




ADVERTIMENT. L'accés als continguts d'aquesta tesi queda condicionat a l'acceptació de les condicions d'ús establertes per la següent llicència Creative Commons:  http://cat.creativecommons.org/?page_id=184

ADVERTENCIA. El acceso a los contenidos de esta tesis queda condicionado a la aceptación de las condiciones de uso establecidas por la siguiente licencia Creative Commons:  <http://es.creativecommons.org/blog/licencias/>

WARNING. The access to the contents of this doctoral thesis it is limited to the acceptance of the use conditions set by the following Creative Commons license:  <https://creativecommons.org/licenses/?lang=en>



Universitat Autònoma
de Barcelona

Detection, activation capture and valorization of CO₂ in green solvents through processes electrochemically triggered

Silvia Mena Fernández

PhD Thesis

PhD in Electrochemistry, Science and Technology

Director

Dr. Gonzalo Guirado

Chemistry Department, Science Faculty

2021

The present work entitled “Detection, activation, capture and valorization of CO₂ in green solvents through processes electrochemically triggered”, is presented by Silvia Mena Fernández to obtain the degree of doctor by Autonomous Barcelona University. This thesis was performed at Green Chemistry and Electrochemistry Group at UAB, under the supervision of Dr. Gonzalo Guirado López.

This thesis was performed under the framework of the PhD Program in Electrochemistry, Science and Technology of Autonomous Barcelona University.

by

Silvia Mena Fernández

Approval:

Thesis supervisor:

Dr. Gonzalo Guirado López

Bellaterra, 2021

Acknowledgments

I would like to thank the financial support from the following institutions:

- The Universitat Autònoma de Barcelona (UAB) and Chemistry Department for the activities involving classes and conferences that help me to growth my knowledge.
- The projects CTQ2015-65439-R and PID2019-106171RB-100 from Spain (MINECO/FEDER).
- The spanish network of Excellence E3TECH ("Environmental and Energy Applications of the Electrochemical Technology", CTQ 2017-90659-REDT).
- The Universitat Autònoma de Barcelona for pre-doctoral PIF fellowships.

Also, I would like to thank to Dr. **Scott Shaw**, from the University of Iowa for his support, and helping me in the searching a place to live and in enjoying the lifestyle in United States! I would like to thank his research group in Iowa city, who received me and help in my three months of stay abroad. I learnt a lot and I am very grateful for all your support. In this sense, I would like to thank **Ramin** for all his help inside the lab and outside; for go with me shopping and included me in his plans. Elmira too!

Also, to **Many, Javy, Niroodha, Andy, Jessica, Colleen, Nathan, Whitney** and all the student which I met in Iowa.

In addition, I would like to thank to **Professor Javier Vela**, for inviting me to Iowa State University, and introducing me to his research group. Thank you so much!!

Finally, I would like to thank all my flat mates in AXS House; **Nyema, Miguel, Michaela, Rachel, Kevin, Ben, Andrew...**

Por otro lado, me gustaría agradecer y dedicar esta tesis a **Gonzalo Guirado**, ya que, sin toda su ayuda, no hubiese sido posible. Por todas las veces que he ido a llorarte con mis dudas existenciales y por toda la ayuda que me has dado. Por todas las veces que viniste al laboratorio porque no funcionaba algo y solo con ponerte al lado de la máquina, ésta sentía tu presencia y funcionaba de nuevo. Por preocuparte de todo para que nosotros pudiésemos trabajar sin toda esa presión. Por enseñarme y ayudarme en todo lo que has podido. No puedo estar más agradecida y de verdad que sin ti esta tesis no hubiese sido posible.

A **Illuminada Gallardo**, agradecerte toda la ayuda y todo lo que me has enseñado. Gracias a ti y tu pasión por la electroquímica, que me ha abierto este mundo y lo bonito que es.

A **Sergio Soler**, gracias por enseñarme todo lo que tenía que saber del laboratorio. Sin ti hubiese estado perdida. A **Marta y Manu**, con los cuáles la hora de las comidas eran súper divertidas. Y a todos los que habéis pasado por el laboratorio: **Neus, Yasmine, Marina, Marian, Jesús, Esteve, Carla y Clara**.

A **Sara Santiago**; aunque no quieras ir como yo vestida en el gym sabes que somos zipi y zape. Des del primer año que hemos estado juntas y ya van para cinco. Estoy super feliz de que la electroquímica nos haya unido y que no nos separe. Gracias por

toda la ayuda, por escucharme y los consejos. Por irnos de congreso juntas. Y todas las risas que nos hemos llevado. De aquí me llevo una amiga para toda la vida.

A **Carolina Gascó**. Muchas gracias por toda la ayuda y esos buenos consejos. Aunque estás un poco loca, des del primer día que te vi sabía que serías una cucada trabajadora. Aunque no quieras admitirlo ya eres más electroquímica que orgánica. ¡Y orgullosas que estamos! Me alegro muchísimo de que te hayas venido al mundo de los electrones porque así he podido conocerte y ya no te vas a librar de mí.

Muchas gracias a las dos por todo el apoyo. Por toda la ayuda. Por apoyarnos mutuamente. Por saber que somos un equipo y que os tengo para sostenerme en cualquier situación. Por irnos a merendar. Por celebrar los éxitos y los fracasos. Estoy orgullosa de vosotras y estoy segura de que vais a llegar a lo más alto.

A **Joan Soldevila**. Muchas gracias por todas las veces que te quedaste conmigo para que no comiese sola. Por todas las charlas para llorar las penas. Por ese humor que solo entendemos nosotros XD. Eres de lo mejor que me llevo de estos años.

A **Kevin Morales**; gracias por estar para mí cuando te he necesitado, por saber que solo subiendo tres pisos te iba a encontrar y me ibas a ayudar con lo que sea.

A **Dionisia Ortiz**, por los días mirando dudas de electroquímica o de becas que nos hacían falta. Por tener siempre todas las respuestas. Por estar para mí para lo que hiciese falta.

Muchas gracias a los dos, y al **Manel**, por todas las veces que hemos quedado para contarnos las penas y reírnos (y perder a juegos). Por saber que puedo contar con vosotros para todo, y que si necesitaba algo solo tenía que subir las escaleras para encontrarlos. Este es un viaje duro, pero con vosotros ha sido mucho más llevadero. Gracias por estar conmigo de principio a fin.

A **Laia García**; gracias por prestarme tu ayuda sin ni siquiera pedirla y saber que puedo contar contigo. Aunque eres una maniática con el formato y no me has perdonado ni una coma mal puesta eres un sol.

A **Francesc Nieto**, muchas gracias por escucharme y ver que te tengo y puedo contar contigo.

Sois muy importantes para mí y me hace mucha ilusión teneros, ponernos al día y reírnos juntos.

A **Mandy**; gracias por estar a mi lado. Por ir a tomar café y ponernos al día semana sí y la otra también.

A **Jessica**, por estar conmigo aún en la distancia. Por saber que solo con pedirlo mueves el mundo.

Las dos estuvisteis conmigo apoyándome des de que comencé esta aventura, y sois de lo más bonito que me llevo.

A **mi familia** por el apoyo que me habéis dado, por no dudar nunca de lo que soy capaz y por estar orgullosos de mí.

Por último, gracias a todos los grandes científicos que he conocido en esta etapa, los cuales de una forma y otra me habéis hecho aprender y crecer.

Table of contents

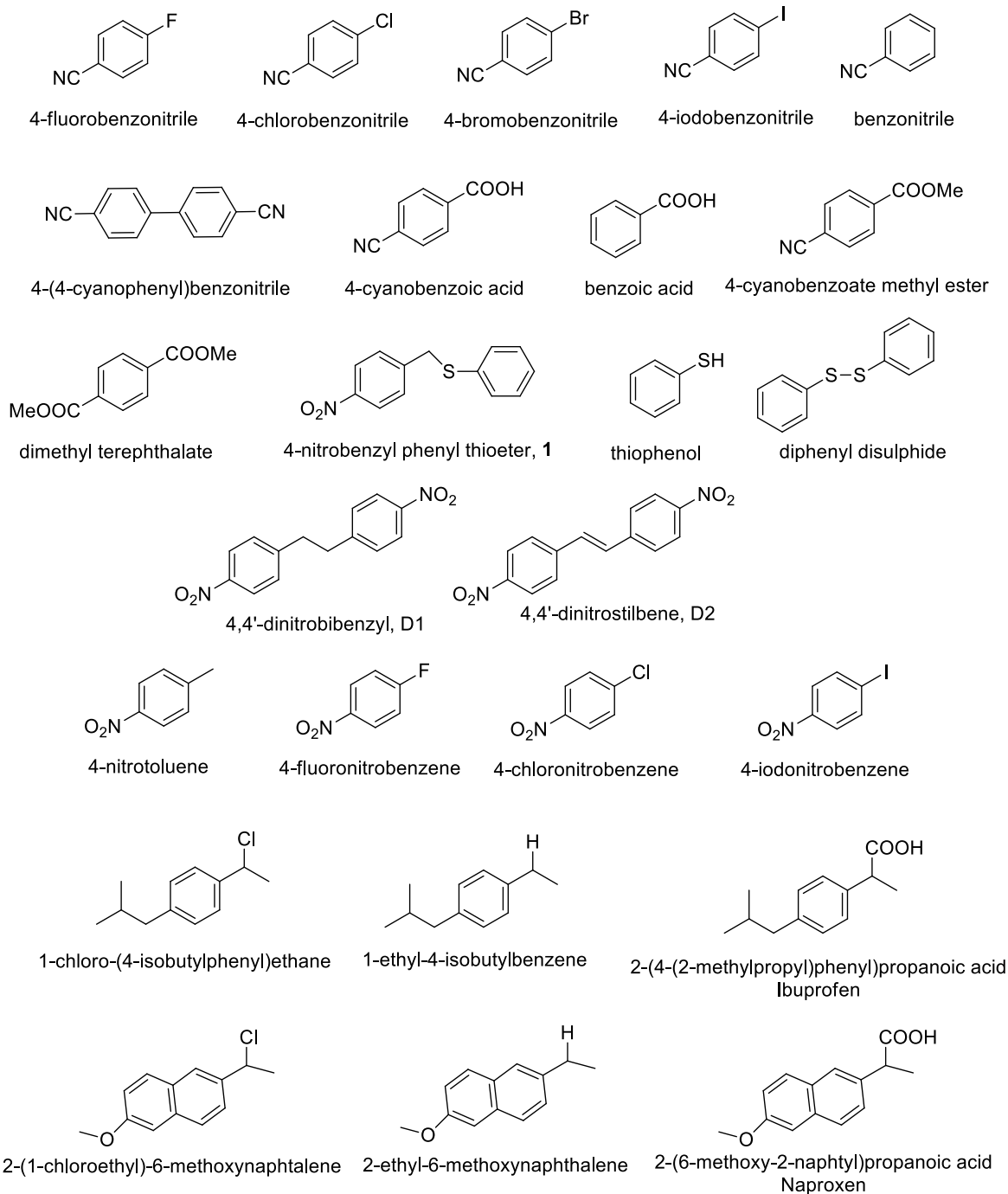
LIST OF ABBREVIATIONS AND SYMBOLS	III
CHART OF STRUCTURES	V
ABSTRACT	VII
RESUMEN	IX
CHAPTER 1. INTRODUCTION.....	3
1.1. GLOBAL WARMING AND GREENHOUSE GASES	3
1.1.1. <i>Consequences of climate change</i>	5
1.2. STRATEGIES TO ADDRESS CO ₂ PROBLEM	6
1.2.1. <i>Carbon-free energy sources</i>	6
1.2.2. <i>Removing or using emitted CO₂</i>	7
1.3. ELECTROCHEMICAL VALORIZATION OF CO ₂	24
1.3.1. <i>Electrochemical reduction of CO₂</i>	24
1.3.2. <i>Electrochemical carboxylation of CO₂</i>	27
1.3.3. <i>CO₂ and Ionic liquids</i>	30
1.4. BIBLIOGRAPHY	40
CHAPTER 2. OBJECTIVES	53
CHAPTER 3. RESULTS AND DISCUSSION	57
3.1. ELECTROCHEMICAL CARBOXYLATION THROUGH CARBON-HALOGEN CLEAVAGE	58
3.2. ELECTROCHEMICAL CARBOXYLATION THROUGH CARBON-SULPHUR CLEAVAGE	66
3.2.1. <i>Electrochemical study of 4-nitrobenzyl phenyl thioether under inert atmosphere</i>	67
3.2.2. <i>Electrochemical study of 4-thionitrobenzyl phenyl thioether under CO₂ saturated atmosphere</i>	73
3.3. SUSTAINABLE SYNTHESIS OF THE IONIC LIQUID TBA TFSI.....	79
3.4. ELECTROCHEMICAL VALORIZATION OF CO ₂ IN IONIC LIQUIDS.....	81
3.4.1. <i>CO₂ reduction mechanism in EMIM OTf</i>	81
3.4.2. <i>Organic molecules in the electrochemical valorization of CO₂ in ionic liquids</i>	87
3.5. ELECTROCHEMICAL VALORIZATION OF CO ₂ TO SYNTHESIZED NSAIDS DRUGS	96
3.5.1. <i>Electrochemical carboxylation approach for synthesis of 2-(4-(2-methylpropyl)phenyl)propanoic acid in ionic liquids</i>	97
3.5.2. <i>Electrochemical carboxylation approach for synthesis of 2-(6-methoxy-2-naphtyl)propanoic acid in ionic liquids</i>	100
3.6. BIBLIOGRAPHY	107
CHAPTER 4. CONCLUSIONS.....	113
CHAPTER 5. PUBLICATIONS	117
APPENDIX. THEORETICAL FUNDAMENTALS OF ELECTROCHEMISTRY	III

List of abbreviations and symbols

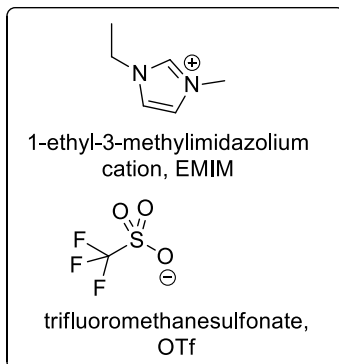
α	Electronic transfer coefficient
η	Overpotential
ν	Frequency
ACN	Acetonitrile
C	Chemical reaction
$^{\circ}\text{C}$	Celsius degree
Cat.	Catalyst
CE	Counter electrode
CCU	Carbon Capture and Utilization
CCS	Carbon Capture and Storage
CV	Cyclic voltammetry
D1	4,4'-dinitrobibenzyl
D2	4,4'-dinitrostilbene
DEA	Diethanolamine
DMF	<i>N,N'</i> -dimethylformamide
DRM	Dry reforming methane
E	Electron transfer
E^0	Standard potential
E_{ap}	Applied potential
E_{p}	Peak potential
ΔE_{p}	Potential average wavelength
EGR	Enhance gas recovery
EOR	Enhance oil recovery
F	Faraday constant ($F = 96485 \text{ C}\cdot\text{mol}^{-1}$) Farads ($F = n\cdot F$)
FTIR-ATR	Infrared spectroscopy with attenuated total reflectance
FTS	Fischer-Tropsch synthesis
GC	Glassy carbon
GC-MS	Gas chromatography coupled to mass spectrometry
GDE	Gas diffusion electrode
GHG	Greenhouse gas
I_{p}	Peak current
IL	Ionic liquid
IR	Infrared reflection
IRRAS	Infrared reflection absorption spectroscopy
k	Chemical reaction constant

k_s^{ap}	Apparent electronic transfer rate constant
MEA	Monoethanolamine
MOF	Metal organic framework
m.p.	Melting point
MWCNT	Multi-walled carbon nanotubes
n	Number of mols
NMR	Nuclear magnetic resonance
NSAIDs	Non-steroidal anti-inflammatory drugs
PMIRRAS	Polarization Modulation- Infrared reflection absorption spectroscopy
ppm	Part per million
RE	Reference electrode
rt	Room temperature
RTIL	Room temperature ionic liquid
SCE	Saturated calomel electrode
TDS	Total dissolved solids
TOF	Turnover frequency
TSIL	Task-specific ionic liquid
v	Scan rate ($V \cdot s^{-1}$)
WE	Working electrode
z	Number of electrons

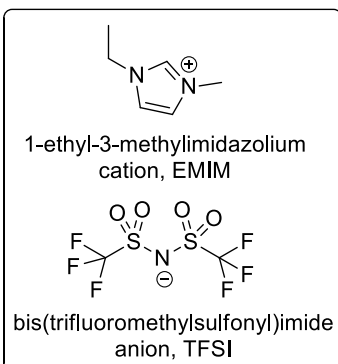
Chart of structure



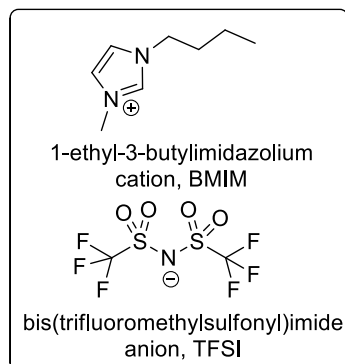
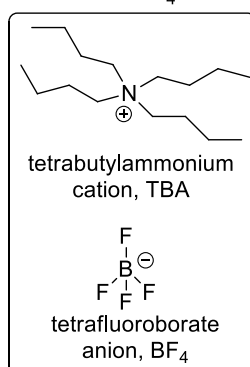
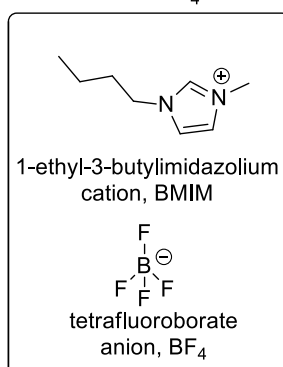
EMIM OTf



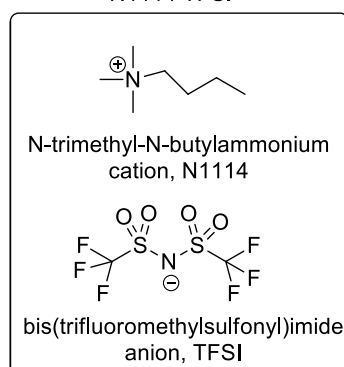
EMIM TFSI



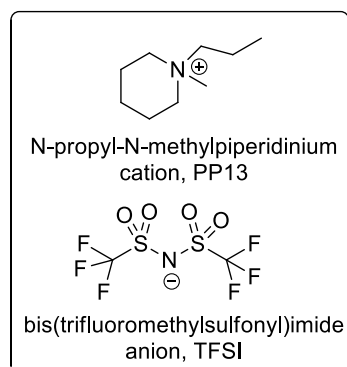
BMIM TFSI

TBABF₄BMIM BF₄

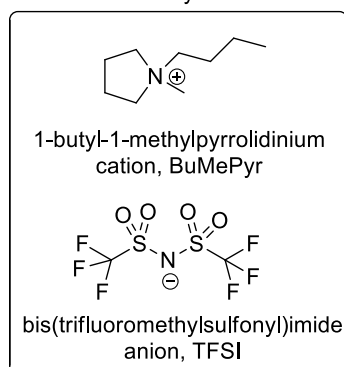
N1114 TFSI



PP13 TFSI



BuMePyr TFSI



Abstract

This thesis presents efficient approaches for producing high value compounds using CO₂ as a building block. The methodology employed is based on electrochemical techniques, which enable eco-friendly chemistry solutions to be used, as well as maintaining the aim of offering a potential long-term strategy for reducing CO₂ emissions in the atmosphere, while obtaining useful compounds, such as carboxylated aromatic acids. The electrochemical approach is relaying on three different strategies to valorize CO₂; firstly, the direct reduction of CO₂ on the electrode surface in presence of an imidazolium-based ionic liquid, obtaining a carboxylated ionic liquid. The second one is based on the electrochemical activation through different C-X cleavages in the presence of CO₂ saturated solutions, producing electrocarboxylation processes. Third one is based on a catalytic process through a homogeneous catalysis, where CO₂ is indirectly reduced in the solution. On the other hand, the ionic liquids are introduced as a greener alternative to the traditional organic aprotic solvents employed in electrochemical experiments, due to their improved characteristics and the removal of the supporting electrolyte. Moreover, is presented a sustainable one-pot synthesis of an ionic liquid, using an ion exchange strategy.

Resumen

Esta tesis presenta diferentes enfoques eficientes para la producción de componentes de alto valor añadido utilizando el CO₂ como base fundamental. La metodología empleada se basa en técnicas electroquímicas, las cuales permiten la utilización de soluciones químicas ecológicas, a la vez que se mantiene el objetivo de ofrecer una potencial estrategia a largo plazo para la reducción de las emisiones de CO₂ a la atmósfera, mientras se obtienen compuestos útiles, como por ejemplo ácidos aromáticos carboxílicos. El enfoque electroquímico se basa en tres estrategias diferentes para valorizar el CO₂; la primera de ellas se basa en la reducción directa del CO₂ en la superficie del electrodo en presencia de un líquido iónico tipo imidazol, obteniendo un líquido iónico carboxilado. La segunda estrategia se basa en la activación electroquímica a través de roturas de enlaces C-X, en presencia de disoluciones saturadas de CO₂, dando lugar a procesos de electrocarboxilación. La tercera estrategia consiste en un proceso catalítico basado en una catálisis homogénea, en la cual el CO₂ es reducido de manera indirecta en la disolución. Por otro lado, son los líquidos iónicos introducidos como una alternativa más ecológica a los disolventes orgánicos apróticos tradicionales utilizados en los experimentos electroquímicos, debido a sus mejoradas características y la eliminación de electrolito soporte. Finalmente, se presenta una síntesis, de un solo paso, sostenible de un líquido iónico, utilizando una estrategia de intercambio iónico.

Chapter 1. Introduction

Chapter 1. Introduction

1.1. Global warming and Greenhouse gases

Global warming is a current issue of concern in the world nowadays. The main source of global climate change is the increasing concentrations of greenhouse gases (GHGs) in the atmosphere, as they develop the worldwide-known greenhouse effect. ^[1] This effect is based on the formation of a layer of different gases over the Earth, which contributes to an entrapment of energy radiation of the Sun (Figure 1), which, instead return to the space, contributes to increase the temperature on the Earth's surface. ^[2]

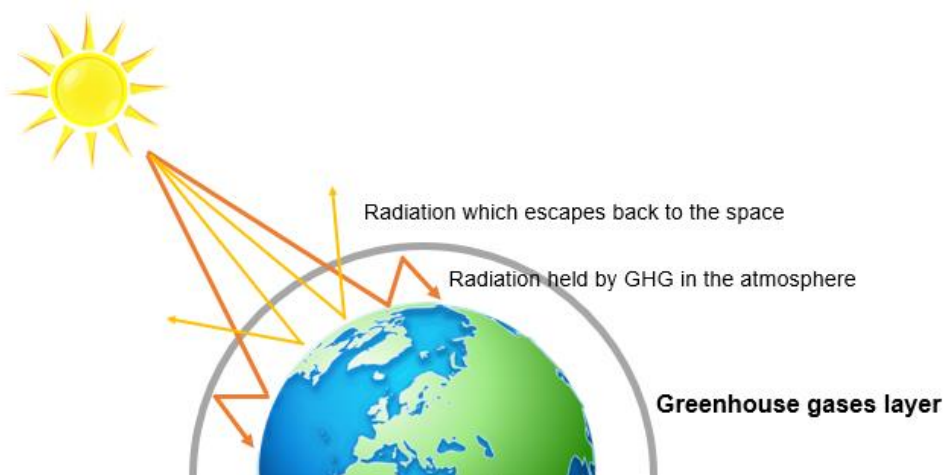


Figure 1. Greenhouse effect.

Despite the fact that greenhouse effect is essential for life, since it prevents an icebound state of the Earth. ^[3] An acceleration of it, due to anthropogenic activities mostly, originates the global warming.

The most important greenhouse gases are carbon dioxide, methane, and water vapor, but to a lesser extent, surface-level ozone, nitrous oxides and fluorinated gases also trap infrared radiation. The concentrations of these greenhouse gases have varied substantially during Earth's history, and these variations have driven substantial climate changes at a wide range of timescales.

On taking a close look at the different GHGs, carbon dioxide, CO₂, is the most important contributor to global warming. Natural sources of atmospheric CO₂ include out-gassing from volcanoes, the combustion and natural decay of organic

matter, and respiration by aerobic (oxygen-using) organisms. These sources are balanced, on average, by a set of physical, chemical, or biological processes that tend to remove CO₂ from the atmosphere. An example of natural sources includes terrestrial vegetation, which takes up CO₂ during photosynthesis. A long-term balance between these natural processes lead to the background level of CO₂ in the atmosphere. [4]

In contrast, human activities increase atmospheric CO₂ concentration levels, primarily through the burning of fossil fuels, and through burning of forests and the clearing of land. Anthropogenic emissions currently account for the annual release of about seven billion tons of carbon into the atmosphere. And this amplified carbon load from human activities far exceeds the offsetting capacity of natural processes. Consequently, CO₂ is accumulated in the atmosphere at an average rate of 1.4 ppm per year between 1959 and 2006 and roughly 2.0 ppm per year between 2006 and 2020. Overall, this rate of accumulation has been linear, and it could be described with the Keeling curve (Figure 2). This is a graph that shows a daily record of global atmospheric carbon dioxide concentration in Mauna Loa (Hawaii). This curve is maintained by the Scripps Institution of Oceanography at University of California, in San Diego, and supervised by Charles David Keeling, who was the first person to perform daily measurements of atmospheric CO₂ concentration at the South Pole and Hawaii since 1958 henceforth. [5]

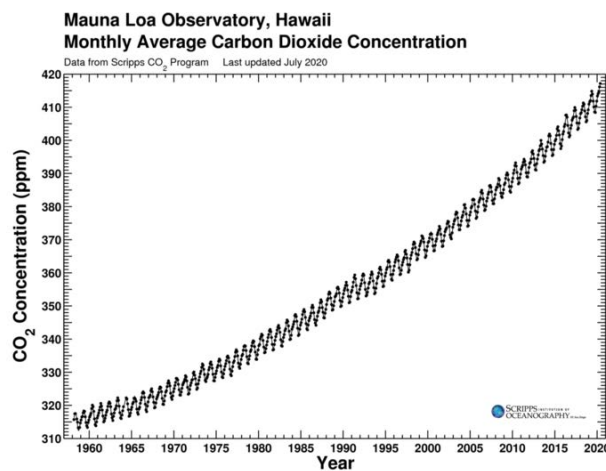


Figure 2. Keeling curve. Atmospheric CO₂ at Mauna Loa Observatory ^a.

^a https://scrippsco2.ucsd.edu/graphics_gallery/mauna_loa_record/mauna_loa_record.html

By the early 21st century, CO₂ levels reached 384 ppm, which is approximately 37 percent above the natural background level of roughly 280 ppm, which existed at the beginning of the Industrial Revolution. Atmospheric CO₂ levels continued to increase, and by 2020 they had reached 415.36 ppm of CO₂ in air, latest read on 5th January 2021 ^b. According to ice core measurements, such levels are believed to be the highest in at least 800,000 years and, according to other lines of evidence, may be the highest in at least 5,000,000 years. ^[6–8]

This tendency makes the need to reduce the emissions of CO₂ urgent, by searching alternative sources of energy and reducing the use of fossil fuels, as well as trying to reduce the CO₂ levels in the atmosphere by directly capturing and valorize this molecule.

1.1.1. Consequences of climate change

The effects of global warming include far-reaching and long-lasting changes to the natural environment, to ecosystems, and to human societies. It also includes the economic and social changes which stem from living in a warmer world. ^[9] For these reasons, anthropogenic climate change is one of the threats to sustainability of the Earth as we know it. ^[10]

Many physical impacts of global warming are already visible, including extreme weather events, glacier retreat, changes in the timing of seasonal events, sea level rise, and declines in Arctic sea ice. ^[11,12]

The future impact of global warming depends on the extent to which nations implement prevention efforts and reduce greenhouse gas emissions. Near-term climate change policies significantly affect long-term climate change impacts. Stringent mitigation policies might be able to limit global warming (in 2100) to around 2 °C or below, relative to pre-industrial levels. Without mitigation, increased energy demand and extensive use of fossil fuels might lead to global warming of around 4 °C. Higher magnitudes of global warming would be more difficult to adapt to and would increase the risk of negative impacts. ^[13]

^b <https://sioweb.ucsd.edu/programs/keelingcurve/>

1.2. Strategies to address CO₂ problem

In order to solve the CO₂ problem, explained in the previous sections, two strategies can be considered: on one hand, preventing the CO₂ emission and, on the other hand, remove or use the emitted CO₂. Both strategies may seem quite logical and self-evident, but the need for complex technological developments and the increasing demand of energy, among other factors, make the use of carbon-free sources difficult, as well as the efficient removal of emitted CO₂. ^[14]

In this sense, some approaches for both strategies to tackle the CO₂ problem are discussed. Firstly, the use of carbon-free energy sources is detailed, as well as alternatives considered to avoid the emission of CO₂ in energy production and industrial processes. Secondly, new systems that allow the removal of emitted CO₂ are mentioned and discussed; Carbon Capture and Storage (CCS) and Carbon Capture and Utilization (CCU) strategies, leading to the use of ionic liquids for these applications.

1.2.1. Carbon-free energy sources

Unlike the combustion of coal, natural gas, and distillate fuel (which produces carbon dioxide), wind, solar, and hydropower energy systems emit no GHGs because their fuel or energy source is carbon-free. Thus, classical renewable energy sources, and biomass, prevent substantial CO₂ emission, by contributing more than 16% of the world energy demand. Moreover, their potential for expansion is considerable, because growing more biomass could play an immediate role in adsorbing excess CO₂ at relatively low cost. ^[6,15]

As a detailed example, the use of biomass energy provides a multitude of environmental benefits. ^[16,17] It reduces acid rain, prevents soil erosion and water pollution, minimizes pressure on landfills, provides wildlife habitat, and helps maintain forest health through better management. Besides, also would reduce greenhouse gas emissions, as fossil fuels emit vast quantities of carbon dioxide into the atmosphere upon combustion, carbon that would otherwise remain trapped underground. Although biomass also freed carbon dioxide as it burns, the carbon dioxide released during combustion is absorbed during the plant's life, and could eventually be released as the organic matter decays, to be absorbed

by other plants that are in the growth stages, creating a closed-carbon cycle (Figure 3).

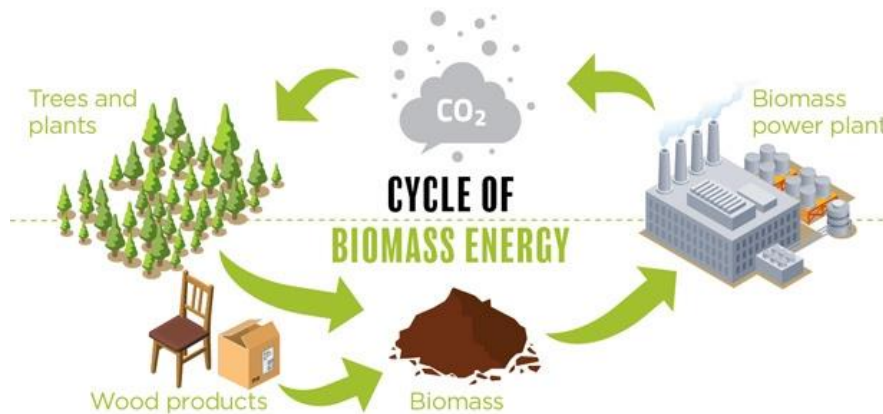


Figure 3. Biomass energy circle °.

Therefore, when fossil fuels are used to generate electric power, carbon dioxide that has been locked away and otherwise would not have been emitted is added to the atmosphere. To the contrary, the use of biomass as an energy source reduces the amount of "fossil" carbon dioxide that is emitted to the atmosphere by displacing fossil fuels.

However, the main barriers for the use of non-emitting sources of energies usually rely on the high cost of the system, low energy density, or non-competitive conversion efficiencies. For these reasons, the use of carbon capture and storages systems (CCS) is crucial, for example, in applications in which fossil fuels have no serious competitor. Carbon capture techniques are taken into account in order to obtain truly emission-free systems and can be helpful in the transition towards a carbon-free economy. In the following section, different carbon capture and storage strategies are detailed, as well as ways to transform the captured CO₂ into valuable products (CCU strategies).

1.2.2. Removing or using emitted CO₂

In the last decade, new concepts have been developed as a suitable approach for facing the challenges of the current global scenario, with biomimetic and circular economy models having been formulated. All the approaches involve a

° <https://www.canadianbiomassmagazine.ca/any-renewable-energy-solution-requires-extracting-the-full-value-of-biomass-6499/>

first capture step for an efficient removal of CO₂ from common point sources prior to the release of gases into the atmosphere.

1.2.2.1. CCS strategies

“CCS technology” could be thought of as a chain of technologies created to separate CO₂ from industrial sources, transport it to a storage location and isolate it for the long-term from the atmosphere. CCS technology can reduce CO₂ emissions from large industrial sources and coal-fired power stations by approximately 85% depending on the kind of CCS chain-capture, transport and storage. [18]

The most expensive element of CCS technology is the initial CO₂ capture. There are three types of well-developed CO₂ capture systems: post-combustion, pre-combustion and oxy-fuel (Figure 4). [19–21]

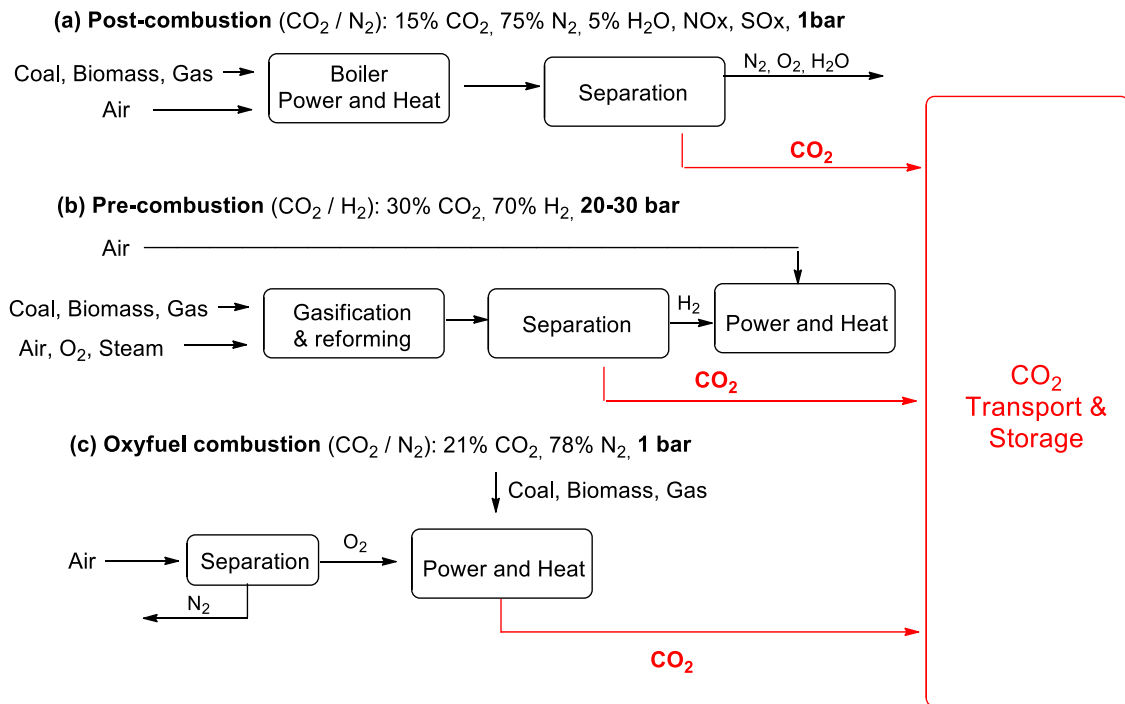


Figure 4. CO₂ capture systems.

Post-combustion capture uses a chemical solvent to remove CO₂ from the exhaust gas of a traditional power plants (gas or coal-fired power plant), or industrial facilities (such as cement kilns, iron and steel production), or in some refinery settings. The solvent, typically an amine solution, binds with the CO₂. The solvent-CO₂ combination is separated from the rest of the exhaust gas and

heated. The heat drives off relatively pure CO₂ which is ready for compression and sequestration. The solvent is cooled and reused.

Pre-combustion capture requires an initial gasification of a fuel source, but it yields a purer stream of CO₂ for capture at the end of the process. Gasification starts by turning coal, refinery wastes, or other materials into *syngas* (a mixture of H₂ + CO + CO₂). The CO₂ capture step from gasification begins with a water shift reaction, where water and carbon monoxide react with carbon dioxide and hydrogen. The shift reaction creates more H₂ and CO₂ in the *syngas*, after which the CO₂ is removed using commercial processes.

Both post- and pre-combustion for CO₂ capture technologies use separation processes, based on solvents, membranes, cryogenic technologies, or other chemical or physical processes that are already being applied in industry. For instance, in the petrochemical industry to increase the yield in the lighter fractions in oil distillation, or in the food industry to produce CO₂ for fizzy drinks.

The other CCS strategy is called, oxy-combustion capture or oxy-fuel. It is a process where coal is burned in oxygen instead of air, resulting exhaust containing only CO₂ and water vapor. Because it yields an almost 100% CO₂ stream that is readily transportable, the process has strong potential, but it is extremely energy intensive.

Once CO₂ is captured, it would be transported, mostly by pipeline. Its cost is an order of magnitude less than capture, and pipeline technology is established and mature. Thus, the key issues in this part of the CCS technology chain are more about the siting and routes of pipelines, the purity of CO₂ transported, and the potential for future pipeline tie-ins, than the intrinsic technologies associated with compression and pipeline integrity.

After transportation, CCS technology follows with the storage. There are several CO₂ injection and storage technology options, of which the most mature are geological storage (Figure 5) (either in depleted oil and gas reservoirs or in deep saline formations), and enhanced oil/gas recovery (EOR/EGR). The costs of geological storage are roughly equivalent to the costs of transportation, and there are relatively constant costs across a wide range of storage capacities.

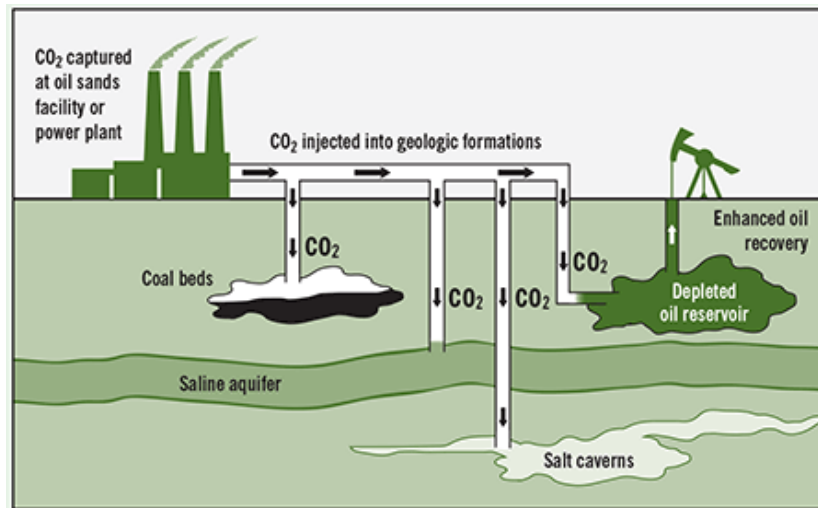


Figure 5. CO₂ geological storage ^d.

Comparing capture technologies, nowadays, post-combustion carbon capture systems are the easiest to adapt, as they can be directly used in current power plants or other sources of CO₂. Moreover, these technologies can be extremely helpful for reducing the emissions in other sectors that are difficult to decarbonize. On the other hand, pre-combustion capture systems are not as easy to adapt. These technologies need to be built in new installations because large equipment, such as a gasifier, is needed. However, pre-combustion capture methods can be really interesting in the transition towards hydrogen consuming systems. Oxy-fuel combustion also allows a greater thermal efficiency of power plants. Nonetheless, oxy-fuel based technologies are more cost-demanding, thus fundamental parts of the power plants, such as turbines, should be readapted.

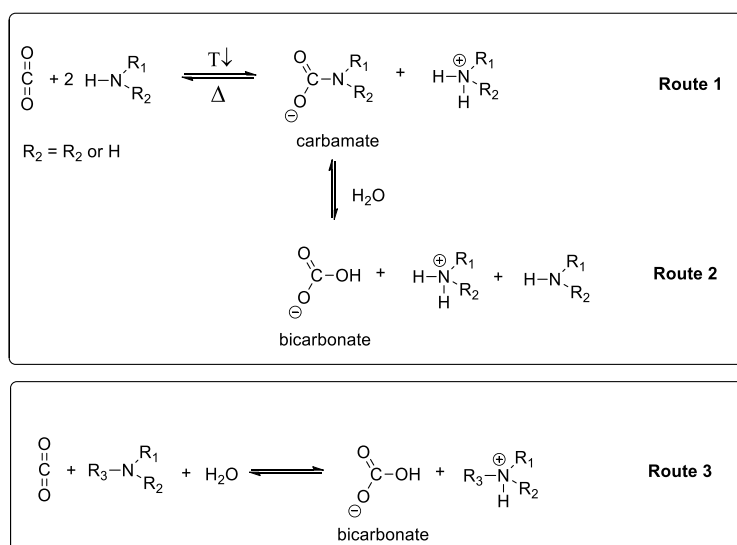
In the next sections some examples of CO₂ capture strategies are detailed. The most important example of post-combustion CCS approaches is based on chemical absorption and desorption using an aqueous amine solution. They are also one of the most promising options for separating CO₂ from fossil-fuel-derived flue gas, due to its simple operation, high absorption efficiency, cost-effectiveness, and maturity. In the same way, the use of MOFs, ionic liquids, and biological methods appear as promising strategies for the capture and storage of CO₂. ^[22,23]

^d <https://energywatch-inc.com/carbon-capture-utilization-storage-pipe-dream-potential-solution/>

Absorption of CO₂: Aqueous amines

In this process, mixing of gaseous CO₂ molecules takes place in an absorbent liquid solvent which is later regenerated. Chemical absorption by aqueous amine-based solvents appears the most promising short-term solution for CO₂ capture from flue gas, because of their ability to capture CO₂ at low pressure with adequate absorption/desorption kinetics. ^[24] For instance, in industry, CO₂ removal from flue gases is practiced on a large scale using an aqueous solution of amines, such as monoethanolamine (MEA) and diethanolamine (DEA), which are more than 90% efficient. To liberate the CO₂ at a higher concentration, these amine solutions are then regenerated by steam stripping. This kind of process is called amine scrubbing. ^[19]

Primary and secondary amines react with CO₂ as a nucleophile and form ammonium carbamates under anhydrous conditions (Scheme 1, Route 1). In the presence of water, primary and secondary amines can act both as nucleophiles and bases to form a mixture of carbamate and bicarbonate/carbonate (Scheme 1, Route 2). To obtain one equivalent of carbamate, two equivalents of amine are necessary, resulting in a CO₂ to amine ratio of 1:2. When bicarbonates/carbonates are formed, a beneficial 1:1 ratio between amine and CO₂ is realized. In contrast to the primary and secondary amines, a tertiary amine can act only as a base due to the lack of –NH proton (unable to form a carbamate) and form bicarbonate/carbonate in water (Scheme 1, Route 3). ^[25]



Scheme 1. CO₂ capture by primary, secondary and tertiary amines.

Figure 6 illustrates the CO₂ capture process using amine scrubbing; [26] the flue gas flows in a counter current direction to the aqueous amine solvent in the absorber, where CO₂ is removed via chemical reactions into the liquid stream at ~40 °C. This liquid stream then goes to a stripper using water vapor and operating at 100–120 °C; here, the solvent is regenerated as CO₂ is released into the gas stream. Then, pure CO₂ can be produced when water is condensed out of the gas stream, followed by CO₂ compression and storage. [22,27]

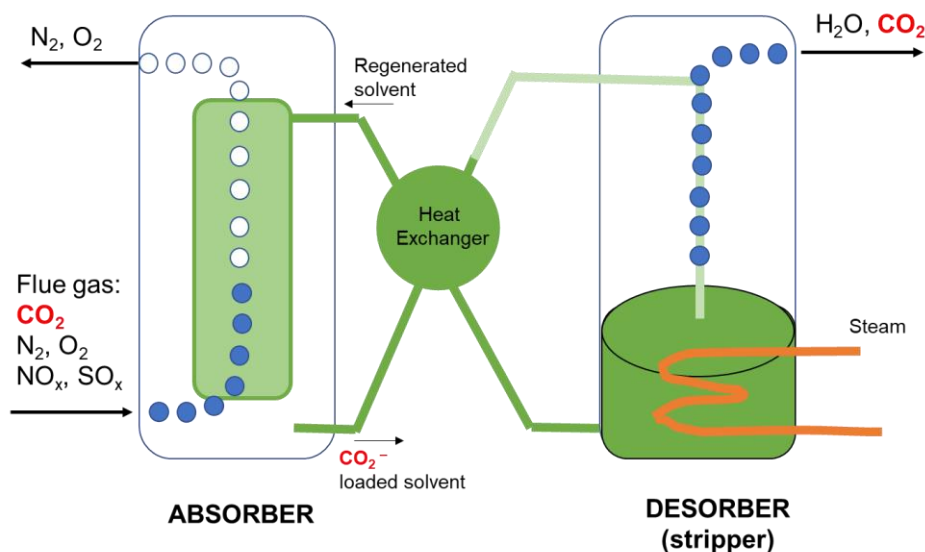


Figure 6. CO₂ capture from flue gas by aqueous amine system.

Unfortunately, widespread implementation of these CO₂ capture systems has been limited, because of the high cost associated with the high parasitic energy consumption during regeneration, as well as solvent degradation, and corrosion. [28] In order to solve the main drawbacks of the use of amines in the carbon capture, alternatives to CO₂ capture are also considered. These alternatives comprise, among other solutions, novel materials which are able to efficiently attach the CO₂, avoiding the regeneration steps and solvent degradations that characterize the chemical carbon absorption.

Absorption of CO₂ in Ionic liquids

The search for alternatives to amines as absorbers has increased enormously in recent years. One of the most fertile research fields on this process has been the ionic liquids (ILs), [26,29] which will be described in depth in the next sections.

ILs are the combination of an organic cation with an inorganic or organic anion. Many combinations of readily available cations and anions lead to ionic liquids, resulting in a wide number of possible candidates.

Designing “task-specific” ionic liquids (TSILs) for many kinds of applications is therefore, in principle, a potentially successful enterprise.

In the field of carbon dioxide capture, Bates et al. were the first to propose task-specific ionic liquid for CO₂ capture.^[30] Ionic liquids have extremely low volatility, so their use could avoid the negative environmental impacts in the atmosphere of the amine processes, and many of them can also solubilize large amounts of carbon dioxide. After that, Ramdin et al.^[29] provided a very extensive review of the advantages and problems of the use of ionic liquids for the purpose of capturing carbon dioxide. The integration of ionic liquids with other materials is a recent strategy that expands the applicability of these solvents. Apart from their high carbon dioxide solubility, they are electrical conductors (because they consist of ions), which might make them the ideal absorber/solvent for the integration of capture with electrochemical transformation of carbon dioxide.^[31]

Adsorption methods for CO₂ capture: Metal organic frameworks (MOFs)

In general, the aim of solid sorbent research is to reduce the cost of CO₂ capture by designing durable sorbents with efficient materials handling schemes, and increased CO₂ carrying capacity. The CO₂ carrying capacity is a key sorbent parameter that depends on the total microscopic surface area of the material. Researchers are thus attempting to identify and design sorbents with very high surface area, pore size, and pore volume, such as mesoporous silica for CO₂ capture.^[32–34]

Metal organic frameworks (MOFs) are a class of porous material that represent one of the promising adsorbents and have gained significant attention during recent years for gas separation applications. MOFs are composed of metal ions or clusters (nodes) bridged by organic ligands (connectors) to form various structures and networks. MOFs are well recognized for their extraordinary surface areas, ultra-high porosity, and the most important, flexibility to tune the porous structure, as well as the surface functionality due to presence of organic ligands that can easily chemical modified. Many MOFs have the capability of capturing

carbon dioxide, but it varies between, approximately, 4 to 26 mmol·g⁻¹ in some cases. [35–37]

Yaghi's group first reported MOFs for CO₂ capture at room temperature. [38] Thereafter they have developed new types of MOFs for CO₂ capture. [39–41] And Zhou's group (among other authors) also reviewed the progress of MOFs for CO₂ capture from experimental to molecular simulation. [42] MOFs could be classified into four different categories, considering the mechanism of carbon adsorption; rigid, flexible, functionalized MOFs, and MOFs with electrostatic interactions that improve the CO₂ capture.

Rigid MOFs are able to adsorb CO₂ due to the molecular sieving effect enhancing the specific electrostatic interactions between the framework and the molecule of CO₂. On the one hand, sieving effect is obtained by selecting the ligands and modifying the MOFs synthesis process in such a way that the pore diameter obtained is like the size of CO₂. The CO₂ could then be separated from a gas mixture, not allowing other molecules to be retained in the MOFs due to the selective pore size (Figure 7). [43] On the other hand, selective adsorption of CO₂ in rigid MOFs can be achieved by exploiting specific interactions between the target molecule and the framework using, for example, amine containing groups. [44]

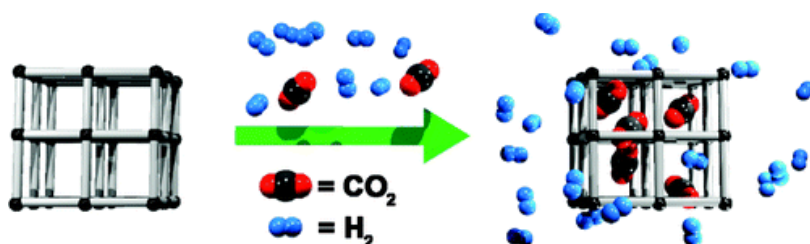


Figure 7. Metal organic framework as adsorbent for pre-combustion of CO₂. Reprinted (adapted) with permission from [43] and the author. Copyright (2011) American Chemical Society.

In flexible MOFs, unlike rigid MOFs, the pore size changes whether the target molecule enters in the crystalline structure or not. Zhou et al. reported a photoactive flexible MOF that was unable to absorb CO₂ (Figure 8). Using azobenzene-functionalized terephthalic acid as a linker, PCN-123 with MOF-505 like rigid framework and photoactive side chains was obtained. Through the control of the trans and cis configuration of the azobenzene motif upon

photochemical or thermal treatment, the pore structure could be regulated, which affected the CO₂ uptake of the resulting material significantly. [45–48]

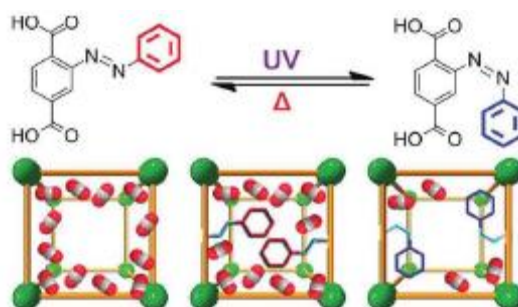


Figure 8. CO₂ adsorption in PCN-123 via photoresponsivity behavior of the linker. Reprinted (adapted) with permission from [48] and the author. Copyright (2012) American Chemical Society.

Electrostatic interactions are another interesting property when considering selective capture of CO₂. As CO₂ presents with a quadrupolar moment, this molecule can be separated from non-polar molecules, such as methane (CH₄), due to electrostatic interactions. Open metal site MOFs take advantage of these types of interactions to selectively adsorb CO₂ from mixtures with different non-polar gases. In open metal site frameworks, metal nodes have free coordination sites, which can establish coordination bonds with the CO₂. One of the most used MOFs of this kind is [Cu₃(BTC)₂], which consist of Cu₂(COO[−])₄ centers linked with 1,3,5-benzenetricarboxylate (BTC^{3−}). In this MOF, the Cu²⁺ centers coordinate with the CO₂. Moreover, when using this MOF in wet environments, the capability of adsorbing CO₂ is increased due to the interaction between the CO₂ and the electric field created by water molecules, coordinated with the metal centers. [49]

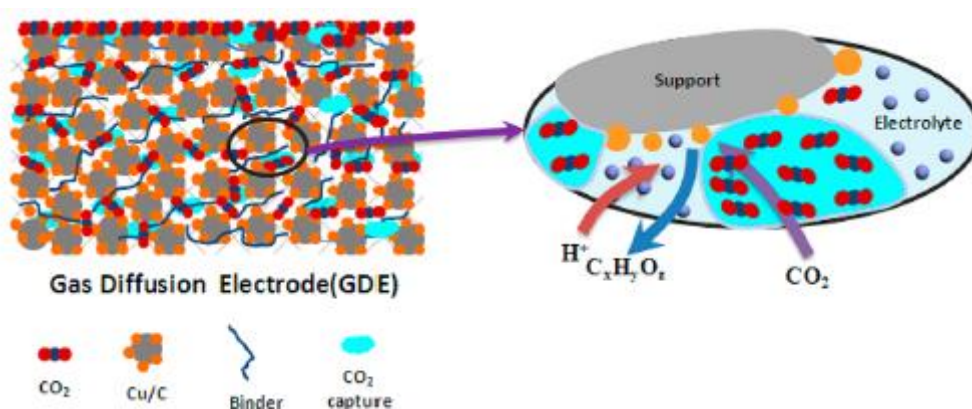


Figure 9. Structural schematic diagram of GDE with Cu₃(BTC)₂ as CO₂ capture agent. Reprinted (adapted) with permission from [49] and the author. Copyright (2018) American Chemical Society.

Finally, as detailed before, the MOFs can be tuned to enhance their capacity to retain CO₂ molecules. The last group of MOFs mentioned is the surface functionalized frameworks. By adding a functional group with great affinity for CO₂, like alkanolamines or other amines, as seen when reviewing the amine scrubbing methods, the selectivity of a MOF for the capture of CO₂ can be really enhanced. [50–53]

Despite the great characteristics of MOFs, several drawbacks should be considered. Most of the MOFs have low thermal stabilities, especially when there are compared with other porous materials, like zeolites. [54] The use of complex ligands can increase the cost of the final product. Furthermore, as stated previously, fabrication processes are difficult to adapt into a large-scale production.

Biological CO₂ fixation: Microalgae green refinery

Of all the different CO₂ capture approaches, the biological CO₂ capture method is a potentially attractive alternative. Carbon dioxide can be converted by photosynthesis into organic matter by using sunlight as a source of energy. This alternative, while valuable, still requires further research and development to be implemented. Generally, terrestrial plants can take CO₂ and produce organic matter through photosynthesis. More specifically, algae can convert CO₂ into organic compounds more efficiently than other terrestrial plants.

Biological CO₂ fixation using microalgae could be combined with other processes, like wastewater treatment. This would be advantageous to offer environmentally sustainability. When microalgae are cultured in wastewater rich of nutrients, this provides a source of food for microalgae to grow. The resulting biomass can be used as a feedstock for biofuel production. Therefore, the combination of CO₂ capture, wastewater treatment and biofuel production, offer an attractive strategy for CO₂ capture methods. [55,56]

1.2.2.2. CCU strategies

All these CO₂ capture and storage strategies only partially solve the problem of removing emitted CO₂ from the atmosphere, so approaches to recover valuable products from its conversion through circular economy vision are highly desirable.

In this sense, some conversion routes are designed for the re-use of fuels, especially when inexpensive renewable energy processes are available.

As a more attractive alternative, carbon capture and utilization (CCU) technologies have received a great deal of attention for turning captured CO_2 , as a renewable carbon feedstock, into valuable products, instead of permanently sequestering it. In fact, CCU treats captured CO_2 as a renewable resource to complement or alternate with the conventional petrochemical feedstocks. [57] Moreover, the long-term effects of sequestration are not a concern for this approach. Despite the significant advantages offered by CCU in comparison to CCS, converting CO_2 and utilizing it in chemical reactions is very challenging, mainly because of the thermodynamically stable nature of CO_2 itself. [58]

The utilization of CO_2 can be considered as a viable option for providing a renewable energy source to produce various valuable products. The process needs to be economically viable, safe, and ecofriendly. The primary utilization route can be classified as enhanced oil/gas recovery (EOR/EGR), mineralization, desalination, and chemical conversion. Figure 10 shows various examples of ways in which CO_2 can be utilized. [59]

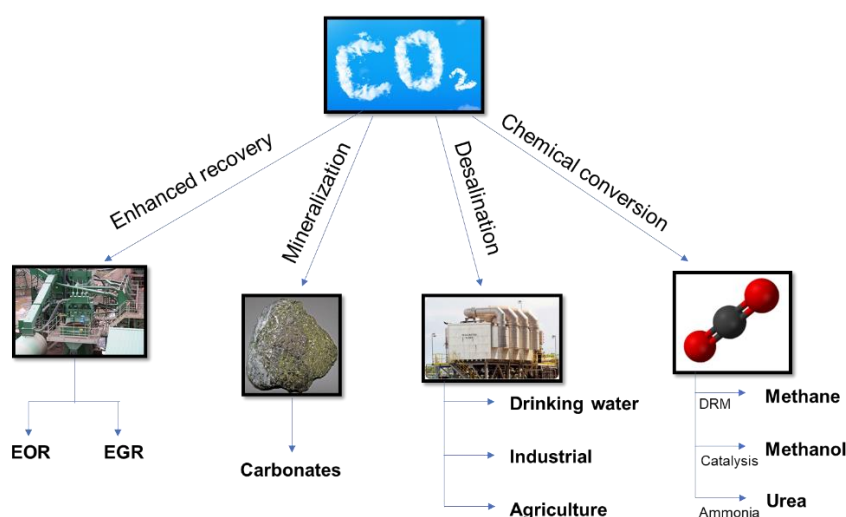


Figure 10. Examples of primary CCU strategies.

Enhanced oil/gas recovery (EOR/EGR)

Enhanced oil/gas recovery refers to a procedure in which a substance is injected into a reservoir to re-pressurize rock formation and to release any oil/gas that may have been trapped in the formation. During the CO_2 EOR process, the

injected CO₂ mixes with the oil and releases it from its otherwise hard-to-recover rock formation. This stream is then pumped to the surface, and the CO₂ emerging with the oil is separated and resupplied into the cycle to repeat the process.

CO₂ flooding is one of the most common and efficient methods used in EOR, as it mixes with the oil, expands it, and makes it lighter and easier to recover. ^[60] Most CO₂ EOR systems use naturally occurring CO₂, but lately, research has focused on using CO₂ captured from potentially hazardous gas streams, such as flue gas and other industrial gas effluents. In general, the efficiency of CO₂ EOR depends largely upon the temperature and pressure of the reservoir involved.

There are numerous challenges faced by CO₂ EOR methods. For instance, owing to the heterogeneity of the rock formation between the wells, fluid properties and capillary pressure reduce the effectiveness of CO₂ flooding.

Overall, CO₂ EOR/EGR is a promising approach in enhanced oil/gas recovery, with applications in most type of reservoirs, but it currently contributes to only 3% of CO₂ utilization.

Mineralization

Non-geologic storage or mineral carbonation of CO₂ consists in the production of stable mineral carbonates by treating CO₂ with metal oxides, such as calcium and magnesium oxides that are naturally abundant in the form of mineral silicates. ^[61,62]

The carbonation of magnesium and calcium silicates through spontaneous reaction with atmospheric CO₂ under ambient conditions is a naturally occurring process (known as natural weathering) that is thermodynamically favored, but not kinetically, because it is very slow. An artificial improvement in the carbonation kinetics can be achieved by injecting fluids with a higher concentration of CO₂, and by increasing the temperature. Despite significant efforts devoted to accelerating this reaction, the slow kinetics are still the main drawback in scaling up the mineralization process. Additionally, this process is energy intensive, as it requires the extraction, processing, and transportation of the rocks, as well as high pressures (10.0 - 15.0 MPa) and temperatures (150 - 600.8 °C) to achieve a carbonation efficiency higher than 80%. Furthermore, the duration of the

carbonation reaction is very long (6 - 24 h), and the rocks should be mined (<37 mm). Large plant sizes and the need for additives to extract reactive species and separate (or dispose of) reaction products are other components with high cost penalties.

In this sense, the mineralization process may be viewed as a sequestration method, because it aims at permanently fixing CO₂, but unlike CCS, which suffers from leakage (geological storage of CO₂), the carbonates are stable and safe. Also, the exothermic nature of the mineralization reaction along with the geothermal gradient contribute to a reduction in energy consumption. Moreover, as pure CO₂ is not required for this process, flue gas can be used directly without removing impurities such as SO_x and NO_x.

Desalination

This is another promising utilization approach; it captures CO₂ that can be used to remove total dissolved solids (TDS) and to transform brine into water. The resulting potable water can be utilized in places for which there is a deficiency. Whereas most desalination plants do not employ CO₂ to perform desalination owing to economic constraints, new technologies are being developed for the cheap and efficient utilization of CO₂ in this process. ^[63]

If sea water, mixed with ammonia (to weaken the salt molecules), is exposed to CO₂, already-weak bonds start to form, which leads to removal of the ions from the water phase. The products formed, Na₂CO₃ and NH₄Cl, are heavy and, thus, can easily settle to the bottom of the tank.

The hydrate-forming method is another technique that is used for desalination, and it involves the formation of CO₂-hydrated (or CO₂-clathrate) by using CO₂ to separate the salts from water. In this approach, CO₂ can be either the gas or liquid form. The CO₂-hydrates are either dumped into the ocean or transported elsewhere.

The ammonia-carbon dioxide forwards osmosis process is yet another desalination technique that employs CO₂. In this process, the driving force is osmotic pressure instead of hydraulic pressure in reverse osmosis, and by using a “draw” solution, the brine and fresh water are separated.

One problem commonly faced by desalination processes is the brine waste that is generated in very large quantities during the process. Additionally, high salt concentrations, solvent chemical residues, and metal corrosion have the capacity to destabilize the local ecosystem. Moreover, desalination is unlikely to penetrate the market without any significant cost advantages. Depending on the source of brine, the cost could vary significantly. The estimated desalination costs are also currently higher than agricultural or municipal water costs, which thus, makes CO₂ based-desalination technology less attractive to address the water market.

CO₂ as feedstock for production of fuels and chemicals

Fuels production

CO₂ conversion into fuels is considered the best route in CO₂ utilization. Methane, methanol, *syngas*, and alkanes are some of the compounds that can be produced by utilizing capture CO₂ as a feedstock. The fuel produced can be used in various sectors, including fuel cells, power plants, and transportation.

Given that CO₂ is a thermodynamically stable molecule, its utilization requires the application of a large amount of heat, and a catalyst inventory to obtain high fuel yields. In the context of fuels production from captured CO₂, hydrogenation and the dry reforming of methane (DRM) are the two most-important pathways.

CO₂ hydrogenation is a very promising route for CO₂ utilization, mainly because it offers the possibility of recycling CO₂, storing H₂, producing fuel, and solving the issue of electric energy storage (Figure 11a). In the hydrogenation of CO₂ into methane, methanol, carbon monoxide, and formic acid, the source of hydrogen from fossil fuel appears to be problematic, as this can itself lead to an increase in CO₂ emissions to the atmosphere. However, renewable energy (e.g., solar, wind, biomass) can be alternatives to fossil sources to mitigate additional CO₂ emissions during hydrogenation (Figure 11b). [64–66]

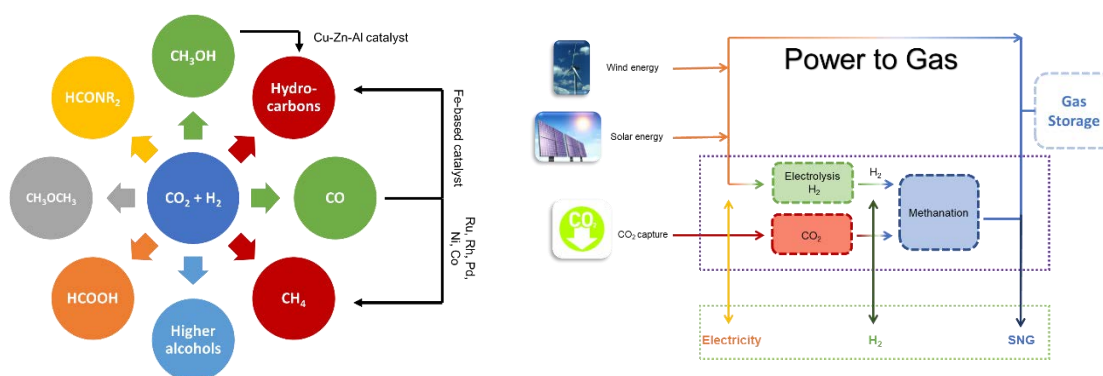


Figure 11. (a) CO₂ hydrogenation products **(b)** Renewable energy sources for CO₂ hydrogenation (methanation).

The catalytic process of dry reforming of methane, DRM, is also considered one of the most-important pathways for production of methanol and a variety of other liquid fuels by the Fischer–Tropsch synthesis (FTS) process. [67]



Furthermore, DRM has recently attracted significant research interest in terms of using CO₂ for *syngas* production, because the H₂/CO₂ molar ratio of the generated *syngas* is less than 1, due to the accompanying reverse water-gas shift reaction. Different metal-based catalysts, such as Ni, Ni–Co, Ru, Ir, and Rh supported on silica, alumina, and lanthanum oxide have been extensively evaluated in the DRM reaction.

Despite significant advances in the development of catalysts with high activity and optimum stability for DRM, finding a suitable catalyst for this reaction still remain a big hurdle, especially at high operation temperatures, as deactivation by coke formation is inevitable at high temperatures (>700 °C).

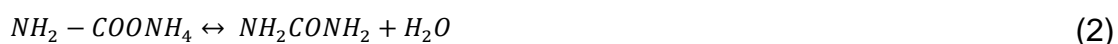
It is apparent from the above discussion that the main hurdle in utilizing captured CO₂ as a feedstock for the production of synthetic fuels lies in the design and development of novel catalysts that not only exhibit high catalytic activity under different reaction conditions, but that are also resistant to coke formation and show long-term chemical and structural stability.

Chemicals production

In addition to synthetic fuels, CO₂ can be used as a feedstock to produce a large array of fine chemicals. The most important applications are urea, inorganic

carbonates, polyurethane, acrylic acid and acrylates, polycarbonates and alkylene carbonates. [68,69]

Urea, as a major fertilizer, has the largest market for CO₂ utilization. It is formed based on the two-steps reaction, where ammonium carbamate is produced from the heterogeneous reaction of ammonia and carbon dioxide (reaction (1)), and after the formation of this intermediate in the liquid state, urea is formed by dehydration of ammonium carbamate by reaction (2):



Urea is non-toxic and has the lowest transportation cost per unit of the nitrogen nutrition. Furthermore, urea is a raw material for the production of many important chemical compounds such as polymer synthesis, pharmaceuticals, fine chemicals, and inorganic chemicals, like melamine and urea resins. [70]

On the other hand, organic carbonates such as acyclic (linear) carbonates [e.g., dimethyl carbonate (DMC)], [71], cyclic carbonates [e.g., propylene carbonate (PC)] and polycarbonates [e.g., poly(propylene carbonate)], [72] ethylene glycol, carbamates [73] and ibuprofen [74,75] that have many applications in pharmaceuticals, agrochemicals, polymers, lubricants, coating, and catalytic reactions are another class of chemicals that can be produced from captured CO₂.

The challenges of this process arise from operating at high temperatures and pressures, and the need for high catalyst inventory. Moreover, the separation of the catalyst from the products is also another challenge. For instance, in the production of polycarbonates from the reaction of CO₂ with epoxides, commercially available Al-based catalysts are widely used, but they are not environmentally friendly. [76] In this regard, the oxidative carboxylation route is an alternative with great potential for the synthesis of high added products (such as urea and urethanes) from CO₂. [77] Polyurethane is another chemical produced by the reaction of CO₂ with cyclic amines, such as aziridines and azetidines, or the N-analogues of epoxides. [78]

CO₂ chemical valorization new approaches

New approaches that transform CO₂ into fine chemicals or value-added products are also being investigated in detail. The remunerability of the product is much higher and can economically support the development of the technologies involved. However, the volume of the potential market of these fine chemicals can hardly match the volume of CO₂ emissions, needing the development of a network of parallel CCU technologies.

In this sense, biological methods, have been developed either for directly producing reduced products (i.e., carbonic anhydrase, hydrogenation of CO₂ to formate, reduction of CO₂ to methane, CO₂ conversion into methanol by enzyme cascade), or to store CO₂ in biomass (e.g., algae). [56,79–81] The advantages offered by this approach include higher growth rate, shorter growth cycle, no competition on land with other plants, and the production of different valuable by-products. However, captured CO₂ should be purified prior to feeding into a photo-bioreactor to remove pollutants such as SO_x, NO_x, and heavy metals that are toxic to the growth of microalgae.

Following this path, photocatalytic reduction approaches also allow the synthesis of a wide spectrum of CO₂ reduction products, such as HCOOH, HCHO, CH₃OH, or CH₄, and can be effectively used by using visible responsive materials. [82–86] Adsorption, CO₂ activation, and further reduction to produce value-added products are crucial steps for photocatalytic processes. For instance, Sharma et al. reported a combined theoretical and experimental study describing the selective reduction of CO₂ into methane through a robust visible light photocatalyst based on single-phase ternary sulfide (CTS). [87] Furthermore, Zhou et al. proposed the use of aqueous suspensions of cubic ZnS nanocrystals for the photocatalytic reduction of CO₂ into formate. [88]

On the other hand, direct carboxylation of carbon nucleophile using CO₂ as an electrophile is a straightforward route to prepare carboxylic acids. The main drawback associated with this process is related to the use of toxic reagents and the production of a large amount of waste. For instance, the conventional route for synthesizing 6-aminonicotinic acid from the corresponding nitriles involves low yields, hazardous chemicals (such as cyanide and ammonia gas), and high

temperatures. ^[89] Nevertheless, Gennaro et al. reported an improvement in this synthesis with the introduction of an electrochemical approach. ^[90]

It is worth highlighting that in the last few years, it has been also reported that the development of electrochemical technologies to capture and transform CO₂ into high-added value products is a suitable and green way for activating CO₂ compared to other Carbon Capture, Utilization and Storage (CCUS) strategies.

1.3. Electrochemical valorization of CO₂

1.3.1. Electrochemical reduction of CO₂

Electrochemical reduction or activation of CO₂ is a well-known technique, which has a number of valuable products, such as oxalic acid, CO, formic acid, methane, methanol, ethane, ethylene, ethanol, as well as other hydrocarbons and oxygenates that can be produced by this technique.

The electroreduction of CO₂ was first studied in twentieth century. Some examples includes the electrochemical reduction of carbon dioxide in aqueous media on platinum, ^[91] with mercury electrodes. ^[92] Moreover, Hori et al. studied the electrochemical reduction of CO₂ with copper crystals, and were the first who shows the formation of carbon dioxide bonds in its reduction. ^[93] On the other hand, in aprotic media, Haynes and Sawyer studied the electrochemical reduction of CO₂ in dimethyl sulfoxide with gold and mercury electrodes. ^[94] The technological challenges of this process have prevented until now, but in the last decades, very significant breakthroughs have been made, and the technology is approaching demonstration phase.

The electrochemical reduction of CO₂ usually requires high overpotential ($\eta > 1$), due to the high potential required to carry out the single electron reduction of CO₂ into CO₂^{•-} anion radical, which depend on electrolytic media and electrode. With gold electrodes, the value of electrochemical carbon dioxide reduction occurs at -1.9 V (vs standard hydrogen electrode, SHE), determined in 0% of water content electrolyte media. ^[94] Thus, highly active and selective electrocatalysts are necessary to reduce the activation energy of the reaction and to enable an energetically efficient process.

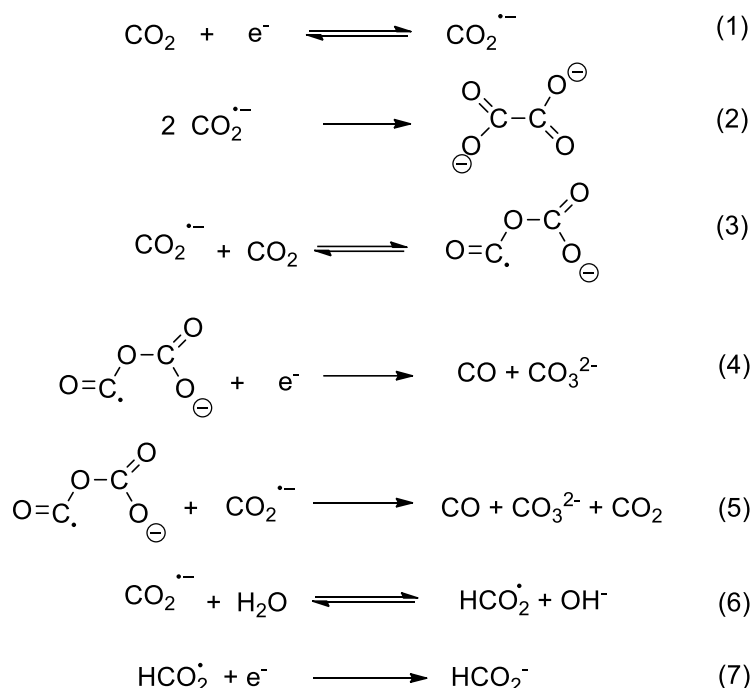
In this sense, a wide variety of new materials have been prepared and tested as heterogeneous catalysts for the reduction of CO₂ dissolved in a liquid electrolyte: metal-based electrodes, nanomaterials, bimetallic catalysts, and metal oxides. On the other hand, homogenous catalysts have been widely studied in order to catalyze the electrochemical reduction of CO₂.^[95–97] Representative examples could be ruthenium complexes like [Ru(bpy)₂(CO)₂]²⁺ or [Ru^{II}(tpy)(phenCO₂)](PF₆).^[98,99]

The other drawback in the progress of carbon dioxide electroreduction is the low solubility of carbon dioxide in aqueous electrolytes, where it has a solubility of c.a. 33 mM at normal room temperature and pressure.^[100] To overcome this low solubility in aqueous electrolytes, two types of strategies have been developed; (i) the utilization of gas diffusion electrodes (GDEs), as already used in fuel-cell technology, and (ii) the use of non-aqueous electrolytes.

GDEs are porous electrodes with a catalyst layer in contact with the electrolyte. Due to high CO₂ mass transport and reduced diffusion lengths within the catalyst layer, GDEs can achieve current densities higher than those traditional electrodes.^[101] Recent developments in GDE technology increased carbon dioxide reduction efficiencies. Ma et al. incorporated multi-walled carbon nanotubes (MWCNT) in the Ag catalyst layer of gas diffusion electrodes and reported a current density up to 350 mA·cm⁻², with 95% faradaic efficiencies towards the formation of CO.^[102]

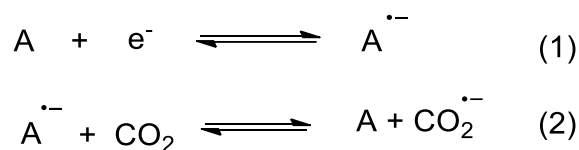
The second above mentioned strategy would be the use of non-aqueous solvents as electrolytes. Organic solvents usually dissolve gases, such as CO₂, much better than water. In this sense, Savéant's group described that direct electrochemical reduction depend on both the chemical nature of the electrode and the reaction medium. In low acidity solvents, such as DMF with supporting electrolyte, and mercury as cathode, the reduction takes place at potentials around the standard potential of CO₂/CO₂^{•-} couple, indicating that the interactions between the electrode and the reactant, intermediates and products are weak. At such, with inert (or outer sphere) electrodes the reduction products are oxalate and CO when the solvent is dry, but the presence of water promotes the obtaining of formate.^[103] Thus, the product distribution depends considerably upon the nature of the electrode material and the reaction media, as well as the

chemisorption of intermediates and/or products. Furthermore, they showed that, in DMF at inert electrodes, the mechanism suggested is depicted in Scheme 2.



Scheme 2. Electroreduction of CO₂.

The same researchers described the possibility of electro-reducing carbon dioxide, but with a homogeneous catalyst based on organic molecules (A), removing metal complexes. They studied the electrochemically generated anion radicals of aromatic nitriles and esters, which have the remarkable property of reducing CO₂ to its anion radical specie, CO₂^{•−}, which lead to oxalate, with negligible formation of carboxylated products in aprotic media (Scheme 3).^[96]



Scheme 3. Electroreduction of CO₂ by organic molecule as homogeneous catalyst.

Also, they show that it is possible to use the catalytic enhancement of the cyclic voltammetry peaks of these catalysts to determine the rate constant of the electron transfer from these aromatic anion radicals to CO₂ as a function of the catalyst standard potential (Figure 12). In this sense, Cyrille and Savéant were able to determine other catalytic parameters through cyclic voltammetry to design of improved catalysts.^[104,105]

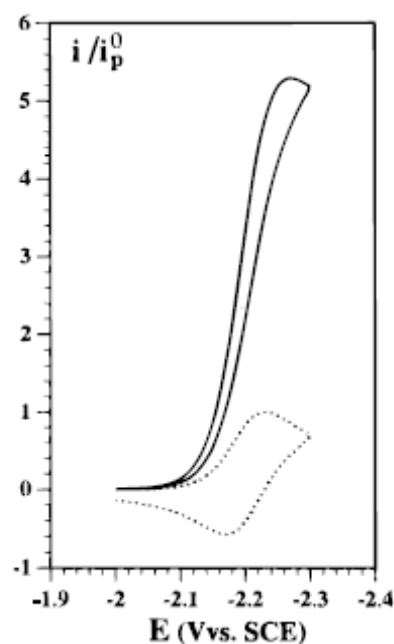


Figure 12. Cyclic voltammetry of an example of methylbenzoate in presence (solid line) and absence (dotted line) of CO_2 in aprotic electrolytic media. Reprinted (adapted) with permission from [96] and the author. Copyright (1996) American Chemical Society.

On the other hand, other approaches related to the obtaining high value-added molecules using CO_2 as C1 skeleton using electrochemistry are available.

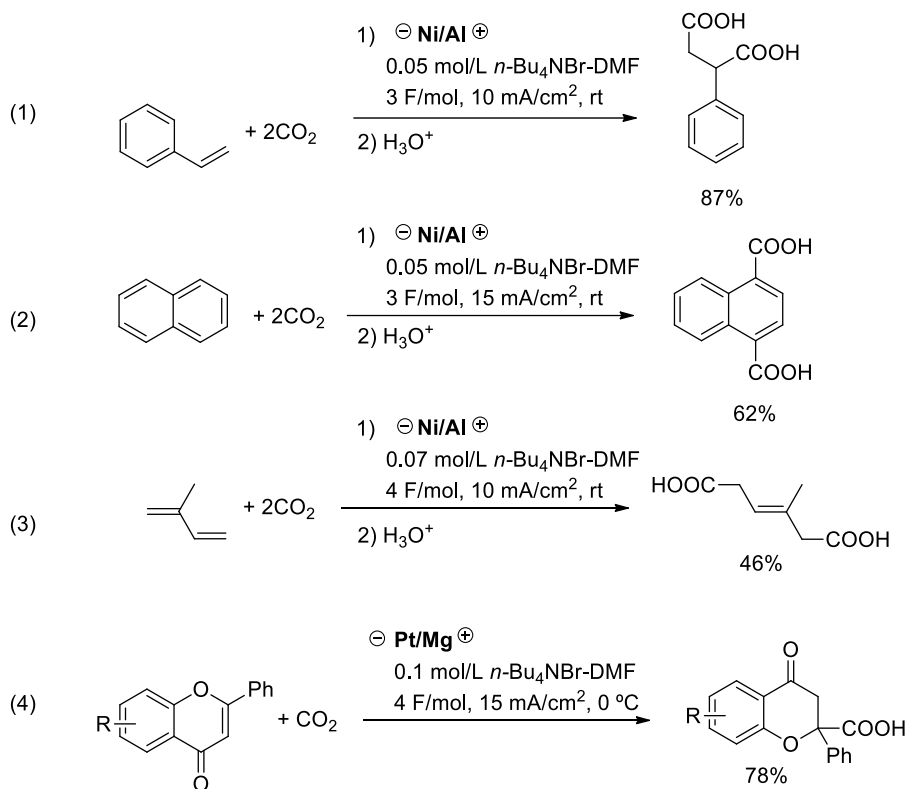
Electrochemical carboxylation is one of the most useful methods for CO_2 fixation to organic molecules, because it is a mild and easy-to-handle process. Carbanions can easily be generated by electrochemical reduction in aprotic media of organic halides, aromatic ketones, and activated olefins, and then carbon dioxide can work as an electrophile in the reaction of anion species to give carboxylic acids with one carbon elongation. [106]

1.3.2. Electrochemical carboxylation of CO_2

The general mechanism of electrochemical carboxylation involves the reduction of substrates, and/or CO_2 , leading to the formation of the corresponding radical anion, and the reaction between radical anion and the other substrates offers the carboxylate anions.

1.3.2.1. Electrocarboxylation of alkenes

There are different kinds of substrates that feature carbon-carbon double bonds, for employing in the synthesis of the corresponding carboxylic acid through an electrocarboxylation process (Scheme 4).



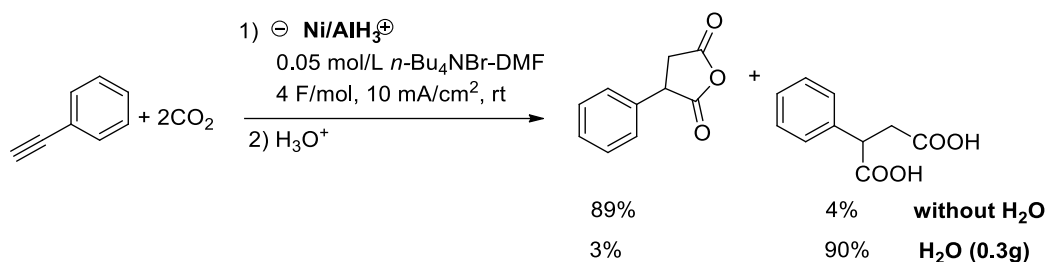
Scheme 4. Various examples of olefins for the electrocarboxylation process.

One example was performed by the Senboku group, which has successfully implemented the electrochemical carboxylation of several flavones at the C2-position of flavones to offer flavanone-2-carboxylic acids with moderate to good yields. ^[107] The set-up consisted of one-compartment cell equipped with Pt cathode and Mg anode in DMF (Scheme 4, Eq. 4).

1.3.2.2. Electrocarboxylation of alkynes

Following the achievements obtained in the electrocarboxylation of styrene derivatives, ^[108] the Jiang group performed a study on the electrochemical decarboxylation of phenylacetylene with CO₂ (Scheme 5). ^[109] An unsaturated aryl-maleic anhydride is produced as the main product under anhydrous

conditions, while the saturated 2-arylsuccinid acid could be obtained as a major product in the presence of H₂O.



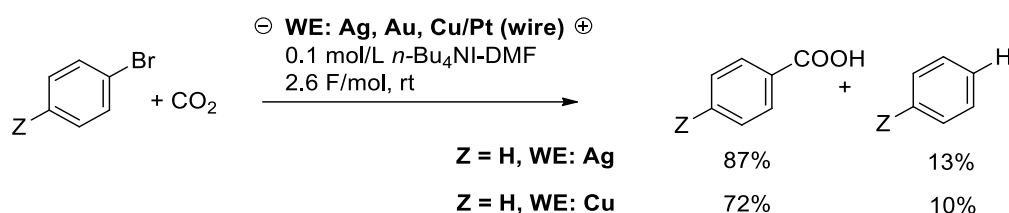
Scheme 5. Electrocarboxylation of phenylacetylene with CO₂.

1.3.2.3. Electrocarboxylation of halides

Electrocarboxylation of organic halides is one of the most studied and mature strategy to synthesize carboxylated products.

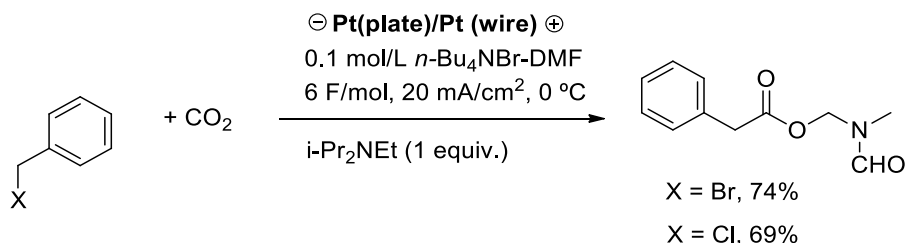
Gennaro et al. showed that the use of silver in the electrochemical reduction of some halides (such as arylethyl chlorides), ^[110] improved the process because of the electrocatalytic properties of silver. ^[111,112] And it is very useful in the electrocarboxylation of the substrates.

Moreover, they reported that the direct CO₂ reduction at Ag and Cu working electrodes occurs at more negative potentials than the reduction potentials of a series of bromobenzenes (ArBr), allowing the selective reduction of ArBr in CO₂-saturated DMF. They also showed that Ag has a better electrocatalytic behavior for the cleavage of C-Br bond. ^[113,114] On the other hand, Au cathodes showed good catalytic properties for the reduction of CO₂, undermining the possibility of exploiting its electrocatalytic properties for the activation of ArBr by carboxylation. It was also shown that hydrodebromination yielding ArH is always in competition with the desirable carboxylation reaction (Scheme 6). The selectivity of the process depends on both the electrode material and molecular structure of the substrate.



Scheme 6. N-methyl-N(phenylacetoxy)methylformamide synthesis through electrocarboxylation in DMF.

On the other hand, the use of a sacrificial anode is important for the efficient electrochemical carboxylation of benzyl halides when the electrolysis is carried out in a one-compartment cell. However, the use of this kind of anode sometimes leads to problems, such as passivation of the cathode. For this reason, Senboku et al. reported an efficient electrochemical three-component coupling reaction of benzyl halides, CO₂, and DMF to produce N-methyl-N(phenylacetoxy)methylformamides in good yields in a one compartment cell equipped with a Pt plate cathode and a Pt wire anode without any sacrificial anode (Scheme 7).^[115]



Scheme 7. N-methyl-N(phenylacetoxy)methylformamide synthesis through electrocarboxylation in DMF.

Overall, there are a lot of examples of electrochemical carboxylation of substrates to obtain carboxylated species, valorizing CO₂ at the same time, in aprotic electrolytic media. However, its high volatility and toxicity^[116] and the low electric conduction of aprotic solvents represents an obstacle for their use as a solvent in many electrochemical reactions.

1.3.3. CO₂ and Ionic liquids

In order to avoid the use of volatile and toxic solvents, and simplify separation, electrocarboxylation in CO₂-saturated room-temperature ionic liquids have been developed. Ionic liquids (ILs), such as electrically conducting “organic” solvents,

which have moderate conductivities and high CO₂ absorption capacity, represent a good compromise for this kind of processes.

1.3.3.1. Ionic Liquids

The ionic liquids (ILs) are generally defined as liquid electrolytes that are composed entirely of ions. A melting point criterion has occasionally been proposed to distinguish between molten salts and ILs (m.p.<100 °C). However, both molten salts and ILs are better described as liquid compounds that display ion-covalent crystalline structures. They represent a class of liquid materials with unique properties originating from the complex interplay of coulombic, hydrogen bonding, and van-der-Waals interactions of their ions.

The first ionic liquid was manufactured in first half of 20th century (in 1948) at Rice university, Houston in Texas, and contained the AlCl₄⁻ species. But, greater interest for ionic liquids came at the end of the 1970's due to the use of not pyrophoric alkylpyridinium and dialkylimidazolium salts, which remain today, with some of them as room temperature ionic liquids (RTILs). [117]

There are three generations of ionic liquids, of which tetrachloroaluminate ionic liquids were first generation. Replacement of this moisture-sensitive anion by tetrafluoroborate ion and other anions in 1992, led to air- and water- stable ILs, which represent the second generation and have since found increasing applications as reaction media for various kinds of organic reactions. Davis et al. introduced the concept of task-specific ionic liquids, TSILs (third generation), which are defined as an IL in which the anion, cation, or both, covalently incorporate a functional group (designed to endow them with particular properties, either chemical or physical, or in reactivity) as a part of the ion structure (Figure 13). [118,119]

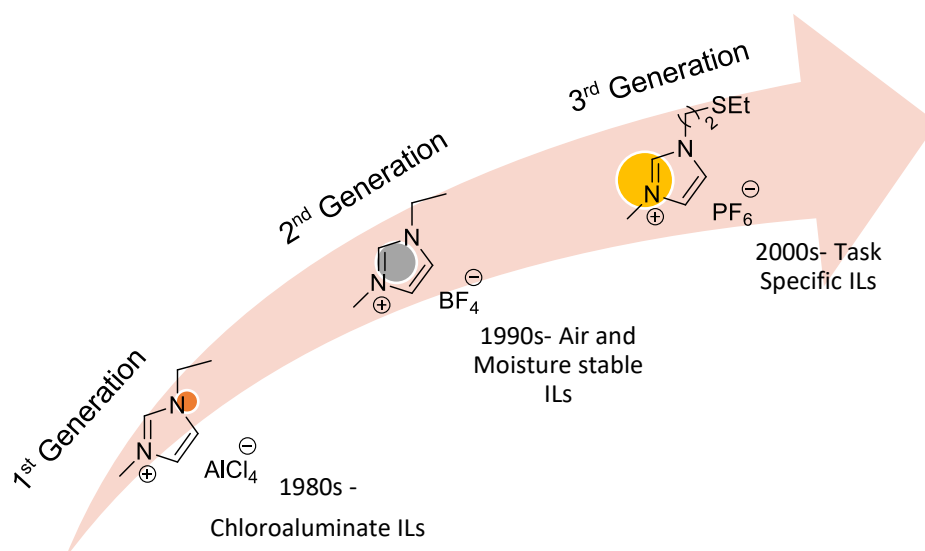


Figure 13. ILs generations.

The modular nature of ILs means that structural modifications can either be made to the anion, the cationic core, or substituents on the anion or cation. Hence, a wide diversity in IL structure is possible, and by altering either the cationic or anionic component of an IL, the physical properties of the IL can readily be fine-tuned (Figure 14). This can be adapted to the requirements of a process, including the melting point, viscosity, density, solubility, and hydrophobicity of the IL. Moreover, reaction products may be separated more easily from an IL than from conventional solvents. These benefits make ILs an attractive choice of solvent in many important chemical processes, ^[31,120] with examples reported in the areas of catalysis, ^[121] biocatalysis, synthetic chemistry, ^[122] and electrochemistry. ^[123]

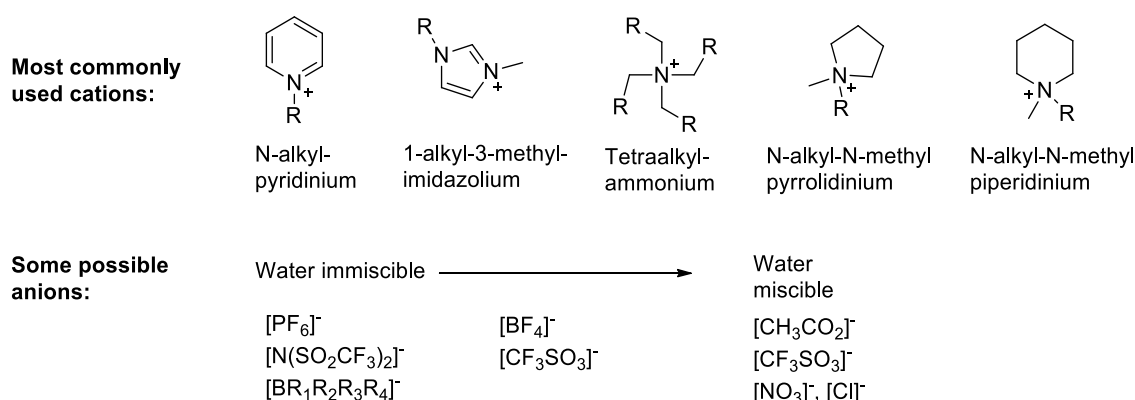


Figure 14. Most common cation and ions in ILs.

Room-temperature ionic liquids (RTILs) have received a lot of attention as potential “green” and “designable” solvents. The liquid state of these substances is created by their structure; RTILs need to have a big non-symmetrical cation and an anion which has a delocalized charge. In addition, almost all reactions can occur in ionic liquids the same way as in common solvents, but chemical interactions occur slightly different in ionic liquids than in molecular solvents. Therefore, thanks to this difference, ionic liquids have better properties than aprotic solvents:

1. They have a very large liquid range (e.g. BMIM TFSI: -89 to 450 °C as compared to EtOH: -114 to 78 °C).
2. They are good solvents for a wide range of inorganic, organic and polymeric materials.
3. They exhibit Brønsted, Lewis and Franklin acidity.
4. They do not have effective vapor pressure.
5. Their water sensitivity does not restrict their industrial applications.
6. They are thermally stable up to 200 °C.
7. They are relatively cheap and easy to prepare.

Besides, RTILs have intrinsic ionic conductivity at room temperature and a wide electrochemical window, exhibiting good electrochemical stability in the range of $4.0 - 5.7$ V. ^[118]

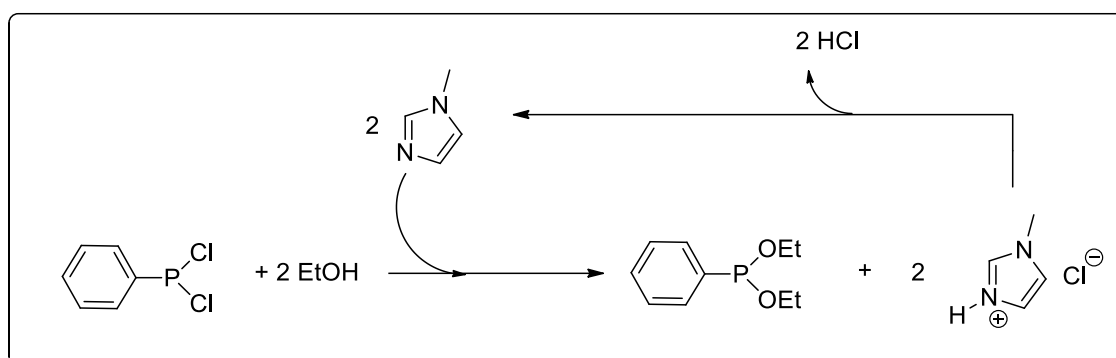
1.3.3.2. Industrial applications of Ionic Liquids

Many industrial processes can be improved with the use of ionic liquids. There are examples of this ranging from chemical processing to consumer-packaged goods. ^[124]

Chemical processing: acid scavenging

BASIL process is probably the most widely known example of industrial implementations of ionic liquids-based processes. It was patented by BASF industry and is based on biphasic acid-scavenging using ionic liquids in the production of alkylphenylphosphines, which are precursors in the production of photo-initiators for UV curing of double bond resins, like used in coatings and printing inks. ^[125]

The BASIL process is commercially important because it improves the aforementioned processes. In the latter one, acid scavenging was achieved using alkylamines, such as triethylamine, obtaining, as byproduct, a thick, dense, insoluble trialkylammonium halide salt, which is difficult to remove. By using 1-methylimidazole ionic liquid precursor, instead of triethylamine, the acid reaction produces, as by-product, 1-methylimidazolium chloride, a protic ionic liquid that is easy to isolate, and could be recycled by deprotonation, regenerating the 1-methylimidazole reactant (Scheme 8).



Scheme 8. BASIL-BASF process.

Polymer processing: cellulose and biomass

Cellulose is an abundant bio-renewable resource. For this reason, people have developed methods for separating it from biomasses and using it for a lot of purposes. Because of cellulose has negligible solubility in water, several solvents systems have been developed for processing cellulose.

Highlighting the use of ionic liquids in cellulose processing, in 1934, Graenacher claimed in a patent that, with the use of molten quaternary ammonium salts, it is possible to prepare cellulose solutions. Fast forward to 2002 when Swarloski et al. found that ionic liquids based on combinations of imidazolium cations and halide anions could directly dissolve cellulose with only mild heating or microwaving. ^[126] Since then, many researchers have found a multitude of ionic liquids combinations and conditions that can dissolve cellulose. ^[127]

Metal processing: electroplating of aluminum

Ionic liquids are attractive for this purpose because the aqueous electrolyte solutions that are typically used in metal plating cannot be used for aluminum,

due to the electrochemical window of the solutions being too narrow. Despite the fact that water is adequate for metals like copper, silver, gold, chromium, and nickel, other metals like aluminum and titanium require something with a broader range.

Functional fluids: gas capture and storage

Even though several gases including hydrogen have very low solubility in ionic liquids compared to molecular solvents, other gases like carbon dioxide exhibit greater solubility in ionic liquids. Blanchard et al. were the first to show that imidazolium-based ionic liquids exhibited high solubilization capacity for carbon dioxide; ^[128] furthermore, carbon dioxide product could be recovered with no contamination of the insoluble ionic liquid.

Ionic liquids are appealing solvents (compared to alkanolamines) for carbon dioxide capture in flue-gas from coal fired power plants because of their environmentally friendly profiles, particularly low volatility, and potential to be recycled/recovered, as was explained in previous sections. However, even though solubility of CO₂ in ionic liquids is relatively high, absorption capacity at low post-combustion partial pressures is lower than 5 mol%, even with the most ideal ionic liquid. Therefore, researchers have modified ionic liquids to be reactive with respect to carbon dioxide and increase the molar absorption capacity of these materials.

Ionic liquids also offer opportunities for safe storage of other hazardous and reactive gases, including boron (III) fluoride, phosphine, and arsine.

Potential applications: Batteries

Ionic liquids also offer promise as electrolytes in other electrochemical devices, like next generation lithium ion batteries. Lithium ion batteries are ubiquitous, and power all our mobile devices from laptops to cell phones to electric cars. However, it is generally agreed that improvements are continually needed to meet the ever-growing demand of increased cycling rate and battery lifetime. Ionic liquids are attractive primarily because of their large electrochemical windows, thus being suitable for energy dense materials and expansion beyond just lithium ion batteries to include metal-air batteries. Furthermore, their low vapor pressures

and non-flammable nature makes them inherently safer and stable materials for this application. Despite the promise, commercial implantation of ionic liquids in modern battery technology has yet to be realized. ^[129]

1.3.3.3. Electrochemistry in Ionic Liquids

Historically, electrochemists have focused mainly on studying the electrochemical properties of conductive solid materials (for instance, battery electrodes, metallic deposition and dissolution), and compounds dissolved in molecular solvents such as acetonitrile (ACN), *N,N'*-dimethylformamide (DMF) and water.

In recent years, ionic liquids have received substantial attention in sustainable chemistry applications because they possess desirable properties. For electrochemical applications, ionic liquids have the additional advantages of intrinsically high conductivity and electrochemical stability, which refers to the voltage range that can be applied across a material before the substance undergoes oxidation or reduction (wide electrochemical window). Furthermore, the electrochemical kinetics, and mass transfer mechanisms associated with charged species, are often unique in ionic liquids, in part due to the high ionic strength of this kind of medium, compared to conventional molecular solvent (electrolyte) media. Nevertheless, despite having a range of attractive properties, ionic liquids also have some significant drawbacks when compared to conventional molecular solvents, such as high viscosity, high production costs, and difficulties in purification. ^[130]

Electrochemical measurements in ILs

Since ILs are defined as liquids solely composed of ions without any solvent, contamination of water and other neutral molecules must be avoided in order to study the phenomenal characteristics of ILs. One of the major impurities is water, which easily absorbs into ILs from the atmosphere. In the case of the amide-type ILs, it is possible to eliminate water from them by heating under vacuum. The dried ILs should be handled under dry atmosphere in a glovebox, for example. The reagents to be added to ILs should be also dried before use, unless they are

shipped under inert and dry atmosphere. Electrochemical measurements should also be conducted in a dry atmosphere.

Common electrochemical techniques can also be used in ILs. Cyclic voltammetry is one of the most popular methods, which will give much useful information on electrode reactions with simple operation. ^[131,132] It is possible to estimate such electrochemical parameters as half-wave potential, diffusion coefficient, and rate constant, with the equations found in textbooks. However, the ohmic drop due to low conductivity of ILs often affects peak potentials and linearity of potential sweep rates. Thus, cyclic voltammetry is not recommended to estimate these electrochemical parameters, unless the effects of the ohmic drop are eliminated properly by such techniques as ultra-microelectrode and IR compensators. Chronopotentiometry is also influenced by the ohmic drop. In contrast, the effects of the ohmic drop are expected to be insignificant in chronoamperometry when enough potential changes are applied.

1.3.3.4. Organic Electrochemistry in Ionic Liquids

ILs are used principally as “inert” reaction media for classical organic chemical reactions. ^[133] However, it is becoming apparent that their rich physico-chemical properties (e.g., Lewis and/or Brønsted acidity/basicity, hydrogen-bonding ability, π - π interactions, etc.) influence chemical reactivity. Considering that organic electrochemical reactions can be complex, and are frequently dependent on experimental conditions (electrode material, solvent, electrolyte, etc.), understanding how many known and electrochemical reactions in molecular solvent systems work, and how they work (is it the same behavior or not) in an IL environment may not be straightforward. For example, although follow-up chemistry may, or may not, be the same in ILs, relative to traditional solvents, there are two common effects of ILs (a) mass transport rates (reported as diffusion coefficients) are smaller by a factor of between 10 and 100 in all IL media, due to the viscous nature of the media; and (b) the heterogeneous electron-transfer rate constants can be smaller by as much as two orders of magnitude for processes controlled by outer-sphere dynamics. ^[134] Ionic liquids offer great potential in this respect by providing a highly stable electrolyte medium of adjustable solvency properties over a wide range, and from which volatile

products can be readily removed by distillation. One of the particularly attractive features of electrosynthetic processes is that they are highly compatible with flow chemistry approaches to large-scale synthesis.

1.3.3.5. Ionic Liquids in the electrochemical valorization of CO₂

Zhao et al. was the first research to use an ionic liquid as electrolyte for the electrochemical reduction of high-pressure CO₂, obtaining *syngas* as the resultant electrolysis product. ^[135]

There are different reviews of electrochemical transformation of carbon dioxide in ionic liquids within the framework of capture and sequestration. ^[31,136] Progress has been achieved through the choice of different electrocatalysts, where the trend has been to move from less abundant substances, such as noble metals, to more commonly available metals and materials. One very important advance was the discovery by Rosen et al. ^[137], who described that some ionic liquids can significantly lower the overpotential of CO₂ reduction. They hypothesized that one of the ionic liquid ions may stabilize the CO₂ anion that is formed in the first step of the electrochemical reaction, through formation of a complex, thus decreasing the activation barrier and the overpotential. Following this path, the Compton group discovered that the ionic liquid 1-butyl-3-ethylimidazolium acetate, showed an abnormally high solubility of carbon dioxide due to the formation of molecular complexes. ^[138] They observed that CO₂ electrochemical reduction was not sustainable, because CO₂ is almost irreversibly absorbed. These results show that, in order to facilitate the electrochemical reduction process, carbon dioxide capture should be a physical absorption (as seen for CO₂ mixing in most ionic liquids), rather than chemical absorption, which optimizes the extent of capture at the expense of down-stream transformation and separation.

Similarly, ionic liquids have been used as electrolytic media for electrochemical reactions because they can act as a solvent as well as supporting electrolyte. For example, Isse et al. showed that benzyl chloride could be carboxylated with an electrochemical reduction in CO₂-saturated acetonitrile. Improving this electrocarboxylation, Lu et al. showed that it was possible to achieve the electrocarboxylation of benzyl chloride by using RTIL, BMIM BF₄, as solvent-

electrolyte media, ^[139] which could be recycled and reused four times. In addition, Senboku et al. demonstrated that electrochemical carboxylation of organohalides was successfully achieved with reasonable yields in ionic liquids. ^[140]

It is important to highlight that the high cost of ionic liquids has been considered a disadvantage for this type of application. However, the enormous potential for structural customization due to the huge number of possible combinations between different cations and anions, together with a wide liquid range, high thermal stability, extremely low volatility, may allow the design of green, low cost, low viscosity solvents with high CO₂ absorption capacity that could pave the way for an effective integration of CO₂ capture with CO₂ conversion.

Therefore, the present methodology could be applied to the synthesis of various carboxylic acids and their derivatives, which are useful chemicals in medical and agrochemical sciences, and thus, could also contribute to a reduction of CO₂ as a greenhouse gas.

1.4. Bibliography

- (1) Nejat, P.; Jomehzadeh, F.; Taheri, M. M.; Gohari, M.; Mueh, M. Z. A Global Review of Energy Consumption, CO₂ emissions and Policy in the Residential Sector (with an Overview of the Top Ten CO₂ Emitting Countries). *Renew. Sustain. Energy Rev.* **2015**, *43*, 843–862.
- (2) Anderson, T. R.; Hawkins, E.; Jones, P. D. CO₂, the Greenhouse Effect and Global Warming: From the Pioneering Work of Arrhenius and Callendar to Today's Earth System Models. *Endeavour* **2016**, *40* (3), 178–187.
- (3) Taylor, F. W. The Greenhouse Effect and Climate Change Revisited. *Reports Prog. Phys.* **2002**, *65* (1), 1–25.
- (4) Holtsmark, B. Quantifying the Global Warming Potential of CO₂ Emissions from Wood Fuels. *GCB Bioenergy* **2015**, *7* (2), 195–206.
- (5) Harris, D. C. Charles David Keeling and the Story of Atmospheric CO₂ Measurements. *Anal. Chem.* **2010**, *82* (19), 7865–7870.
- (6) Sims, R. E. H. Renewable Energy: A Response to Climate Change. *Sol. Energy* **2004**, *76* (1–3), 9–17.
- (7) Szulejko, J. E.; Kumar, P.; Deep, A.; Kim, K. H. Global Warming Projections to 2100 Using Simple CO₂ greenhouse Gas Modeling and Comments on CO₂ climate Sensitivity Factor. *Atmos. Pollut. Res.* **2017**, *8* (1), 136–140.
- (8) López, J. C.; Quijano, G.; Souza, T. S. O.; Estrada, J. M.; Lebrero, R.; Muñoz, R. Biotechnologies for Greenhouse Gases (CH₄, N₂O, and CO₂) Abatement: State of the Art and Challenges. *Appl. Microbiol. Biotechnol.* **2013**, *97* (6), 2277–2303.
- (9) Bekhet, H. A.; Matar, A.; Yasmin, T. CO₂ Emissions, Energy Consumption, Economic Growth, and Financial Development in GCC Countries: Dynamic Simultaneous Equation Models. *Renew. Sustain. Energy Rev.* **2017**, *70* (November 2016), 117–132.
- (10) Veríssimo, D.; Macmillan, D. C.; Smith, R. J.; Crees, J.; Davies, Z. G. Has Climate Change Taken Prominence over Biodiversity Conservation? *Bioscience* **2014**, *64* (7), 625–629.
- (11) Karmalkar, A. V.; Bradley, R. S. Consequences of Global Warming of 1.5 °C and 2 °C for Regional Temperature and Precipitation Changes in the Contiguous United States. *PLoS One* **2017**, *12* (1), 1–17.
- (12) Matthews, T. K. R.; Wilby, R. L.; Murphy, C. Communicating the Deadly Consequences of Global Warming for Human Heat Stress. *Proc. Natl. Acad. Sci. U. S. A.* **2017**, *114* (15), 3861–3866.
- (13) Schleussner, C. F.; Lissner, T. K.; Fischer, E. M.; Wohland, J.; Perrette, M.; Golly, A.; Rogelj, J.; Childers, K.; Schewe, J.; Frieler, K.; et al. Differential Climate Impacts for Policy-Relevant Limits to Global Warming: The Case of 1.5 °C and 2 °C. *Earth Syst. Dyn.* **2016**, *7* (2), 327–351.
- (14) Song, C. Global Challenges and Strategies for Control, Conversion and Utilization of CO₂ for Sustainable Development Involving Energy, Catalysis, Adsorption and Chemical Processing. *Catal. Today* **2006**, *115* (1–4), 2–32.

-
- (15) Gielen, D.; Boshell, F.; Saygin, D.; Bazilian, M. D.; Wagner, N.; Gorini, R. The Role of Renewable Energy in the Global Energy Transformation. *Energy Strateg. Rev.* **2019**, 24 (January), 38–50.
- (16) He, Y.; Peng, S.; Liu, Y.; Li, X.; Wang, K.; Ciais, P.; Arain, M. A.; Fang, Y.; Fisher, J. B.; Goll, D.; et al. Global Vegetation Biomass Production Efficiency Constrained by Models and Observations. *Glob. Chang. Biol.* **2020**, 26 (3), 1474–1484.
- (17) Parikka, M. Global Biomass Fuel Resources. *Biomass and Bioenergy* **2004**, 27 (6), 613–620.
- (18) Bowen, F. Carbon Capture and Storage as a Corporate Technology Strategy Challenge. *Energy Policy* **2011**, 39 (5), 2256–2264.
- (19) De Guido, G.; Compagnoni, M.; Pellegrini, L. A.; Rossetti, I. Mature versus Emerging Technologies for CO₂ Capture in Power Plants: Key Open Issues in Post-Combustion Amine Scrubbing and in Chemical Looping Combustion. *Front. Chem. Sci. Eng.* **2018**, 12 (2), 315–325.
- (20) Cuéllar-Franca, R. M.; Azapagic, A. Carbon Capture, Storage and Utilisation Technologies: A Critical Analysis and Comparison of Their Life Cycle Environmental Impacts. *J. CO₂ Util.* **2015**, 9, 82–102.
- (21) Tapia, J. F. D.; Lee, J. Y.; Ooi, R. E. H.; Foo, D. C. Y.; Tan, R. R. A Review of Optimization and Decision-Making Models for the Planning of CO₂ Capture, Utilization and Storage (CCUS) Systems. *Sustain. Prod. Consum.* **2018**, 13 (September), 1–15.
- (22) Yu, C. H.; Huang, C. H.; Tan, C. S. A Review of CO₂ Capture by Absorption and Adsorption. *Aerosol Air Qual. Res.* **2012**, 12 (5), 745–769.
- (23) Creamer, A. E.; Gao, B. Carbon-Based Adsorbents for Postcombustion CO₂ Capture: A Critical Review. *Environ. Sci. Technol.* **2016**, 50 (14), 7276–7289.
- (24) Gomes, J.; Santos, S.; Bordado, J. Choosing Amine-Based Absorbents for CO₂ Capture. *Environ. Technol. (United Kingdom)* **2015**, 36 (1), 19–25.
- (25) Kothandaraman, J.; Goeppert, A.; Czaun, M.; Olah, G. A.; Surya Prakash, G. K. CO₂ Capture by Amines in Aqueous Media and Its Subsequent Conversion to Formate with Reusable Ruthenium and Iron Catalysts. *Green Chem.* **2016**, 18 (21), 5831–5838.
- (26) Environ, E.; Ferrari, M.; Gross, R.; Hallett, J. P. Carbon Capture and Storage Update. *R. Soc. Chem.* **2014**, No. 7, 130–189.
- (27) Stowe, H. M.; Hwang, G. S. Fundamental Understanding of CO₂ Capture and Regeneration in Aqueous Amines from First-Principles Studies: Recent Progress and Remaining Challenges. *Ind. Eng. Chem. Res.* **2017**, 56 (24), 6887–6899.
- (28) Jiang, B.; Kish, V.; Fauth, D. J.; Gray, M. L.; Pennline, H. W.; Li, B. Performance of Amine-Multilayered Solid Sorbents for CO₂ Removal: Effect of Fabrication Variables. *Int. J. Greenh. Gas Control* **2011**, 5 (5), 1170–1175.
- (29) Ramdin, M.; De Loos, T. W.; Vlugt, T. J. H. State-of-the-Art of CO₂ Capture with Ionic Liquids. *Ind. Eng. Chem. Res.* **2012**, 51 (24), 8149–8177.
- (30) Bates, E. D.; Mayton, R. D.; Ntai, I.; Davis, J. H. CO₂ Capture by a Task-Specific Ionic Liquid. *J. Am. Chem. Soc.* **2002**, 124 (6), 926–927.
-

- (31) Liu, R.; Zhang, P.; Zhang, S.; Yan, T.; Xin, J.; Zhang, X. Ionic Liquids and Supercritical Carbon Dioxide: Green and Alternative Reaction Media for Chemical Processes. *Rev. Chem. Eng.* **2016**, 32 (6), 587–609.
- (32) Salazar Duarte, G.; Schürer, B.; Voss, C.; Bathen, D. Adsorptive Separation of CO₂ from Flue Gas by Temperature Swing Adsorption Processes. *ChemBioEng Rev.* **2017**, 4 (5), 277–288.
- (33) Kaithwas, A.; Prasad, M.; Kulshreshtha, A.; Verma, S. Industrial Wastes Derived Solid Adsorbents for CO₂ Capture: A Mini Review. *Chem. Eng. Res. Des.* **2012**, 90 (10), 1632–1641.
- (34) Azmi, A. A.; Aziz, M. A. A. Mesoporous Adsorbent for CO₂ Capture Application under Mild Condition: A Review. *J. Environ. Chem. Eng.* **2019**, 7 (2), 103022.
- (35) Mohamedali, M.; Nath, D.; Ibrahim, H.; Henni, A. Review of Recent Developments in CO₂ Capture Using Solid Materials: Metal Organic Frameworks (MOFs). In *Greenhouse Gases*; Llamas, B., Ed.; IntechOpen, 2016; pp 115–154.
- (36) Chen, C.; Lee, Y. R.; Ahn, W. S. CO₂ Adsorption over Metal-Organic Frameworks: A Mini Review. *J. Nanosci. Nanotechnol.* **2016**, 16 (5), 4291–4301.
- (37) Trickett, C. A.; Helal, A.; Al-Maythaly, B. A.; Yamani, Z. H.; Cordova, K. E.; Yaghi, O. M. The Chemistry of Metal-Organic Frameworks for CO₂ Capture, Regeneration and Conversion. *Nat. Rev. Mater.* **2017**, 2 (8), 1–16.
- (38) Millward, A. R.; Yaghi, O. M. Metal-Organic Frameworks with Exceptionally High Capacity for Storage of Carbon Dioxide at Room Temperature. *J. Am. Chem. Soc.* **2005**, 127 (51), 17998–17999.
- (39) Britt, D.; Furukawa, H.; Wang, B.; Glover, T. G.; Yaghi, O. M. Highly Efficient Separation of Carbon Dioxide by a Metal-Organic Framework Replete with Open Metal Sites. *Proc. Natl. Acad. Sci. U. S. A.* **2009**, 106 (49), 20637–20640.
- (40) Banerjee, R.; Furukawa, H.; Britt, D.; Knobler, C.; O’Keeffe, M.; Yaghi, O. M. Control of Pore Size and Functionality in Isoreticular Zeolitic Imidazolate Frameworks and Their Carbon Dioxide Selective Capture Properties. *J. Am. Chem. Soc.* **2009**, 131 (11), 3875–3877.
- (41) Banerjee, R.; Phan, A.; Wang, B.; Knobler, C.; Furukawa, H.; O’Keeffe, M.; Yaghi, O. M. High-Throughput Synthesis of Zeolitic Imidazolate Frameworks and Application to CO₂ Capture. *ReVision* **2008**, 939 (February), 939–944.
- (42) Liu, Y.; Wang, Z. U.; Zhou, H.-C. Recent Advances in Carbon Dioxide Capture with Metal-Organic Frameworks. *Greenh. Gases Sci. Technol.* **2012**, 2, 239–259.
- (43) Herm, Z. R.; Swisher, J. A.; Smit, B.; Krishna, R.; Long, J. R. Metal-Organic Frameworks as Adsorbents for Hydrogen Purification and Precombustion Carbon Dioxide Capture. *J. Am. Chem. Soc.* **2011**, 133 (15), 5664–5667.
- (44) Sabouni, R.; Kazemian, H.; Rohani, S. Carbon Dioxide Capturing Technologies: A Review Focusing on Metal Organic Framework Materials (MOFs). *Environ. Sci. Pollut. Res.* **2014**, 21 (8), 5427–5449. <https://doi.org/10.1007/s11356-013-2406-2>.
- (45) Devic, T.; Salles, F.; Bourrelly, S.; Moulin, B.; Maurin, G.; Horcajada, P.; Serre, C.; Vimont, A.; Lavalley, J. C.; Leclerc, H.; et al. Effect of the Organic Functionalization of Flexible MOFs on the Adsorption of CO₂. *J. Mater. Chem.*

2012, 22 (20), 10266–10273.

- (46) Schneemann, A.; Bon, V.; Schwedler, I.; Senkovska, I.; Kaskel, S.; Fischer, R. A. Flexible Metal-Organic Frameworks. *Chem. Soc. Rev.* **2014**, 43 (16), 6062–6096.
- (47) Chang, Z.; Yang, D. H.; Xu, J.; Hu, T. L.; Bu, X. H. Flexible Metal-Organic Frameworks: Recent Advances and Potential Applications. *Adv. Mater.* **2015**, 27 (36), 5432–5441.
- (48) Yanai, N.; Kitayama, K.; Hijikata, Y.; Sato, H.; Matsuda, R.; Kubota, Y.; Takata, M.; Mizuno, M.; Uemura, T.; Kitagawa, S. Gas Detection by Structural Variations of Fluorescent Guest Molecules in a Flexible Porous Coordination Polymer. *Nat. Mater.* **2011**, 10 (10), 787–793.
- (49) Qiu, Y. L.; Zhong, H. X.; Zhang, T. T.; Xu, W. Bin; Su, P. P.; Li, X. F.; Zhang, H. M. Selective Electrochemical Reduction of Carbon Dioxide Using Cu Based Metal Organic Framework for CO₂ Capture. *ACS Appl. Mater. Interfaces* **2018**, 10 (3), 2480–2489.
- (50) Olajire, A. A. Synthesis Chemistry of Metal-Organic Frameworks for CO₂ Capture and Conversion for Sustainable Energy Future. *Renew. Sustain. Energy Rev.* **2018**, 92 (May), 570–607.
- (51) Masoomi, M. Y.; Stylianou, K. C.; Morsali, A.; Retailleau, P.; Maspoch, D. Selective CO₂ Capture in Metal-Organic Frameworks with Azine-Functionalized Pores Generated by Mechanochemistry. *Cryst. Growth Des.* **2014**, 14 (5), 2092–2096.
- (52) Lau, C. H.; Konstas, K.; Doherty, C. M.; Kanehashi, S.; Ozcelik, B.; Kentish, S. E.; Hill, A. J.; Hill, M. R. Tailoring Physical Aging in Super Glassy Polymers with Functionalized Porous Aromatic Frameworks for CO₂ Capture. *Chem. Mater.* **2015**, 27 (13), 4756–4762.
- (53) Haldar, R.; Reddy, S. K.; Suresh, V. M.; Mohapatra, S.; Balasubramanian, S.; Maji, T. K. Flexible and Rigid Amine-Functionalized Microporous Frameworks Based on Different Secondary Building Units: Supramolecular Isomerism, Selective CO₂ Capture, and Catalysis. *Chem. - A Eur. J.* **2014**, 20 (15), 4347–4356.
- (54) Wilson, S. M. W.; Tezel, F. H. Direct Dry Air Capture of CO₂ Using VTSA with Faujasite Zeolites. *Ind. Eng. Chem. Res.* **2020**, 59 (18), 8783–8794.
- (55) Razzak, S. A.; Ali, S. A. M.; Hossain, M. M.; deLasa, H. Biological CO₂ Fixation with Production of Microalgae in Wastewater – A Review. *Renew. Sustain. Energy Rev.* **2017**, 76 (September 2015), 379–390.
- (56) Cheah, W. Y.; Ling, T. C.; Juan, J. C.; Lee, D. J.; Chang, J. S.; Show, P. L. Biorefineries of Carbon Dioxide: From Carbon Capture and Storage (CCS) to Bioenergies Production. *Bioresour. Technol.* **2016**, 215, 346–356.
- (57) Murcia Valderrama, M. A.; van Putten, R. J.; Gruter, G. J. M. The Potential of Oxalic – and Glycolic Acid Based Polyesters (Review). Towards CO₂ as a Feedstock (Carbon Capture and Utilization – CCU). *Eur. Polym. J.* **2019**, 119 (August), 445–468.
- (58) Huang, C. H.; Tan, C. S. A Review: CO₂ Utilization. *Aerosol Air Qual. Res.* **2014**, 14 (2), 480–499.

- (59) Al-Mamoori, A.; Krishnamurthy, A.; Rownaghi, A. A.; Rezaei, F. Carbon Capture and Utilization Update. *Energy Technol.* **2017**, 5 (6), 834–849.
- (60) Hamouda, A. A.; Chughtai, S. Miscible CO₂ Flooding for EOR in the Presence of Natural Gas Components in Displacing and Displaced Fluids. *Energies* **2018**, 11 (2), 1–12.
- (61) Xie, H.; Yue, H.; Zhu, J.; Liang, B.; Li, C.; Wang, Y.; Xie, L.; Zhou, X. Scientific and Engineering Progress in CO₂ Mineralization Using Industrial Waste and Natural Minerals. *Engineering* **2015**, 1 (1), 150–157.
- (62) Chiang, P. C.; Pan, S. Y. *Carbon Dioxide Mineralization and Utilization*, 1st ed.; Springer Singapore, 2017.
- (63) Kim, I.; Nole, M.; Jang, S.; Ko, S.; Daigle, H.; Pope, G. A.; Huh, C. Highly Porous CO₂-Hydrate Generation Aided by Silica Nanoparticles for Potential Secure Storage of CO₂ and Desalination. *RSC Adv.* **2017**, 7 (16), 9545–9550.
- (64) Ye, R. P.; Ding, J.; Gong, W.; Argyle, M. D.; Zhong, Q.; Wang, Y.; Russell, C. K.; Xu, Z.; Russell, A. G.; Li, Q.; et al. CO₂ Hydrogenation to High-Value Products via Heterogeneous Catalysis. *Nat. Commun.* **2019**, 10 (1), 5698.
- (65) Li, W.; Wang, H.; Jiang, X.; Zhu, J.; Liu, Z.; Guo, X.; Song, C. A Short Review of Recent Advances in CO₂ Hydrogenation to Hydrocarbons over Heterogeneous Catalysts. *RSC Adv.* **2018**, 8 (14), 7651–7669.
- (66) Liu, M.; Yi, Y.; Wang, L.; Guo, H.; Bogaerts, A. Hydrogenation of Carbon Dioxide to Value-Added Chemicals by Heterogeneous Catalysis and Plasma Catalysis. *Catalysts* **2019**, 9 (3).
- (67) Jin, B.; Shang, Z.; Li, S.; Jiang, Y. B.; Gu, X.; Liang, X. Reforming of Methane with Carbon Dioxide over Cerium Oxide Promoted Nickel Nanoparticles Deposited on 4-Channel Hollow Fibers by Atomic Layer Deposition. *Catal. Sci. Technol.* **2020**, 10 (10), 3212–3222.
- (68) Omae, I. Aspects of Carbon Dioxide Utilization. *Catal. Today* **2006**, 115 (1–4), 33–52.
- (69) Alper, E.; Yuksel Orhan, O. CO₂ Utilization: Developments in Conversion Processes. *Petroleum* **2017**, 3 (1), 109–126.
- (70) Koohestanian, E.; Sadeghi, J.; Mohebbi-Kalhari, D.; Shahraki, F.; Samimi, A. A Novel Process for CO₂ Capture from the Flue Gases to Produce Urea and Ammonia. *Energy* **2018**, 144, 279–285.
- (71) Honda, M.; Tamura, M.; Nakagawa, Y.; Tomishige, K. Catalytic CO₂ Conversion to Organic Carbonates with Alcohols in Combination with Dehydration System. *Catal. Sci. Technol.* **2014**, 4 (9), 2830–2845.
- (72) Ma, J.; Song, J.; Liu, H.; Liu, J.; Zhang, Z.; Jiang, T.; Fan, H.; Han, B. One-Pot Conversion of CO₂ and Glycerol to Value-Added Products Using Propylene Oxide as the Coupling Agent. *Green Chem.* **2012**, 14 (6), 1743–1748.
- (73) Ren, Y.; Rousseaux, S. A. L. Metal-Free Synthesis of Unsymmetrical Ureas and Carbamates from CO₂ and Amines via Isocyanate Intermediates. *J. Org. Chem.* **2018**, 83 (2), 913–920.
- (74) Fauvarque, J. F.; Jutand, A.; Francois, M. Nickel Catalysed Electrosynthesis of

- Anti-Inflammatory Agents. Part I - Synthesis of Aryl-2 Propionic Acids, under Galvanostatic Conditions. *J. Appl. Electrochem.* **1988**, 18 (1), 109–115.
- (75) Fauvarque, J. F.; Jutand, A.; Francois, M.; Petit, M. A. Nickel Catalysed Electrosynthesis of Anti-Inflammatory Agents. Part II - Monitoring of the Electrolyses by HPLC Analysis. Role of the Catalyst. *J. Appl. Electrochem.* **1988**, 18 (1), 116–119.
- (76) Darensbourg, D. J.; Mackiewicz, R. M.; Phelps, A. L.; Billodeaux, D. R. Copolymerization of CO₂ and Epoxides Catalyzed by Metal Salen Complexes. *Acc. Chem. Res.* **2004**, 37 (11), 836–844.
- (77) Pawar, G. G.; Robert, F.; Grau, E.; Cramail, H.; Landais, Y. Visible-Light Photocatalyzed Oxidative Decarboxylation of Oxamic Acids: A Green Route to Urethanes and Ureas. *Chem. Commun.* **2018**, 54 (67), 9337–9340.
- (78) Tamura, M.; Honda, M.; Nakagawa, Y.; Tomishige, K. Direct Conversion of CO₂ with Diols, Aminoalcohols and Diamines to Cyclic Carbonates, Cyclic Carbamates and Cyclic Ureas Using Heterogeneous Catalysts. *J. Chem. Technol. Biotechnol.* **2014**, 89 (1), 19–33.
- (79) Schlager, S.; Dibenedetto, A.; Aresta, M.; Apaydin, D. H.; Dumitru, L. M.; Neugebauer, H.; Sariciftci, N. S. Biocatalytic and Bioelectrocatalytic Approaches for the Reduction of Carbon Dioxide Using Enzymes. *Energy Technol.* **2017**, 5 (6), 812–821.
- (80) Bhatia, S. K.; Bhatia, R. K.; Jeon, J.-M.; Kumar, G.; Yang, Y.-H. Carbon Dioxide Capture and Bioenergy Production Using Biological System – A Review. *Renew. Sustain. Energy Rev.* **2019**, 110, 143–158.
- (81) Mateos, R.; Escapa, A.; Vanbroekhoven, K.; Patil, S. A.; Moran, A.; Pant, D. Microbial Electrochemical Technologies for CO₂ and Its Derived Products Valorization. In *Microbial Electrochemical Technology*; Mohan, S. V., Varjani, S., Pandey, A., Eds.; Elsevier B.V., 2018; pp 777–796.
- (82) Oh, Y.; Hu, X. Organic Molecules as Mediators and Catalysts for Photocatalytic and Electrocatalytic CO₂ Reduction. *Chem. Soc. Rev.* **2013**, 42 (6), 2253–2261.
- (83) Compagnoni, M.; Ramis, G.; Freyria, F. S.; Armandi, M.; Bonelli, B.; Rossetti, I. Innovative Photoreactors for Unconventional Photocatalytic Processes: The Photoreduction of CO₂ and the Photo-Oxidation of Ammonia. *Rend. Lincei* **2017**, 28 (s1), 151–158.
- (84) Windle, C. D.; Perutz, R. N. Advances in Molecular Photocatalytic and Electrocatalytic CO₂ Reduction. *Coord. Chem. Rev.* **2012**, 256 (21–22), 2562–2570.
- (85) Jiang, X.; Nie, X.; Guo, X.; Song, C.; Chen, J. G. Recent Advances in Carbon Dioxide Hydrogenation to Methanol via Heterogeneous Catalysis. *Chem. Rev.* **2020**, 120, 7984–8034.
- (86) Dey, G. R.; Belapurkar, A. D.; Kishore, K. Photo-Catalytic Reduction of Carbon Dioxide to Methane Using TiO₂ as Suspension in Water. *J. Photochem. Photobiol. A Chem.* **2004**, 163 (3), 503–508.
- (87) Sharma, N.; Das, T.; Kumar, S.; Bhosale, R.; Kabir, M.; Ogale, S. Photocatalytic Activation and Reduction of CO₂ to CH₄ over Single Phase Nano Cu₃SnS₄: A Combined Experimental and Theoretical Study. *ACS Appl. Energy Mater.* **2019**, 2

- (8), 5677–5685.
- (88) Zhou, R.; Guzman, M. I. CO₂ Reduction under Periodic Illumination of ZnS. *J. Phys. Chem. C* **2014**, *118* (22), 11649–11656.
- (89) Ramesh Raju, R.; Krishna Mohan, S.; Jayarama Reddy, S. Electroorganic Synthesis of 6-Aminonicotinic Acid from 2-Amino-5-Chloropyridine. *Tetrahedron Lett.* **2003**, *44* (21), 4133–4135.
- (90) Gennaro, A.; Sánchez-Sánchez, C. M.; Isse, A. A.; Montiel, V. Electrocatalytic Synthesis of 6-Aminonicotinic Acid at Silver Cathodes under Mild Conditions. *Electrochem. commun.* **2004**, *6* (7), 627–631.
- (91) Giner, J. Electrochemical Reduction of CO₂ on Platinum Electrodes in Acid Solutions. *Electrochim. Acta* **1963**, *8* (11), 857–865.
- (92) Teeter, T. E.; Van Rysselberghe, P. Reduction of Carbon Dioxide on Mercury Cathodes. *J. Chem. Phys.* **1954**, *22* (4), 759–760.
- (93) Hori, Y.; Takahashi, I.; Koga, O.; Hoshi, N. Electrochemical Reduction of Carbon Dioxide at Various Series of Copper Single Crystal Electrodes. *J. Mol. Catal. A Chem.* **2003**, *199* (1–2), 39–47.
- (94) Haynes, L. V.; Sawyer, D. T. Electrochemistry of Carbon Dioxide in Dimethyl Sulfoxide at Gold and Mercury Electrodes. *Anal. Chem.* **1967**, *39* (3), 332–338.
- (95) Damodar, J.; Krishna Mohan, S.; Khaja Lateef, S. K.; Jayarama Reddy, S. Electrosynthesis of 2-Arylpropionic Acids from α -Methylbenzyl Chlorides and Carbon Dioxide by [Co(Salen)]. *Synth. Commun.* **2005**, *35* (9), 1143–1150.
- (96) Gennaro, A.; Isse, A. A.; Savéant, J. M.; Severin, M. G.; Vianello, E. Homogeneous Electron Transfer Catalysis of the Electrochemical Reduction of Carbon Dioxide. Do Aromatic Anion Radicals React in an Outer-Sphere Manner? *J. Am. Chem. Soc.* **1996**, *118* (30), 7190–7196.
- (97) Al-Omari, A. A.; Yamani, Z. H.; Nguyen, H. L. Electrocatalytic CO₂ Reduction: From Homogeneous Catalysts to Heterogeneous-Based Reticular Chemistry. *Molecules* **2018**, *23* (11), 1–13.
- (98) Das, B.; Jia, C.; Ching, K.; Bhadbhade, M.; Chen, X.; Ball, G. E.; Colbran, S. B.; Zhao, C. Ruthenium Complexes in Homogeneous and Heterogeneous Catalysis for Electroreduction of CO₂. *ChemCatChem* **2020**, *12*, 1292–1296.
- (99) Ishida, H.; Tanaka, K.; Tanaka, T. Electrochemical CO₂ Reduction Catalyzed by [Ru(Bpy)₂(CO)₂]²⁺ and [Ru(Bpy)₂(CO)Cl]⁺. The Effect of pH on the Formation of CO and HCOO⁻. *Organometallics* **1987**, *6* (1), 181–186.
- (100) Machado, A. S. R.; Nunes, A. V. M.; da Ponte, M. N. Carbon Dioxide Utilization-Electrochemical Reduction to Fuels and Synthesis of Polycarbonates. *J. Supercrit. Fluids* **2017**, *134*, 150–156.
- (101) Hernandez-Aldave, S.; Andreoli, E. Fundamentals of Gas Diffusion Electrodes and Electrolysers for Carbon Dioxide Utilisation: Challenges and Opportunities. *Catalysts* **2020**, *10* (6), 1–34.
- (102) Ma, S.; Luo, R.; Gold, J. I.; Yu, A. Z.; Kim, B.; Kenis, P. J. A. Carbon Nanotube Containing Ag Catalyst Layers for Efficient and Selective Reduction of Carbon Dioxide. *J. Mater. Chem. A* **2016**, *4* (22), 8573–8578.

-
- (103) Gennaro, A.; Isse, A. A.; Severin, M.-G.; Vianello, E.; Bhugun, I.; Savéant, J.-M. Mechanism of the Electrochemical Reduction of Carbon Dioxide at Inert Electrodes in Media of Low Proton Availability. *J. Chem. Soc., Faraday Trans.* **1996**, 92 (20), 3963–3968.
- (104) Costentin, C.; Savéant, J. M. Homogeneous Molecular Catalysis of Electrochemical Reactions: Catalyst Benchmarking and Optimization Strategies. *J. Am. Chem. Soc.* **2017**, 139 (24), 8245–8250.
- (105) Costentin, C.; Robert, M.; Savéant, J. M. Catalysis of the Electrochemical Reduction of Carbon Dioxide. *Chem. Soc. Rev.* **2013**, 42 (6), 2423–2436.
- (106) Cao, Y.; He, X.; Wang, N.; Li, H. R.; He, L. N. Photochemical and Electrochemical Carbon Dioxide Utilization with Organic Compounds. *Chinese J. Chem.* **2018**, 36 (7), 644–659.
- (107) Senboku, H.; Yamauchi, Y.; Kobayashi, N.; Fukui, A.; Hara, S. Some Mechanistic Studies on Electrochemical Carboxylation of Flavones to Yield Flavanone-2-Carboxylic Acids. *Electrochim. Acta* **2012**, 82, 450–456.
- (108) Filardo, G.; Gambino, S.; Silvestri, G.; Gennaro, A.; Vianello, E. Electrocarboxylation of Styrene through Homogeneous Redox Catalysis. *J. Electroanal. Chem.* **1984**, 177, 303–309.
- (109) Yuan, G. Q.; Jiang, H. F.; Lin, C. Efficient Electrochemical Dicarboxylations of Arylacetylenes with Carbon Dioxide Using Nickel as the Cathode. *Tetrahedron* **2008**, 64 (25), 5866–5872.
- (110) Isse, A. A.; Ferlin, M. G.; Gennaro, A. Homogeneous Electron Transfer Catalysis in the Electrochemical Carboxylation of Arylethyl Chlorides. *J. Electroanal. Chem.* **2003**, 541, 93–101.
- (111) Isse, A. A.; Gottardello, S.; Durante, C.; Gennaro, A. Dissociative Electron Transfer to Organic Chlorides: Electrocatalysis at Metal Cathodes. *Phys. Chem. Chem. Phys.* **2008**, 10 (17), 2409–2416.
- (112) Isse, A. A.; Falciola, L.; Mussini, P. R.; Gennaro, A. Relevance of Electron Transfer Mechanism in Electrocatalysis: The Reduction of Organic Halides at Silver Electrodes. *Chem. Commun.* **2006**, 1 (3), 344–346.
- (113) Isse, A. A.; De Giusti, A.; Gennaro, A.; Falciola, L.; Mussini, P. R. Electrochemical Reduction of Benzyl Halides at a Silver Electrode. *Electrochim. Acta* **2006**, 51 (23), 4956–4964.
- (114) Isse, A. A.; Durante, C.; Gennaro, A. One-Pot Synthesis of Benzoic Acid by Electrocatalytic Reduction of Bromobenzene in the Presence of CO₂. *Electrochem. commun.* **2011**, 13 (8), 810–813.
- (115) Senboku, H.; Nagakura, K.; Fukuhara, T.; Hara, S. Three-Component Coupling Reaction of Benzylic Halides, Carbon Dioxide, and *N,N*-Dimethylformamide by Using Paired Electrolysis: Sacrificial Anode-Free Efficient Electrochemical Carboxylation of Benzylic Halides. *Tetrahedron* **2015**, 71 (23), 3850–3856.
- (116) Hudlicky, T. Benefits of Unconventional Methods in the Total Synthesis of Natural Products. *ACS Omega* **2018**, 3 (12), 17326–17340.
- (117) Endres, F. Ionic Liquids: Promising Solvents for Electrochemistry. *Zeitschrift für Phys. Chemie* **2004**, 218 (2), 255–283.
-

- (118) Vekariya, R. L. A Review of Ionic Liquids: Applications towards Catalytic Organic Transformations. *J. Mol. Liq.* **2017**, 227, 44.
- (119) Seddon, K. R. Review Ionic Liquids for Clean Technology. *J. Chem. Tech. Biotechnol.* **1997**, 68, 351–356.
- (120) Holbrey, J. D.; Seddon, K. R. Ionic Liquids. *Clean Prod. Process.* **1999**, 1 (December), 223–236.
- (121) Xie, J. N.; Yu, B.; Zhou, Z. H.; Fu, H. C.; Wang, N.; He, L. N. Copper(I)-Based Ionic Liquid-Catalyzed Carboxylation of Terminal Alkynes with CO₂ at Atmospheric Pressure. *Tetrahedron Lett.* **2015**, 56 (50), 7059–7062.
- (122) Marrucho, I. M.; Branco, L. C.; Rebelo, L. P. N. Ionic Liquids in Pharmaceutical Applications. *Annu. Rev. Chem. Biomol. Eng.* **2014**, 5 (1), 527–546.
- (123) Armand, M.; Endres, F.; Mac Farlane, D. R.; Ohno, H.; Scrosati, B. Ionic-Liquid Materials for the Electrochemical Challenges of the Future. *Nat. Mater.* **2010**, 8 (8), 129–137.
- (124) Gutowski, K. E. Industrial Uses and Applications of Ionic Liquids. *Phys. Sci. Rev.* **2018**, 1–10.
- (125) Welton, T. Ionic Liquids : A Brief History. *Biophys. Rev.* **2018**, 10, 691–706.
- (126) Swatloski, R. P.; Spear, S. K.; Holbrey, J. D.; Rogers, R. D. Dissolution of Cellulose with Ionic Liquids. *J. Am. Chem. Soc.* **2002**, 124 (18), 4974–4975.
- (127) Remsing, R. C.; Swatloski, R. P.; Rogers, R. D.; Moyna, G. Mechanism of Cellulose Dissolution in the Ionic Liquid 1-n-Butyl-3- Methylimidazolium Chloride: A ¹³C and ^{35/37}Cl NMR Relaxation Study on Model Systems. *Chem. Commun.* **2006**, No. 12, 1271–1273.
- (128) Blanchard, L. A.; Hancu, D.; Beckman, E. J.; Brennecke, J. F. Green Processing Using Ionic Liquids and CO₂. *Nature* **1999**, 399, 28–29.
- (129) Yang, B.; Li, C.; Zhou, J.; Liu, J.; Zhang, Q. Pyrrolidinium-Based Ionic Liquid Electrolyte with Organic Additive and LiTFSI for High-Safety Lithium-Ion Batteries. *Electrochim. Acta* **2014**, 148, 39–45.
- (130) Brooks, C. A. *Electrochemistry in Ionic Liquids*; Springer International Publishing: London, 2002; Vol. 2.
- (131) Barrosse-Antle, L. E.; Bond, A. M.; Compton, R. G.; O'Mahony, A. M.; Rogers, E. I.; Silvester, D. S. Voltammetry in Room Temperature Ionic Liquids: Comparisons and Contrasts with Conventional Electrochemical Solvents. *Chem. - An Asian J.* **2010**, 5 (2), 202–230.
- (132) Reche, I.; Gallardo, I.; Guirado, G. The Role of Cations in the Reduction of 9- Fluorenone in Bis(Trifluoromethylsulfonyl)Imide Room Temperature Ionic Liquids. *New J. Chem.* **2014**, 38 (10), 5030–5036.
- (133) Doherty, A. P.; Brooks, C. A. Organic Electrochemistry in Ionic Liquids. In *Ionic Liquids as Green Solvents*; American Chemical Society: Washington DC, 2003; pp 410–420.
- (134) Bornemann, S.; Handy, S. T. Synthetic Organic Electrochemistry in Ionic Liquids: The Viscosity Question. *Molecules* **2011**, 16 (7), 5963–5974.

-
- (135) Zhao, G.; Jiang, T.; Han, B.; Li, Z.; Zhang, J.; Liu, Z.; He, J.; Wu, W. Electrochemical Reduction of Supercritical Carbon Dioxide in Ionic Liquid 1- n- Butyl-3-Methylimidazolium Hexafluorophosphate. *J. Supercrit. Fluids* **2004**, 32 (1–3), 287–291.
- (136) Alvarez-Guerra, M.; Albo, J.; Alvarez-Guerra, E.; Irabien, A. Ionic Liquids in the Electrochemical Valorisation of CO₂. *Energy Environ. Sci.* **2015**, 8 (9), 2574–2599.
- (137) Rosen, B. A.; Salehi-Khojin, A.; Thorson, M. R.; Zhu, W.; Whipple, D. T.; Kenis, P. J. A.; Masel, R. I. Ionic Liquid-Mediated Selective Conversion of CO₂ to CO at Low Overpotentials. *Science*. **2011**, 334 (6056), 643–644.
- (138) Barrosse-Antle, L. E.; Compton, R. G. Reduction of Carbon Dioxide in 1-Butyl-3-Methylimidazolium Acetate. *Chem. Commun.* **2009**, 25, 3744–3746.
- (139) Niu, D.; Zhang, J.; Zhang, K.; Xue, T.; Lu, J. Electrocatalytic Carboxylation of Benzyl Chloride at Silver Cathode in Ionic Liquid BMIM BF₄. *Chinese J. Chem.* **2009**, 27 (6), 1041–1044.
- (140) Tateno, H.; Nakabayashi, K.; Kashiwagi, T.; Senboku, H.; Atobe, M. Electrochemical Fixation of CO₂ to Organohalides in Room-Temperature Ionic Liquids under Supercritical CO₂. *Electrochim. Acta* **2015**, 161, 212–218.

Chapter 2. Objectives

Chapter 2. Objectives

This doctoral thesis looks at the development of new and sustainable electrochemical processes; therefore, the general objective of this PhD thesis is built around three main concepts: electro-induced reactions, the capture and valorization of CO₂, and the use of ionic liquids as green solvents.

In order to carry out the main objective, the following specific objectives were established:

- To disclose the electrochemical reduction mechanism of organic molecules as well as CO₂ under inert and CO₂ atmosphere in organic aprotic solvents and ionic liquids.
- To analyze the effect of the working electrode and the solvent in order to design and propose electrochemical reduction routes to valorize CO₂.
- To understand the composition and properties of ionic liquids and their influence in the electrochemical valorization of CO₂ by conventional electrochemical techniques and using in-situ spectroelectrochemistry techniques.
- To valorize CO₂ after electrochemical activation in aprotic solvents and ionic liquids through:
 - Homogenous catalysis with small organic molecules.
 - Electrocarboxylation processes.
- To propose new environmentally friendly approaches for synthesizing ionic liquids in order to improve the actual commercial or synthetic routes proposed.

Chapter 3.

Results and discussion

Chapter 3. Results and discussion

This section is centered on the experimental results obtained during this PhD thesis related to the development and application of different ways to valorize CO₂ with electrochemistry and aprotic organic solvents and/or ionic liquids electrolytes, opening the door to use this very versatile and sustainable methodology with the aim of obtaining high-added value products through CO₂ electrochemical reduction.

The results have been published in different scientific journals as six original research papers, which are able to look up in Chapter 5.

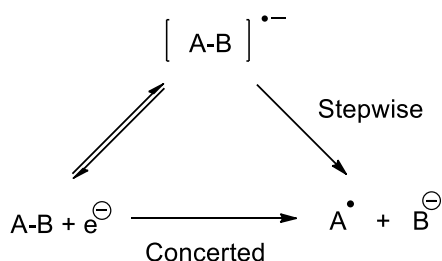
- 1) Reche, I.; Mena, S.; Gallardo, I.; Guirado, G. Electrocarboxylation of Halobenzonitriles: An Environmentally Friendly Synthesis of Phthalate Derivatives. *Electrochimica Acta*, **2019**, 320, 134576–134585.....**p.117**
- 2) Mena, S.; Guirado, G. One-Pot Sustainable Synthesis of Tetrabutylammonium Bis(Trifluoromethanesulfonyl)Imide Ionic Liquid. *Journal of Molecular Liquids*, **2020**, 312, 113393–113398.**p.127**
- 3) Mena, S.; Gallardo, I.; Guirado, G. Electrocatalytic Processes for the Valorization of CO₂: Synthesis of Cyanobenzoic Acid Using Eco-Friendly Strategies. *Catalysts*, **2019**, 9 (5), 413–424.....**p.133**
- 4) Mena, S.; Guirado, G. Electrochemical Tuning of CO₂ Reactivity in Ionic Liquids Using Different Cathodes: From Oxalate to Carboxylation Products. *Journal of Carbon Research*, **2020**, 6, 34–54.....**p.145**
- 5) Mena, S.; Sanchez, J.; Guirado, G. Electrocarboxylation of 1-Chloro-(4-Isobutylphenyl)Ethane with a Silver Cathode in Ionic Liquids: An Environmentally Benign and Efficient Way to Synthesize Ibuprofen. *RSC Advances* **2019**, 9 (1), 15115–15123.....**p.166**
- 6) Mena, S.; Santiago, S.; Gallardo, I.; Guirado, G. Sustainable and Efficient Electrosynthesis of Naproxen Using Carbon Dioxide and Ionic Liquids. *Chemosphere* **2020**, 245, 125557–125566.**p.175**

A summary of the experimental results is present below; firstly, there are two studies for electrochemical carboxylation processes using a C-X cleavage reaction in aprotic media in order to optimize the electrochemical strategy. A greener way is than presented in order to synthesize an ionic liquid, as well as the electrochemical behavior of CO₂ in an ionic liquid solution, characterized in situ by spectroelectrochemistry approaches. Finally, there are different ways to

valorize CO₂ in ionic liquids; by using a homogeneous catalysis, and through nucleophilic-electrophilic reactions.

3.1. Electrochemical carboxylation through carbon-halogen cleavage

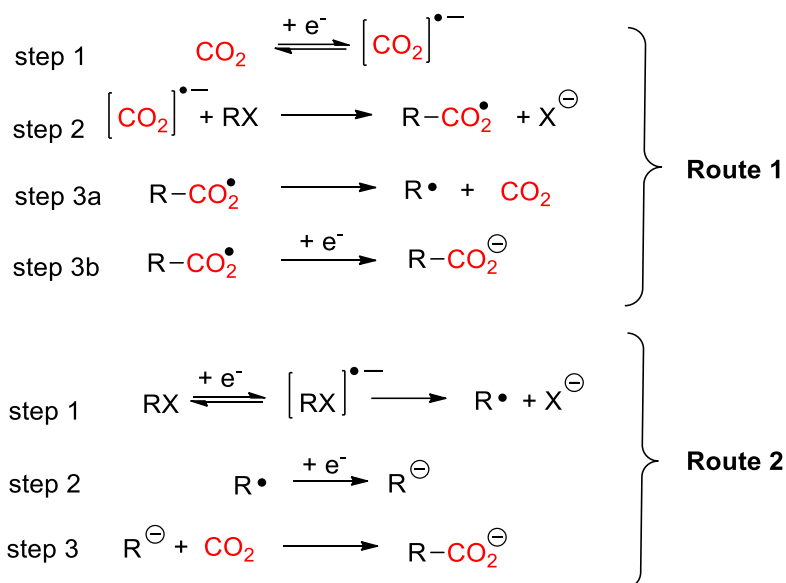
There are many ways to activate and cleave C-X bonds, mainly based on transition-metal-mediated. However, this chemistry requires a high loading of toxic and air-sensitive transition metals and extremely high temperatures and is only feasible with more reactive methyl and ethyl esters. In this sense, electrochemistry has been widely used in the activation and cleavage of C-X bonds. Electron-transfer reactions may not only lead to chemically stable species, but also to bond cleavage or bond formation. A discussion is also presented on general reactivity models that have been built for this kind of reaction in different extensive reports on the mechanisms of carbon-halogen bond cleavage. The general mechanism consists of the electrochemical activation of organic molecules by producing a radical anion after the electron transfer, which then cleaves to produce a radical and an anion in two steps (stepwise process), or in a one-step (concerted process) pathway (Scheme 9).^[1]



Scheme 9. Dissociative electron transfer pathways electrochemically triggered.

In the same way, the electrochemical-promoted approaches for achieving carboxylated organic valuable products through CO₂ can mainly be tackled by strategies; in the first approach, the electrochemical generation of carbon dioxide radical anion, CO₂^{•-}, requires a fairly negative potential (Scheme 10, Route 1), making this option costly in terms of energy consumed, as has been discussed in previous chapters. On the other hand, in the second approach (Scheme 10, Route 2), the electrochemical reduction takes place in the organic molecule (for instance, an organic halide, RX), which is a more easily reducible compound than

CO₂. In this case, after being reduced, RX^{•-} cleaves into the halide anion (X⁻) and the organic radical (R[•]) (step 1, Route 2). The electro-generated radical can be further reduced forming corresponding organic anion (R⁻) (step 2, Route 2). If this organic anion is stable enough in the electrolyte media, it would nucleophilically attack the CO₂ dissolved in the solution, and therefore, the CO₂ would be added to the organic molecule skeleton, leading to a carboxylate derivative (RCO₂⁻) (step 3, Route 2).



Scheme 10. Electrocarboxylation approaches.

As regards this second approach, an electrochemical study has been conducted to establish the optimal experimental conditions for the electrochemical capture of CO₂ with a series of four 4-halobenzonitriles (F, Br, Cl, and I derivatives). Their electrochemical behavior was determined with two different working electrodes; silver and glassy carbon cathode materials. The aprotic electrolyte media selected for the electrochemical study was DMF, using 0.1 M of tetrabutylammonium tetraborate (TBABF₄) as supporting electrolyte.

Figure 15 shows the cyclic voltammetry response under inert atmosphere of 4- fluorobenzonitrile, 4-chlorobenzonitrile, 4-bromobenzonitrile, and 4- iodobenzonitrile with a carbon working electrode and a silver working electrode.

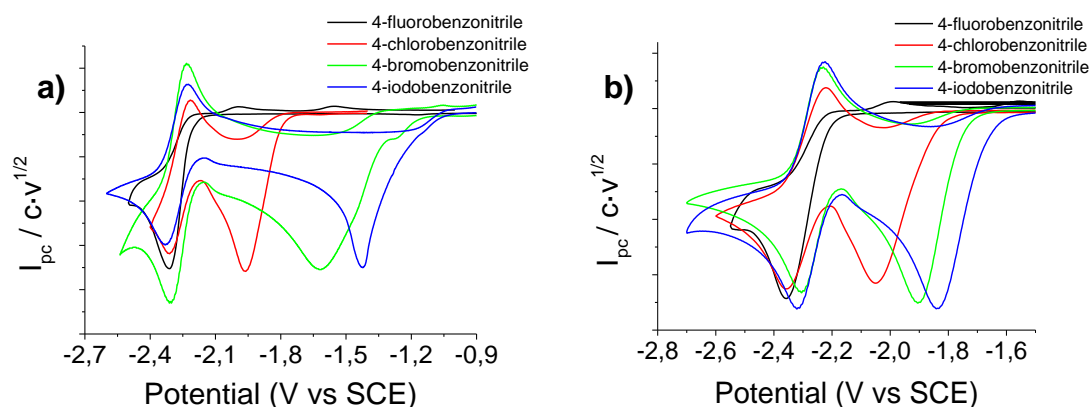


Figure 15. Cyclic voltammetry of 5-10 mM of 4-halobenzonitriles in DMF/0.1 M TBABF₄, under inert atmosphere. Scan rate: 0.5 V·s⁻¹. At working electrodes **(a)** Ag **(b)** GC.

The cyclic voltammetry response of the four halogen compounds showed a bielectronic, irreversible, slow first electron transfer, which has a reduction potential following the order, $I > Br > Cl > F$, which indicates that the halogen ion pair can be incorporated into the conjugation of the systems affecting the reduction potential values. Moreover, glassy carbon and silver working electrodes show the same voltammetry response, but silver cathode material has electrocatalytic features which reduce the first electron transfer potential between 30 and 380 mV, depending on halogen atom, improving the energy efficiency (Table 1).

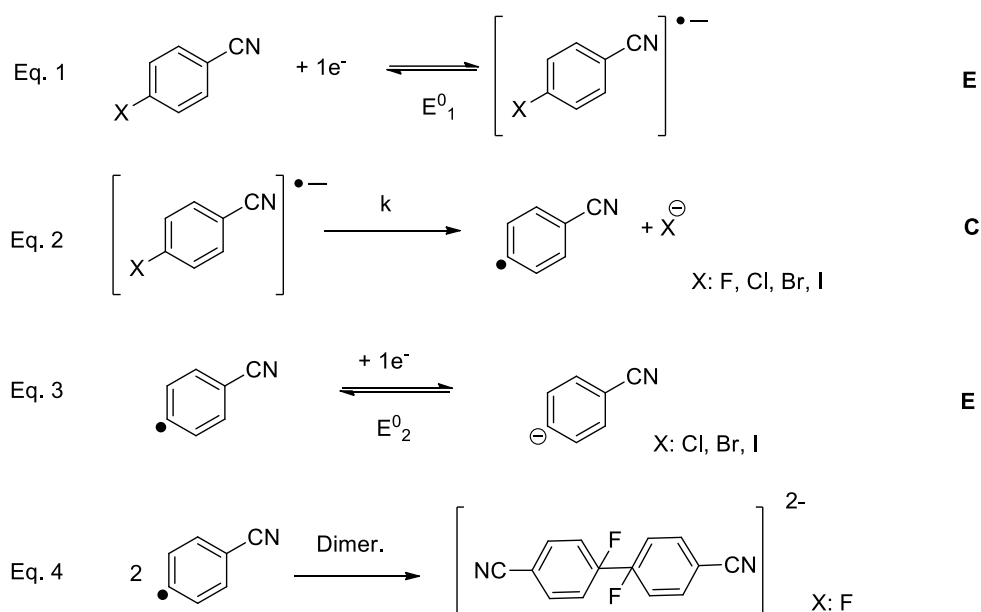
Table 1. Electrochemical parameters associated to first electrochemical reduction of 4-halobenzonitrile solutions (X: F, Cl, Br, I) under N₂ atmosphere.

4-halobenzonitriles	E _{pc} (V)		Electrocatalytic effect (mV): E _{pc} (Ag) – E _{pc} (GC)
	Ag	GC	
F	-2.35	-2.38	30
Cl	-1.95	-2.04	90
Br	-1.75	-1.94	190
I	-1.46	-1.84	380

Taking a close look at CVs, 4-fluorobenzonitrile only shows one electron transfer process at E_{pc} = -2.45 V (vs SCE), whereas the other derivatives show a second one, which would be related to benzonitrile reduction. [2]

To determine the nature of the product obtained after the first electron transfer, controlled-potential electrolysis were performed at ~0.1 V more negative potential, obtaining 4-(4-cyanophenyl)benzonitrile as main product when the reagent was 4-fluorobenzonitrile, while benzonitrile was obtained with the other three 4-halobenzonitriles.

With these data, an Electron transfer–Chemical reaction–Electron transfer (ECE) and an Electron transfer–Chemical reaction (EC) mechanisms could be proposed for the 4-halobenzonitriles (Scheme 11). After first reduction the radical anion of the 4-halobenzonitrile is obtained. It is followed by a C-X bond cleavage which led to a benzonitrile radical and the corresponding halide. Finally, this radical is then reduced into a benzonitrile anion with 4-chloro, 4-bromo, and 4-iodobenzonitrile (Scheme 11, Eq. 1-3). On the other hand, with 4-fluorobenzonitrile, the benzonitrile radical would dimerize to obtain 4-(4-cyanophenyl)benzonitrile following an EC mechanism instead of an ECE one (Scheme 11, Eq. 1-2 and 4).



Scheme 11. Proposed mechanism for 4-halobenzonitriles (F, Cl, Br, I).

Both cathode materials have the same tendency with 4-halobenzonitriles. Only 4-fluorobenzonitrile shows a different distribution of products with the use of silver, probably because there were adsorption processes of reduction intermediates on the electrode surface, obtaining benzonitrile apart from 4-(4-cyanophenyl)benzonitrile.

On knowing 4-halobenzonitrile behavior under inert atmosphere, it is possible to use its electrochemical C-halogen cleavage to perform an electrocarboxylation process. This would be obtained by an electrophile-nucleophile reaction between the benzonitrile anion and CO₂, with the use of 4-chloro, 4-bromo, and 4-iodobenzonitriles, whereas in the case of 4-fluorobenzonitrile, the reaction would be triggered through its radical anion and CO₂.

With the aim of valorizing CO₂ with the electrochemical approach, the same electrochemical study as N₂ atmosphere was performed, but under saturated CO₂ atmosphere, showing different electrochemical behavior. Furthermore, there were significant differences with the use of carbon or silver cathode materials.

The silver electrode shows two different electron transfers as a cyclic voltammetry response of 4-halocompounds (X: Cl, Br, I) when the amount of CO₂ in the solution is big enough to overlay the electron transfer related to benzonitrile reduction (Figure 16a). When the amount is around 0.05 M of CO₂, cyclic voltammetry shows three different electron transfers; a first electron transfer that is the same as that shown under N₂ atmosphere. It is followed by a new reduction peak around $E_{pc} = -2.2$ V (vs SCE), which is related to CO₂ reduction on the silver working electrode surface. And the third one is the same as in an inert atmosphere, which shows the reduction of benzonitrile (Figure 16b). In the case of 4-fluorobenzonitrile, this third electron transfer did not appear.

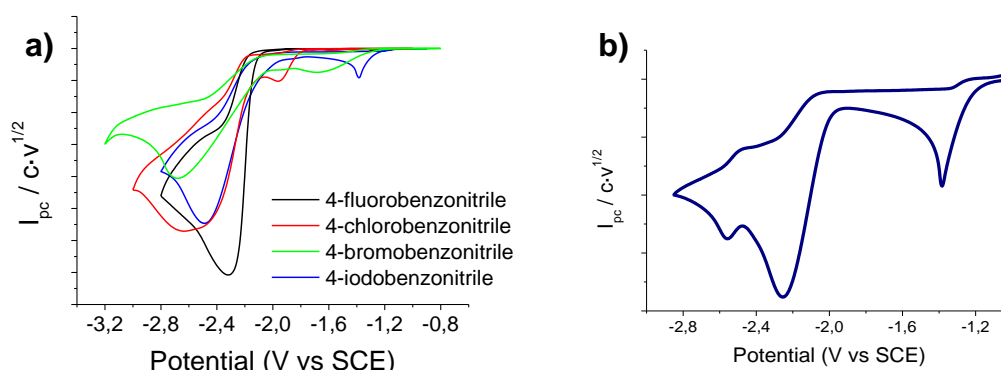


Figure 16. Cyclic voltammetry in DMF/0.1 M TBABF₄ with silver working electrode. Scan rate: 0.5 V·s⁻¹. **(a)** 5-10 mM of 4-halobenzonitriles under 0.3-0.4 M [CO₂] **(b)** 4-iodobenzonitrile under 0.05 M [CO₂].

On the other hand, with the use of a glassy carbon working electrode (Figure 17), 4-chloro, 4-bromo, and 4-iodobenzonitrile showed two reduction peaks at the same reduction potential that were previously determined under inert atmosphere. Hence, the first wave is related to the reduction of 4-halobenzonitrile, whereas the second one is related to benzonitrile reduction. Noting that under saturated CO₂ atmosphere, the benzonitrile reduction peak loses its reversibility and dramatically increases its peak current value, which indicates that benzonitrile was acting as an organic mediator (catalyst) for a homogeneous catalysis in the reduction of CO₂. 4-fluorobenzonitrile only had an

increase in the cathode peak current value due to the reactant and products (benzonitrile and 4- (4- cyanophenyl)benzonitrile), which act as catalyst, appearing at the same potential values.

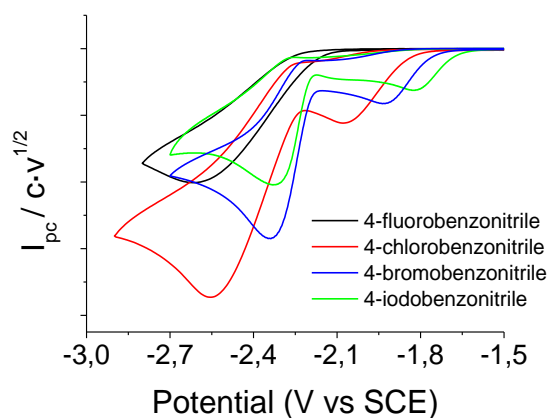


Figure 17. Cyclic voltammetry of 5-10 mM of 4-halobenzonitriles in DMF/0.1 M TBABF₄, under saturated CO₂ atmosphere with carbon working electrode. Scan rate: 0.5 V·s⁻¹.

Therefore, by tuning the potential and working electrode it is possible to produce a wide range of high value-added products of CO₂ reduction through different electrochemical processes; since the nucleophilic attack between the 4- halobenzonitrile reduction derivative and CO₂, to a catalysis for reduction of CO₂ into a radical anion triggered by the product of the reduction of 4- halobenzonitrile (organic mediator). But, to avoid having mixture of products and obtain higher selectivity of the process, controlled-potential electrolysis only was performed after first reduction wave, hence products of nucleophilic attack would only be obtained.

Characterizing the product obtained after the electrocarboxylation processes, a general trend is observed in all cases, independently of the nature of the electrode or charge. When 4-chloro, 4-bromo and 4-iodohalobenzonitriles solutions were electrolyzed, a mixture of mono- (4-cyanobenzoate methyl ester) and di-carboxylated (dimethyl terephthalate) products were obtained after the chemical treatment of the sample. In contrast, with 4-fluorobenzonitrile, only dimethyl terephthalate is formed. Moreover, when exhaustive electrolysis is performed, the percentage of di-carboxylated product increases.

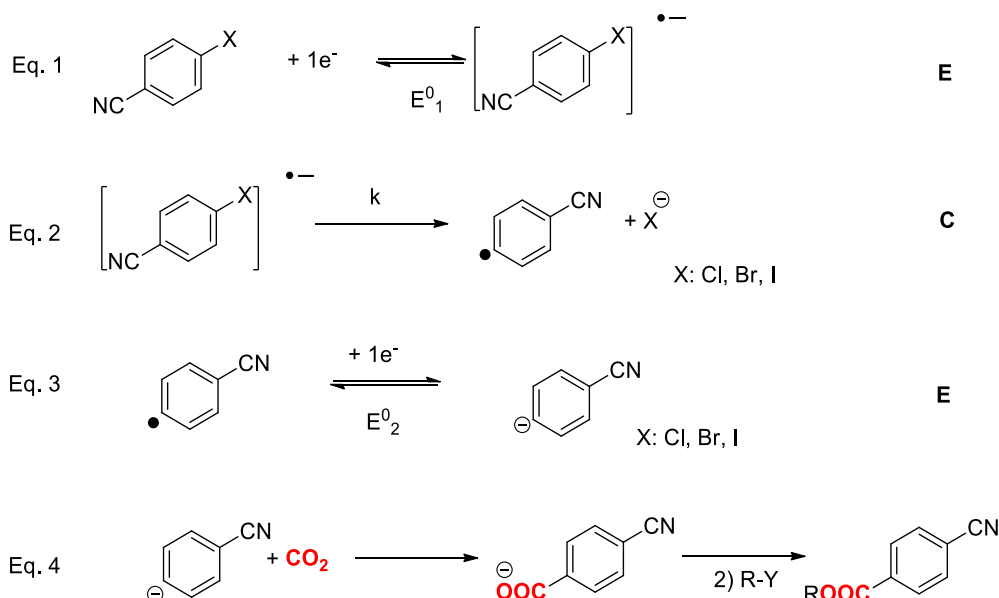
On comparing both cathode electrodes, the Ag electrode is recognized as a powerful catalytic electrode in organic solvent, with its catalytic property being ascribed to the absorption between metal surface and halogenated substrate, as well as its reduction intermediates and products. Hence, owing to these

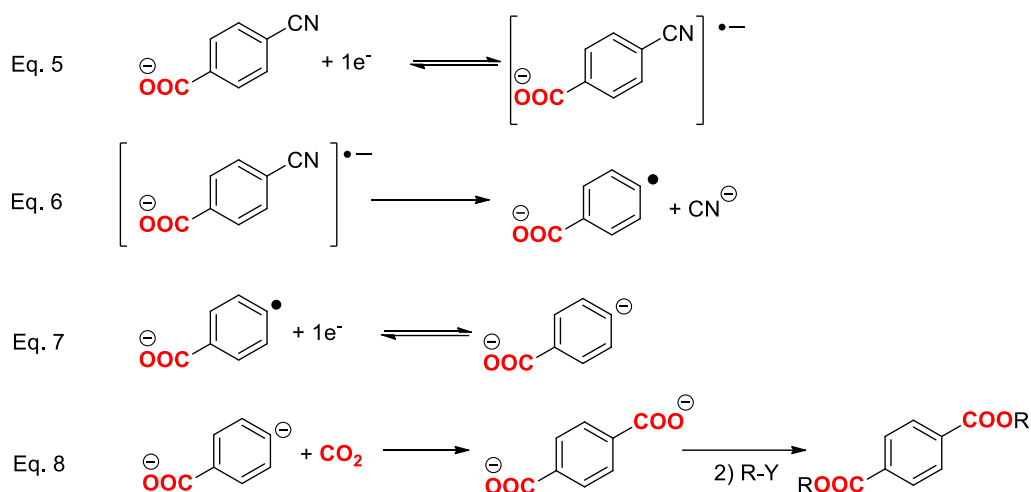
adsorption processes that favor the stability of reduction intermediates after the total charge passed, at the same consumption of charge, the yield of carboxylation is about 2-3 times higher with Ag than with C in global terms.

In addition, it is worth noting that, after passing the same number of Farads ($n \cdot F$), the total yield of electrocarboxylation products is as follows; $I > Br > Cl > F$. This fact could be explained by considering the bond dissociation energies (BDEs) of the Ar-X bonds.

On observing the data, it is plausible to propose the following mechanism for the insertion of CO_2 in 4-halobenzonitriles (X: Cl, Br and I). In a first step, 4-halobenzonitrile is reduced to its corresponding radical anion, which rapidly cleaves to give the benzonitrile radical and the corresponding halide. In a third step, the radical is reduced at the electrode surface leading to the benzonitrile anion. In a further step, this anion can react with CO_2 , producing 4-cyanobenzoate anion, which is alkylated by an alkylating agent (R-Y) to yield the corresponding ester (Scheme 12. Eq 1-4).

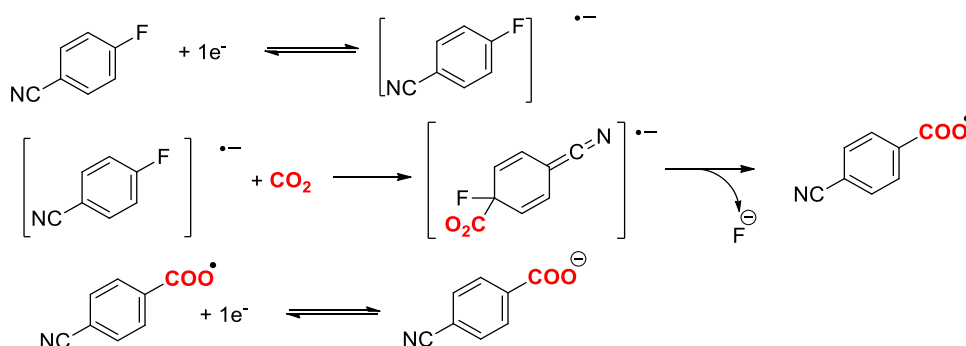
The formation of the carboxylated di-substituted products is related to the reactivity of the nitrile group in the presence of CO_2 when more charge is passed (Scheme 12. Eq. 5-8).





Scheme 12. Proposed mechanism for 4-halobenzonitriles (Cl, Br, I) electrocarboxylation process.

In the case of 4-fluorobenzonitrile, only electrocarboxylated products were obtained when silver was employed as working electrode but enabling a yield of 40% to be obtained. A plausible electrocarboxylation mechanism could be described as follows; 4-fluorobenzonitrile anion radical reacts with CO_2 instead of a dimerization process, leading to a benzonitrile carboxylated derivative (Scheme 13). This derivative is not stable at high negative potentials, and further reduction are taking place following the same mechanism as the other three 4-halobenzonitriles (Scheme 12. Eq. 5-8).



Scheme 13. Proposed mechanism for 4-fluorobenzonitriles electrocarboxylation process.

Focusing in the products obtained in the electrolysis processes, the use of 4-halobenzonitrile in CO_2 -saturated DMF solutions, employing carbon and silver electrodes, lead to the formation of mono- and di-substituted carboxylated products. Obtaining the greater efficiency of the carboxylation process (87% yield of dimethyl terephthalate) with the use of 4-bromobenzonitrile and silver cathodic material applying c.a. -1.8 V (vs SCE), after the passage of 4.5 F. Besides,

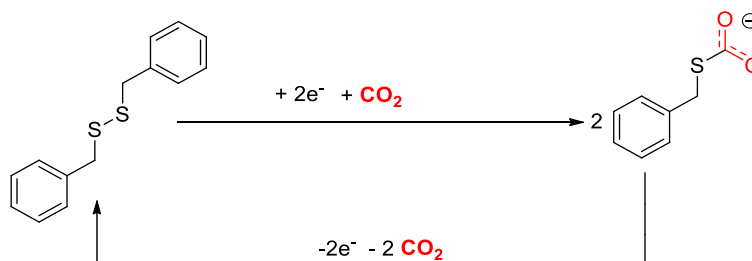
demonstrating that the use of “small” alkylating agents enables higher yields, because it was increased a 45% yield in an 87-90% yield of dimethyl terephthalate, only reducing the size of the alkylating agent.

This study allowed the development of the article published in the 320 volume of the *Electrochimica Acta* journal entitled “**Electrocarboxylation of halobenzonitriles: An environmentally friendly synthesis of phthalate derivatives**”.^[3]

3.2. Electrochemical carboxylation through carbon-sulphur cleavage

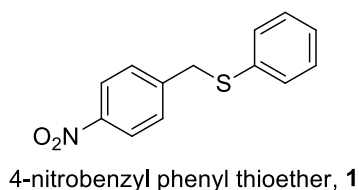
Once it is possible to use the electrochemistry to cleave the carbon-halogen bond and use it as strategy for electro-induced carboxylation reactions, it is proposed to expand this methodology for other C-X bonds.

In this sense, C-O and C-S bond cleavages in ether and thioether have been notably studied, owing to their interest in different biological phenomena. For instance, for the DNA stand break of the C3'-O3' bond,^[4] or for photo-cleavage of benzyl-sulfide bond in a ribonucleoside is interesting for its successful photo-affinity labelling of a membrane transport protein.^[5,6] Also, it has a high importance in the fuel and coal industry for decades. Focusing on the C-S bond cleavage reaction, it has been recently published by Singh et al.^[7] that it is possible to generate benzylthiolate anion moieties (PhCH_2S^-) through an electrochemical reduction process of benzyldisulfide ($\text{PhCH}_2\text{-S-S-CH}_2\text{Ph}$) of a high-negative potential, and these benzylthiolate anions are able to reversibly capture CO_2 (Scheme 14).



Scheme 14. Electrochemical cycle that enables capture and release of carbon dioxide with the use of benzylthiolate as capture agent.

Therefore, it seems to be possible to valorize CO₂ with an electrochemically activated compound through C-S cleavage. In this section, CO₂ is valorized at low potential values using 4-nitrobenzyl phenyl thioether, **1**, an arylthioether compound with a nitro-group substituent. Thus, the electrochemical reduction mechanism of **1** under inert atmosphere will be previously established using electrochemical techniques (cyclic voltammetry and controlled potential electrolysis). After that, the electrochemical reactivity of **1** under CO₂ will be evaluated.



3.2.1. Electrochemical study of 4-nitrobenzyl phenyl thioether under inert atmosphere

Compound **1** has been electrochemically studied by cyclic voltammetry under inert atmosphere. The typical CV of 5 mM solution of compound **1** in DMF/0.1 M TBABF₄ is depicted in Figure 18. A cathode scan shows three different electron transfers; A first monoelectronic fast reversible electron transfer, with $E_{pc,1} = -1.11$ V (vs SCE), followed by a second irreversible electron transfer, $E_{pc,2} = -1.9$ V (vs SCE), and a third multi-electron cathodic wave at $E_{pc,3} = -2.43$ V (vs SCE), which is related to the reduction of the nitro-group in the molecule to a nitroso compound.

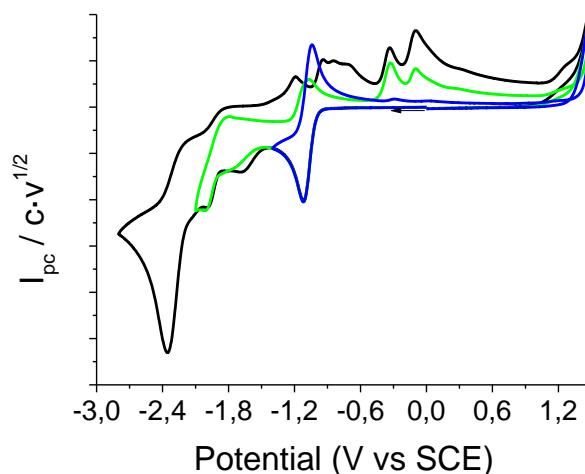


Figure 18. Cyclic voltammetry of 5.01 mM of **1** in DMF/0.1 M TBABF₄ on glassy carbon disk, under inert atmosphere. Scan rate: 0.5 V·s⁻¹. First electron transfer (blue line), second electron transfer (green line), third electron transfer (black line).

As the generation of nitroso compounds will be not discussed, the current study will be focused only on the two first electron transfers.

Electrochemical study of **1** under inert atmosphere at first electron transfer

The first wave corresponds to the reversible reduction of **1**, so the compound takes a first electron reversibly, which is localized on the nitro group according to the value of the standard potential (-1.16 V vs SCE) to form an anion radical, **1**^{•-}, (Figure 19). No oxidation products were detected after the reduction scan.

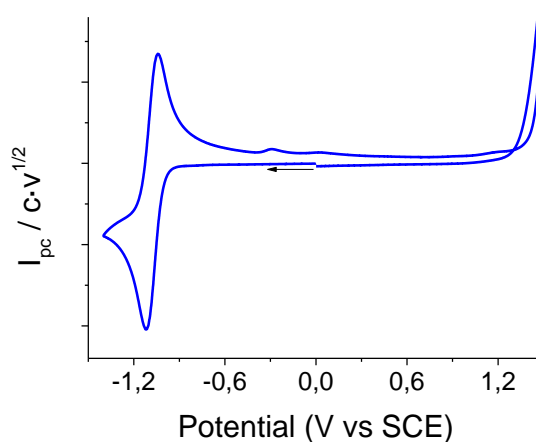


Figure 19. Cyclic voltammetry of 5.01 mM of **1** in DMF/0.1 M TBABF₄ on glassy carbon disk, under inert atmosphere. Scan rate: 0.5 V·s⁻¹.

Electrochemical study of **1** under inert atmosphere at second electron transfer

The electrochemical behavior related to second electron transfer, Figure 20, shows a pseudoreversible monoelectronic wave, because slow scan rates gives an irreversible peak (Figure 20a), but when scan rate was increased it turns reversible (Figure 20b). Moreover, when the scan rate is slow, oxidation peaks are produced in an anodic scan after reduction.

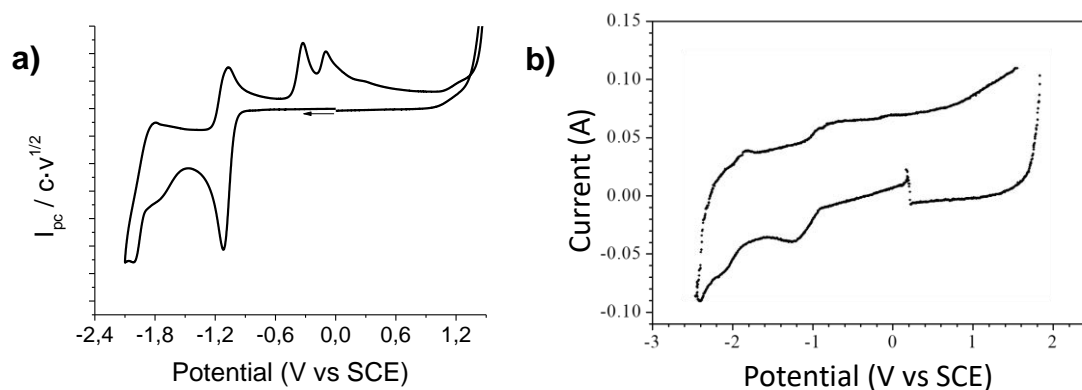


Figure 20. Cyclic voltammetry of 5.01 mM of **1** in DMF/0.1 M TBABF₄ under inert atmosphere. **(a)** glassy carbon disk, Scan rate: 0.5 V·s⁻¹ **(b)** glassy carbon disk ultra-micro-electrode (Φ = 9.7 μ m). Scan rate: 700 V·s⁻¹.

In order to obtain the value of the second transfer electrochemical parameters of compound **1**, CVs at different scan rates were recorded in the same conditions. The reversibility of the second reduction wave is achieved at high scan rates (700 V·s⁻¹), hence it is possible to determine the standard potential value of this second reduction process ($E^0 = -1.63$ V vs SCE). Note that the oxidation peaks related to the second electron transfer coupled reaction disappeared (Figure 20b). Thus, it is possible to propose that after the second electron transfer is produced a chemical reaction. The electrochemical parameters obtained for the second electron transfer were $E^0_2 = -1.63$ V, $k_s^{ap} = 9 \cdot 10^{-4}$ cm·s⁻¹, $\alpha = 0.34$, and $k = 90$ s⁻¹, were determined experimentally, as well as confirmed by simulation of the experimental curves using DIGISIM® software.

With the aim to know the nature of the products obtained after the second electron transfer, a control potential electrolysis at $E_{ap} = -2$ V (vs SCE) was performed. After 2 F of charge and chemical treatment only, 16% of the reagent remained, and the products obtained are summarized in Table 2.

Table 2. Results of electrochemical reduction of **1** under inert atmosphere.

Entries	Electrolysis parameters		% Yield					
	E_{ap} (V)	Charge (Q = nzF)	Reagent	Product	4-nitrotoluene	Ph-S-S-Ph	p-NO ₂ -Ph-CHO	D1+D2
1	-2.0	1F	1	Thiophenol	23	17	2	-
2	-2.0	2F	16	6	34	36	3	5

Taking a close look at Table 2, the products obtained confirmed that the C-S cleavage is produced efficiency after passing the charge corresponding to two electrons. Obtaining, on the one hand 4-nitrotoluene, and on the other hand, diphenyl disulphide, Ph-S-S-Ph, as main products. Moreover, aldehyde and dimer derivatives (4,4'-dinitrobibenzyl and 4,4'- dinitrostilbene, D1 and D2) were detected at low yields.

Highlighting in the products obtained after the electrolysis, it is possible to relate the oxidation peaks obtained, at slow scan rates, after second electron transfer with the oxidation of nitrobenzyl anion ^[8] ($E_{pa,1} = -0.33$ V (vs SCE)), and the other with the thiophenolate oxidation ^[9] ($E_{pa,2} = -0.09$ V (vs SCE)). The second one was determined by comparison with CV obtained by commercial analog, sodium thiophenolate, NaSPh, (Figure 21a).

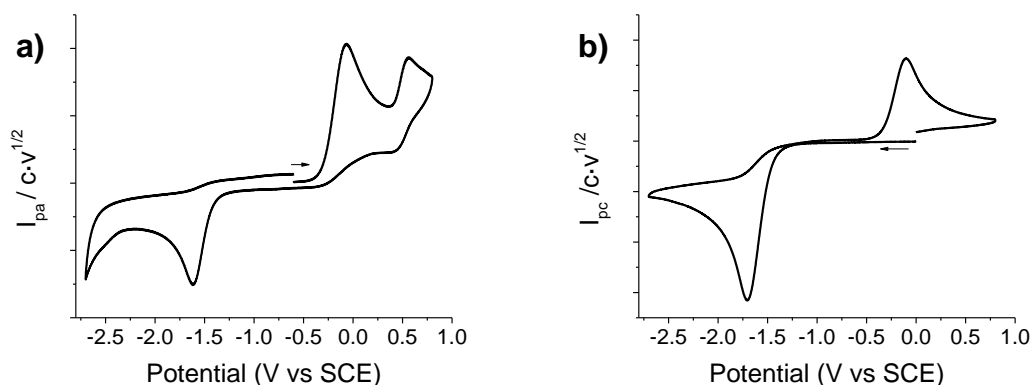
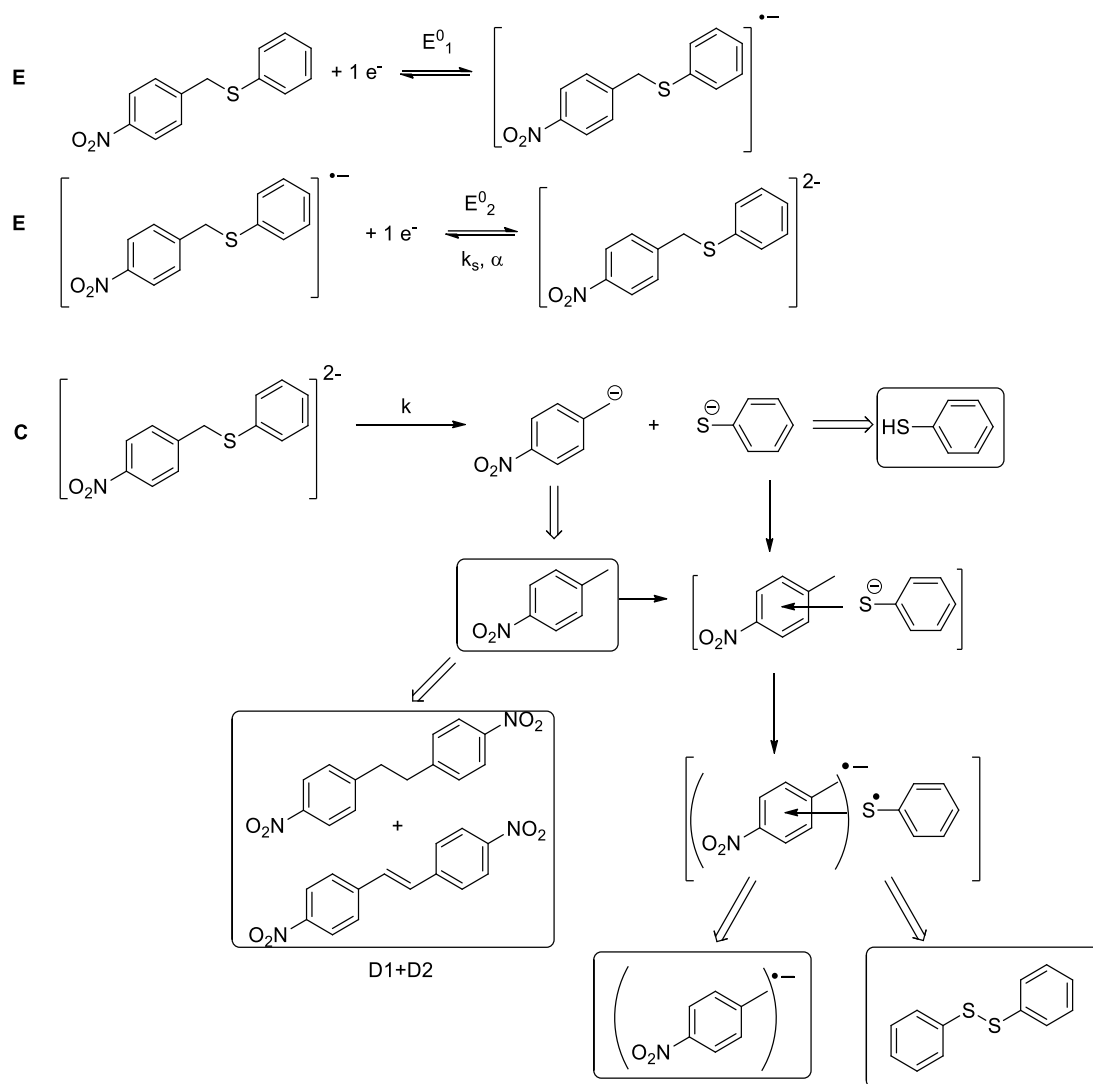


Figure 21. Cyclic voltammetry in DMF/0.1 M TBABF₄ on glassy carbon disk, under inert atmosphere. Scan rate: 0.5 V·s⁻¹. Solution of 5.01 mM **(a)** NaSPh **(b)** Ph-S-S-Ph.

Besides, sodium thiophenolate electrochemical characterization shown two oxidation peaks ($E_{pa,1} = -0.09$ V vs SCE and $E_{pa,2} = +0.55$ V vs SCE) and a reduction wave at $E_{pc} = -1.60$ V (vs SCE). The first oxidation wave would correspond to the oxidation of sodium thiophenolate to its radical form, which could evolve following two different reaction pathways; It can either abstract a

hydrogen atom leading to benzenethiol, which would be oxidized at $E_{pa} = +0.55$ V (vs SCE), or would evolve to dimerize into diphenyl disulphide, Ph-S-S-Ph, which has the reduction wave at $E_{pc} = -1.60$ V (vs SCE), Figure 21b. This second pathway seems to be favored in the electrolysis of **1** because is obtained much more diphenyl disulphide (36% yield) than thiophenol (16% yield) with the passage of 2 F.

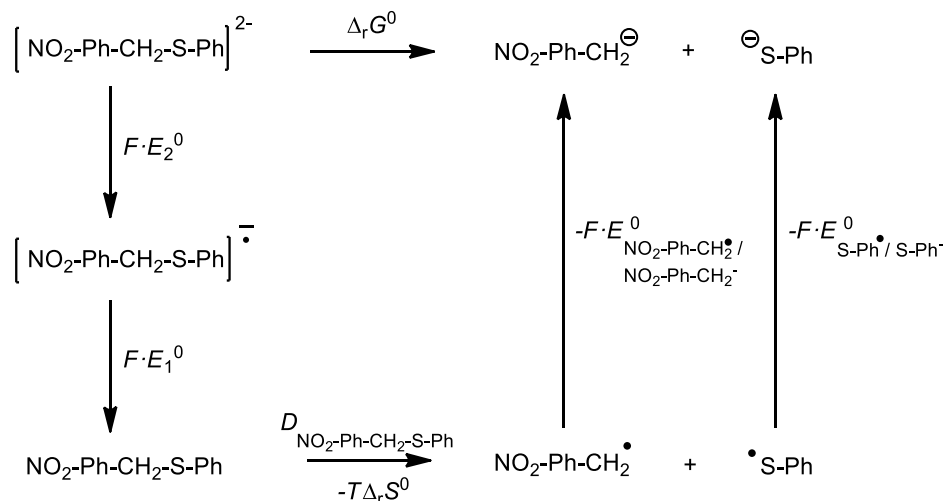
As regards the CV and electrolysis experiments, it is possible to propose a mechanism for the electrochemical reduction of **1**, following an EEC mechanism (Scheme 15), where compound **1** is reduced to obtain its radical anion, **1**^{•-}, with an Electronic transfer (E), which is followed by another one (E), obtaining the dianion **1**²⁻, that is broken through a chemical reaction (C) where there is a C-S bond cleavage. Giving as products 4-nitrobenzyl and thiophenolate derivatives.



Scheme 15. Proposal EEC mechanism for the electrochemical reduction of **1**.

Thermodynamics and kinetics of C-S bond cleavage

The experimental data (standard potentials E^0_1 and E^0_2 , heterogeneous electron transfer rate constants, k_s , and first order constant, k) are treated following the theoretical model of dissociative electron transfer developed by Savéant. ^[10]



Scheme 16. Thermodynamic cycle for dianion cleavage.

According to the thermodynamic cycle presented in Scheme 16, the standard free energy of the cleavage reaction is:

$$\Delta_r G^0 = D_{NO_2PhCH_2SPh} + F(E_1^0 + E_2^0 - E_{(SPh)^-}^0 / (SPh)^- - E_{NO_2PhCH_2^{\bullet}/NO_2PhCH_2^-}^0) - T\Delta_r S^0 \quad (3)$$

The D and E^0 values are the bond dissociation energies and the standard potentials of the subscript species, respectively. $\Delta_r S^0$ is approximately $1 \text{ meV} \cdot \text{K}^{-1}$ ($96.5 \text{ J} \cdot \text{K}^{-1} \cdot \text{mol}^{-1}$). The effect of the solvent reorganization is considered negligible. The activation free energy $\Delta_r G^\ddagger$ is obtained from the first order constant, where the pre-exponential factor A are taken to be equal to $5 \cdot 10^{12} \text{ s}^{-1}$:

$$k = A \exp\left(\frac{-\Delta_r G^\ddagger}{RT}\right) \quad (4)$$

The activation free energy, $\Delta_r G^\ddagger$, is related quadratically to the standard free energy of the cleavage reaction:

$$\Delta_r G^\ddagger = \frac{4\Delta_r G^{0\ddagger}}{4} \left(1 + \frac{\Delta_r G^0}{4\Delta_r G^{0\ddagger}}\right)^2 \quad (5)$$

So, the standard activation free energy, $\Delta_r G^{0\ddagger}$, is:

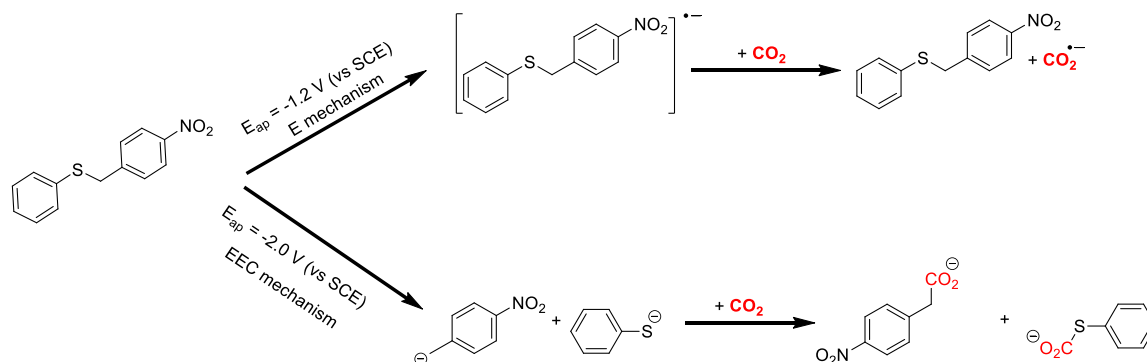
$$\Delta_r G^{0\neq} = \frac{\Delta_r G^\neq - \frac{\Delta_r G^0}{2} + \sqrt{\left(\Delta_r G^\neq - \frac{\Delta_r G^0}{2}\right)^2 - \frac{(\Delta_r G^0)^2}{4}}}{2} \quad (6)$$

The results are summarized in Table 3, where compound **1** has related negative standard free energy ($\Delta_r G^0$). Therefore, the reaction is thermodynamically favorable.

Table 3. Thermodynamic parameters for compound **1**.

$D_{NO_2PhCH_2SPh}$	- F E^0_1	- F E^0_2	- F $E^0_{SPh-/SPh-}$	- F $E^0_{NO_2PhCH_2-/NO_2PhCH_2-}$	$T\Delta_r S^0$	$-\Delta_r G^0$	k (s ⁻¹)	$\Delta_r G^\neq$	$\Delta_r G^{0\neq}$
218	112	158	9.65	33.8	27.8	55.7	90	59.3	84.9

At this point, it is possible to envisage the electrochemical control of CO₂ reactivity by tuning the electrochemical reduction process of **1** in function of the applied potential. As the first electron transfer yields a stable anion radical, it is possible to use this reactant as a homogenous catalyst for CO₂ reduction. Whereas, the second electron transfer yields carbon and sulphur anions, which can potentially react with CO₂ to yield carboxylate products (Scheme 17).



Scheme 17. Reactivity of **1** and CO₂ depending on potential.

3.2.2. Electrochemical study of 4-thionitrobenzyl phenyl thioether under CO₂ saturated atmosphere

The electrochemical behavior of 4-thionitrobenzyl phenyl thioether under CO₂ atmosphere was completely different than under inert atmosphere, and it could be divided into two reduction electron transfer processes.

3.2.2.1. First reduction electron transfer process

Figure 22 shows the cyclic voltammetry response of **1** under CO₂ saturated atmosphere. The first wave, which was reversible under inert atmosphere, loses its reversibility, and its peak current values increase significantly when the solution is saturated with CO₂ (Figure 22a). These electrochemical features are characteristic of an electrocatalytic process where compound **1** acts as a redox mediator (organic catalysts) in a homogeneous catalysis leading to CO₂ reduction. In addition, the new peak at $E_{pa} = +0.26$ V (vs SCE) is related to the oxidation of oxalate in aprotic media, which is in agreement with that of tetrabutylammonium oxalate, TBA₂Ox, pattern (Figure 22b), and in the literature. [11–13]

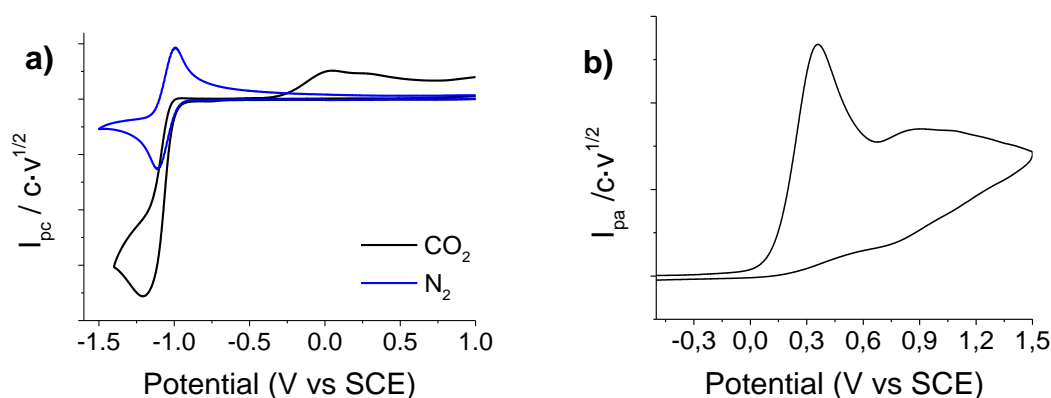


Figure 22. Cyclic voltammetry in DMF/0.1 M TBABF₄ on glassy carbon disk. Scan rate: 0.5 V·s⁻¹. Solution of 5.01 mM (a) Compound **1** (b) TBA₂Ox.

In order to determine the nature of products obtained after catalytic process, a control potential electrolysis was performed at $E_{ap} = -1.2$ V (vs SCE). The CO₂ reduction products were characterized in situ by Fourier transform infrared – attenuated total reflectance (FTIR–ATR) spectroscopy (Figure 23a) after the passage of 1 F. The IR data show new peaks at frequencies $\nu = 1580$ cm⁻¹, $\nu = 1380$ cm⁻¹, and $\nu = 1350$ cm⁻¹, which would correspond with the formation of formate, HCOO⁻. [14–16] The reduction process was monitored by cyclic voltammetry (Figure 23b). The cyclic voltammogram recorded at the end of the electrolysis showed two new peaks at anodic scan and cathodic scan related to the oxalate oxidation ($E_{pa} = +0.20$ V vs SCE), and a formate radical reduction formed upon oxalate oxidation ($E_{pc} = -0.89$ V vs SCE), respectively. It is important to note that 73% of compound **1**, which as a redox organic mediator, is recovered

at the end of the process. Therefore, compound **1** is reduced with an electron transfer giving a radical anion species that, through a homogeneous catalysis, would reduce CO_2 into a radical anion, which evolves into a formate anion, recovering the catalyst (Scheme 18).

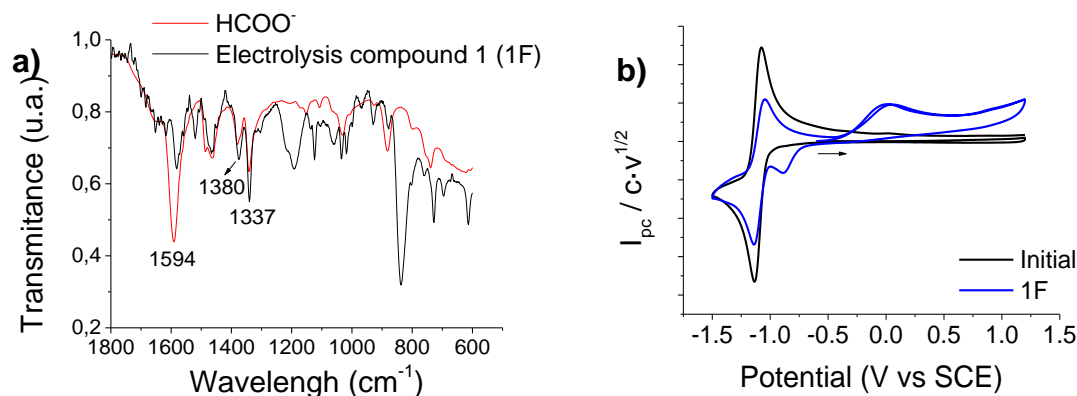
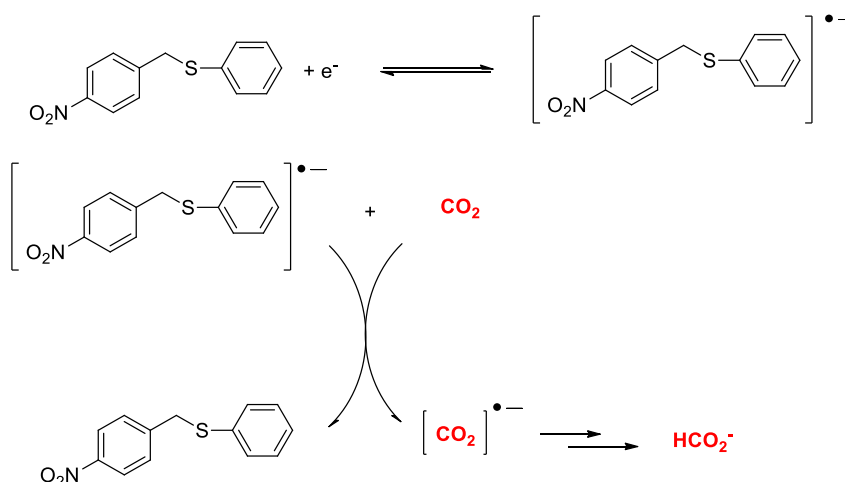


Figure 23. Characterization of compound **1** electrolysis **(a)** IR (ATR) of formate pattern and electrolysis product of **1** **(b)** Cyclic voltammogram of **1** (5.1 mM) in DMF/0.1 M TBABF₄ at 15 °C under inert atmosphere. Glassy carbon disk. Scan rate: 0.5 V·s⁻¹.



Scheme 18. Proposed mechanism for compound **1** reduction after first electron transfer, under CO_2 saturated atmosphere.

3.2.2.2. Second reduction electron transfer process

After the second reduction wave of **1**, a completely different behavior is seen under CO_2 atmosphere (Figure 24). Cathodic scan shows that as the amount of CO_2 is rising in the solution, the peak related to first electron transfer is losing its reversibility and increasing its intensity, acting as an organic mediator in a catalysis process. At the same time, the peak related to second electron transfer disappear.

On the other hand, anodic peaks related to C-S cleavage products changed; the peak of nitrobenzyl anion oxidation, $E_{pa,1} = -0.33$ V (vs SCE) disappears as CO_2 concentration rises in the solution. Moreover, the oxidation peak related to thiophenolate moves into more positive potentials and it may be overlapped with the oxalate oxidation peak $E_{pa,3} = +0.04$ V (vs SCE).

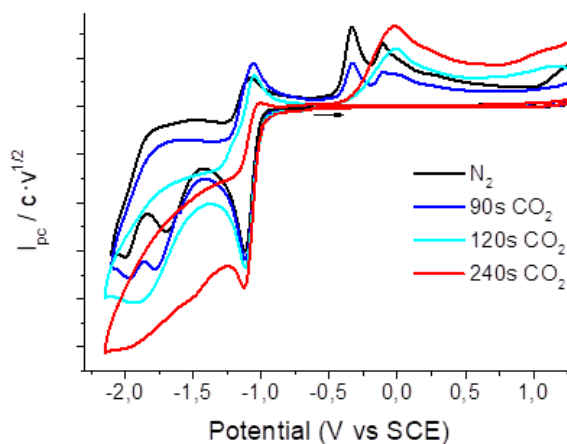
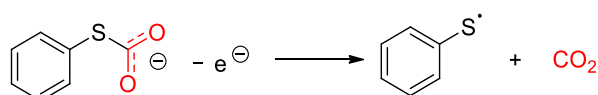


Figure 24. Cyclic voltammogram of **1** (5.1 mM) in DMF/0.1 M TBABF₄ at 15 °C, under different CO₂ concentrations. Glassy carbon disk. Scan rate: 0.5 V·s⁻¹.

Figure 25 shows a CV of sodium thiophenolate under nitrogen and CO₂ atmosphere, where the peak potential value related to its reduction increases, as was previously described by Singh et al. for similar thiophenolate derivatives.^[7] This fact can be explained by the formation of the corresponding carboxylate derivative ((phenylsulfanyl)formate, (Scheme 19).



Scheme 19. (Phenylsulfanyl)formate oxidation proposed mechanism.

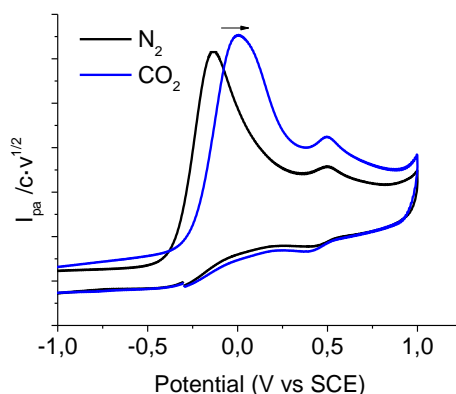
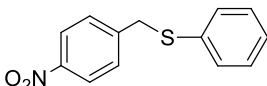


Figure 25. Cyclic voltammogram of thiophenolate, NaPhS, (5.1 mM) in DMF/0.1 M TBABF₄ at 15 °C. Glassy carbon disk. Scan rate: 0.5 V·s⁻¹.

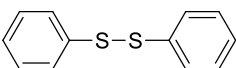
With the aim of determining the nature of the products formed upon reduction obtained by **1**, after a second electron transfer, and a controlled potential electrolysis under CO₂ atmosphere were performed. Note, at this point that it is expected to obtain products coming from homogeneous catalysis, which is produced after first electron transfer, as well as products arising from the electrocarboxylation through C-S cleavage that occurs after the second electron transfer. The results are summarized in Table 4. The nature of the products obtained was determined by nuclear magnetic resonance (¹H-NMR) and gas chromatography coupled with mass spectrometry (GC-MS).

Table 4. Results of electrochemical carboxylation of compound **1**.

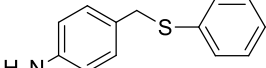
Entries	Electrochemical Parameters		Yield (%)					
	E _{ap} (V vs SCE)	Charge (Q=znF)	1	2	3	4	Carboxylation product 5	Catalysis product Formate
1	-1.9	3F	41	7	47	5	-	20.8 mM
2	-2.3	3F	48.7	51.3	-	-	10	22 mM



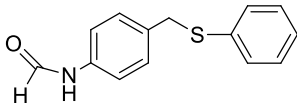
1



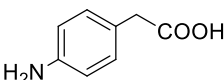
2



3



4



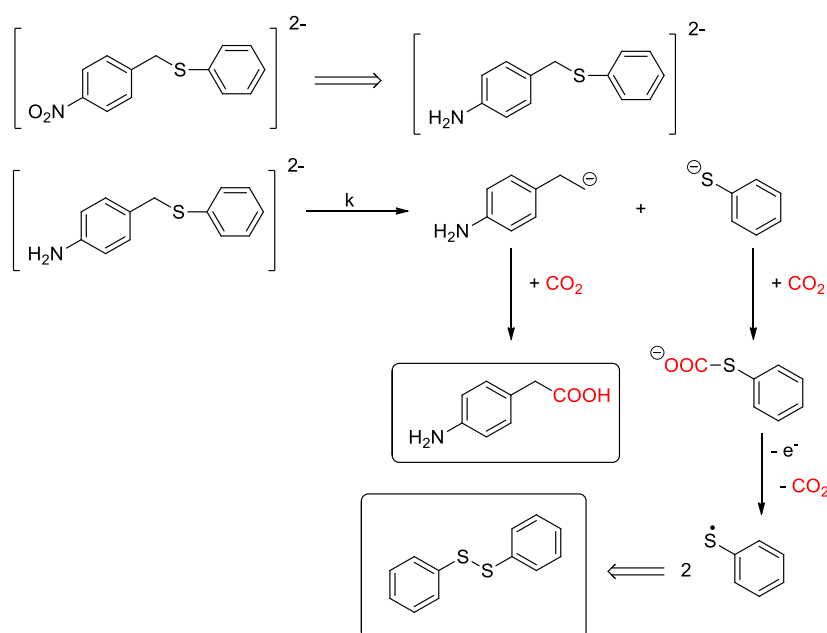
5

At this point, it is possible to propose three different processes occurring at the same time. First, a homogeneous catalysis (anion radical level), which gives rise to formate anion, and the recovery of the reagent in 40-50% yield, as it was explained in Scheme 18.

When a controlled potential electrolysis is performed at -2.3 V (vs SCE) (Table 4, entry 2); a C-S cleavage reaction is taking place, leading to the corresponding carboxylated products, such as **5**, due to a nucleophile-electrophile reaction between CO₂ and the formed aromatic and sulfur anion moieties. Note that the nitro group of the reagent is reduced to its amine analog, **3**. It seems that this reduction reaction occurs before the C-S bond cleavage, since compound **4** and **5** have an amine group instead of a nitro group in the molecule. According to literature results, it may be due to an acidification of the electrolyte solvent by the

CO₂ bubbling.^[17,18] To analyze this effect, a controlled potential electrolysis of **1** in the conditions depicted in Table 4, entry 1, after adding one equivalent of acid (HClO₄) instead CO₂ was performed. In this latter case compound **3** with 20% yield after 2 F, seems to verify the previous hypothesis.

On the other hand, it was obtained compound **4**, which agrees with an N-formylation^[19] of the amine analogue (compound **3**) with formic acid. And the dimer, diphenyl disulfide would be obtained as a result of the oxidation of (phenylsulfanyl)methanoate, losing CO₂ and dimerizing instead. Note, as was previously pointed out, that the (phenylsulfanyl)methanoate anion is not stable enough under these experimental conditions (Scheme 20).



Scheme 20. Proposal mechanism for the electrochemical reduction of **1** under CO₂ at -2.3 V (vs SCE).

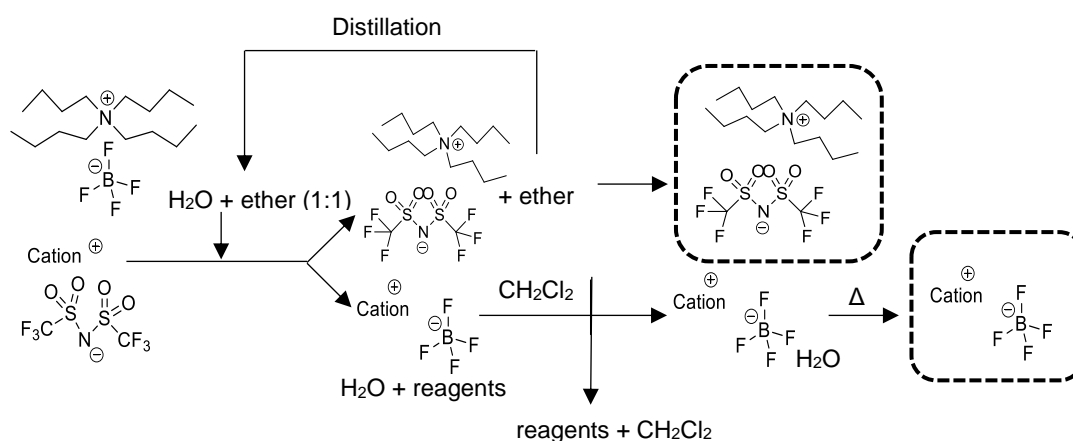
The above-mentioned studies of carbon-sulfur cleavages, performed in CO₂ saturated-DMF solutions, will be gathered in research paper in a scientific journal.

Although it is possible to valorize this gas with electrochemical approaches as it was explained in the above sections, with the aim of introducing greener strategies for the valorization of this gas is needed to synthesize ionic liquids in an easily way.

3.3. Sustainable synthesis of the ionic liquid TBA TFSI

An easy and friendly environmental approach to synthesize an ionic liquid is presented, published in the volume 312 of the Journal of Molecular Liquids as an article entitled “**One-pot sustainable synthesis of tetrabutylammonium bis(trifluoromethanesulfonyl)imide ionic liquid**”. [20]

One-pot synthesis was presented for tetrabutylammonium bis(trifluoromethanesulfonyl)imide, TBA TFSI, by mixing an organic bis(trifluoromethanesulfonyl)imide ionic liquid and tetrabutylammonium tetrafluoroborate salt (TBABF₄), based on a simple ion exchange process. Scheme 21 describes the entire ion exchange process, and how all the solvents employed in the synthesis could be recycled.



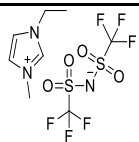
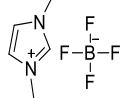
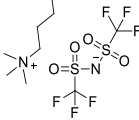
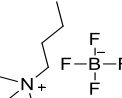
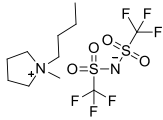
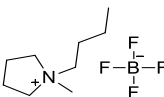
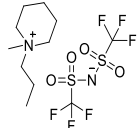
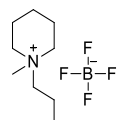
Scheme 21. Ion exchange process between TBABF₄ and TFSI ionic liquid.

An equimolar amount of above-mentioned salt and ionic liquid are dissolved in DMF by stirring the mixture at room temperature. DMF solution was poured into a separator funnel, which contained the same amount of water/diethyl ether. As neither the ionic liquid nor TBABF₄ are soluble in water an ion exchange process takes place. Hence, in the organic phase the desirable TBA TFSI is obtained, after washing and drying the phase with water and anhydrous sodium sulphate. Moreover, as a by-product of the ion exchange, another ionic liquid is obtained, which remains in the aqueous phase. It consists in the cationic part of ionic liquid (C⁺) and the BF₄⁻ anion. It is purified by washings with dichloromethane and recovered by removing the water with heat.

Table 5 summarizes the yields obtained in different ion exchange processes, showing that EMIM TFSI, as ionic liquid, presented the best results. In terms of cost-effectiveness analysis, the present strategy of an ion exchange approach is a low-cost alternative, since the products obtained at the end of the synthesis (ILs) have increased their value by c.a. 40% in comparison with starting materials. Moreover, about 80% of the solvent and reagent used in the synthesis could be recycled and reused.

This methodology could be extended to different bis(trifluoromethanesulfonyl)imide based ionic liquids. However, the ionic liquid exchange process is dependent on the length of the alkyl chain present in the tetraalkylammonium salt. For instance, no ion exchange reaction took place when tetraethylammonium tetrafluoroborate (TEABF₄) salt was used as reagent.

Table 5. Ionic liquid yields obtained after the ion exchange process.

Reactive + TBABF ₄	Products + TBA TFSI	TBA TFSI Yield (%)	C ⁺ BF ₄ ⁻ Yield (%)
		89.0	66.7
		73.4	31.2
		67.3	35.4
		71.2	41.4

A detailed characterization of the different products obtained was performed by nuclear magnetic resonance (NMR) and infrared spectroscopy (IR) is collected in the article, where is shown that these techniques are very useful as characterization techniques for these kinds of reactions, because they show significant differences in the spectral responses between products obtained and starting materials.

3.4. Electrochemical valorization of CO₂ in ionic liquids

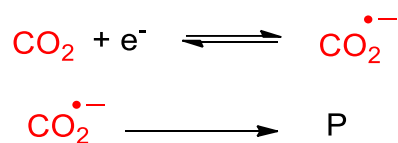
It has been widely showed how CO₂ has very good solubility in ionic liquids. For this reason, different studies have been conducted to determine the different ways that CO₂ could be valorized in this electrolyte media.

On the one hand is related to the direct reduction of CO₂ in an ionic liquid, which is characterized with spectroscopy and electrochemical techniques. On the other hand, there are presented different electrocarboxylations of organic reagents with an electrochemical activation in presence of CO₂.

3.4.1. CO₂ reduction mechanism in EMIM OTf

Taking into account that the Electrochemistry and Green Chemistry Group of UAB has studied the valorization of CO₂ with ionic liquids and electrochemistry, using CO₂ mainly as an electrophile. The electrocarboxylation of EMIM OTf was performed during a short stay abroad at Iowa University, in Scott Shaw's Group who valorize the CO₂ with ionic liquids and electrochemistry together with spectroscopy techniques. Up to know these results are not published.

The main idea in this case was the obtaining of carbon dioxide reduction products through its direct reduction on the surface of silver material in the ionic liquid EMIM OTf (Scheme 22), and its characterization *in situ* by spectroelectrochemistry.



Scheme 22. Electrochemical reduction of CO₂ proposed in EMIM OTf.

Thus, EMIM OTf was electrochemically characterized with spectroelectrochemistry based on cyclic voltammetry coupled with PMIRRAS and IRRAS, under N₂, CO, and CO₂ atmospheres. Noting that it was characterized under CO atmosphere in order to have a pattern of this gas in order to confirm whether it is one of the products obtained.

3.4.1.1. EMIM OTf characterization under N₂ atmosphere

Figure 26 shows the cyclic voltammetry response for EMIM OTf, which is reduced at $E_{pc} = -2.0$ V (vs Pt), due to its imidazolium ring.

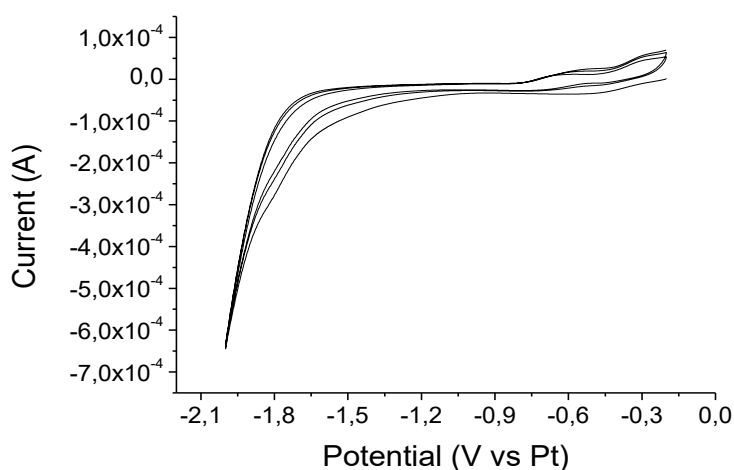


Figure 26. Cyclic voltammetry of EMIM OTf with silver working electrode, CE Pt and Quasi RE Pt. Scan rate $0.5 \text{ V} \cdot \text{s}^{-1}$. Under N₂ atmosphere.

IRRAS and PMIRRAS spectra (Figure 27) show the functional groups which have the ionic liquid in the cationic and anionic part of its structure. The IRRAS spectroscopy also shows ionic liquid functional groups and the environmental interactions (water and carbon dioxide vapor inside the cell). On the other hand, PMIRRAS only shows the electrode surface.

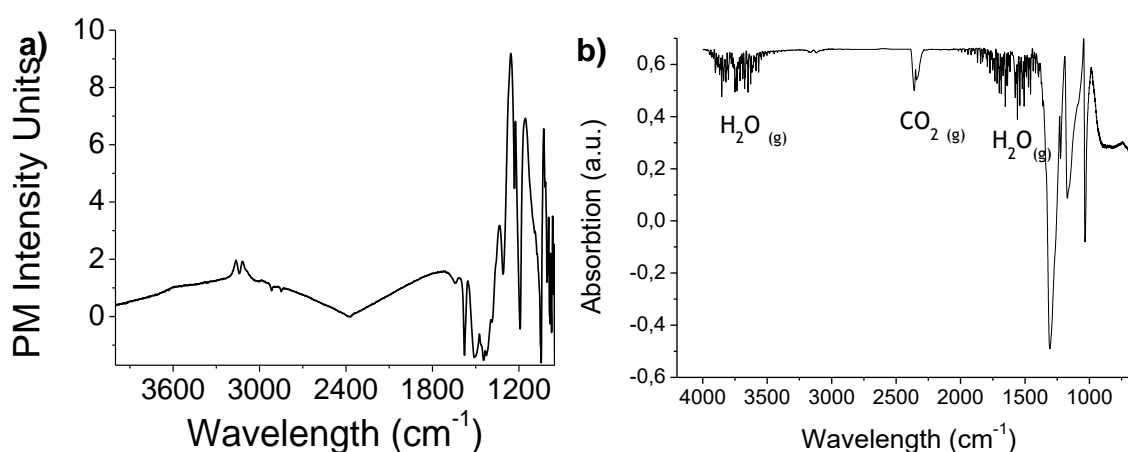


Figure 27. Spectroscopy of EMIM OTf under inert atmosphere on a silver surface (a) PMIRRAS spectra (b) IRRAS spectra.

PMIRRAS shows an improvement in the spectra since there are removed the environmental interactions, so it is possible to see region of $1600\text{--}1300\text{ cm}^{-1}$, where there are peaks arising from C=C stretching, C-H bending, and C-N ring stretching vibrations in the cation structure of EMIM OTf. ^[21,22] The spectroscopic data related to the functional groups of EMIM OTf are summarized in Table 6.

Table 6. EMIM OTf spectroscopy characterization.

Assignments	IRRAS (cm^{-1})	PMIRRAS (cm^{-1})
SO_3 asym str	1263, 1270	1263, 1270
CF_3 sym str	1226	1226
CF_3 asym str	1165	1165
SO_3 sym str	1032	1032
CH_3 asym str	3163	3163
CH_3 sym str	3120	3120
C=C str / C-N str / C-H b	-	1300-1600

To determine how the ionic liquid is reorganized when applying negative potentials, four different potentials were applied across the electrochemical window of the ionic liquid. The imidazolium ring ($1600\text{--}1300\text{ cm}^{-1}$) modes increase with more negative potentials (Figure 28). It is concluded from these data, that the cationic part of EMIM OTf would move nearer to the electrode surface as the potential becomes more negative.

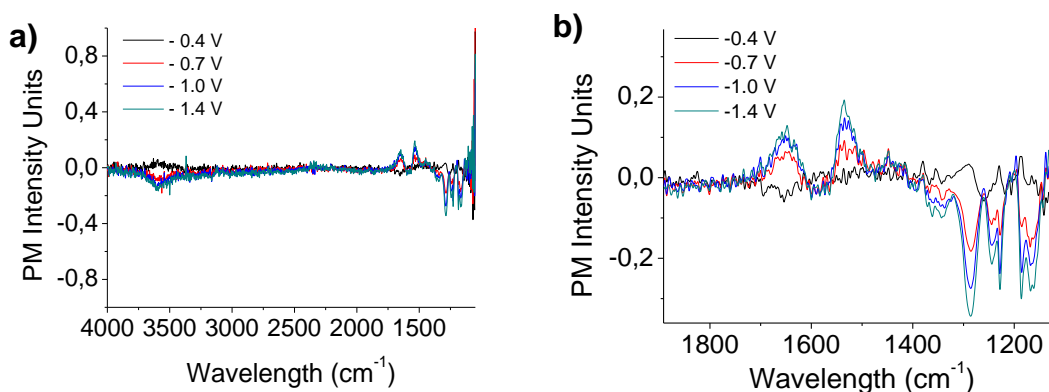


Figure 28. PMIRRAS of amperometric determinations of EMIM OTf at different applied potentials, after subtraction of blanks, under inert atmosphere. **(a)** all wavelength **(b)** zoom at determined wavelength ($1100\text{--}1900\text{ cm}^{-1}$).

3.4.1.2. EMIM OTf characterization under CO and CO₂ atmospheres

Figure 29 shows the cyclic voltammetry response and IRRAS spectroscopy of the ionic liquid in the three different atmospheres; when the solution was saturated with CO or CO₂, IRRAS spectra changed and new peaks appear at frequencies related to CO (2143 cm⁻¹) or CO₂ (2235 cm⁻¹), indicating that CO or CO₂ is present in the solution. However, PMIRRAS spectra is the same as inert atmosphere (Figure 27a), because this method is 'surface sensitive' and only shows what is happening at the electrochemical surface. Therefore, just bubbling the gas into the solution of ionic liquid was not enough to show the presence of CO or CO₂ at the working electrode surface.

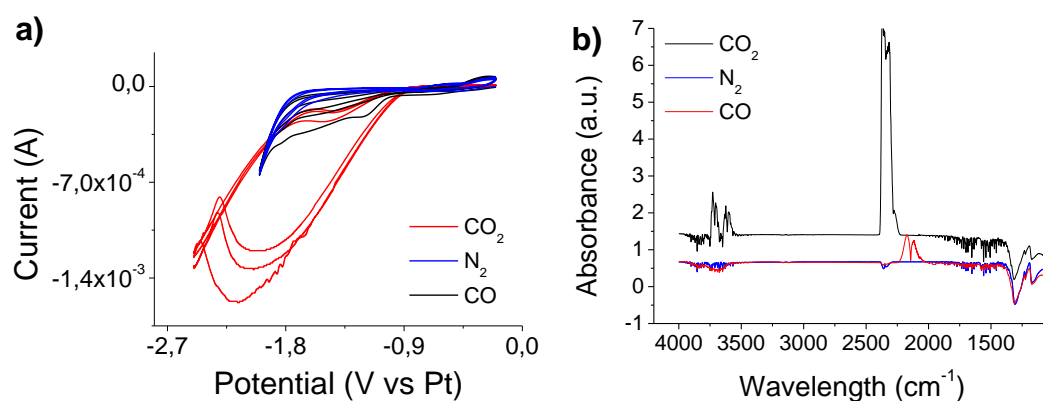


Figure 29. Characterization of EMIM OTf ionic liquid under N₂ (blue line), CO (black line) CO₂ (red line) saturated atmospheres by **(a)** Cyclic voltammetry. WE Ag. Scan rate: 0.5 V·s⁻¹ **(b)** IRRAS spectroscopy.

Cyclic voltammetry shows a huge peak related to the reduction of CO₂ on the silver surface. But under CO and N₂ atmospheres CV response is not shown, because there was no reduction in the electrochemical potential window of EMIM OTf. To determine what is happening in the ionic liquid and on surface of the working electrode when CO₂ is reduced, different determinations of PMIRRAS were performed, coupled to amperometric determinations at E_{pc} = -1.5 V, -1.8 V and -2.0 V (vs Pt) in a carbon dioxide saturated atmosphere.

Figure 30 shows PMIRRAS spectra of the different applied potentials after 1 h. No change in the structure of the ionic liquid is initially observed, but when the negative potential is applied, the peaks related to cationic part of ionic liquid

increase in intensity, which means that imidazolium ring is oriented towards the silver surface.

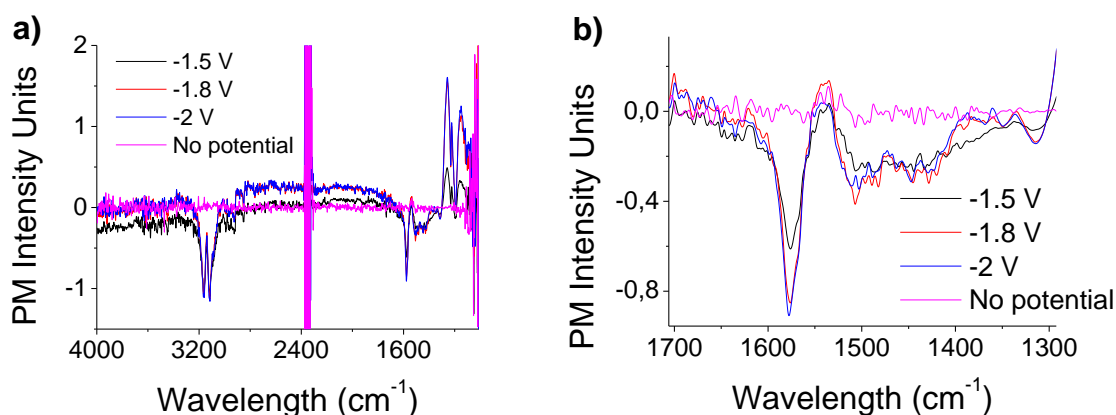


Figure 30. PMIRRAS of amperometric determinations of EMIM OTf at different applied potentials, after 1 h. After subtractions of blank, under CO_2 atmosphere. **(a)** all wavelength **(b)** zoom at determined wavelength (1300-1700 cm^{-1}).

New peaks (1577 cm^{-1} , 1508 cm^{-1} and 1477 cm^{-1}) also appeared and increased in intensity with potential applied. These new peaks could be related to a carboxylated species on the structure of the ionic liquid, because when the ionic liquid was characterized under inert atmosphere, these new peaks did not appear.

If we focus on the 1577 cm^{-1} peak, intensity value increases as potential increases (Figure 31), because a larger amount of carbon dioxide is reduced.

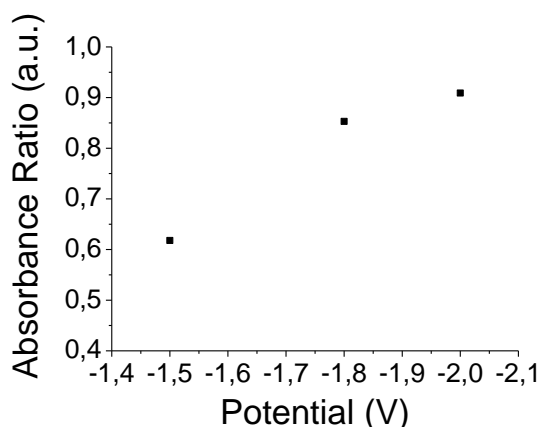


Figure 31. Absorbance ratio versus potential applied at 1577 cm^{-1} peak.

To check that the new peaks are related to CO_2 reduction products, additional experiments were conducted, wherein an applied potential of -2.0 V (vs Pt) was held on the system for 2 h, followed by a brief nitrogen purge to remove carbon dioxide (Figure 32).

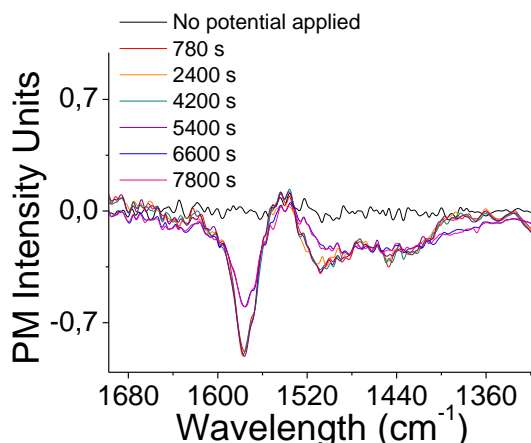


Figure 32. PMIRRAS of amperometric determination at -2.0 V (vs Pt) of EMIM OTf, after subtractions of blank, at determined wavelength (1300-1700 cm⁻¹). 2 h under CO₂ atmosphere and last 10 min under N₂ atmosphere.

This experiment showed that the peaks rise with CO₂, and when CO₂ amount is reduced in the solution these peaks also decreased. This could be checked by looking at the current vs time response in the amperometry experiment (Figure 33).

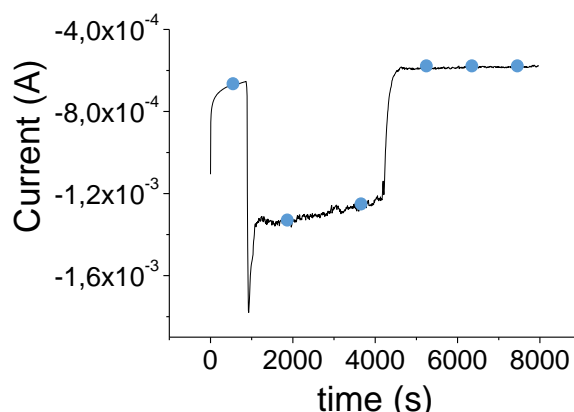
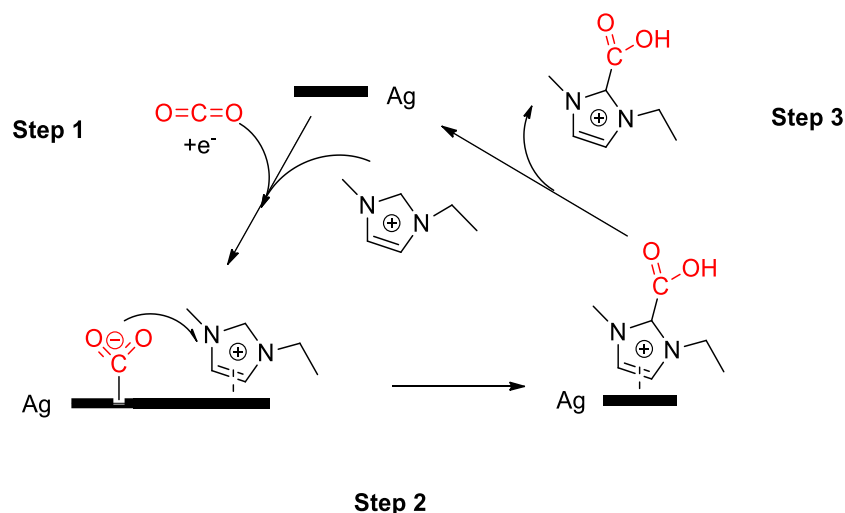


Figure 33. Current (A) versus time (s) response of amperometry experiment at -2.0 V (vs Pt). Blue dots represent the time where amperometry determinations were done.

With all these data, it is possible to see that CO₂ is reduced in EMIM OTf, but instead of obtaining CO as a product, a carboxylated ionic liquid was produced. It is believed that the CO₂ radical anion is generated, which attaches to the ionic liquid structure (Scheme 23), because the frequencies at which the new peaks appear are in the same region of EMIM ring functional groups, which is in agreement with the literature.^[23-28] Moreover, it is known that imidazolium ring is oriented into the surface, and it is easy for the carbon dioxide reduced species to be attached by it.



Scheme 23. Proposed carboxylation process for synthesis of EMIM OTf carboxylated ionic liquid.

3.4.2. Organic molecules in the electrochemical valorization of CO_2 in ionic liquids

A way to reduce directly CO_2 in an imidazolium-based ionic liquid has been shown, with a carboxylated analog being obtained and characterized *in situ* by spectroelectrochemistry, as a way of CO_2 electrochemical valorization in ionic liquids. Later on, another way will be shown on how to valorize this gas in ionic liquids through the electrochemical activation of an organic molecule which activates CO_2 , through a nucleophilic-electrophilic reaction as well as a homogenous catalysis process.

In this sense, taking into account that 4-iodobenzonitrile has the minor bond dissociation energy (BDEs) of the Ar-X bonds, in the article published in the volume 9 of journal *Catalysts* entitled “**Electrocatalytic processes for the valorization of CO_2 : Synthesis of cyanobenzoic acid using eco-friendly strategies**”,^[29] details are presented on the electrochemical behavior of 4-iodobenzonitrile with silver (Ag) and carbon (GC) cathode electrodes in different bis(trifluoromethanesulfonyl)imide ionic liquids.

Figure 34 shows the cyclic voltammetry response for 4-iodobenzonitrile in DMF/0.1 M TBABF₄ and ionic liquids solutions with glassy carbon and silver working electrodes. It is shown that 4-iodobenzonitrile shows the same behavior in ionic liquid solutions than in aprotic media. Moreover, silver cathodic material

shows electrocatalytic properties, decreasing first electron transfer potential about 0.4 V with the use of Ag instead of GC.

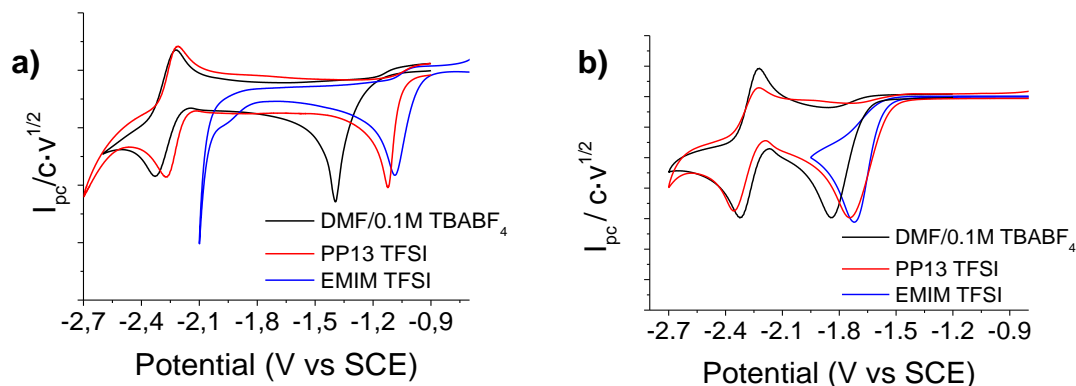


Figure 34. Cyclic voltammetry of 5-10 mM of 4-iodobenzonitrile in DMF/0.1 M TBABF₄ (black line) and the ionic liquid EMIM TFSI (blue line), PP13 TFSI (red line) under inert atmosphere with **(a)** silver and **(b)** carbon working electrode. Scan rate: 0.5 V·s⁻¹.

The electrocatalytic effect when DMF is replaced by ionic liquids is shown in Table 7. When 1-ethyl-3-methylimidazolium bis(trifluoromethanesulfonyl)imide, EMIM TFSI, and 1-methyl-1-propylpiperidinium bis(trifluoromethanesulfonyl)imide, PP13 TFSI, were used as electrolytes, the reduction potential value of 4-iodobenzonitrile was reduced by approximately 0.5 V (17.5 kcal·mol⁻¹) with a silver cathode. Hence, ILs can also act as co-catalysts when silver is used as a working electrode, because the solvation process of the benzonitrile anion appeared to be more effective when a high concentration of cations (ILs) is used instead of tetrabutylammonium salts at low concentration (0.1M TBABF₄ in DMF). Besides, it seemed that the presence of piperidinium cations in the IL composition led to stronger coulombic interactions, which led to better solvation of the benzonitrile anion.

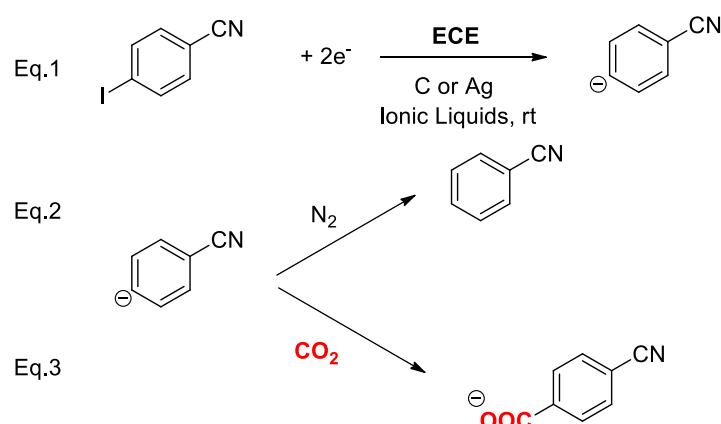
Table 7. Electrochemical parameters associated with first electrochemical reduction of 4-iodobenzonitrile solution under N₂ atmosphere.

Solvent	E _{pc} (V vs SCE)		Electrocatalytic effect (kcal·mol ⁻¹): E _{pc} (Ag) – E _{pc} (GC)
	Ag	GC	
DMF/0.1M TBABF ₄	-1.37	-1.85	10.4
EMIM TFSI	-1.29	-1.84	12.7
PP13 TFSI	-1.07	-1.83	17.5

With the aim of checking that the electrochemical reduction mechanism is the same as in DMF/0.1 M TBABF₄ under inert atmosphere, a control potential electrolysis with ~0.1 V more negative than E_{pc} was performed under inert atmosphere, using either carbon graphite or silver electrodes. In all cases

benzonitrile was the only product (yield 90-95%) obtained after the passage of 2 F. Therefore, an ECE mechanism could describe 4-iodobenzonitrile's reduction in ionic liquids, as occurs in aprotic electrolyte media. In a first Electrochemical step (E), the radical anion of 4-iodobenzonitrile is generated. A Chemical reaction (C) coupled with this first electrochemical transfer led to a benzonitrile radical and iodide through C-I bond cleavage. Finally, the radical is reduced to an anion at the electrode surface by another Electrochemical step (E), which is protonated by reacting with the solvent to obtain benzonitrile.

The obtaining of the benzonitrile anion is the key step to carboxylate 4-iodobenzonitrile through nucleophilic attack with CO₂ (Scheme 24).



Scheme 24. Proposed mechanism for 4-halobenzonitriles (Cl, Br, I) under inert and CO₂ atmosphere.

Taking into account that when CO₂ is reduced in presence of an imidazolium ionic liquid, a complex based on a carboxylated ionic liquid is formed, as was shown in section 3.4.1, the electrochemical study of 4-iodobenzonitrile under CO₂ saturated atmosphere was performed in a piperidinium based ionic liquid, PP13 TFSI. Obtaining the same results that were shown in organic aprotic solvent were obtained (Figure 35).

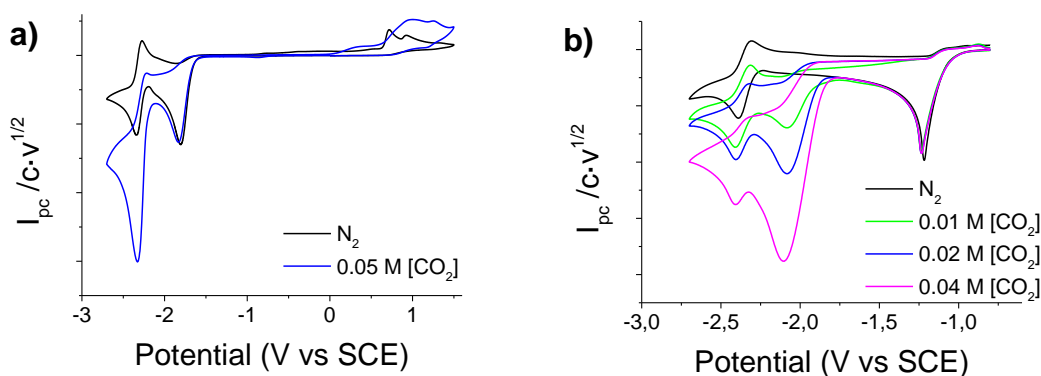


Figure 35. Cyclic voltammetry of 10 mM of 4-iodobenzonitrile in PP13 TFSI ionic liquid with different amounts of CO₂. Scan rate: 0.5 V·s⁻¹ **(a)** WE GC **(b)** WE Ag.

4-iodobenzonitrile and benzonitrile reductions waves were obtained in both electrodes in the same potentials as under inert atmosphere. But, with carbon cathodic material, benzonitrile acts as an organic mediator in a catalysis process, losing its reversibility and increasing its intensity value (Figure 35a). Whereas, with a silver cathodic material, a new peak appears at -2.0 V (vs SCE) instead of -2.3 V (vs SCE) as DMF, which is related to CO₂ reduction on the electrode surface (Figure 35b). Moreover, since the electrochemical reduction of CO₂ occurs prior to the benzonitrile reduction, no electrocatalytic processes were observed related to the role of benzonitrile as a redox mediator.

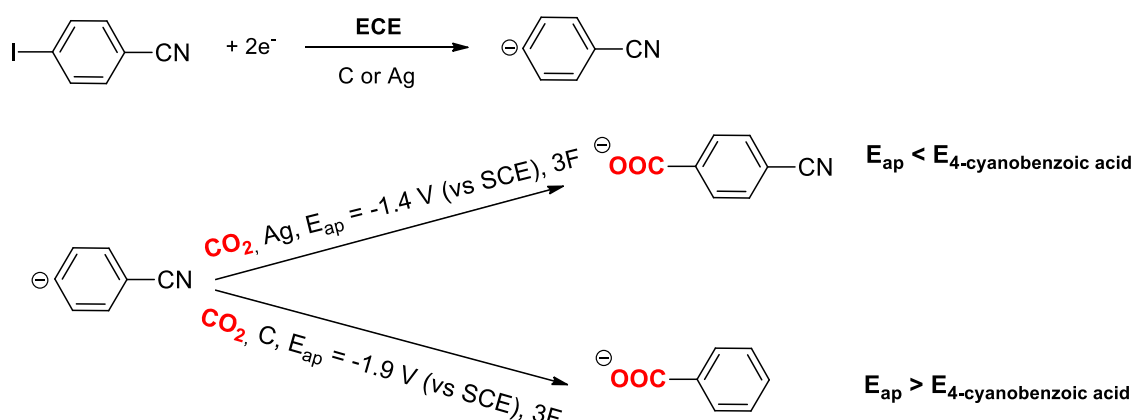
On the other hand, when EMIM TFSI was used as ionic liquid, the electrochemical reduction of benzonitrile was not detected in any electrode due to the fact that the reduction of imidazolium cation appears at a less negative potential under inert or CO₂ saturated atmosphere (-2.2 V vs SCE) and the potential window is not broad enough to arrive at a potential where benzonitrile is reduced. [30]

To determine whether the same carboxylated products are obtained with ionic liquids like DMF/0.1 M TBABF₄, electrocarboxylation processes were performed using carbon graphite rod and a silver foil after ~0.1 V of first reduction wave under a CO₂ saturated atmosphere.

The results obtained showed that, when PP13 TFSI was used, around 10% of electrocarboxylated products were obtained with carbon cathode materials. In addition, at high applied reduction potential values, benzoic acid was obtained, which is in agreement with the reduction of 4-iodobenzonitrile in DMF/0.1 M TBABF₄, described in Scheme 12, Eq. 5-6 (explained in 3.1). It shows

that when the passage of charge increases, 4-cyanobenzoic acid loses a cyanide group. Thus, the reagent has the same behavior in ionic liquid and aprotic media. Moreover, an electrochemical characterization was performed, as well as a control potential electrolysis of 4-cyanobenzoic acid in the same electrochemical conditions, and it was observed that it is reduced at $E_{pc} = -1.6$ V (vs SCE).

Hence, when control potential electrolysis with carbon electrodes was performed, 4-cyanobenzoic acid is reduced at the same time as the reagent, leading to benzoic acid ($E_{ap} < E_{pc, 4\text{-cyanobenzoic acid}}$). On the other hand, using silver cathodes enables working under milder conditions, and, as a consequence, not only were the electrocarboxylation yields almost three times higher, but also the selectivity increases, obtaining only 4-cyanobenzoic acid as a carboxylated product. This is because the applied potential is greater than the reduction potential of 4-cyanobenzoic acid ($E_{ap} > E_{pc, 4\text{-cyanobenzoic acid}}$).



Scheme 25. Electrocarboxylation products obtained in the electrochemical reduction of 4-iodobenzonitrile under CO_2 atmosphere in PP13 TFSI depending on working electrode.

These results can also be reproduced with another two different ionic liquids, such as 1-butyl-1-methylpyrrolinium bis(trifluoromethanesulfonyl)imide, BMPyr TFSI, and N-trimethyl-N-butylammonium methylimidazolium bis(trifluoromethanesulphonyl)imide, N1114 TFSI.

Taking into account the results obtained in the electrocarboxylation process of 4-iodobenzonitrile in ionic liquids, the electrocarboxylation process of 4-chlorobenzonitrile and 4-bromobenzonitrile were shown as an example of nucleophilic-electrophilic reaction between them and CO_2 in ionic liquids solutions, in the experimental research published in volume 6 of the Journal of

Carbon Research entitled as “**Electrochemical tuning of CO₂ reactivity in ionic liquids using different cathodes: from oxalate to carboxylation products**”. [31]

In this case, it presented the electrochemical study of 4-chloro and 4-bromobenzonitrile under CO₂ in DMF/0.1 M TBABF₄ and ionic liquids with carbon, silver and copper working electrodes.

Cyclic voltammetry response of 4-chlorobenzonitrile with three cathodic materials in two different ionic liquids (EMIM TFSI and PP13 TFSI) are represented in Figure 36, where EMIM TFSI shows a smaller potential window than PP13 TFSI, and only the first electron transfer is shown. Dotted lines represent the electrochemical behavior under saturated CO₂ atmosphere, while straight lines are under inert atmosphere. Taking a close look of the CVs, the carbon working electrode did not show any change in both atmospheres, only with PP13 TFSI, which shows a benzonitrile reduction, it is able to appreciate that the second peak loses its reversibility and increases its current value slightly, representing a catalytic process, as was expected.

On the other hand, silver and copper have the same trend, showing a new peak related to CO₂ reduction on the electrode surface, which increases with the CO₂ amount, and overlays the peak related to 4-chlorobenzonitrile reduction. Due to being in ionic liquids, both reduction potentials have very similar values. A benzonitrile reduction peak is also shown, which was not associated with any catalytic feature, but only in PP13 TFSI because EMIM TFSI did not have enough potential window.

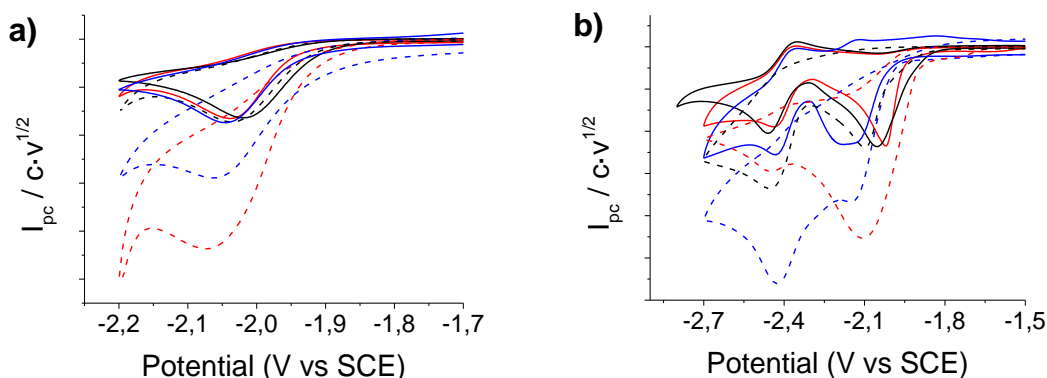


Figure 36. Cyclic voltammetry of 10 mM of 4-chlorobenzonitrile with carbon (black line) silver (red line) and copper (blue line) working electrodes. Scan rate: 0.5 V·s⁻¹. Under inert (straight line) and saturated CO₂ (dotted line) atmospheres in ionic liquids **(a)** EMIM TFSI **(b)** PP13 TFSI.

With the aim of only obtaining nucleophilic-electrophile reactions, both 4- halobenzonitriles were electrocarboxylated with only a carbon cathode, obtaining 4-cyanobenzoic acid and benzoic acid, as happened in the same electrocarboxylation reactions of 4-iodobenzonitrile. Therefore, an ECE mechanism, as in aprotic solvents, could be proposed, and it may be possible to use them as reagents for electrocarboxylation reactions.

In the same publication, the electrochemical behavior of different 4- nitrocompounds (X: CH₃, F, Cl, I derivatives) were presented in order to show how small organic compounds could be used for valorizing CO₂, acting as organic mediators in homogeneous catalysis. Employing electrochemistry and ionic liquids, in this case, to obtain oxalate as a high added value product.

In this sense, 4-nitrotoluene, 4-fluoronitrobenzene, 4-chloronitrobenzene and 4-iodonitrobenzene were characterized by terms of cyclic voltammetry under inert atmosphere in DMF/0.1 M TBABF₄ and EMIM TFSI (Figure 37).

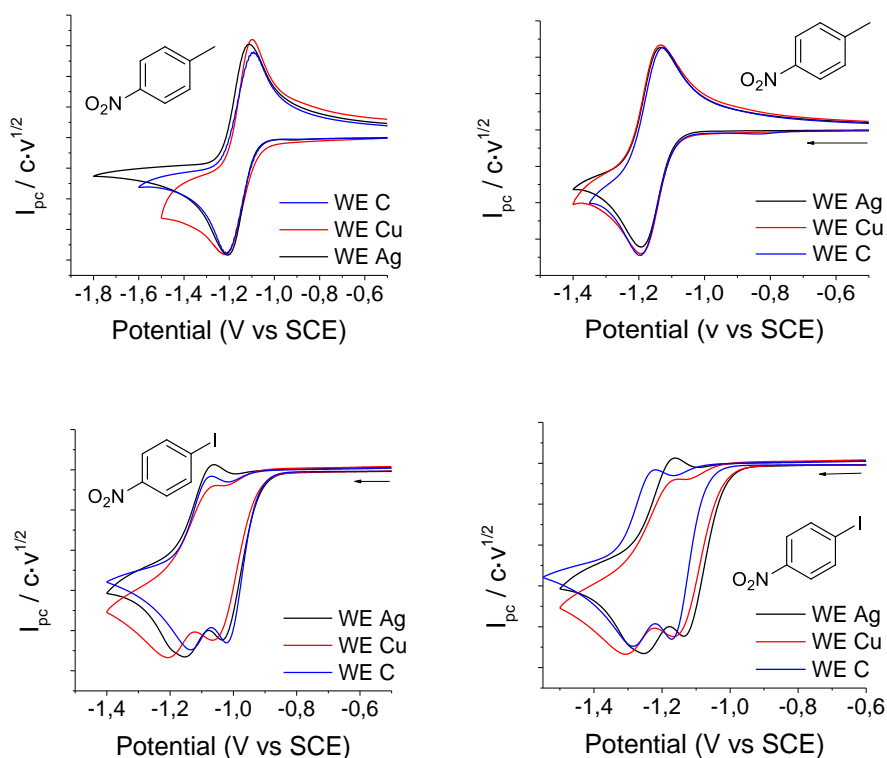


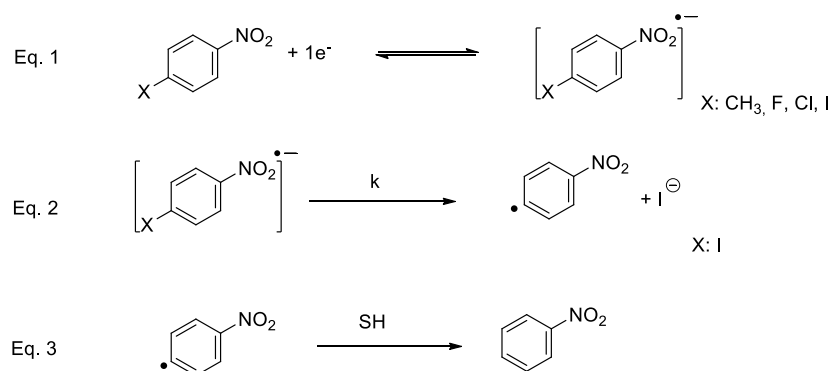
Figure 37. Cyclic voltammetry of 10 mM 4-nitrotoluene and 4-iodonitrobenzene with Ag (black line), Cu (red line) and C (blue line), under nitrogen atmosphere. Scan rate: 0.5 V·s⁻¹. Solution of 10 mL DMF/0.1 M TBABF₄ (left) and solution of 3 mL EMIM TFSI (right).

It was obtained that the cyclic voltammetry response of 4-nitrotoluene (which has the same behavior as 4-fluoro and 4-chloronitrobenzene) was a first reversible

monoelectronic fast electron transfer in both electrolytic media. Only 4-iodonitrobenzene shows a different response in which it shows a first pseudo-reversible monoelectronic electron transfer, which has a k parameter of $2 \cdot 10^4 \text{ s}^{-1}$, whereas the other 4-nitrocompounds have k values of about 2 s^{-1} . It is also followed by another reversible monoelectronic peak.

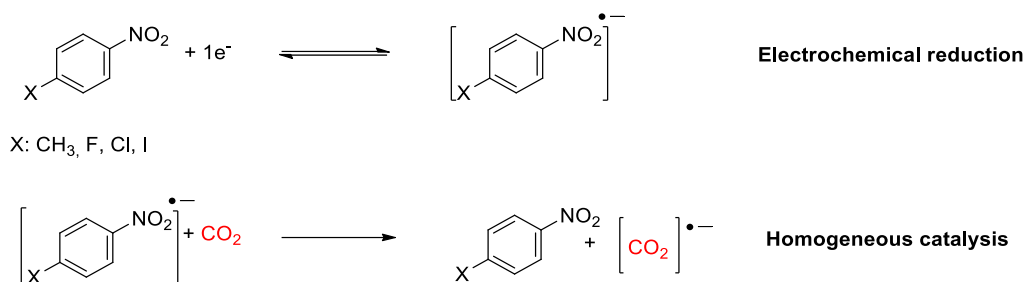
The pseudo-reversibility of the 4-iodonitrobenzene first wave leads to believe that there is a chemical reaction coupled to electrochemical reaction. Hence, to determine the nature of the product obtained after first electron transfer, a controlled potential electrolysis of 4-iodonitrobenzene under inert atmosphere was performed, with 4-nitrobenzene being the only product obtained in both electrolytic media and with three working electrodes.

Considering the cyclic voltammetry and control potential electrolysis experiments performed, it could be proposed that 4-nitrocompounds follow the mechanism depicted in Scheme 26. Where 4-nitrotoluene, 4-fluoronitrobenzene, and 4-chloronitrobenzene follow an electrochemical reduction (Scheme 26, Eq. 1). On the other hand, 4-iodonitrobenzene would follow an EC mechanism where an electrochemical reduction (E) is first produced, followed by C-I cleavage, leading to a nitrobenzene radical and iodide, which could obtain hydrogen atom through an abstraction reaction with the solvent (Scheme 26, Eq 1-3)).



Scheme 26. Proposed mechanism for 4-nitrocompounds (CH₃, F, Cl, I) under inert atmosphere.

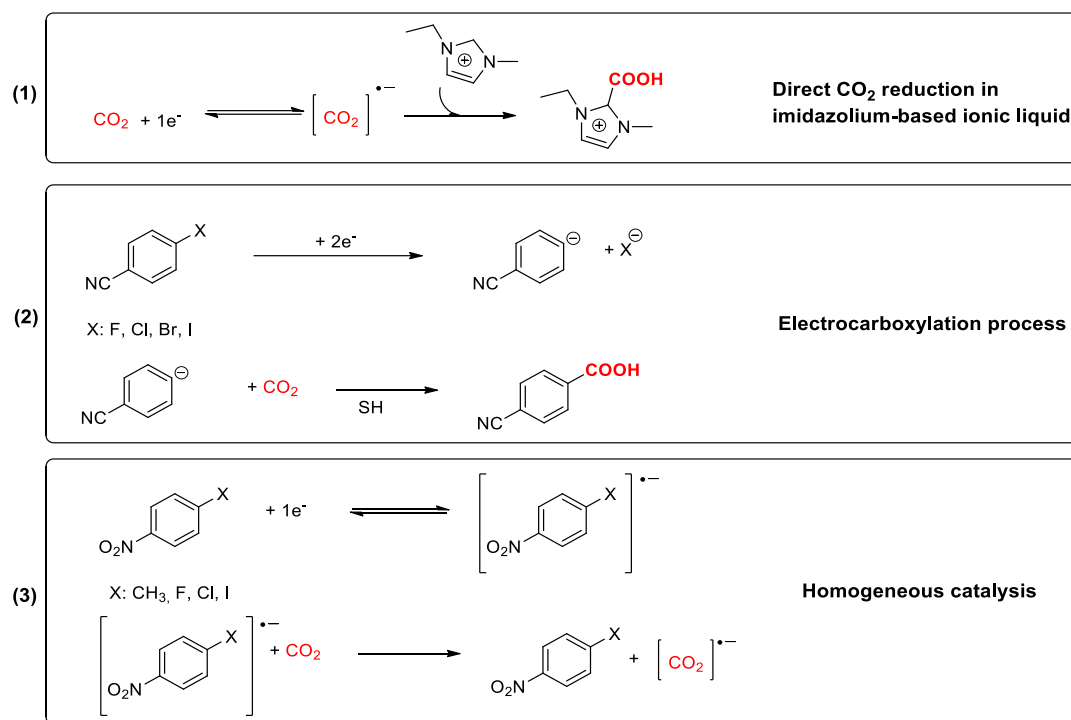
Once the electrochemical behavior of 4-nitrocompounds is determined, the same study under CO₂ saturated atmosphere were performed. In all cases, the reversibility is lost and increases its current value, which indicates that it is producing a homogeneous catalysis, where the 4-nitrocompounds would act as a redox mediator leading to CO₂ reduction (Scheme 27).



Scheme 27. Proposed mechanism for 4-nitrocompounds (CH₃, F, Cl, I) under CO₂ atmosphere.

Moreover, with the electrochemical parameters obtained through CV determinations, it is possible to see that changing methyl group by halides, the standard potential is lowered between 0.08-0.2 V depending on the electrode and halide, having the best results with 4-chloronitrobenzene. In addition, due to low viscosity and coefficient diffusion of CO₂ in EMIM TFSI, turnover frequency (TOF) values and faraday efficiencies determined for both electrolytic media, were better in DMF than in ionic liquid. But in both cases, with the use of small organic molecules such as 4-nitrocompounds, it is possible to obtain similar TOF values (in order of s⁻¹) as with the use of organometallic or more sophisticated compounds, and in a greener way.

To sum up, in this section, three different strategies to valorized CO₂ have been shown (Scheme 28). The first one, the direct electrochemical reduction of CO₂ into an ionic liquid solution. After that, three examples of nucleophilic-electrophilic reaction have been described, where, through carbon-halogen electrochemical cleavage in a saturated CO₂-ionic liquid solution, an electrocarboxylation process is produced that leads to the formation of 4-cyanobenzoic acid. Finally, a catalytic approach in ionic liquids is shown, where through an organic mediator (avoiding the use of metals), it is possible to reduce CO₂ to obtain oxalate species with a homogeneous catalysis.



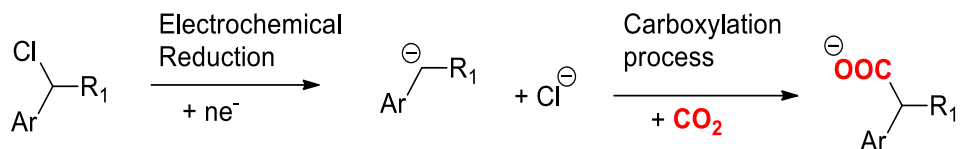
Scheme 28. Strategies to valorized CO₂ in ionic liquids.

Taking into account how well the electrochemical approach works in ionic liquids in order to valorize CO₂, in the following section an attractive electrochemical carboxylation process was developed in which; (1) there is the replacement of conventional electrochemical solvents by ionic liquids, and (2) it is using silver cathode for decreasing the reduction potential values required for C-X bond, removing toxic mediators. For synthesizing two kinds of non-steroidal anti-inflammatory drugs (NSAIDs).

3.5. Electrochemical valorization of CO₂ to synthesized NSAIDs drugs

The electrochemical approach has been previously used to synthesize these kinds of non-steroidal anti-inflammatory drugs, obtaining moderate to good yields [32,33]. However, these electrochemical approaches have the drawbacks of using organic solvents, which are well-known to be hazardous and flammable, as well as the use of large quantities of supporting electrolyte, and the use of toxic organic mediators or high reduction potentials. In this sense, the addition of ionic liquids into the synthetic route could improve these approaches, lowering the reduction potentials and improving the atom economy of the process.

For this reason, focusing on the last steps of the current commercial synthesis of ibuprofen and naproxen, it was decided to introduce our electrochemical approach. This started with an analog with a C-Cl bond, which will be broken to attach CO₂ through an electrochemical carboxylation reaction (Scheme 29).



Scheme 29. Electrochemical carboxylation reaction.

An anion species would be obtained in the electrochemical reduction, which increases its nucleophilic behavior, and would attack the CO₂ attaching it in its structure (carboxylation process). After a chemical treatment, 2- (4- (2- methylpropyl)phenyl)propanoic acid, ibuprofen, or 6- methoxy- α - methyl- 2-naphthaleneacetic acid, naproxen, would be obtained, recycling the ionic liquid employed in the synthesis.

3.5.1. Electrochemical carboxylation approach for synthesis of 2-(4-(2-methylpropyl)phenyl)propanoic acid in ionic liquids

In the case of ibuprofen, the C-Cl reagent was 1-chloro-(4-isobutylphenyl)ethane, which was electrochemically studied with cyclic voltammetry and control potential electrolysis under inert atmosphere in order to determine what could be its proposed mechanism and, then, under CO₂, to perform the electrocarboxylation reaction. These studies were performed in DMF and ionic liquids, and employing carbon and silver working electrodes.

Figure 38 shows the cyclic voltammetry response for 1- chloro- (4- isobutylphenyl)ethane with a carbon working electrode in different electrolytic media (Figure 38a), and a solution of the reagent in the ionic liquid PP13 TFSI in both N₂ and CO₂ atmospheres (Figure 38b).

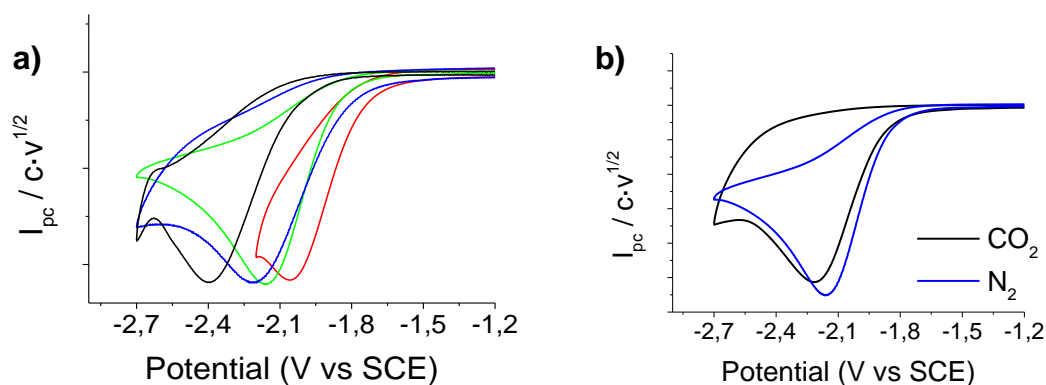


Figure 38. Cyclic voltammetry of 10 mM 1-chloro-4-(isobutylphenyl)ethane with GC. Scan rate: 0.5 V·s⁻¹. **(a)** DMF/0.1 M TBABF₄ (black line), DMF-PP13 TFSI (50:50) (blue line), PP13 TFSI (green line) and EMIM TFSI (red line) **(b)** in PP13 TFSI with N₂ and CO₂ saturated atmospheres.

In cathodic scan, a two-electron irreversible slow reduction wave appears between -1.9 V and -2.4 V (vs SCE) depending on the solvent, which means that there is a chemical reaction coupled to electrochemical reduction. The analysis of the peak current values and their dependence on the concentration and scan rate, indicates that the chemical reaction is a first-order reaction.

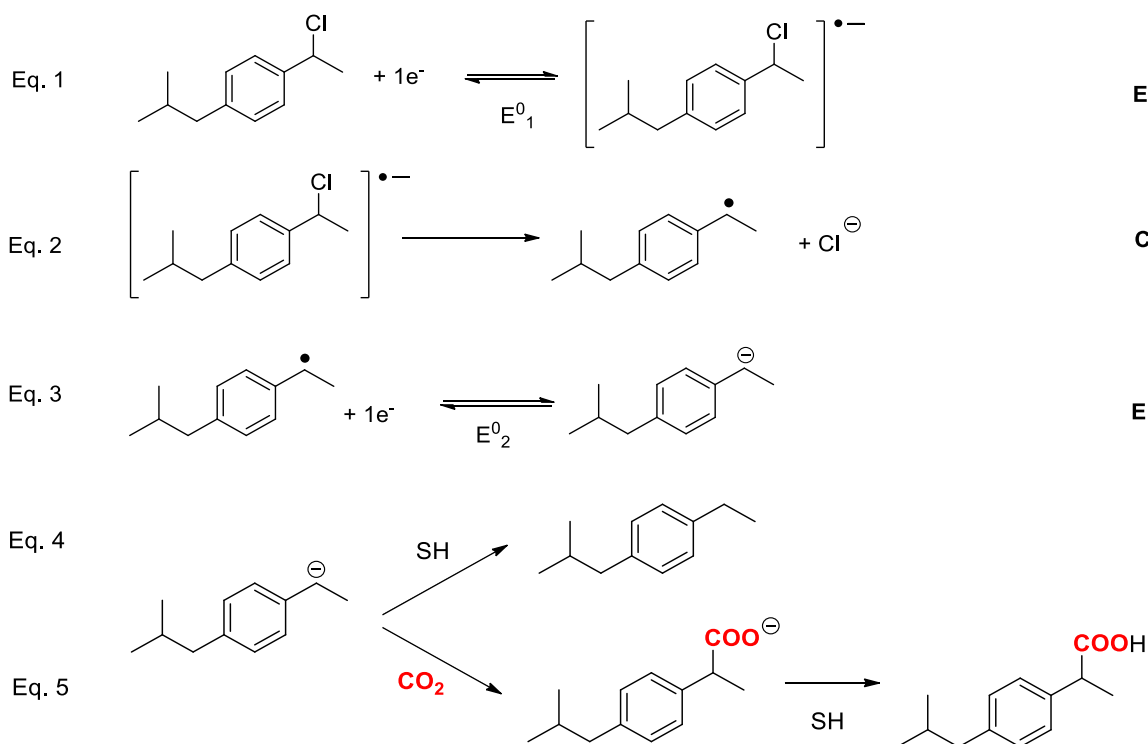
Comparing the E_{pc} values obtained by the electrochemical reduction of 1-chloro-(4-isobutylphenyl)ethane, as happened with 4-halocompounds, ILs are positively shifted, which means that the cations of the ionic liquids act as a catalyst, lowering the reduction potential to more than 0.3 V (7 kcal·mol⁻¹).

After the electrochemical study performed with CV, a controlled potential electrolysis under inert atmosphere was performed to determine the nature of the product obtained after electron transfer. 1-ethyl-4-isobutylbenzene was obtained as unique quantitative product in all electrolyte medias. Overall, the electrochemical reduction mechanism for 1-chloro-(4-isobutylphenyl)ethane has a two electron ECE mechanism in which a C-Cl cleavage reaction is produced (Scheme 30, Eq. 1-4). With these data, CO₂ was bubbled into the solution and the voltammetry response, depicted in Figure 38b, was obtained, where it shows no changes in the electrochemical behavior of the C-Cl reagent. In this case, there is no catalytic process.

The electrocarboxylation reaction was performed with a carbon electrode, using a controlled potential electrolysis of ~0.1 V after the electron transfer reduction potential, and ibuprofen was obtained in moderate to good yields. With the use

of a mixture of DMF and PP13 TFSI, the reaction became greener, and increased the yield up to 75%. It is important to highlight that with the use of dried PP13 TFSI, the obtaining of by-product 1-ethyl-4-isobutylbenzene is avoided.

Hence, following and ECE electrochemical mechanism, 1-chloro- (4- isobutylphenyl)ethane could be converted in ibuprofen through a nucleophile-electrophile reaction between it and CO₂ (Scheme 30, Eq. 1-3 and 5) employing electrochemical techniques and ionic liquid as a solvent.



Scheme 30. Proposed mechanism for 1-chloro-(4-isobutylphenyl)ethane reduction with carbon cathode material under inert and CO₂ saturated atmosphere.

As it is well known that silver cathodes reduce the reduction potential of C-Cl cleavage reactions, it was decided to use them at the same time as ionic liquids in order to improve the electrocarboxylation process.

Hence, the same electrochemical studies of the C-Cl reagent were performed with silver working electrodes in the same ionic liquids and showed the same electrochemical behavior, except that the E_{pc} had considerably positively shifted. The reduction potential could be lowered to about 0.49 V (11 kcal·mol⁻¹) with the use of silver electrode and PP13 TFSI ionic liquid, respectively, on a carbon electrode (Figure 39a). When the solution is bubbled with CO₂, a new reduction peak is detected, which rises as the concentration of CO₂ increases, showing that

this peak is related to CO₂ reduction on the silver surface (Figure 39b), although the 1-chloro-(4-isobutylphenyl)ethane reduction peak remains constant.

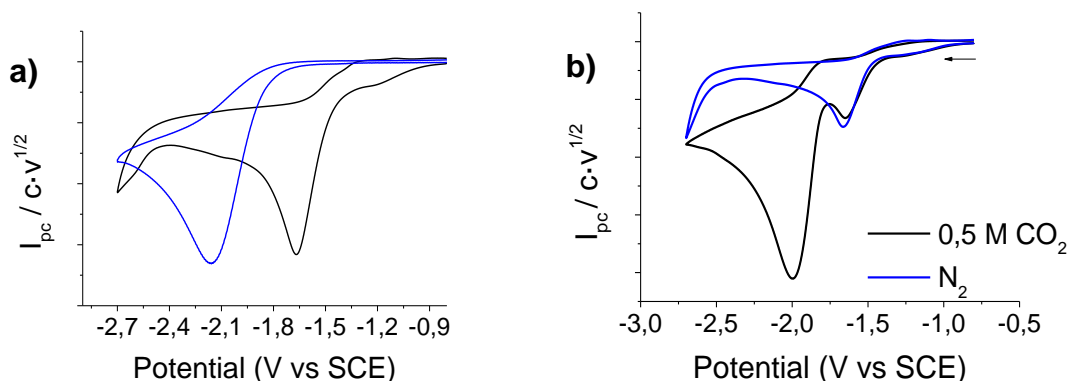


Figure 39. Cyclic voltammetry of 10 mM 1-chloro-4-(isobutylphenyl)ethane in PP13 TFSI. Scan rate: 0.5 V·s⁻¹. **(a)** Comparison of reduction potentials between silver (black line) and carbon (blue line) working electrodes **(b)** N₂ and CO₂ saturated atmospheres with silver electrode.

Therefore, the electrocarboxylation is performed through a control potential electrolysis after 1-chloro-(4-isobutylphenyl)ethane reduction wave (~ 0.1 V after $E_{pc} = -1.7$ V vs SCE in PP13 TFSI), and ibuprofen was obtained with moderate to good yields. This was taken as the most efficient way with the use of dried PP13 TFSI ionic liquid (82% ibuprofen yield) and a silver working electrode.

All these data led to the publishing of the article entitled “**Electrocarboxylation of 1- chloro-(4-isobutylphenyl)ethane with a silver cathode in ionic liquids: an environmentally benign and efficient way to synthesize Ibuprofen**” in volume 9 of RSC Advances journal. [34]

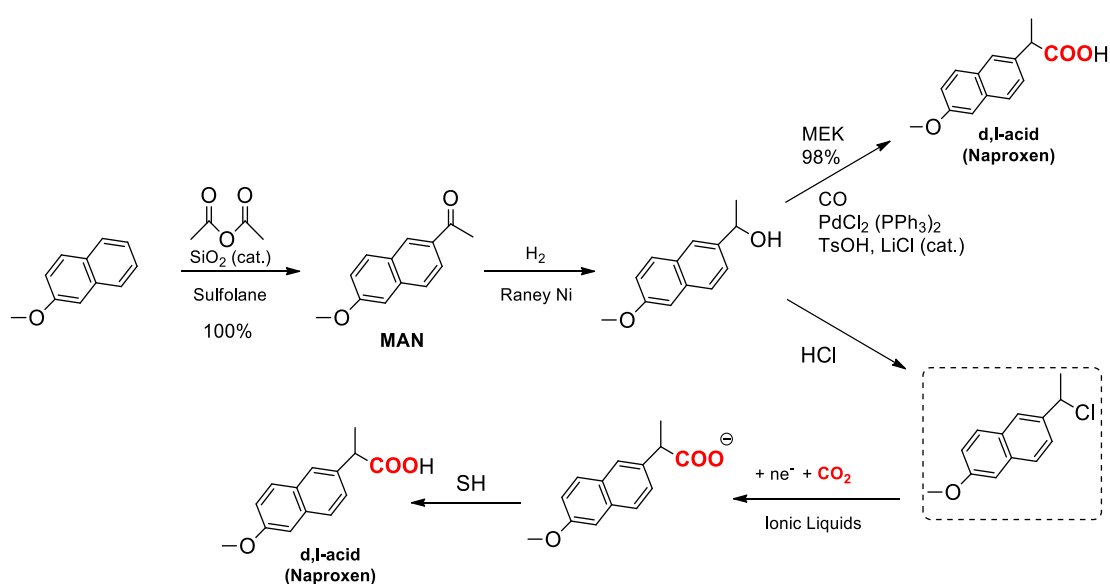
3.5.2. Electrochemical carboxylation approach for synthesis of 2-(6-methoxy-2-naphtyl)propanoic acid in ionic liquids

Following this path, an in-depth study was performed on current manufacturing strategies for obtaining 2-(6-methoxy-2-naphtyl)propanoic acid, Naproxen, to provide a sustainable strategy using electrochemical methods, ILs and CO₂ feedstock.

The manufacture of Naproxen started when it was first commercialized by Syntex in 1976 [35]. But in order to remove some the handicaps of the initial process, it was improved by the same company in 1993, increasing the yield obtained from

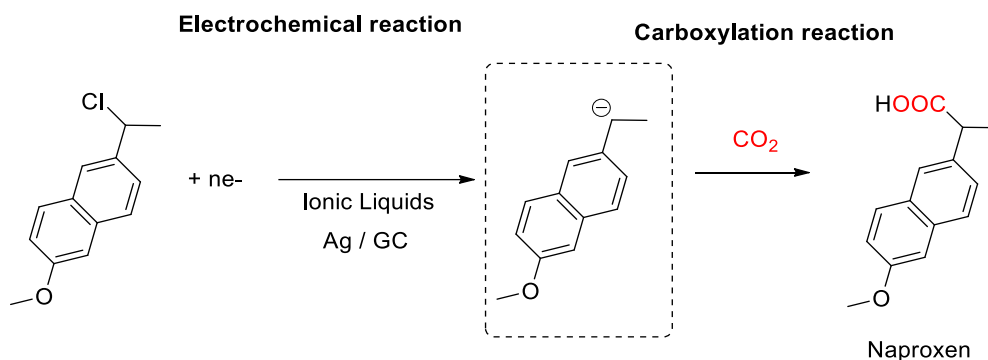
less 50% to 90%. New approaches have also been explored and discussed in the last few years. One of these developed by Nate Shaw and Steve Schlitzer, who introduced the use of safer solvents and auxiliaries (such as catalysts). With that new approach, atom economy increases from 39.4% to 77.7% (taking into account recoverability of the resolving agent).

In this sense, an electrocarboxylation approach was presented, where it was proposed to the change of the reagent employed by Shaw and Schlitzer, which has an C-OH bond instead a C-Cl one, as the good behavior that this kind of C- halide bond has in electrochemistry has been studied. Then, with the use of an electrochemical carboxylation process, CO₂ would be incorporated into the structure of the reactant. It also presents an atom economy analysis of the proposed approach, which showed 36% (65% considering the recoverability of the resolving agent). The results obtained were very similar to those obtained in Shaw and Schlitzer's approach (Scheme 31).



Scheme 31. Both Shaw/Schlitzer adapted synthesis and our proposed synthesis for naproxen.

Focusing on the electrochemical procedure, 2- (1- chloroethyl)- 6- methoxynaphtalene was characterized under an inert and CO₂ saturated atmosphere to determine whether the relative anion is stable enough to perform the attachment of CO₂ (Scheme 32). These characterizations were performed in different electrolytic media (DMF/0.1 M TBABF₄, BMIM TFSI, BMIM BF₄, N1114 TFSI, and BMPyr TFSI ionic liquids), using glassy carbon (GC) and silver (Ag) cathodic materials.



Scheme 32. Electrochemical carboxylation proposed of 2-(1-chloroethyl)-6-methoxynaphthalene based on nucleophilic-electrophilic reaction.

Under inert atmosphere, 2-(1-chloroethyl)-6-methoxynaphthalene shows a two-electron slow irreversible reduction peak as a cyclic voltammetry response, followed by a one-electron reversible one in both working electrodes (Figure 40).

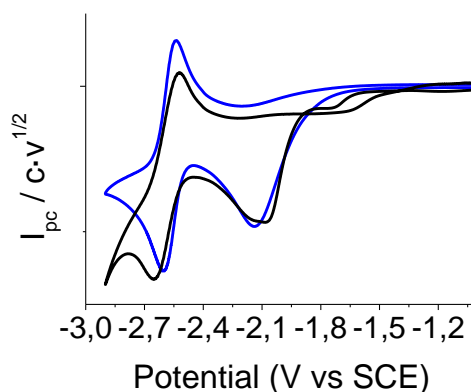
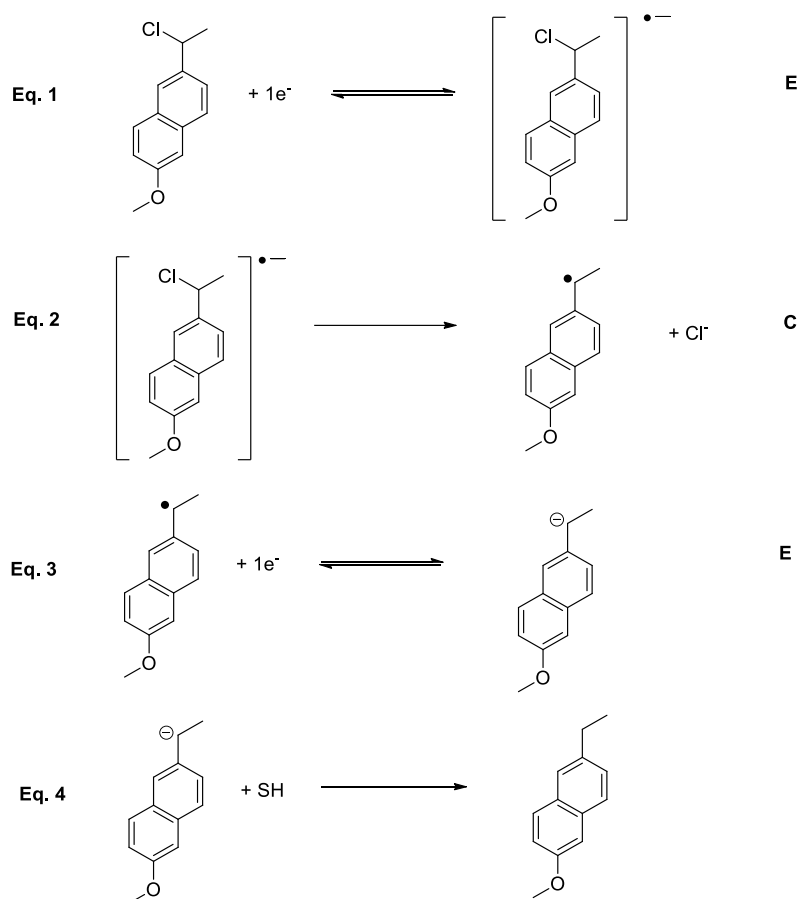


Figure 40. Cyclic voltammetry of 10 mM 2-(1-chloroethyl)-6-methoxynaphthalene in DMF/0.1 M TBABF₄. Scan rate: 0.5 V·s⁻¹. Comparison of reduction potentials between silver (black line) and carbon (blue line) working electrodes.

The analysis of peak current and potential values depending on concentration and scan rate, revealed that the chemical reaction coupled to the electrochemical reduction is a first-order reaction. Therefore, a second reversible one-electron transfer can be assigned to the reduction of 2-ethyl-6-methoxynaphthalene, which was demonstrated with the product obtained after controlling potential electrolysis at $E_{ap} = -2.2$ V (~ 0.1 V after first electrochemical reduction) after 2 F.

The combined use of these electrochemical techniques means that an ECE mechanism for the electrochemical reduction of 2-(1-chloroethyl)-6-methoxynaphthalene can be proposed (Scheme 33).



Scheme 33. ECE proposed mechanism for the reduction of 2-(1-chloroethyl)-6-methoxynaphthalene.

Is important to highlight that when the CV characterization in BMIM TFSI and BMIM BF₄ (imidazolium ionic liquids) was performed, a second electron transfer was not shown as the ionic liquids do not have a sufficiently broad electrochemical window to achieve their reduction potential.

On the other hand, taking into account the E_{pc} values of first electron transfer in all electrolytic media, with the use of ionic liquids, reduction potentials are positively shifted. Showing that it could be lowered to more than 0.24 V (5.5 kcal·mol⁻¹) and 0.33 V (7.6 kcal·mol⁻¹) with the use of carbon and silver electrodes, respectively, as regards the potentials in DMF/0.1 M TBABF₄. Moreover, due to the electrocatalytic behavior that shows a silver electrode in C- halogen cleavage reactions, a 0.07 V (4.8 kcal·mol⁻¹) lowering of reduction potential could be observed when silver is used as cathode.

By bubbling CO₂ into the solution there was a change in cyclic voltammetry response in both electrodes (Figure 41), with the same trend being observed in all electrolyte media tested.

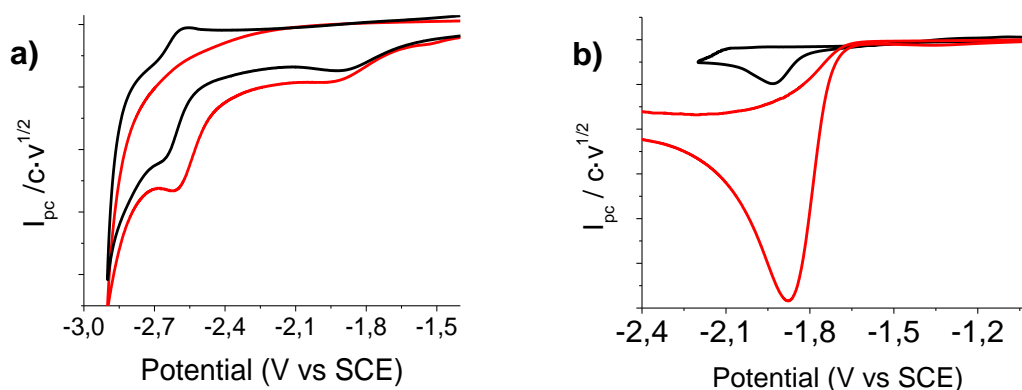
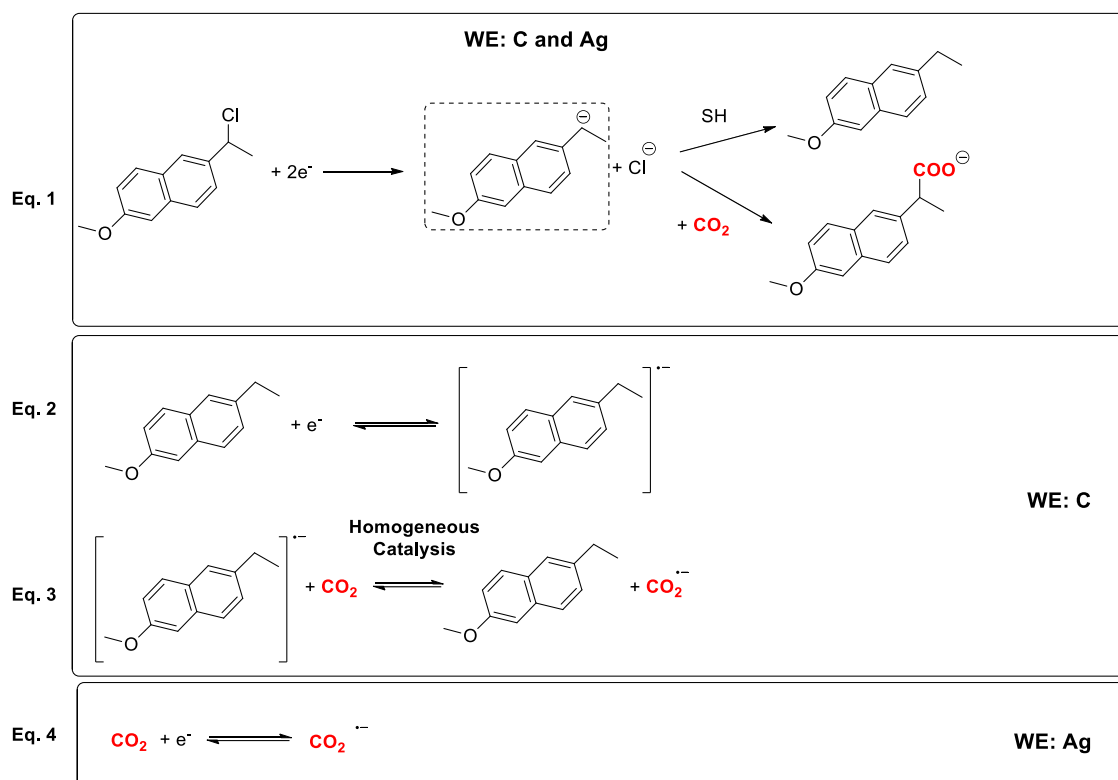


Figure 41. Cyclic voltammetry of 10 mM 2-(1-chloroethyl)-6-methoxynaphthalene in BMPyr TFSI, under N₂ (black line) and CO₂ (red line) saturated atmospheres. Scan rate: 0.5 V·s⁻¹. **(a)** Glassy carbon working electrode, GC **(b)** Silver carbon working electrode, Ag.

By using a carbon working electrode, there is a two-electron reduction wave like the one observed under inert atmosphere, but the second reduction wave becomes irreversible and increases its intensity current value. This behavior describes a catalytic process, where 2-ethyl-6-methoxynaphthalene would act as catalyst to reduce CO₂ through a homogeneous catalytic process producing CO₂ radical anion (Scheme 34, Eq.1-3).

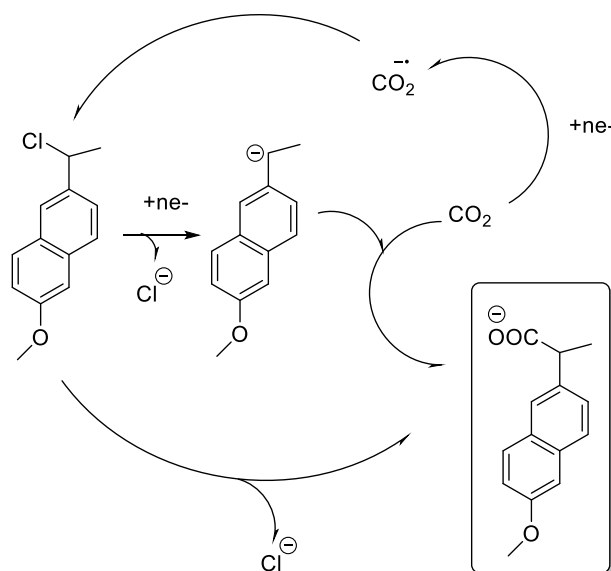
On the other hand, when silver is employed as a working electrode, in a reduction scan, a new reduction peak is detected between c.a. -1.8 V and -2.40 V (vs SCE) depending on the solvent that was assigned to the reduction of CO₂ on the surface of the working electrode. This peak, which increases with the concentration of CO₂, overlays the 2-(1-chloroethyl)-6-methoxynaphthalene reduction wave when the solution is saturated with CO₂. Hence, in some ionic liquid solutions, the reduction of CO₂ occurs before the reduction of the reagent (Scheme 34, Eq.1 and 4).



Scheme 34. Proposed mechanism for electrochemical behavior of 2-(1-chloroethyl)-6-methoxynaphthalene under CO_2 with C and Ag electrodes.

At this point, several electrocarboxylation processes were attempted under CO_2 saturated atmosphere, applying a controlled potential ~ 0.1 V after the first electrochemical reduction potential of 2-(1-chloroethyl)-6-methoxynaphthalene in all electrolyte media using a carbon graphite bar and silver foil as working electrodes.

In all cases naproxen was obtained in a reasonable yield. The best results were obtained when silver was employed as cathodic material and BMIM BF_4 as ionic liquid. This could be because there are two simultaneous carboxylation processes with the use of silver and this ionic liquid through the nucleophilic-electrophilic reaction. In one of them, the nucleophile species would be the anion obtained from the two-electron reduction of 2-(1-chloroethyl)-6-methoxynaphthalene, which would attack CO_2 . The other nucleophile species would be the radical anion of carbon dioxide obtained through its direct reduction on the silver foil surface, which would attack the 2-(1-chloroethyl)-6-methoxynaphthalene reagent (Scheme 35).



Scheme 35. Nucleophilic substitution mechanism operates concurrently.

Hence, the electrochemical triggered dual reactivity enhances the yield of naproxen, showing an environmental approach for this kind of synthesis. The results were collected in the volume 245 of Chemosphere scientific journal as the article entitled “**Sustainable and efficient electrosynthesis of naproxen using carbon dioxide and ionic liquids**”. [36]

In summary, the experimental results of this Doctoral Thesis show a novel set of more sustainable strategies to valorize CO₂ based on synergetic processes, which include the used of electrochemistry and/or green solvents. The ionic liquids give greener features to the process, owing to (1) removing supporting electrolyte and avoiding volatile organic solvents, and (2) the improved energy efficiencies, due to their capacity to lower the reduction potentials, since their particular electrocatalytic behavior, as well as acting as co-catalysts when they are involved with silver cathodic materials.

3.6. Bibliography

- (1) Bouchet, L. M.; Peñeñory, A. B.; Robert, M.; Argüello, J. E. Breaking Bonds with Electrons: Stepwise and Concerted Reductive Cleavage of C-S, C-Se and Se-CN Bonds in Phenacylthiocyanates and Phenacylselenocyanates. *RSC Adv.* **2015**, *5* (16), 11753–11760.
- (2) Bartak, D. E.; Houser, K. J.; Rudy, B. C.; Hawley, M. D. Electrochemical Studies of the Formation and Decomposition of Halogenated Benzonitrile Anion Radicals. *J. Am. Chem. Soc.* **1972**, *94* (21), 7526–7530.
- (3) Reche, I.; Mena, S.; Gallardo, I.; Guirado, G. Electrocarboxylation of Halobenzonitriles: An Environmentally Friendly Synthesis of Phthalate Derivatives. *Electrochim. Acta* **2019**, *320*, 134576.
- (4) Gu, J.; Wang, J.; Leszczynski, J. Electron Attachment-Induced DNA Single Strand Breaks: C3'-O3' σ -Bond Breaking of Pyrimidine Nucleotides Predominates. *J. Am. Chem. Soc.* **2006**, *128* (29), 9322–9323.
- (5) Fleming, S. A.; Jensen, A. W. Photocleavage of Benzyl-Sulfide Bonds. *J. Org. Chem.* **1993**, *58* (25), 7135–7137.
- (6) Fleming, S. A.; Rawlins, D. B.; Samano, V.; Robins, M. J. Photochemistry of Nucleoside Transport Inhibitor 6-S-Benzylated Thiopurine Ribonucleosides. Implications for a New Class of Photoaffinity Labels. *J. Org. Chem.* **1992**, *57* (22), 5968–5976.
- (7) Singh, P.; Rheinhardt, J. H.; Olson, J. Z.; Tarakeshwar, P.; Mujica, V.; Buttry, D. A. Electrochemical Capture and Release of Carbon Dioxide Using a Disulfide-Thiocarbonate Redox Cycle. *J. Am. Chem. Soc.* **2017**, *139* (3), 1033–1036.
- (8) Álvarez-Griera, L.; Gallardo, I.; Guirado, G. Estimation of Nitrobenzyl Radicals Reduction Potential Using Spectro-Electrochemical Techniques. *Electrochim. Acta* **2009**, *54* (22), 5098–5108.
- (9) Borsari, M.; Cannio, M.; Gavioli, G. Electrochemical Behavior of Diphenyl Disulfide and Thiophenol on Glassy Carbon and Gold Electrodes in Aprotic Media. *Electroanalysis* **2003**, *15* (14), 1192–1197.
- (10) Savéant, J. M. Dynamics of Cleavage and Formation of Anion Radicals into and from Radicals and Nucleophiles. Structure-Reactivity Relationships in SRN1 Reactions. *J. Phys. Chem.* **1994**, *98* (14), 3716–3724.
- (11) Chang, M. M.; Saji, T.; Bard, A. J. Electrogenenerated Chemiluminescence. 30. Electrochemical Oxidation of Oxalate Ion in the Presence of Luminescers in Acetonitrile Solutions. *J. Am. Chem. Soc.* **1977**, *99* (16), 5399–5403.
- (12) Rodman, G. S.; Bard, A. J. Electrogenenerated Chemiluminescence. 52. Binuclear Iridium(III) Complexes. *Inorg. Chem.* **1990**, *29* (23), 4699–4702.
- (13) Kai, T.; Zhou, M.; Johnson, S.; Ahn, H. S.; Bard, A. J. Direct Observation of $\text{C}_2\text{O}_4^{\cdot-}$ and $\text{CO}_2^{\cdot-}$ by Oxidation of Oxalate within Nanogap of Scanning Electrochemical Microscope. *J. Am. Chem. Soc.* **2018**, *140* (47), 16178–16183.
- (14) Gomes, J. F.; Garcia, A. C.; Gasparotto, L. H. S.; De Souza, N. E.; Ferreira, E. B.; Pires, C.; Tremiliosi-Filho, G. Influence of Silver on the Glycerol Electro-Oxidation over AuAg/C Catalysts in Alkaline Medium: A Cyclic Voltammetry and in Situ FTIR

- Spectroscopy Study. *Electrochim. Acta* **2014**, *144*, 361–368.
- (15) Pérez, E. R.; Garcia, J. R.; Cardoso, D. R.; McGarvey, B. R.; Batista, E. A.; Rodrigues-Filho, U. P.; Vielstich, W.; Franco, D. W. In Situ FT-IR and Ex Situ EPR Analysis for the Study of the Electroreduction of Carbon Dioxide in *N,N*-Dimethylformamide on a Gold Interface. *J. Electroanal. Chem.* **2005**, *578* (1), 87–94.
- (16) Desilvestro, J.; Pons, S. The Cathodic Reduction of Carbon Dioxide in Acetonitrile. An Electrochemical and Infrared Spectroelectrochemical Study. *J. Electroanal. Chem.* **1989**, *267* (1–2), 207–220.
- (17) Aubakirov, Y. A.; Sassykova, L. R.; Tashmukhambetova, Z. K.; Karymbayev, S. Y.; Sendilvelan, S.; Zharkyn, M.; Zhussupova, A. K.; Batyrbayeva, A. A.; Kayrdynov, S. A. Catalytic Reduction of Aromatic Nitro Compounds: General Questions, Equipment, Enlarged Laboratory Tests. *Int. J. Biol. Chem.* **2018**, *11* (2), 89–98.
- (18) Pearson, J. The Reduction of Nitrocompounds at the Dropping-Mercury Cathode. *Trans. Faraday Soc.* **1948**, *44* (V), 683.
- (19) Dhake, K. P.; Tambade, P. J.; Singhal, R. S.; Bhanage, B. M. An Efficient, Catalyst- and Solvent-Free N-Formylation of Aromatic and Aliphatic Amines. *Green Chem. Lett. Rev.* **2011**, *4* (2), 151–157.
- (20) Mena, S.; Guirado, G. One-Pot Sustainable Synthesis of Tetrabutylammonium Bis(Trifluoromethanesulfonyl)Imide Ionic Liquid. *J. Mol. Liq.* **2020**, 113393.
- (21) Cione, A. M.; Mazyar, O. A.; Booth, B. D.; McCabe, C.; Jennings, G. K. Deposition and Wettability of [Bmim][Triflate] on Self-Assembled Monolayers. **2009**, 2384–2392.
- (22) Anareddy, R. S.; Shaw, S. K. Developing Distinct Chemical Environments in Ionic Liquid Films. *J. Phys. Chem. C* **2018**, *122*, 19731–19737.
- (23) Jr, D. F.; Gonçalves, W. D. G.; Dupont, J. CO₂ Electroreduction in Ionic Liquids. *Front. Chem.* **2019**, *7* (March), 1–8.
- (24) Lau, G. P. S.; Schreier, M.; Vasilyev, D.; Scopelliti, R.; Gra, M.; Dyson, P. J. New Insights Into the Role of Imidazolium-Based Promoters for the Electroreduction of CO₂ on a Silver Electrode. *J. Am. Chem. Soc.* **2016**, *138*, 7820–7823.
- (25) Lim, H. K.; Kim, H. The Mechanism of Room-Temperature Ionic-Liquid-Based Electrochemical CO₂ Reduction: A Review. *Molecules* **2017**, *22* (4).
- (26) Mei, K.; He, X.; Chen, K.; Zhou, X.; Li, H.; Wang, C. Highly Efficient CO₂ Capture by Imidazolium Ionic Liquids through a Reduction in the Formation of the Carbene –CO₂ Complex. *Ind. Eng. Chem. Res.* **2017**, *56*, 8066–8072.
- (27) Rosen, B. A.; Salehi-Khojin, A.; Thorson, M. R.; Zhu, W.; Whipple, D. T.; Kenis, P. J. A.; Masel, R. I. Ionic Liquid-Mediated Selective Conversion of CO₂ to CO at Low Overpotentials. *Science* **2011**, *334*, 643–644.
- (28) Sun, L.; Ramesha, G. K.; Kamat, P. V.; Brennecke, J. F. Switching the Reaction Course of Electrochemical CO₂ Reduction with Ionic Liquids. *Langmuir* **2014**, *30*, 6302–6308.
- (29) Mena, S.; Gallardo, I.; Guirado, G. Electrocatalytic Processes for the Valorization of CO₂: Synthesis of Cyanobenzoic Acid Using Eco-Friendly Strategies. *Catalysts*
-

2019, 9 (5), 413.

- (30) Reche, I.; Gallardo, I.; Guirado, G. The Role of Cations in the Reduction of 9-Fluorenone in Bis(Trifluoromethylsulfonyl)Imide Room Temperature Ionic Liquids. *New J. Chem.* **2014**, 38 (10), 5030–5036.
- (31) Mena, S.; Guirado, G. Electrochemical Tuning of CO₂ Reactivity in Ionic Liquids Using Different Cathodes : From Oxalate to Carboxylation Products. *J. Carbon Research.* **2020**, 6, 34.
- (32) Fauvarque, J. F.; Jutand, A.; Francois, M. Nickel Catalysed Electrosynthesis of Anti-Inflammatory Agents. Part I - Synthesis of Aryl-2 Propionic Acids, under Galvanostatic Conditions. *J. Appl. Electrochem.* **1988**, 18 (1), 109–115.
- (33) Fauvarque, J. F.; Jutand, A.; Francois, M.; Petit, M. A. Nickel Catalysed Electrosynthesis of Anti-Inflammatory Agents. Part II - Monitoring of the Electrolyses by HPLC Analysis. Role of the Catalyst. *J. Appl. Electrochem.* **1988**, 18 (1), 116–119.
- (34) Mena, S.; Sanchez, J.; Guirado, G. Electrocarboxylation of 1-Chloro-(4-Isobutylphenyl)Ethane with a Silver Cathode in Ionic Liquids : An Environmentally Benign and Efficient Way to Synthesize Ibuprofen. *RSC Adv.* **2019**, 9 (1), 15115–15123.
- (35) Harrington, P. J.; Lodewijk, E. Twenty Years of Naproxen Technology. *Org. Process Res. Dev.* **1997**, 1 (1), 72–76.
- (36) Mena, S.; Santiago, S.; Gallardo, I.; Guirado, G. Sustainable and Efficient Electrosynthesis of Naproxen Using Carbon Dioxide and Ionic Liquids. *Chemosphere* **2020**, 245, 125557.

Chapter 4. Conclusions

Chapter 4. Conclusions

Below is presented the main conclusions extracted from the experimental results:

- ❖ An electrochemical study and control-potential electrolysis of 4-halobenzonitriles in CO₂-saturated aprotic solutions employing carbon and silver cathodic materials have been performed, obtaining mono-, and di-carboxylated substituted products from moderate to almost quantitative yields. The use of Ag electrodes enables to perform electrolysis at less negative potential values, because of electrocatalytic features of silver electrode in the C-halogen electrochemical cleavage.
- ❖ 4-nitrobenzyl phenyl thioether could be used as reagent for CO₂ valorization. At low negative potential, first reduction wave level, it is possible to reduce CO₂ by catalytic process where 4-nitrobenzyl phenyl thioether would be an organic mediator, obtaining formate applying only -1.2 V (vs SCE). On the other hand, taking advantage of C-S cleavage, could be obtained high-value added products through nucleophile-electrophile reaction between anions (thiophenolate and 4-ethylanyline) obtained after C-S cleavage and CO₂ applying -2.3 V (vs SCE); on the one hand, obtaining 4-aminobenzylacetic acid. On the other hand, the capture and released of CO₂ by thiophenolate anion.
- ❖ A new route for synthesizing tetrabutylammonium bis(trifluoromethanesulfonyl)imide ionic liquid (TBA TFSI) has been performed, following a sustainable one-pot methodology based on an ionic exchange process. In terms of cost-effectiveness analysis, the proposed approach is a low-cost alternative because the product obtained and the by-product are ionic liquids, which increased their value c.a. 40% in comparison with the starting materials. Besides, around 80% of the solvent and reagent could be recycled and reused at the end of the process.
- ❖ The use of electrochemistry and spectroscopy techniques are sustainable and useful toolkits to valorize carbon dioxide, and to know the mechanism which is happening. EMIM OTf ionic liquid could be characterized with spectroelectrochemistry approaches and it showed that when is applied negative potentials, its structure is reorganized on the surface of the working electrode, where imidazolium part of the ionic liquid is oriented to the electrode surface. On the other hand, when CO₂ is reduced on the surface of silver electrode, the radical anion obtained is attached to the imidazolium part of the ionic liquid and it is formed a carboxylate analogue of EMIM OTf.

- ❖ The obtention of 4-cyanobenzoic acid with an electrochemical activation of 4-iodobenzonitrile with an electrochemical approach in CO₂-saturated ionic liquids media is a new “environmentally-friendly” strategy for producing highly valuable compounds using CO₂ as a building block in ILs. The use of silver instead of carbon cathodes enables 4-cyanobenzoic acid to be obtained from electrochemical reduction under milder conditions with moderate yields and conversion rates.
- ❖ A tuned CO₂ valorization could be obtained depending on the functional group, nitro or cyano, of a series of aromatic halides in CO₂-saturated ionic liquids. An electrocatalytic process using a homogeneous catalysis is seen when nitro derivatives are used, removing metal complexes as a catalyst. The use of cyano derivatives allows to tune the reactivity in function of the reduction potential value applied from electrocarboxylated products (nucleophile-electrophile reaction) to oxalate.
- ❖ A description of a sustainable and highly efficient chemical route for synthesizing useful compounds using CO₂ as a C1 synthon through electrocarboxylation reactions has been presented. This strategy deals with the use of electrochemical techniques and ILs, which allow introduce some of the Green Chemistry principles for the synthesis of NSAIDs. Cyclic voltammetry study and controlled potential electrolysis of 1-chloro-(4-isobutylphenyl)ethane and 2-(1-chloroethyl)-6-methoxynaphthalene in CO₂-saturated ionic liquids solutions obtains Ibuprofen and Naproxen in around 90% yields and excellent atom economy compared with commercial ones. This methodology offers a “green” way for the synthesis of different carboxylic acids that could potentially displace the petrochemical process in a future.

Chapter 5. Publications

Chapter 5. Publications

Electrochimica Acta 320 (2019) 134576



Contents lists available at ScienceDirect

Electrochimica Acta

journal homepage: www.elsevier.com/locate/electacta

Electrocarboxylation of halobenzonitriles: An environmentally friendly synthesis of phthalate derivatives

Irene Reche, Silvia Mena, Iluminada Gallardo, Gonzalo Guirado*

Departament de Química, Universitat Autònoma de Barcelona, Campus UAB, 08193-Bellaterra, Barcelona, Spain



ARTICLE INFO

Article history:

Received 21 May 2019
 Received in revised form
 19 July 2019
 Accepted 22 July 2019
 Available online 23 July 2019

Keywords:

Carboxylation
 Electrochemistry
 Electrolysis
 4-Halobenzonitrile
 Cyclic voltammetry

ABSTRACT

This manuscript presents an efficient approach for producing high valuable compounds using CO₂ as building block. The methodology employed is based on electrochemical techniques, which allow performing eco-friendly chemistry solutions and maintaining the aim of offering a potential long-term strategy for reducing the CO₂ emissions in the atmosphere, while obtaining useful compounds, such as aromatic acids and phthalate derivatives. This work describes the electrochemical reduction behavior of 4-halobenzonitrile compounds using Glassy Carbon and Silver as cathodes under inert and carbon dioxide atmosphere. Controlled potential electrolysis of 4-halobenzonitriles under CO₂ allows obtaining, in very good yields, the corresponding mono- and di-carboxylated organic compounds in CO₂-saturated solutions of dimethylformamide containing 0.1 M of tetrabutylammonium tetrafluoroborate. Electro-catalytic effects are seen when Ag is used as a cathode, which give very high yields, especially as regards di-carboxylated products. The methodology offers a new "green" route for the synthesis of different phthalate derivatives, which can be potentially used for making plastic polymers in a more environmentally friendly way.

© 2019 Elsevier Ltd. All rights reserved.

1. Introduction

The increasing concentration of CO₂ in the atmosphere is a fact that threatens the economy and the sustainability of the planet. In spite of the precautions and actions that have been taken for reducing the emissions arising from fuel consumption processes, more efficient and sustainable ways to ameliorate the climate change problem still need to be investigated, not only for improving the quality life, but also because non-renewable sources are, indeed, limited and still in high demand world-wide [1–3]. Possible alternatives for reducing CO₂ emissions are using low carbon-rich forms as fuel, and capturing and storing CO₂, and for what seems to be the most practical approach is to use it as a carbon building block for producing high valuable compounds [4,5]. In this sense, one of the problems associated with the chemical utilization of CO₂ is related to its inherent thermodynamic stability and kinetic inertness, hence, direct or indirect activation of the functionalization process is required. On the other hand, the use of CO₂ as C1 feedstock has some advantages as an abundant, non-toxic, non-

flammable, and a quite easily available resource [6].

Transformation of CO₂ studies to either convert the CO₂ into more reduced forms or use it as a carboxylating agent in combination with different molecules, have been widely described in the literature. There are also a few examples reported where the CO₂ acts as a C1 building block, including: methane [7–9], methanol [10,11], ethylene glycol [12,13], polyurethanes, urea [14] cyclic carbonates (propylene carbonate) [15–18], carbamates [19–21], and ibuprofen [22–25]. Nevertheless, these transformations are normally associated with high pressures and/or temperatures, low efficiency processes, formation of byproducts, multiple synthetic steps, etc. In the present work, we have developed an electrochemical method in order to overcome those disadvantages, that is, a more environmentally respectful strategy for the utilization of CO₂ to produce high value-added products, and at the same time, a potential way to confront the climatic change at a long-term perspective. In fact, electrochemistry can be seen as a branch of Green Chemistry as it is in accordance with a set of principles for reducing the use of hazardous substances in the design of processes and manufacture of chemical products [26]. The benefits of using electrochemical experiments include mild chemical and process conditions, easy control, high process selectivity, novel chemistry available, safer operation, electrons as inexpensive reagents in

* Corresponding author.

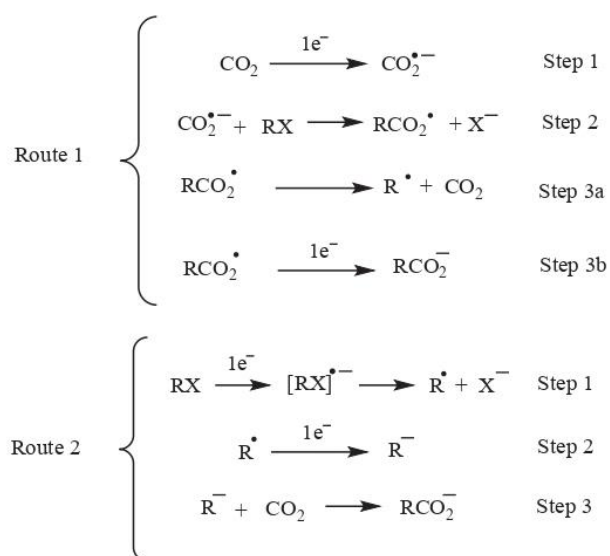
E-mail addresses: gonzalo.guirado@uab.cat, gonzalo.guirado@uab.es (G. Guirado).

comparison with the typical redox agents. In addition, the electrons are capable of acting as heterogeneous catalysts able to be easily isolated from the products.

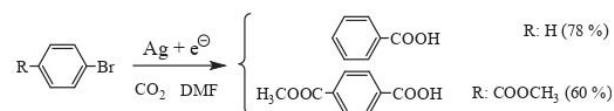
Classical electrochemistry of CO₂ consists of the electro-reduction of the molecule in the presence of an organic aprotic or protic solvent and supporting electrolyte. Apart from the solvent, the nature of the working electrode (WE), the temperature, and the concentration are other important factors. These can be more or less adjustable, not only for tuning the reduction potential of CO₂ but also to modulate the subsequent formation of different products (such as oxalate, carbonate, carbon monoxide, etc.) [27,28].

The electrochemical promoted approaches for achieving carboxylated organic valuable products can mainly be tackled in strategies (Scheme 1). In the first approach, the electrochemical generation of the CO₂ radical anion (CO₂^{•-}) requires a fairly negative potential (Scheme 1, route 1) [29], making this option costly in terms of energy consumed. In the second approach (Scheme 1, route 2), the electrochemical reduction takes places in the organic molecule (for instance, an organic halide RX); which is a more easily reducible compound than CO₂. After being reduced (RX^{•-}), cleaves into the anion halide (X⁻) and the organic radical (R[•]) (step 1). The electro-generated radical can be further reduced to form the corresponding organic anion (R⁻) (step 2). If this organic anion is stable enough in the electrolytic media, it will nucleophilically attack the CO₂ dissolved in the solution, and therefore the CO₂ molecule would be added, leading to a carboxylate derivative (RCO₂⁻) (step 3).

There are some examples in the literature following the second carboxylation strategy. Gennaro et al. have reported electro-reduction processes that lead to carboxylation of different organic [30–32], and non-organic compounds in various solvents and/or working electrodes [33–36]. In one of these studies, they showed that exhaustively controlled potential electrolysis (at –1.5 V vs SCE) of electrochemical reduction of benzyl halides in acetonitrile, using silver as working electrode, under of CO₂ atmosphere at 25 °C, yielded up to c.a. 45% of phenylacetic acid [36]. Zhang et al. also investigated the electro-catalytic carboxylation of bromobenzene derivative using a silver cathode in the presence of CO₂ (at 0 °C) achieving a 78% yield, Scheme 2 [37].



Scheme 1. Electrochemical strategies used for the synthesis of carboxylated products.



Scheme 2. Electrolysis of aryl bromides in the presence of CO₂ in DMF using Ag as working electrode [37].

According to the above mentioned electrocarboxylation strategies and previous studies published [36,37], the use of halobenzenitriles seems to be an ideal starting material for obtaining carboxylated products. The presence of the CN group in the molecule would help to reduce the energy required for the reduction process, since it would act as an electrophore. Thus, the carbon-halogen bond cleavage reaction will occur at less negative potential. Note, that the nature of the electrode would also modify the reduction potential value, so the use of Ag as cathode due to its electrocatalytic properties would also help to decrease the reduction potential value.

Thus, the aim of this study is to valorize CO₂ using halobenzenitriles as a starting material for obtaining carboxylated derivatives using a “green” electrochemical route. The electrocatalytic properties of using Ag instead of C as cathode in the electrochemical reduction mechanism of 4-halobenzenitriles will also be analyzed. It is important to note that the synthesis of dicarboxylated compounds using this strategy would potentially open a very versatile and sustainable approach for making plastic polymers in a foreseeable future (Scheme 3).

2. Experimental section

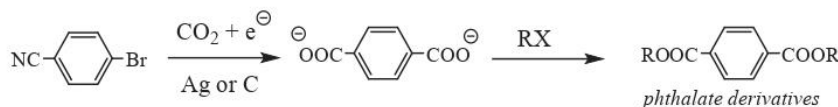
2.1. Reagents

All the commercially available reagents were purchased with the maximum purity and used without previous purification. **Solvents:** Chloroform, SDS, Carlo Erba, for HPLC stabilized with ethanol, ≥ 99.9%. Deuterated chloroform (CDCl₃), Euriso-top, 99.8%. Dichloromethane, Carlo Erba, for HPLC, stabilized with ethanol, ≥ 99.9%. Diethyl ether, SDS, Carlo Erba, purity ≥ 99.0% (GC). *N, N'*-dimethylformamide (DMF), SDS, for synthesis. Toluene, SDS, pure for synthesis. **Supporting electrolytes:** tetrabutylammonium tetrafluoroborate (TBABF₄), Sigma-Aldrich, 99%. **Electro-active substances:** 4-Bromobenzonitrile, Sigma-Aldrich, 99%. 4-Cyanobenzoate methyl ester, Sigma-Aldrich, 99%. 4-Chlorobenzonitrile, Sigma-Aldrich, 99%. 4-Fluorobenzonitrile, Sigma-Aldrich, 99%. 4-Iodobenzonitrile, Sigma-Aldrich, 99%. 9-Fluorenone puriss., Fluka, ≥ 99%. Benzonitrile, Sigma-Aldrich, 99%. Carbon Dioxide, Linde, purity ≥ 99.9993%. Dimethyl terephthalate, Fluka, ≥ 99.0% (GC). **Other reagents:** 2-Bromoethylbenzene, Sigma-Aldrich, 98%. Hydrochloric acid (HCl), Sigma-Aldrich, reactive 37%. Bromoethane (BrEt), Sigma-Aldrich, 98%. Methyl iodide (CH₃I), Sigma-Aldrich, 2.0 M solution in tert-butylmethyl ether, and anhydrous sodium sulfate, Na₂SO₄, Sigma-Aldrich, 99.0%.

2.2. Methodology

2.2.1. Cyclic voltammetry

Firstly, a solution of the electro-active substance is prepared with a known concentration (between 10 and 16 mM) containing 0.10 M of a supporting electrolyte (tetrabutylammonium tetrafluoroborate, TBABF₄) in 10 ml of dimethylformamide (DMF). Once the solution is introduced into the cell, it is deoxygenated (or CO₂



Scheme 3. Electrochemical strategy used in this work for synthesizing phthalate derivatives.

removed) through an influx of an inert gas, Ar or N₂, a process that is repeated between measurements when the cell is opened to clean the working electrode. The working electrode is a vitreous carbon disk of 1 mm diameter. It is polished using a 1 mm diamond paste before each new measurement with a mixture of lubricant and ethanol. The electrochemical used for the set-up of the three-electrode system is conical. The counter electrode is a Pt disk of <1 mm diameter. All the potentials are reported versus an aqueous saturated calomel electrode (SCE) isolated from the working electrode compartment by a salt bridge. The salt solution of the reference calomel electrode is separated from the electrochemical solution by a salt-bridge ended with a frit, which is made of a ceramic material, allowing ionic conduction between the two solutions and avoiding appreciable contamination. Ideally, the electrolyte solution present in the bridge is the same as the one used for the electrochemical solution, to minimize junction potentials. The cyclic voltammetry studies are performed for each concentration of electro-active substance at different scan rates between 0.1 and 1.0 V s⁻¹. Overall, the I-E curves obtained lead to the determination of the electrochemical (E_p, ΔE_p, I_p/(c·v)^{1/2}), and thermodynamic parameters (E°) of the target molecule.

2.2.2. Controlled potential electrolysis

For preparing the solutions to be electrolyzed, a known amount of the 4-halobenzonitrile is firstly dissolved in DMF/0.1 M TBABF₄. The solution is then deoxygenated with an influx of an inert gas (N₂ or Ar), and an initial voltammogram is recorded before starting the electrolysis. The solution is then saturated with CO₂ (determined because no increase in intensity is observed in the I-E response, despite continuing bubbling CO₂ into it), and the electrolysis is immediately started. The applied potential for the reduction of the electro-active substance is about 100 mV more negative than the corresponding reduction wave. A graphite rod was used as a working electrode and a Pt as a counter electrode, isolated from the solution by a salt bridge with electrolyte solution, and an SCE was used as a reference electrode, which was also separated from the solution by a salt bridge. The electrolysis is finished, either when the desired charge is consumed according to the Faraday's Law, or when the initial intensity has been reduced by over 90% (exhaustive electrolysis). At this point, 4 equivalents of an alkylating agent are added (R-Y: R: methyl, ethyl, or 2-ethylbenzene; Y: I or Br) to the solution and kept under constant N₂ bubbling for 15–20 min.

The electrolyzed samples are then extracted with ether/HCl 1 M in the same proportion. The products that are more soluble in acid water (HCl 1 M) (x3) being extracted from the organic phase, and later with H₂O (x2). The aqueous acid phase is finally extracted using ether. The resulting organic phase is dried with anhydrous sodium sulphate, filtered, and evaporated in a rotating evaporator. To finish, the crude reaction is analyzed using ¹H NMR and GC-MS and compared with pure samples.

Typical Procedure for Preparative Electrolysis – Generation of isolated carboxylated products by preparative Electrolysis: a solution of the halobenzonitrile (50–100 mg), which contains 0.1 M TBABF₄ is electrolyzed following the above-mentioned procedure. Four equivalents of the alkylating agent were added at the end of the electrolysis. After that the electrochemical cell was bubbled with nitrogen for 10 min. Later an extraction with ether/HCl 1 M

was performed, and the crude product [or mixture of product(s)] was purified or separated by chromatography on silica gel eluting with mixtures of hexane/dichloromethane (40:60). The yield obtained for isolated products in pure form were a 5% less than the firstly determined for the non-purified crude.

Benzonitrile: GC-MS (70 eV): m/z (%): 103.0 (100) [M⁺], 76.0 (36) [M⁺ – CN], 63.0 (4), 52.0 (6), 51.0 (12).

4-cyanobenzoate methyl ester: GC-MS (70 eV): m/z (%): 161.0 (22) [M⁺], 130.0 (100) [M⁺ – CH₃O], 102.0 (44) [M⁺ – C₂H₃O₂], 75.0 (14%), 51.0 (8). ¹H NMR (250 MHz, CDCl₃) δ (ppm): 3.96 (s, 3H), 7.75 (d, 8.33 Hz, 2H), 8.14 (d, 8.33 Hz, 2H).

Dimethyl terephthalate: GC-MS (70 eV): m/z (%): 194.0 (18) [M⁺], 163.0 (100) [M⁺ – CH₃O], 135.0 (22) [M⁺ – C₂H₃O₂], 120.0 (8) [M⁺ – C₃H₆O₂], 103.0 (13) [M⁺ – C₃H₆O₃], 92.0 (3), 76.0 (13) [M⁺ – C₄H₆O₄]. ¹H NMR (250 MHz, CDCl₃) δ (ppm): 3.95 (s, 6H), (s, 8.10 Hz, 4H).

Diethyl terephthalate: GC-MS (70 eV): 175.0 (13) [M⁺], 147.0 (34) [M⁺ – C₂H₅], 130.0 (100) [M⁺ – C₂H₅O], 102.0 (42) [M⁺ – C₃H₅O₂], 87.0 (5), 75.0 (13) [M⁺ – C₄H₅O₂N].

Terephthalic acid monoethyl ester: GC-MS (70 eV): m/z (%) 194.0 (11) [M⁺], 166.0 (35) [M⁺ – C₂H₅], 149.0 (100) [M⁺ – C₂H₅O], 121.0 (17) [M⁺ – C₃H₅O₂], 104.0 (6) [M⁺ – C₃H₆O₃], 76.0 (9) [M⁺ – C₄H₆O₄], 65.0 (20), 51.0 (5).

4-cyanobenzoate ethyl ester: GC-MS (70 eV): m/z (%): 222.1 (6) [M⁺], 194.1 (20) [M⁺ – C₂H₅], 177.1 (100) [M⁺ – C₂H₅O], 166.0 (35), 149.0 (86) [M⁺ – C₃H₅O₂], 132.0 (2) [M⁺ – C₄H₁₀O₂], 121.0 (19) [M⁺ – C₅H₁₀O₂], 104.0 (24) [M⁺ – C₅H₁₀O₃], 76.0 (23) [M⁺ – C₆H₁₀O₄], 65.1 (21), 51.0 (4).

Diethyl terephthalate: GC-MS (70 eV): 175.0 (13) [M⁺], 147.0 (34) [M⁺ – C₂H₅], 130.0 (100) [M⁺ – C₂H₅O], 102.0 (42) [M⁺ – C₃H₅O₂], 87.0 (5), 75.0 (13) [M⁺ – C₄H₅O₂N].

Terephthalic acid monoethyl ester: GC-MS (70 eV): m/z (%) 194.0 (11) [M⁺], 166.0 (35) [M⁺ – C₂H₅], 149.0 (100) [M⁺ – C₂H₅O], 121.0 (17) [M⁺ – C₃H₅O₂], 104.0 (6) [M⁺ – C₃H₆O₃], 76.0 (9) [M⁺ – C₄H₆O₄], 65.0 (20), 51.0 (5).

4-cyanobenzoate ethyl ester: GC-MS (70 eV): m/z (%): 222.1 (6) [M⁺], 194.1 (20) [M⁺ – C₂H₅], 177.1 (100) [M⁺ – C₂H₅O], 166.0 (35), 149.0 (86) [M⁺ – C₃H₅O₂], 132.0 (2) [M⁺ – C₄H₁₀O₂], 121.0 (19) [M⁺ – C₅H₁₀O₂], 104.0 (24) [M⁺ – C₅H₁₀O₃], 76.0 (23) [M⁺ – C₆H₁₀O₄], 65.1 (21), 51.0 (4).

Diphenethyl terephthalate: GC-MS (70 eV): m/z (%) 374.4 [M⁺], 253.1 (6) [M⁺ – C₈H₉O], 149.0 (12) [M⁺ – C₁₆H₁₈O], 121.1 (5) [M⁺ – C₁₇H₁₈O₂], 104.1 (100) [M⁺ – C₁₇H₁₈O₃], 91.1 (5) [M⁺ – C₁₇H₁₅O₄], 77.1 (3) [M⁺ – C₁₈H₁₇O₄], 65.1 (5), 51.1 (1).

4-cyanobenzoate phenethyl ester: GC-MS (70 eV): m/z (%) 251.3 [M⁺], 130.0 (28) [M⁺ – C₈H₉O], 104.1 (100) [M⁺ – C₉H₉ON], 91.1 (13) [M⁺ – C₉H₆O₂N], 77.1 (M⁺ – C₁₀H₈O₂N), 65.1 (5), 51.1 (5).

3-Phenylpropionitrile: GC-MS (70 eV): m/z (%): 131.1 (25) [M⁺], 103.1 (3) [M⁺ – 91.1 (100) [M⁺ – C₂H₂N], 77.1 (5) [M⁺ – C₃H₄N], 65.1 (12), 51.1 (7).

Benzoate phenethyl ester: GC-MS (70 eV): 226.3 [M⁺], 104.1 (100) [M⁺ – C₈H₉O], 91.1 (8) [M⁺ – C₈H₇O₂], 77.0 (33) [M⁺ – C₉H₉O₂], 65.0 (4), 51.0 (10).

2.2.3. Instrumentation

The cyclic voltammetry at different scan rates and controlled potential electrolysis are performed using a PAR 273A potentiostat

controlled by a computer. Powersuite software is used for data acquisition and data treatment.

^1H NMR spectra were recorded on a Bruker DPX360 (360 MHz) spectrometer and GC-MS analysis were performed using an Agilent Technologies 6850 GC instrument with a 5975C detector.

3. Results and discussion

3.1. Electrochemistry of 4-halobenzonitriles under N_2 atmosphere

A study has been conducted in order to establish the optimal experimental conditions for the optimal electrochemical capture of CO_2 , the electrochemical behavior of 4-halobenzonitriles (F, Br, Cl and I derivatives). Cyclic voltammograms of a 10 ml solution in DMF using 0.1 M of tetrabutylammonium tetrafluoroborate (TBABF₄) were recorded at different scan rates (from 0.10 to 1.0 V s^{-1}) using Ag (solid lines) or Glassy Carbon (GC, dotted line) as working electrodes under N_2 atmosphere for each halobenzonitrile derivative (Fig. 1).

As it can be deduced from Fig. 1, two different electrochemical pathways can be distinguished. The 4-fluorobenzonitrile shows only an electron transfer process, whereas the other halobenzonitrile derivatives show two electron transfer processes up to -2.5 V . Focusing on the first electron transfer process, all the compounds

show an irreversible two electron reduction wave (Table 1). The peak width values (ΔE_{pc}) greater than 56 mV reveal a slow electron transfer process. According to previously reported cyclic voltammetry studies performed in our laboratory [38–40], the second electron transfer process seen when $\text{X} \neq \text{F}$ corresponds to one electron transfer process, is attributed to the electrochemical reduction of benzonitrile. Thus, the benzonitrile moiety is the initial electron acceptor, and the cyano group acts as an intramolecular catalyst of the halogen atom removal when $\text{X} \neq \text{F}$. The electrochemical parameters of the electrochemical reduction of 4-halobenzonitriles are summarized in Table 1. It is worth noting the shape of the cyclic voltammograms recorded at the same for each compound when either GC or Ag is used as a working electrode. The presence of halogen substituents in the aromatic compounds, electron withdrawing groups (because of higher electronegativity), makes easier to reduce them. A closer look to the E_{pc} values of halobenzonitriles reveals. However, there is another effect related to the fact that their lone pair can be incorporated that their tendency to gain electrons and get reduced follows the order $\text{I} > \text{Br} > \text{Cl} > \text{F}$, which indicated that the halogen lone pair can be incorporated in conjugation of the systems affecting the reduction potential values. However, a closer look reveals that, for all the halobenzonitriles studied, the use of Ag to enable the compound to be reduced at less negative potential values

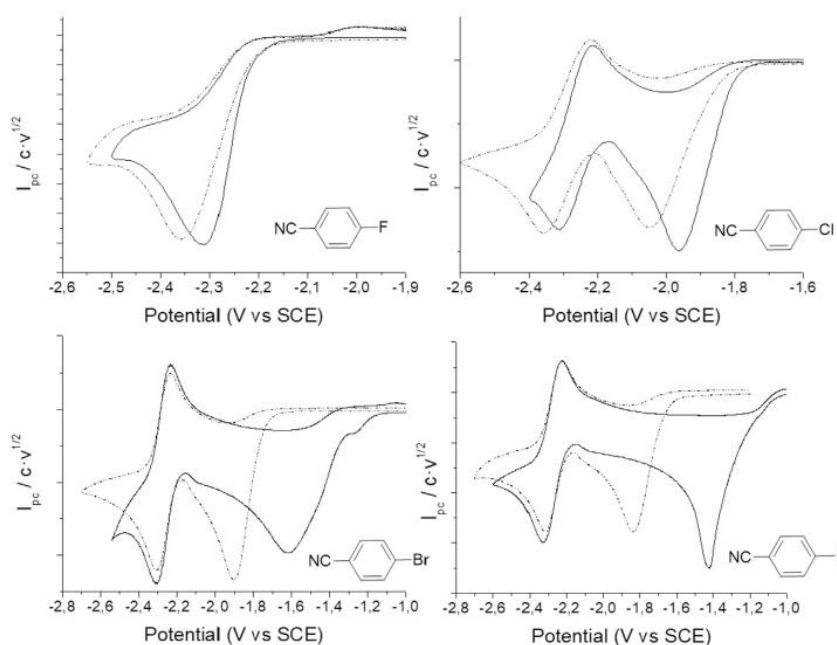


Fig. 1. Cyclic voltammograms of 5–15 mM 4-halobenzonitriles (X: F, Cl, Br and I) solutions using Ag (solid line) and GC (dotted lines) in DMF/0.1 M TBABF₄ under nitrogen atmosphere. Scan rate: 0.5 V s^{-1} .

Table 1

Electrochemical parameters associated to the first reduction wave of 5–15 mM of 4-halobenzonitrile solutions (X: F, Cl, Br, and I) contained in 10 ml DMF/0.1 M TBABF₄ under N_2 atmosphere, using Ag or GC as WEs, respectively, Pt as counter-electrode, and SCE as reference electrode.

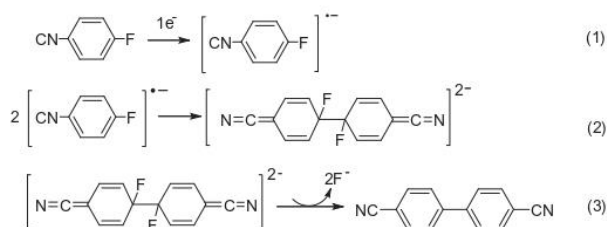
4-Halobenzonitriles	Ag			GC		Electrocatalytic effect: $E_{\text{pc}}(\text{Ag}) - E_{\text{pc}}(\text{GC})$ (mV)
	Number of electrons	E_{pc} (V)	ΔE_{pc} (mV)	E_{pc} (V)	ΔE_{pc} (mV)	
F	2	−2.35	80	−2.38	80	30
Cl	2	−1.95	90	−2.04	100	90
Br	2	−1.75	210	−1.94	110	190
I	2	−1.46	50	−1.84	110	380

demonstrates the electrocatalytic effects of this material.

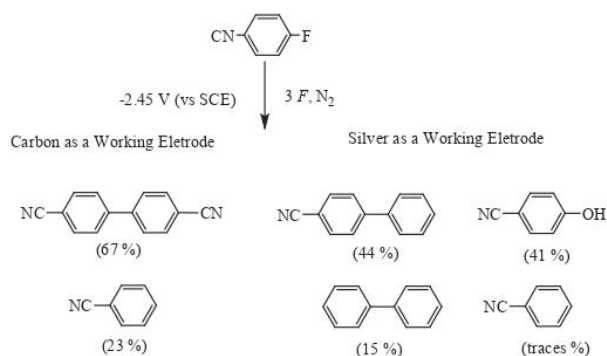
In order to demonstrate the electrochemical reduction mechanism of halobenzonitriles in our experimental conditions, controlled-potential electrolysis was performed after the first reduction wave. In the case of 4-fluorobenzonitrile, exhaustively controlled potential electrolysis experiments were performed at -2.45 V (vs SCE), using 20 mM solutions in DMF/ 0.1 M TBABF₄. The distribution of products obtained after the reduction of the sample depended on the nature of the electrode. In the case of using a carbon graphite rod as cathode, the products obtained were benzonitrile and 4,4'-dicyanobibenzene, which is in good agreement with previously reported studies using Pt as a cathode (Scheme 4). The formation of 4,4'-biphenyldicarbonitrile from 4-fluorobenzonitrile can be rationalized by a dimerization reaction of 4-fluoro-benzonitrile anion radical (Scheme 4, step 2), which decomposes by the elimination of two fluoride anions, leading to the corresponding dimer (step 3).

Benzonitrile and dimer derivatives are also obtained when silver (Ag) foil was used as working electrode, (Scheme 5). In this sense, the electrochemical reduction mechanism appears to be the same in both cases, although the use of silver seems to favor a decyanidation process of the products formed, probably due to an adsorption process of the reduction intermediates at the electrode surface. The presence of 4-hydroxybenzonitrile can be explained due to the reactivity of the reactant (4-F-benzonitrile) in the medium after the electrolysis.

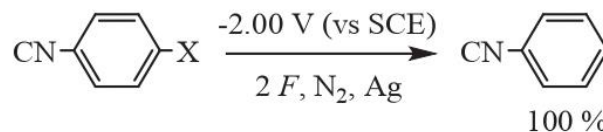
Controlled potential electrolysis experiments of Cl, Br, and I halobenzonitriles (applying a reduction potential value of -0.1 V more negative than its first reduction potential wave using either using C graphite or Ag) reveal the quantitative formation of benzonitrile after the passage of 2 F under nitrogen atmosphere (Scheme 6). The formation of benzonitrile is related to a bond cleavage reaction coupled to the initial electron transfer process.



Scheme 4. Proposed mechanism for the formation of 4,4'-biphenyldicarbonitrile from 4-F-benzonitrile.



Scheme 5. Electrolysis of a 16 mM solution of 4-F-benzonitrile in DMF/ 0.1 M TBABF₄, applying a potential of -2.45 V (vs SCE), consuming 3 F of charge, under a N₂ atmosphere, using silver foil as WE, a Pt counter-electrode, and a SCE reference electrode.



Scheme 6. Electrolysis of 10 mM of 4-halobenzonitrile solutions in DMF/ 0.1 M TBABF₄ under N₂ atmosphere using Ag as a working electrode.

The benzonitrile radical formed is reduced at this potential value, yielding the corresponding anion, which is protonated in last step. Those results are in good agreement with previous work published in the literature using a C electrode, as a working electrode [38,39,41].

From these electrochemical results obtained under inert atmosphere, it is possible to conclude that in the case of Cl, Br and I benzonitrile derivatives the electrocarboxylation process should take place through a nucleophilic attack between the benzonitrile anion and CO₂. Whereas, in the case of 4-F-benzonitrile the electrocarboxylation process would be triggered through a reaction between of 4-F-benzonitrile radical anion and CO₂.

3.2. Electrochemistry of 4-halobenzonitriles under CO₂ atmosphere

Cyclic voltammetry of the different 4-halobenzonitriles (X: F, Cl, Br and I) are performed using Ag and GC under CO₂ atmosphere (Fig. 2). In the case of 4-Br, 4-Cl and 4-I, when either GC or Ag were used as a working electrode two reduction peaks were observed at the same reduction potential values, which were previously determined under inert atmosphere for each electrode. Hence, the first one is related to the reduction of the 4-halobenzonitrile, whereas the second one is related to the reduction of benzonitrile. Note that under CO₂ atmosphere, the benzonitrile reduction peak turns irreversible and increases dramatically its peak current value, which indicates that benzonitrile is acting as an organic mediator (catalyst) for the reduction of CO₂ (Scheme 7). In the case of 1-Fluorobenzonitrile only an increase in the cathodic peak current value is detected since the reactant and products (benzonitrile and 4,4'-biphenyldicarbonitrile), which act as a catalyst appear at the same potential values [28,42]. Note that at low CO₂ concentration (5 mM, Fig. 2D), it is possible to distinguish a third reduction peak at c.a. -2.4 V vs. SCE. According to previous studies performed in our research group, this new reduction peak corresponds to a CO₂ direct reduction at the surface of silver electrode [43].

Electrolysis of 4-halobenzonitriles (X: F, Cl, Br, and I) are performed using a Ag foil or C_{graphite} bar, applying potentials -0.1 V more negative than the previously determined the first reduction wave of each 4-halobenzonitrile (Table 2) in CO₂-saturated solutions with ~ 12 mM of the organic compound in DMF and an excess of supporting electrolyte (0.1 M of TBABF₄ for Ag or TEABF₄ for C). After the consumption of the desired charge, an alkylating agent, methyl iodide (CH₃I), was added to facilitate the separation of the products.

The results of these experiments are depicted in Table 2 (entries 1–7 and 10–14). A general trend is observed in all the cases independently of the nature of the electrode, Ag or C, and the total charge passed (from 1.7 to 4.5 F). When 4-Br-, 4-Cl-, and 4-I-halobenzonitriles solutions are electrolyzed a mix of mono- (4-cyanobenzoate methyl ester) and di-carboxylated (dimethyl terephthalate) products are obtained after the chemical treatment of the sample (Scheme 8 and Table 2, entries 1–7, and 10–14). In contrast, with X = 4-F-, only the di-carboxylated compound is formed (Table 2, entries 1–3). In addition, in all the cases when the total charge passed increases, less reactant remains, and the

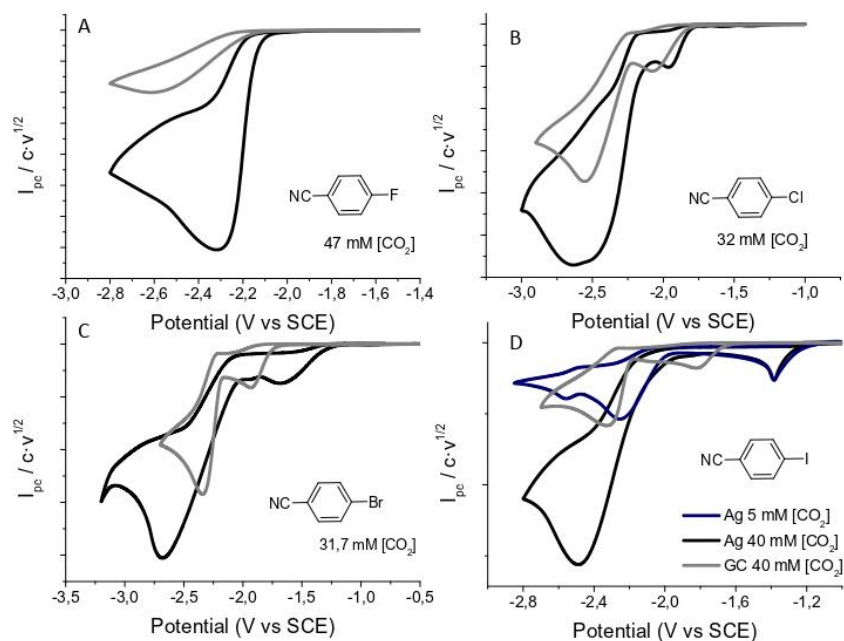
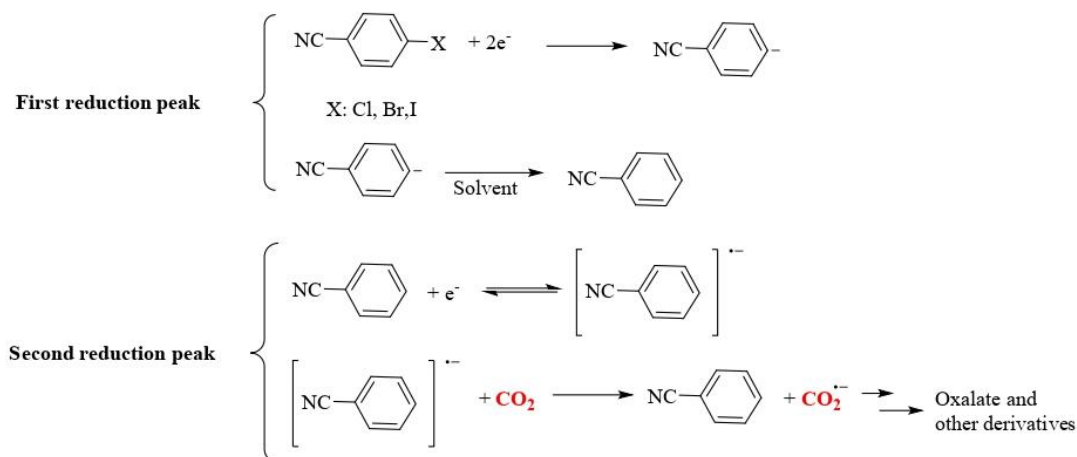


Fig. 2. Cyclic voltammograms of 5–15 mM 4-halobenzonitriles (X: F, Cl, Br and I) solutions using Ag (black lines) and GC (grey lines) in DMF/0.1 M TBABF₄ under at scan rate: 0.5 V s⁻¹ under CO₂ atmosphere.



Scheme 7. Mechanism proposal for the reduction of 4-Cl, 4-Br and 4-I using GC electrode under saturated CO₂ atmosphere.

percentage of di-carboxylation increases.

A closer look at Table 2 revealed that, when C is used as a cathode, moderate yields of carboxylated products were obtained (from 24% to 45%) using high reduction potential values (c.a. -2.00 V vs. SCE, entries 12–14) when non-fluorinated benzonitrile is used. When fluorobenzonitrile is used as a starting material, no carboxylated products were obtained using C graphite as a working electrode. The observed reactivity can be related to the ability of the aromatic radical anions to undergo cleavage of the carbon halogen bond, with the peculiarity that in our case there is a stable fluoride radical anion that dimerises [45].

Replacing C cathode, which acts as an inert electrode, by Ag cathode not only allows reducing the reduction potential value applied but also increasing the yield of carboxylation products

(entries 4–11). Ag electrode is recognized as a powerful catalytic electrode in organic solvent, being its catalytic property ascribed to the adsorption between metal surface and halogenated substrate as well as its reduction intermediates and products. Hence, due to these adsorption processes that favors the stability of reduction intermediates after the same total charge passed, the same consumption of charge, the yield of carboxylation is higher for Ag, but also in global terms, carboxylation is 2–3 times for Ag.

The maximum yield of dimethyl terephthalate (87%, entry 7) is reached for controlled potential electrolysis of a bromobenzonitrile solution at -1.80 V (vs SCE) after the passage of 4.5 F under CO₂ atmosphere using Ag as a cathode. The use of 4-I-benzonitrile also allows obtaining carboxylation yields close to 100% after the passage of 3.5 F. The ratio of % of di-carboxylation/charge consumed is

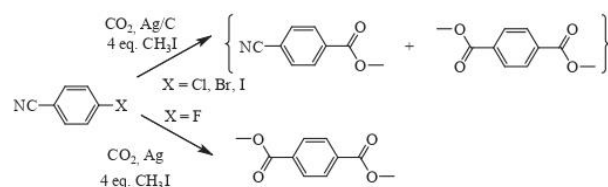
Table 2

Products distribution obtained by electrolysis of 10 mM 4-halobenzonitriles (X: F, Cl, Br, and I) CO₂-saturated solutions in DMF/0.1 M TBABF₄ or TEABF₄, with a Ag foil or C_{graphite}, respectively, after adding 4 equivalents of the corresponding alkylating agent indicated on the right column. "Mono-" and "di-" terms refer to mono-carboxylated or di-carboxylated product.

WE	Entry	Halobenzonitrile (X)	C mol ⁻¹	E _{applied} (V vs SCE)	Alkylating agent	Yield (%) of carboxylated products	
						mono-	di-
Ag ^a	1	F	2.0	-2.45	CH ₃ I	0	11
	2	F	3.5	-2.45	CH ₃ I	0	20
	3	F	4.5	-2.75	CH ₃ I	0	40
	4	Cl	2.1	-2.05	CH ₃ I	20	40
	5	Cl	3.5	-2.05	CH ₃ I	31	49
	6	Br	2.3	-1.80	CH ₃ I	36	29
	7 ^b	Br	4.5	-1.90	CH ₃ I	1	87
	8	Br	4.5	-1.80	Br-CH ₂ CH ₃	10	90
	9	Br	4.5	-1.80	2-Br-CH ₂ CHPh	17	49
	10	I	2.0	-1.80	CH ₃ I	39	31
	11	I	3.5	-1.80	CH ₃ I	28	67
C _{graphite}	12	Cl	1.7	-2.15	CH ₃ I	15	23
	13	Br	2.0	-2.10	CH ₃ I	27	18
	14	I	1.7	-2.10	CH ₃ I	16	12

^a 100% of conversion ratios, the reactant was the only product apart from the electrocarboxylation products recovered at the end of the experiment.

^b In this case a 12% of benzonitrile was obtained at the end of the process, it can be attributed to the application of a higher negative reduction potential value. Under these conditions, CO₂ can be also reduced and react with the halobenzonitrile derivative (Scheme 1 – Steps 1-3a). Finally, a radical cleavage in the Kolbe reaction of the mono-carboxylated product (R-CO₂·) will occur leading to benzonitrile and CO₂ [44].



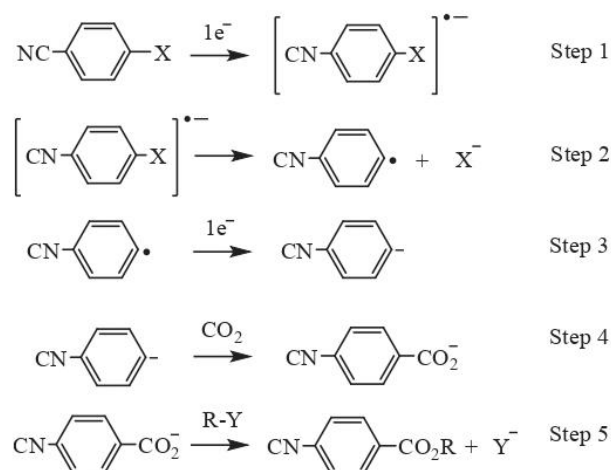
Scheme 8. Electrolysis of 10–14 mM 4-halobenzonitrile (X: F, Cl, Br, I) CO₂-saturated solutions in DMF/0.1 M TBABF₄ or TEABF₄, with an Ag foil or a C_{graphite} rod as WEs and adding 4 equivalents of CH₃I at the end of each experiment.

the same in both cases, thus this could suggest that maybe the adsorption of the I-derived reactant (Fig. 1) plays an important role for the carboxylation process.

As it was previously mention, no carboxylated products were obtained using C graphite as a working electrode for fluoro-benzonitrile. However, the use of silver as a working electrode enables a maximum yield of 40% of dimethyl terephthalate (entry 3) to be obtained after the passage of 4.5 F at of -2.75 V (vs SCE). It is worth noting that, after the passage of the same number of Farads, the total yield of electrocarboxylation products is as follows; I > Br > Cl > F. This fact can be explained by considering the bond dissociation energies (BDEs) of the Ar-X bonds.

On observing the above-mentioned results, it is plausible to propose a mechanism for the insertion of CO₂ in 4-halobenzonitriles (X: Cl, Br, and I) the following mechanism (Scheme 9). In a first step, the reduction of the 4-halobenzonitrile forms the correspondent radical anion, which rapidly cleaves to give the benzonitrile radical, and the corresponding halide (step 2). In a third step, the radical reduces at the electrode surface leading to the benzonitrile anion. In a further step, this anion can react with CO₂ under CO₂-saturated atmosphere, leading to 4-cyanobenzoate anion (step 4). Finally, the addition of iodomethane as alkylating agent (R-Y) yields the correspondent ester (step 5).

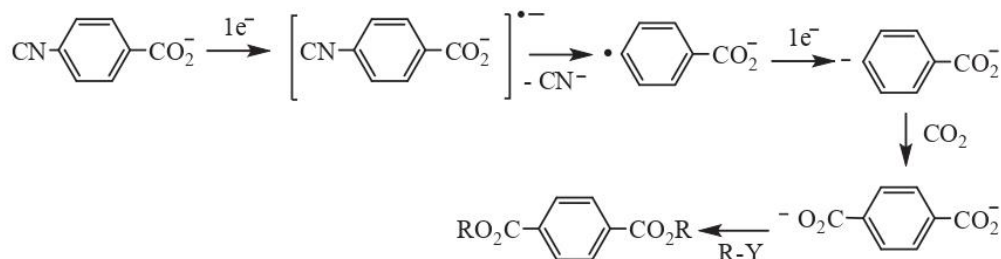
Note that the ratio of carboxylated products (4-cyanobenzoate methyl ester vs. dimethyl terephthalate) can be tune in function of the charge passed during the electrolysis. This fact should be related to the reduction of the 4-cyanobenzoate formed upon the



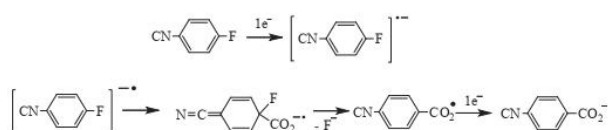
Scheme 9. Electrochemical Strategy for inserting CO₂ in 4-halobenzonitriles (X: Cl, Br, and I).

electrolysis, this dianion can act as a nucleophile and react with the CO₂ (Scheme 10). Lately, the decyanation of dianion has taken place. This mechanism is supported by the detection of cyanide anion at the end of the electrolysis. Hence, the formation of the carboxylated di-substituted products is related to the reactivity of the nitrile group in presence of CO₂. Moreover, reductive decyanation processes for similar compounds has been previously reported in the literature [46–48].

In the case of 4-fluorobenzonitrile then only carboxylated product obtained after the electrocarboxylation process in Ag was the dimethyl terephthalate. In this case, the electrocarboxylation is very selective and enables yields of 40% to be obtained, as has been previously pointed. The plausible electrocarboxylation mechanism is depicted in Scheme 10. The fluorobenzonitrile anion radical reacts with CO₂ instead of dimerization leading to a benzonitrile carboxylated derivate (Scheme 11). This derivate is not stable at high negative reduction processes values and further reduction are



Scheme 10. Electrochemical reduction mechanism of 4-halobenzonitriles (X: Cl, Br, and I) under CO₂ atmosphere after the passage of 3–4 F.



Scheme 11. 4-fluorobenzonitriles under CO₂ atmosphere electrochemical reduction mechanism.

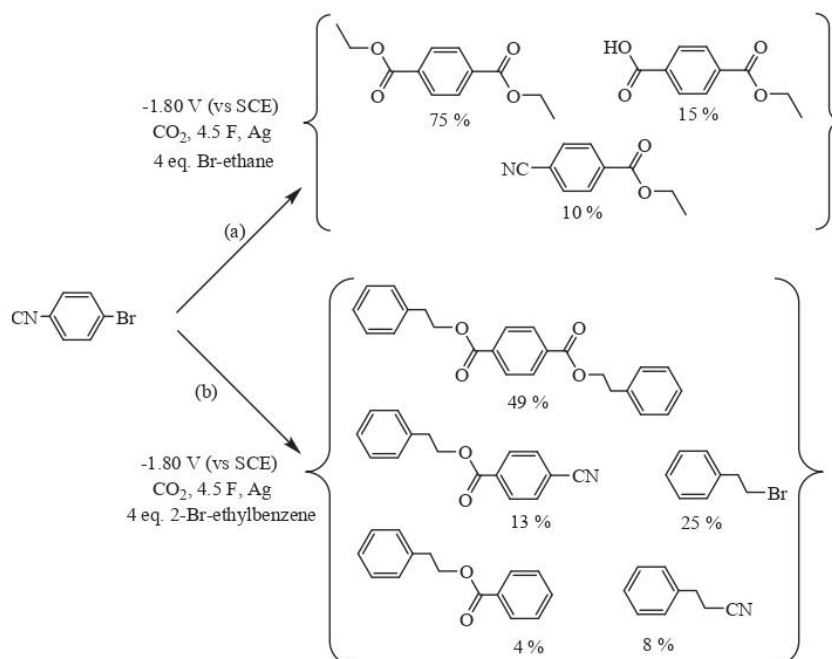
taking place following the same mechanism that the previously described for the rest of halobenzonitriles (Scheme 9). The process ends with the capture of CO₂, and further alkylation processes.

Once halobenzonitrile in CO₂ cathode electrochemical reduction mechanism as well as the electrocarboxylation conditions were optimized at the silver, other alkylation agents were used in other to check the potentiality of the methodology. 4-bromo-benzonitrile was selected as a starting material, since almost a 100% of electrocarboxylation products were obtained using methyl iodide as a methylated agent (Table 2, Entry 9). Hence, controlled potential electrolysis, at –1.80 V vs. SCE, of a 10 mM DMF/0.1 M TBABF₄ solution of 4-bromo-benzonitrile in a CO₂-saturated were performed

using Ag foil as a working electrode. After, the passage of 4.5 F, four equivalents of two different alkylating agents: 1) bromoethane and (2-bromoethyl) benzene were added at the end of the electrolysis. In the first case, the analysis of the electrocarboxylation process yields 75% of diethyl terephthalate, 15% of terephthalic acid monoethyl ester, and 10% 4-cyanobenzoate ethyl ester, Scheme 12 (Table 2, entry 8). Changing the alkylating agent for (2-bromoethyl) benzene, the analysis of the electrocarboxylation process revealed a 49% diphenethyl terephthalate, 13% 4-cyanobenzoate phenethyl ester, 8% 3-phenylpropionitrile, and 4% benzoate phenethyl ester, and 25% of the alkylating agent is recovered (Scheme 12, Table 2, entry 9). As mentioned before, the presence of the 3-phenylpropionitrile molecule can be explained by the reaction between the removed cyanide from the reactant and the alkylating agent. Note that there is a steric hindrance effect on the efficiency of alkylation reaction.

4. Conclusions

Electrolysis of 4-halobenzonitrile in CO₂-saturated employing a carbon graphite rods or silver foils as a cathode lead to the



Scheme 12. Electrolysis of 10–14 mM 4-bromobenzonitrile CO₂-saturated solutions in DMF/0.1 M TBABF₄ with an Ag foil. At the end of the electrocarboxylation process the alkylating agent was added: a) bromoethane b) for (2-bromoethyl)benzene.

formation of mono-, and di-substituted products from moderate to almost quantitative yields. The maximum efficiency of the carboxylation process is achieved with the passage of c.a. 4F. It has also been demonstrated that the use of “small” alkylating agents, such as iodomethane or bromoethane, enables higher yields to be obtained in terms of carboxylation products, probably due to hindrance effects. The use of Ag as working electrode enables controlled potential electrolysis to be performed at less negative potential values. Hence, electrocatalytic effects are seen when Ag is used as cathode, giving very high yields in terms of di-carboxylated products, where two units of CO₂ are incorporated to one unit of halobenzonitrile. This “new” methodology offers a new “green” route for the synthesis of different phthalate derivatives, which can potentially be used for making plastic polymers in a more environmentally friendly way.

Acknowledgements

This work was supported by projects CTQ2015-65439-R from the MINECO/FEDER and APOSTA UAB. S.M. thanks the Universitat Autònoma de Barcelona for pre-doctoral PIF fellowships.

References

- [1] C.F. Schleussner, T.K. Lissner, E.M. Fischer, J. Wohland, M. Perrette, A. Golly, J. Rogelj, K. Childers, J. Schewe, K. Frieler, M. Mengel, W. Hare, M. Schaeffer, Differential climate impacts for policy-relevant limits to global warming: the case of 1.5 °C and 2 °C, *Earth Syst. Dyn.* 7 (2016) 327–351, <https://doi.org/10.5194/esd-7-327-2016>.
- [2] B. Holtsmark, Quantifying the global warming potential of CO₂ emissions from wood fuels, *GCB Bioenergy* 7 (2015) 195–206, <https://doi.org/10.1111/gcbb.12110>.
- [3] J.E. Szulejko, P. Kumar, A. Deep, K.H. Kim, Global warming projections to 2100 using simple CO₂ greenhouse gas modeling and comments on CO₂ climate sensitivity factor, *Atmos. Pollut. Res.* 8 (2017) 136–140, <https://doi.org/10.1016/j.apr.2016.08.002>.
- [4] A. Dokania, A. Ramirez, A. Bavykina, J. Gascon, Heterogeneous catalysis for the valorization of CO₂: role of bifunctional processes in the production of chemicals, *ACS Energy Lett.* 4 (2018) 167–176, <https://doi.org/10.1021/acsenenergylett.8b01910>.
- [5] R. Mateos, A. Escapa, K. Vanbroekhoven, S.A. Patil, A. Moran, D. Pant, Microbial electrochemical Technologies for CO₂ and its derived products valorization, in: S.V. Mohan, S. Varjani, A. Pandey (Eds.), *Microb. Electrochem. Technol.*, Elsevier B.V., 2018, pp. 777–796, <https://doi.org/10.1016/B978-0-444-64052-9.00032-7>.
- [6] E. Alper, O. Yuksel Orhan, CO₂ utilization: developments in conversion processes, *Petroleum* 3 (2017) 109–126, <https://doi.org/10.1016/j.petlm.2016.11.003>.
- [7] G.R. Dey, A.D. Belapurkar, K. Kishore, Photo-catalytic reduction of carbon dioxide to methane using TiO₂ as suspension in water, *J. Photochem. Photobiol. A Chem.* 163 (2004) 503–508, <https://doi.org/10.1016/j.jphotochem.2004.01.022>.
- [8] J.V. Veselovskaya, P.D. Parunin, O.V. Netskina, L.S. Kibis, A.I. Lysikov, A.G. Okunev, Catalytic methanation of carbon dioxide captured from ambient air, *Energy* 159 (2018) 766–773, <https://doi.org/10.1016/j.energy.2018.06.180>.
- [9] G. Iaquaniello, S. Setini, A. Salladini, M. De Falco, CO₂ valorization through direct methanation of flue gas and renewable hydrogen: a technical and economic assessment, *Int. J. Hydrogen Energy* 43 (2018) 17069–17081, <https://doi.org/10.1016/j.ijhydene.2018.07.099>.
- [10] E.E. Barton, D.M. Rampulla, A.B. Bocarsly, Selective solar-driven reduction of CO₂ to methanol using a catalyzed, *J. Am. Chem. Soc.* 130 (2008) 6342–6344, <https://doi.org/10.1021/ja0776327>.
- [11] S. Saeidi, N.A.S. Amin, M.R. Rahimpour, Hydrogenation of CO₂ to value-added products - a review and potential future developments, *J. CO₂ Util.* 5 (2014) 66–81, <https://doi.org/10.1016/j.jcou.2013.12.005>.
- [12] I. Omae, Aspects of carbon dioxide utilization, *Catal. Today* 115 (2006) 33–52, <https://doi.org/10.1016/j.cattod.2006.02.024>.
- [13] F.D. Bobbink, F. Menoud, P.J. Dyson, Synthesis of methanol and diols from CO₂ via cyclic carbonates under metal-free, ambient pressure, and solvent-free conditions, *ACS Sustain. Chem. Eng.* 6 (2018) 12119–12123, <https://doi.org/10.1021/acssuschemeng.8b02453>.
- [14] A.W. Kleij, M. North, A. Urakawa, CO₂ Catalysis, *ChemSusChem* 10 (2017) 1036–1038, <https://doi.org/10.1002/cssc.201700218>.
- [15] M. Tamura, M. Honda, Y. Nakagawa, K. Tomishige, Direct conversion of CO₂ with diols, aminoalcohols and diamines to cyclic carbonates, cyclic carbamates and cyclic ureas using heterogeneous catalysts, *J. Chem. Technol. Biotechnol.* 89 (2014) 19–33, <https://doi.org/10.1002/jctb.4209>.
- [16] N.A. Tappe, R.M. Reich, V. D'Elia, F.E. Kühn, Current advances in the catalytic conversion of carbon dioxide by molecular catalysts: an update, *Dalton Trans.* 47 (2018) 13281–13313, <https://doi.org/10.1039/c8dt02346h>.
- [17] M. Honda, M. Tamura, Y. Nakagawa, K. Tomishige, Catalytic CO₂ conversion to organic carbonates with alcohols in combination with dehydration system, *Catal. Sci. Technol.* 4 (2014) 2830–2845, <https://doi.org/10.1039/c4cy00557k>.
- [18] J. Ma, J. Song, H. Liu, J. Liu, Z. Zhang, T. Jiang, H. Fan, B. Han, One-pot conversion of CO₂ and glycerol to value-added products using propylene oxide as the coupling agent, *Green Chem.* 14 (2012) 1743–1748, <https://doi.org/10.1039/c2gc35150a>.
- [19] Y. Ren, S.A.L. Rousseaux, Metal-free synthesis of unsymmetrical ureas and carbamates from CO₂ and amines via isocyanate intermediates, *J. Org. Chem.* 83 (2018) 913–920, <https://doi.org/10.1021/acs.joc.7b02905>.
- [20] J. Rintjema, R. Epping, G. Fiorani, E. Martín, E.C. Escudero-Adán, A.W. Kleij, Substrate-controlled product divergence: conversion of CO₂ into heterocyclic products, *Angew. Chem. Int. Ed.* 55 (2016) 3972–3976, <https://doi.org/10.1002/anie.201511521>.
- [21] Y. Liu, W.M. Ren, K.K. He, W.Z. Zhang, W.B. Li, M. Wang, X.B. Lu, CO₂-Mediated formation of chiral carbamates from meso-epoxides via polycarbonate intermediates, *J. Org. Chem.* 81 (2016) 8959–8966, <https://doi.org/10.1021/acs.joc.6b01616>.
- [22] M. Tokuda, Efficient fixation of carbon dioxide by electrolysis - facile synthesis of useful carboxylic acids-, *J. Nat. Gas Chem.* 15 (2006) 275–281, [https://doi.org/10.1016/S1003-9953\(07\)60006-1](https://doi.org/10.1016/S1003-9953(07)60006-1).
- [23] J. Damodar, S. Krishna Mohan, S.K. Khaja Lateef, S. Jayarama Reddy, Electro-synthesis of 2-arylpropionic acids from α -methylbenzyl chlorides and carbon dioxide by [Co(Salen)], *Synth. Commun.* 35 (2005) 1143–1150, <https://doi.org/10.1081/SCC-200054748>.
- [24] J.F. Fauvarque, A. Jutand, M. Francois, Nickel catalysed electrosynthesis of anti-inflammatory agents. Part I - synthesis of aryl-2 propionic acids, under galvanostatic conditions, *J. Appl. Electrochem.* 18 (1988) 109–115, <https://doi.org/10.1007/BF01016213>.
- [25] J.F. Fauvarque, A. Jutand, M. Francois, M.A. Petit, Nickel catalysed electrosynthesis of anti-inflammatory agents. Part II - monitoring of the electrolyses by HPLC analysis. Role of the catalyst, *J. Appl. Electrochem.* 18 (1988) 116–119, <https://doi.org/10.1007/BF01016214>.
- [26] A.J. Bard, L.A. Faulkner, *Fundamentals and Applications*, 2nd ed., 1990. Austin.
- [27] T.C. Berto, L. Zhang, R.J. Hamers, J.F. Berry, Electrolyte dependence of CO₂-electroreduction: tetraalkylammonium ions are not electrocatalysts, *ACS Catal.* 5 (2015) 703–707, <https://doi.org/10.1021/cs501641z>.
- [28] A. Gennaro, A.A. Isse, J.M. Savéant, M.G. Severin, E. Vianello, Homogeneous electron transfer catalysis of the electrochemical reduction of carbon dioxide. Do aromatic anion radicals react in an outer-sphere manner? *J. Am. Chem. Soc.* 118 (1996) 7190–7196, <https://doi.org/10.1021/ja960605o>.
- [29] A.A. Isse, A. Gennaro, Electrochemical synthesis of cyanoacetic acid from chloroacetonitrile and carbon dioxide, *J. Electrochem. Soc.* 149 (2002) D113, <https://doi.org/10.1149/1.1490358>.
- [30] A. Gennaro, A.A. Isse, M.-G. Severin, E. Vianello, I. Bhugun, J.-M. Savéant, Mechanism of the electrochemical reduction of carbon dioxide at inert electrodes in media of low proton availability, *J. Chem. Soc., Faraday Trans.* 92 (1996) 3963–3968, <https://doi.org/10.1039/FT9969203963>.
- [31] A. Gennaro, C.M. Sánchez-Sánchez, A.A. Isse, V. Montiel, Electrocatalytic synthesis of 6-aminonicotinic acid at silver cathodes under mild conditions, *Electrochem. Commun.* 6 (2004) 627–631, <https://doi.org/10.1016/j.elecom.2004.04.019>.
- [32] H. Khoshro, H.R. Zare, A. Gorji, M. Namazian, A.A. Jafari, R. Vafazadeh, The effect of electronic structure on electrocatalytic behaviors of cobalt Schiff base complexes: electrosynthesis of 2-phenylacetic acid using carbon dioxide, *J. Electroanal. Chem.* 732 (2014) 117–121, <https://doi.org/10.1016/j.jelechem.2014.07.039>.
- [33] C. Durante, A.A. Isse, F. Todesco, A. Gennaro, Electrocatalytic activation of aromatic carbon-bromine bonds toward carboxylation at silver and copper cathodes, *J. Electrochem. Soc.* 160 (2013) G3073–G3079, <https://doi.org/10.1149/2.008307jes>.
- [34] A. Gennaro, A.A. Isse, F. Maran, Nickel(I)(salen)-electrocatalyzed reduction of benzyl chlorides in the presence of carbon dioxide, *J. Electroanal. Chem.* 507 (2001) 124–134, [https://doi.org/10.1016/S0022-0728\(01\)00373-4](https://doi.org/10.1016/S0022-0728(01)00373-4).
- [35] O. Scialdone, A. Galia, G. Filardo, A.A. Isse, A. Gennaro, Electrocatalytic carboxylation of chloroacetonitrile at a silver cathode for the synthesis of cyanoacetic acid, *Electrochim. Acta* 54 (2008) 634–642, <https://doi.org/10.1016/j.electacta.2008.07.012>.
- [36] A.A. Isse, A. De Giusti, A. Gennaro, L. Falcioni, P.R. Mussini, Electrochemical reduction of benzyl halides at a silver electrode, *Electrochim. Acta* 51 (2006) 4956–4964, <https://doi.org/10.1016/j.electacta.2006.01.039>.
- [37] J. Zhang, D. Niu, Y. Lan, H. Wang, G. Zhang, J. Lu, Electrocatalytic carboxylation of aryl bromides at silver cathode in the presence of carbon dioxide, *Synth. Commun.* 41 (2011) 3720–3727, <https://doi.org/10.1080/00397911.2010.520399>.
- [38] I. Gallardo, S. Soler, Electrochemically promoted arylation of iodoaromatics, *J. Electroanal. Chem.* 799 (2017) 9–16, <https://doi.org/10.1016/j.jelechem.2017.05.034>.
- [39] S. Mena, I. Gallardo, G. Guirado, Electrocatalytic processes for the valorization of CO₂: synthesis of cyanobenzoic acid using eco-friendly strategies, *Catalysts* 9 (2019) 413, <https://doi.org/10.3390/catal9050413>.

- [40] S. Mena, J. Sanchez, G. Guirado, Electrocarboxylation of 1-chloro-(4-isobutylphenyl)ethane with a silver cathode in ionic liquids: an environmentally benign and efficient way to synthesize ibuprofen, *RSC Adv.* 9 (2019) 15115–15123, <https://doi.org/10.1039/C9RA01781J>.
- [41] M.R. Asirvatham, M.D. Hawley, Electrochemical studies of the formation and decomposition of p-nitrobenzenesulfonamide radical anions, *J. Electroanal. Chem.* 53 (1974) 293–305, [https://doi.org/10.1016/S0022-0728\(74\)80142-7](https://doi.org/10.1016/S0022-0728(74)80142-7).
- [42] C. Costentin, M. Robert, J.-M. Savéant, Catalysis of the electrochemical reduction of carbon dioxide, *Chem. Soc. Rev.* 42 (2013) 2423–2436, <https://doi.org/10.1039/C2CS35360A>.
- [43] I. Reche, I. Gallardo, G. Guirado, Electrochemical studies of CO₂ in imidazolium ionic liquids using silver as a working electrode: a suitable approach for determining diffusion coefficients, solubility values, and electrocatalytic effects, *RSC Adv.* 4 (2014) 65176–65183, <https://doi.org/10.1039/C4RA11297K>.
- [44] C.P. Andrieux, F. Gonzalez, J.M. Savéant, Homolytic and heterolytic radical cleavage in the Kolbe reaction: electrochemical oxidation of arylmethyl carboxylate ions, *J. Electroanal. Chem.* 498 (2001) 171–180, [https://doi.org/10.1016/S0022-0728\(00\)00365-X](https://doi.org/10.1016/S0022-0728(00)00365-X).
- [45] I. Gallardo, G. Guirado, J. Marquet, Mechanistic studies on the reactivity of halodinitrobenzene radical-anion, *J. Electroanal. Chem.* 488 (2000) 64–72, [https://doi.org/10.1016/S0022-0728\(00\)00189-3](https://doi.org/10.1016/S0022-0728(00)00189-3).
- [46] T. Kawamoto, K. Oritani, D.P. Curran, A. Kamimura, Thiol-catalyzed radical decyanation of aliphatic nitriles with sodium borohydride, *Org. Lett.* 20 (2018) 2084–2087, <https://doi.org/10.1021/acs.orglett.8b00626>.
- [47] J.-M. Mattalia, C. Marchi-Delapierre, H. Hazimeh, M. Chanon, The reductive decyanation reaction: chemical methods and synthetic applications, *Arman. Lattes Ark* (2006) 90–118, <https://doi.org/10.3998/ark.5550190.0007.408>.
- [48] A.M. Romanin, A. Gennaro, E. Vianello, Electrode reduction mechanism of aromatic nitriles in aprotic solvents, *Benzonitrile*, *J. Electroanal. Chem.* 88 (1978) 175–185, [https://doi.org/10.1016/S0022-0728\(78\)80265-4](https://doi.org/10.1016/S0022-0728(78)80265-4).



Contents lists available at ScienceDirect

Journal of Molecular Liquids

journal homepage: www.elsevier.com/locate/molliq

Short Communication

One-pot sustainable synthesis of tetrabutylammonium bis(trifluoromethanesulfonyl)imide ionic liquid

Silvia Mena, Gonzalo Guirado *

Departament de Química, Universitat Autònoma de Barcelona, 08193, Bellaterra, Barcelona, Spain

ARTICLE INFO

Article history:

Received 6 March 2020

Received in revised form 20 April 2020

Accepted 18 May 2020

Available online 20 May 2020

ABSTRACT

Tetrabutylammonium bis(trifluoromethanesulfonyl)imide (TBA TFSI) and tetrafluoroborate-based anion ionic liquids (ILs) were obtained simultaneously by using a fast, versatile, cheap, low cost, and one-pot process. The process relies on dissolving tetrabutylammonium tetrafluoroborate salt, an organic-based bis(trifluoromethanesulfonyl) imide, ILs, such as 1-ethyl-3-methylimidazolium, *N*-trimethyl-*N*-butylammonium, 1-butyl-1-methylpyrrolidinium, 1-methyl-1-propylpiperidinium derivatives in dimethylformamide. A further extraction process using water and ether allows the selective recovery of the TBA TFSI in the organic phase, and the organic-based tetrafluoroborate IL in the aqueous phase. All the ionic liquids synthesized were characterized using Infrared Spectroscopy and Nuclear Magnetic Resonance, and compared with commercially available samples.

© 2020 Elsevier B.V. All rights reserved.

1. Introduction

Solvents define a major part of the performance of processes in the chemical industry, and have an impact on cost, safety, and health issues. The use of alternative solvents represents a major entry in the general green chemistry toolkit, and is the subject of an enormous research effort [1–8]. In this sense, an attractive alternative to conventional organic solvents is the use of ionic liquids, ILs, due to both their benign chemical features (non-flammable, non-volatile, and thermally stable over a wide range of temperatures) [9–15] and their electrochemical characteristics. ILs have from moderate to high conductivities because they are liquids consisting of only ions and have good electrochemical stability (stable from -3.00 V to $+1.7$ V vs. Saturated Calomel Electrode (SCE) for reduction-oxidation processes) [16–20]. However, the processes and the reactant used for synthesizing ILs require a critical analysis from an environmental point of view. In most of the cases, it is not possible to obtain the IL with the desired anion in one single step, so two main different reaction pathways are used: 1) Lewis-acid-base reaction, or 2) anion metathesis [21–25]. Both types of reactions are performed from the halide salts of ionic liquids, producing a considerable amount of non-desired byproducts. In this regard, one important drawback associated with synthetic routes is to remove the impurities or byproducts of the ILs, which is a hard and tedious task (Scheme 1). Note that pure ILs are specially required for homogeneous catalysis, supporting electrolyte and electronic applications, such as gating in transistors [26,27].

In this sense the tetrabutylammonium bis(trifluoromethylsulfonyl) imide (TBA TFSI) is one of the most promising IL for electronic applications, more exactly, for transistor design. However, up until now, there are only three synthetic routes for obtaining TBA TFSI IL, and all of them generate a considerably amount of lithium salts or other byproducts [9,10,21,28]. The aim of this work is to design a cleaner strategy for obtaining TBA TFSI by mixing an organic TFSI ionic liquid and a tetrabutylammonium tetrafluoroborate salt (TBA BF₄) in dimethylformamide (DMF). This new synthetic route will potentially allow two different ionic liquids, TBA TFSI and organic cation, C⁺ BF₄[−] to be produced after an ion exchange process. It is important to highlight that following this new approach, then main product (TBA TFSI) and the byproducts formed in the ion exchange process are also ILs, which will potentially have their own market. Finally, it is remarkable there is the higher recyclability of the solvents involved in the chemical process.

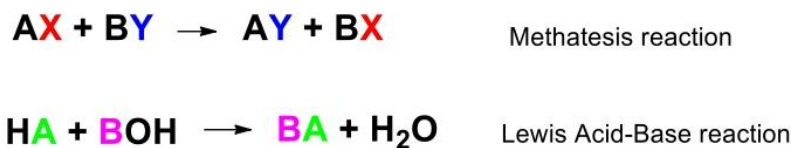
2. Experimental

2.1. Chemicals

Ionic liquids (1-Ethyl-3-methylimidazolium bis(trifluoromethanesulfonyl)imide (EMIM TFSI), *N*-Trimethyl-*N*-butylammonium bis(trifluoromethanesulfonyl)imide (N₁₁₁₄ TFSI), 1-Butyl-1-methylpyrrolidinium bis(trifluoromethanesulfonyl)imide (Pyr14 TFSI), 1-Methyl-1-propylpiperidinium bis(trifluoromethanesulfonyl)imide (PP13 TFSI)) were purchased from Solvionic and used without further purification. Tetrabutylammonium tetrafluoroborate (TBA BF₄), Tetraethylammonium tetrafluoroborate

* Corresponding author.

E-mail address: gonzalo.guirado@uab.es (G. Guirado).



Scheme 1. Reaction pathways.

(TEA BF₄), Tetramethylammonium hexafluorophosphate (TMA PF₆), Tetrabutylammonium bis (trifluoromethanesulfonyl)imide (TBA TFSI) and *N,N*-dimethylformamide (DMF), 99.8%, were supplied by Sigma-Aldrich and used as received (Scheme 2).

2.2. Analysis and product characterization

Products obtained were characterized by Nuclear Magnetic Resonance and Near Infrared Spectroscopy and compared with commercially available samples.

2.2.1. Nuclear magnetic resonance (NMR)

Synthesized ionic liquids and commercially available samples of the synthesized ionic liquids were characterized by ¹H NMR, ¹³C NMR and ¹⁹F NMR. Measurements were performed in a Bruker DPX360 (360 MHz) (Billerica, MA, USA) spectrometer, and Bruker DPX250 (250 MHz) with a Quattro Nucleus Probe (QNP). Proton chemical shifts were reported in ppm (δ) (CDCl₃, δ = 7.26 or CD₃CN, δ = 1.94). Carbon chemical shifts are reported in ppm (δ) (CDCl₃, δ = 77.2 or CD₃CN, δ = 1.32). The *J* values are reported in Hz. Fluor chemical shifts are reported in ppm (δ) (CDCl₃).

2.2.2. Infrared spectroscopy (IR)

Near infrared spectra were recorded in attenuated total reflectance (ATR) mode on a Model Tensor 27 spectrophotometer from Bruker that was governed via the software OPUS 5.5, also from Bruker.

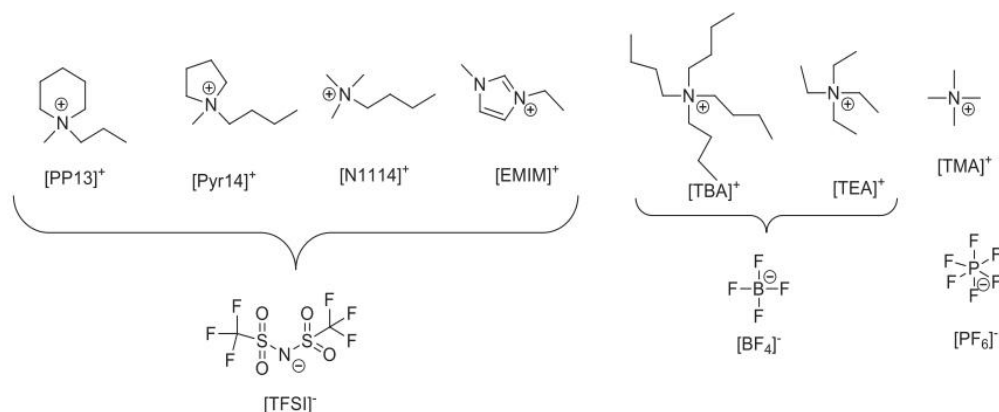
3. Results and discussion

Scheme 3 describes the simple ionic exchange process between TBA BF₄ (organic salt) and EMIM TFSI (ionic liquid). An equimolar amount of the above-mentioned salt and IL are dissolved in dimethylformamide (DMF) by stirring the mixture for 5 min at room temperature. After that the DMF solution was poured into a separator funnel, which contained the same amount of water and ether. Due to the fact that

neither EMIM TFSI nor TBA BF₄ is soluble in water, an ion exchange process takes place. Hence, in the organic phase, after washing and drying this phase with water and anhydrous sodium sulphate, the desired IL (tetrabutylammonium bis(trifluoromethanesulfonyl)imide) is obtained with an 89% yield. Moreover, the byproduct of the ion exchange between tetrabutylammonium tetrafluoroborate and 1-ethyl-3-methylimidazolium bis(trifluoromethanesulfonyl)imide, EMIM BF₄, is easily recovered from the aqueous phase after several washings with dichloromethane. Distillation of dichloromethane enables EMIM BF₄ to be obtained in a 66.7% yield. It is important to highlight that the one-pot synthetic process above described enables two highly pure ionic liquids to be obtained following several principles of Green Chemistry, such as high atom economy, the utilization of by-products, recovery of the solvents, as well as recyclability of the reactants.

Standard spectroscopy techniques were used as useful tools to identify and characterize the products formed. Quick comparisons between the spectroscopic features of pure reactants, compounds obtained, and pure commercial available samples of the compounds obtained verified the exchange process [28–30]. Fig. 1(a–b) shows the different IR spectra for the TBA BF₄ and EMIM TFSI reagents, and the synthesized ionic liquids, TBA TFSI and EMIM BF₄. All frequencies described in IR for the EMIM⁺, TBA⁺ cations, and TFSI[−], BF₄[−] anions are summarized in Table S1. The stretching/bending vibrations for the cation part could be distinguished, focusing between 2880 and 2970 cm^{−1} for TBA⁺ cation and between 2950 and 3165 cm^{−1} for EMIM⁺. Furthermore, the imidazolium ring of EMIM⁺ shows characteristic vibrations between 1300 and 1600 cm^{−1}. In the anion part, the spectra for BF₄[−] is easily described as it shows a huge peak at 1050 cm^{−1}; however, in the case of the TFSI[−] anion the spectra show four different peaks that describe the stretching and bending for CF₃, SO₂, and S–N–S bonds.

On the other hand, Figs. 2 and 3 show the ¹H NMR spectrum for EMIM BF₄, EMIM TFSI, TBA BF₄ and TBA TFSI. It is easy to distinguish between cation EMIM⁺ and TBA⁺ because they have very different kind of protons in their structure; TBA⁺ presents 4 different signals of its alkyl



Scheme 2. Chart of structures/

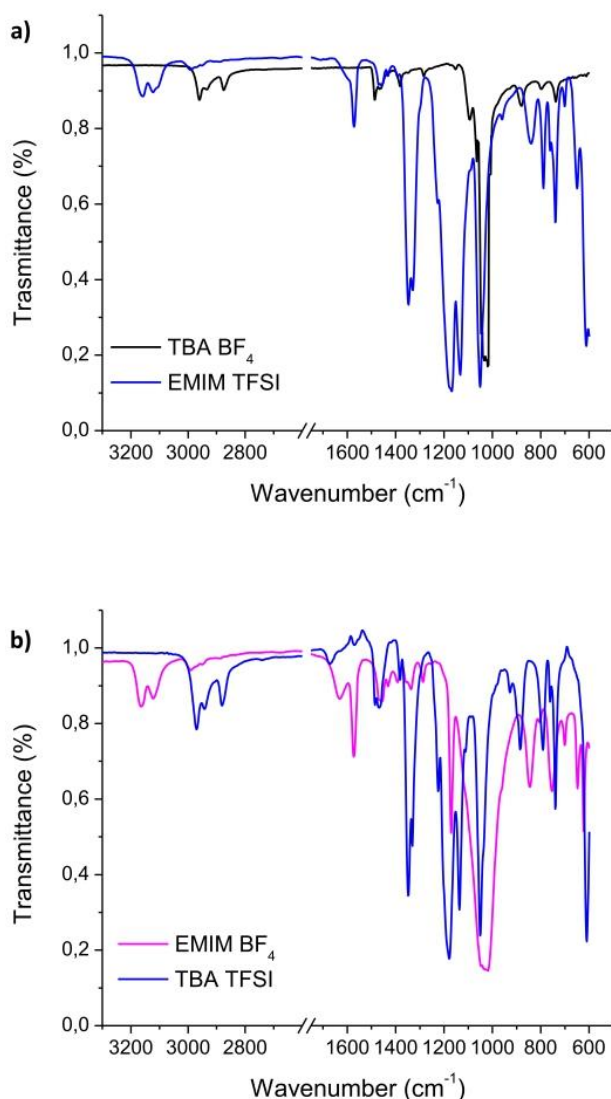
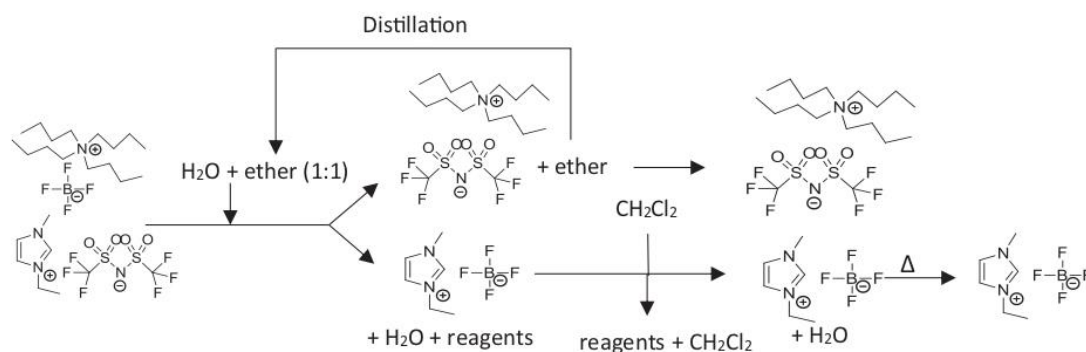


Fig. 1. IR spectra of ionic exchange process between TBA BF₄ and EMIM TFSI a) before mixing and b) after a mixing and a purification process.

protons, whereas EMIM⁺ has 6 different proton types, which appear at a higher chemical shift because of the resonance of the imidazolium ring. Moreover, the EMIM⁺ cation described an ion-pair formation equilibrium with BF₄⁻ and TFSI⁻ anions in dilute low dielectric solutions, such as chloroform [31]. Hence, ¹H NMR describes two concurrent sets of signals due to the presence in the sample of freely dissolved ions and ion-pair aggregates, these signals are different depending on.

Furthermore, the combined use of ¹³C NMR and ¹⁹F NMR allow the nature of the counter anion present to be identified in the ILs formed. Fig. 4 shows the ¹³C NMR for the TBA⁺ cation paired with TFSI⁻ and BF₄⁻. An extra signal (C5) TBA TFSI, which is related to CF₃ group. Table S2 summarizes the ¹H NMR and ¹³C NMR signals for TBA TFSI. ¹⁹F NMR data are reported in Fig. S1, according to previously published data [32–34] two different signals are observed for BF₄⁻ and TFSI⁻ anions at 152.4 and 79.9 ppm, respectively.

The current methodology can be extended to other similar bis(trifluoromethanesulfonyl)imide based ionic liquids by a simple mixture with TBA BF₄. Table 1 summarizes the yields obtained after the ionic exchange and phase separation process described in Scheme 3, when *N*-Trimethyl-*N*-butylammonium bis(trifluoromethanesulfonyl)imide (N₁₁₁₄ TFSI), 1-Butyl-1-methylpyrrolidinium bis(trifluoromethanesulfonyl)imide (Pyr14 TFSI), 1-Methyl-1-propylpiperidinium bis(trifluoromethanesulfonyl)imide (PP13 TFSI) are used as reagents. Notice that in all cases are obtained TBA TFSI is obtained a good yield, whereas the by-product (BF₄⁻ based ionic liquid) is obtained in moderate yields. However, the ionic exchange process is strongly dependent on the length of the alkyl chain present in the tetraalkylammonium salt, as it was previously described in the literature [9] Hence, no ionic exchange products were obtained when Tetraethylammonium tetrafluoroborate (TEA BF₄) or salt is used as starting material. This fact can be rationalized by taking into account the different hydrophobicity of both cations, TEA⁺ and TBA⁺; therefore, it is soluble in aqueous phase.

The purity of the ionic liquids synthesized following this methodology are determined employing the ¹H NMR data using of ¹³C satellites of imidazolium *N*-methyl group as internal standard [35] as well as the integration of similar protons in non-imidazolium ILs. In the case of TBA TFSI the purity of IL obtained was from 96.2% to 99.3% depending on the type of C⁺ TFSI used as reagent. For the rest of the ILs obtained as a byproducts purities obtained were the following: 99.2% for Pyr14 TFSI, 93.5% for PP13 TFSI, 98.0% for N₁₁₁₄ TFSI and 99.1% for EMIM TFSI. Finally, it is remarkable that a comparison in terms of atom economy between our methodology and a classical one starting from similar products reveals that are very similar in both cases (c.a. 80%). However, the byproducts obtained using our methodology are also ILs and the solvent used are recyclable, whereas in the case the classical route the byproduct obtained is a salt (lithium bromide).

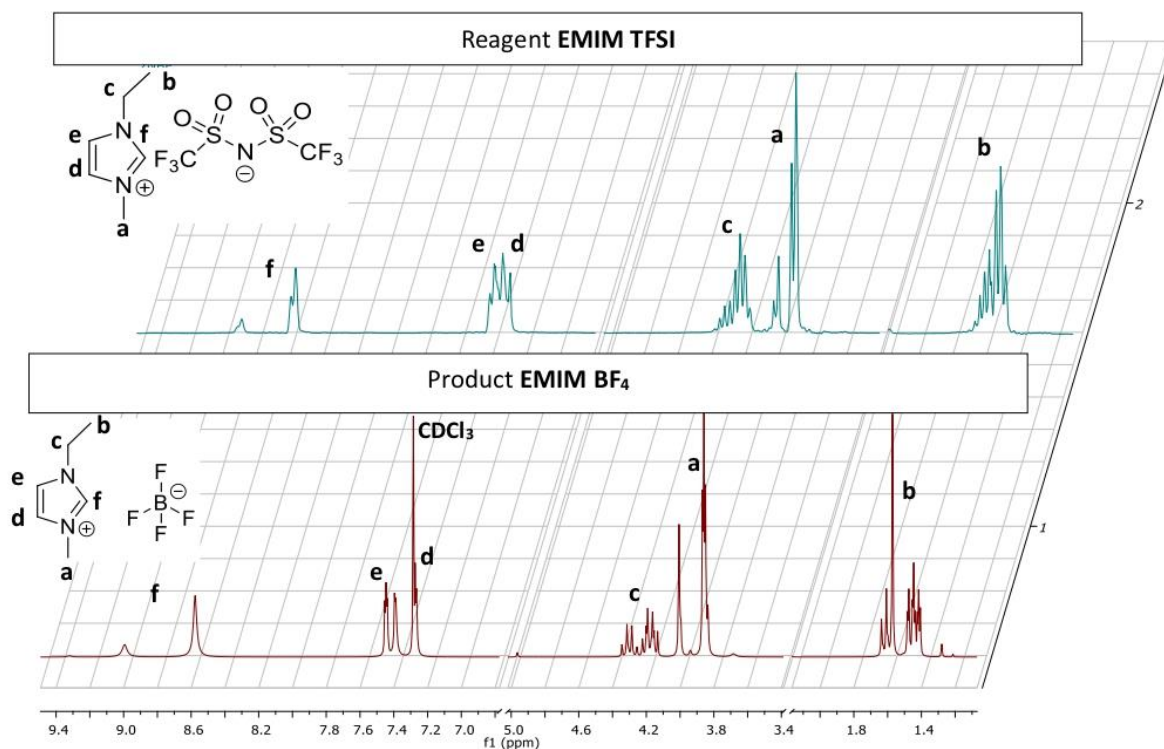


Fig. 2. ^1H NMR of EMIM BF_4 and EMIM TFSI ILs.

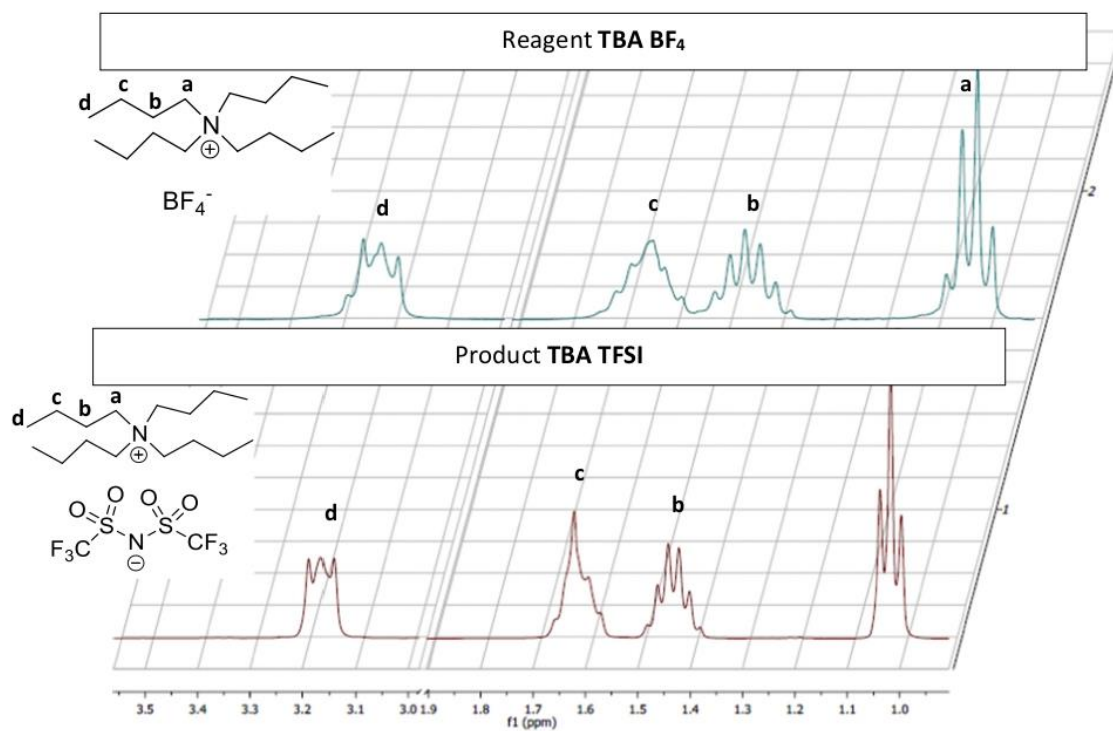


Fig. 3. ^1H NMR of TBA BF_4 salt and TBA TFSI IL.

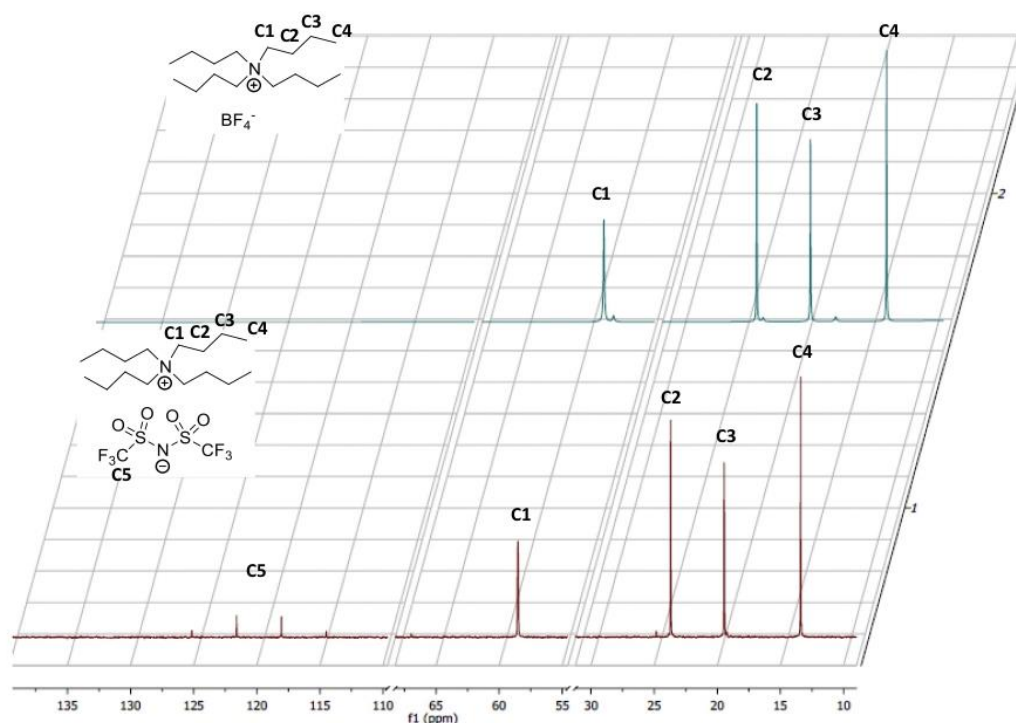


Fig. 4. ^{13}C NMR for TBA BF_4 and TBA TFSI.

4. Conclusions

In the current manuscript we have been able to design a new synthetic route for synthesizing the tetrabutylammonium bis(trifluoromethanesulfonyl) imide ionic liquid (TBA TFSI) following a sustainable one-pot methodology based on an ion exchange process with purities from 96 to 99%. It is important to highlight tetrafluoroborate based ionic liquids are also obtained as a secondary product with purities from 98 to 99%. In terms of cost-effectiveness analysis, our exchange ionic approach is a low-cost alternative since the products obtained at the end (ILs) have increased their value by ca 40% in comparison with the starting IL and salt used. Moreover, ca 80% of the solvent and reagents used can be recycled and reused at the end of the process. Hence, the above described methodology allows the previous synthetic methodologies reported in the literature to be improved, avoiding the use of multistep processes, non-desirable byproducts, as well as strong experimental conditions.

Author contributions

G.G. conceptualized the research topic, conceived and designed the experiments; S.M. perform the experiments, G.G. and S.M. analyzed and interpreted the results. S.M. and G.G. prepared the manuscript. All authors corrected the draft. G.G. obtained the funds for the research.

Declaration of competing interest

The authors declare no conflicts of interest.

Acknowledgments

The authors thank financial support through the project CTQ 2015-65439-R from the MINECO/FEDER. S.M. acknowledges the Autonomous University of Barcelona for her predoctoral PIF grant.

Table 1
Ionic liquid yields obtained after ionic exchange and purification processes.

Reactive + TBA BF_4	Products + TBA TFSI	TBA TFSI Yield (%)	$\text{C}^+ \text{BF}_4^-$ Yield (%)
		73.4	31.2
		67.3	35.4
		71.2	41.4

Appendix A. Supplementary data

Supplementary data to this article can be found online at <https://doi.org/10.1016/j.molliq.2020.113393>.

References

- [1] A. Kamimura, K. Murata, T. Kawamoto, An efficient and selective conversion of sorbitol in ionic liquids: use of ion exchange resin as a solid acid catalyst, *Tetrahedron Lett.* 58 (37) (2017) 3616–3618, <https://doi.org/10.1016/j.tetlet.2017.07.105>.
- [2] Y. Takashima, M. Yokoyama, A. Horikoshi, Y. Sato, T. Tsuruoka, K. Akamatsu, Ionic liquid/metal-organic framework hybrid generated by ion-exchange reaction: synthesis and unique catalytic activity, *New J. Chem.* 41 (23) (2017) 14409–14413, <https://doi.org/10.1039/C7NJ03269B>.
- [3] X. Mao, M. Wu, X. Xu, L. Jiang, J. Yan, Z. Du, J. Li, S. Hou, Fabrication of an electrochemical sensor for NO_x based on ionic liquids and MoS₂, *Int. J. Electrochem. Sci.* 13 (11) (2018) 11038–11048, <https://doi.org/10.20964/2018.11.79>.
- [4] H. Tahara, K. Uraoka, M. Hirano, T. Ikeda, T. Sagara, H. Murakami, Electrochromism of ferrocene- and Viologen-based redox-active ionic liquids composite, *ACS Appl. Mater. Interfaces* 11 (2018) 6–11, <https://doi.org/10.1021/acsami.8b16410>.
- [5] R. Liu, P. Zhang, S. Zhang, T. Yan, J. Xin, X. Zhang, Ionic liquids and supercritical carbon dioxide: green and alternative reaction Media for Chemical Processes, *Rev. Chem. Eng.* 32 (6) (2016) 587–609, <https://doi.org/10.1515/revce-2015-0078>.
- [6] K.R. Seddon, Review Ionic Liquids for Clean Technology^a, 50(lii), 1997 1–6.
- [7] P. Wasserscheid, T. Welton, Ionic Liquids Ionic Liquids, *Top. Curr. Chem.* 1 (December) (2017) 1–4.
- [8] M. Piquet, I. Tkatchenko, I. Tommasi, P. Wasserscheid, J. Zimmermann, Ionic liquids, 3. Synthesis and utilisation of Protic imidazolium salts in homogeneous catalysis, *Adv. Synth. Catal.* 345 (8) (2003) 959–962, <https://doi.org/10.1002/adsc.200303025>.
- [9] D.P. Fagnant, M.A. Desilva, J.F. Brennecke, Solid-liquid equilibria measurements of mixtures of Lithium Bis(Trifluoromethanesulfonyl)imide with varying alkyl chain length ammonium Bis(Trifluoromethanesulfonyl)imide ionic liquids, *J. Chem. Eng. Data* 61 (2) (2016) 958–967, <https://doi.org/10.1021/acs.jced.5b00807>.
- [10] Y. Kohno, H. Arai, S. Saita, H. Ohno, Material Design of Ionic Liquids to show temperature-sensitive Lcst-type phase transition after mixing with water, *Aust. J. Chem.* 64 (12) (2011) 1560–1567, <https://doi.org/10.1071/CH11278>.
- [11] R. Marcilla, J.A. Blazquez, J. Rodriguez, J.A. Pomposo, D. Mecerreyes, Tuning the solubility of polymerized ionic liquids by simple anion-exchange reactions, *J. Polym. Sci. Part A Polym. Chem.* 42 (1) (2004) 208–212, <https://doi.org/10.1002/pola.11015>.
- [12] M.W. Thompson, R. Matsumoto, R.L. Sacchi, N.C. Sanders, P.T. Cummings, Scalable screening of soft matter: case study of mixtures of ionic liquids and organic solvents, *J. Phys. Chem. B* (2019) <https://doi.org/10.1021/acs.jpcc.8b11527> acs.jpcc.8b11527.
- [13] F. Zhou, S. Liu, B. Yang, P. Wang, A.S. Alshammari, Y. Deng, Electrochemistry communications highly selective and stable electro-catalytic system with ionic liquids for the reduction of carbon dioxide to carbon monoxide, *Electrochem. Commun.* 55 (2015) 43–46.
- [14] M. Deetlefs, K.R. Seddon, M. Shara, Predicting physical properties of ionic liquids, *Phys. Chem. Chem. Phys.* 8 (5) (2006) 642–649, <https://doi.org/10.1039/b513453f>.
- [15] M.J. Earle, J.M.S.S. Esperança, M.A. Gilea, J.N.C. Lopes, L.P.N. Rebelo, J.W. Magee, K.R. Seddon, J.A. Widegren, The distillation and volatility of ionic liquids, *Nature* 439 (7078) (2006) 831–834, <https://doi.org/10.1038/nature04451>.
- [16] H. Cruz, I. Gallardo, G. Guirado, Electrochemically promoted nucleophilic aromatic substitution in room temperature ionic liquids – an environmentally benign way to functionalize nitroaromatic compounds, *Green Chem.* 13 (9) (2011) 2531–2542, <https://doi.org/10.1039/c1gc15303j>.
- [17] M. Hayyan, F.S. Mjalli, M.A. Hashim, I.M. AlNashef, T.X. Mei, Investigating the electrochemical windows of ionic liquids, *J. Ind. Eng. Chem.* 19 (1) (2013) 106–112, <https://doi.org/10.1016/j.jiec.2012.07.011>.
- [18] T.M. Pappenfus, K. Lee, L.M. Thoma, C.R. Dukart, Wind to Ammonia: electrochemical processes in room temperature ionic liquids, *ECS Trans.* 16 (49) (2009) 89–93, <https://doi.org/10.1149/1.3159311>.
- [19] H. Cruz, I. Gallardo, G. Guirado, Understanding specific effects on the standard potential shifts of Electrogenerated species in 1-Butyl-3-Methylimidazolium ionic liquids, *Electrochim. Acta* 53 (20) (2008) 5968–5976, <https://doi.org/10.1016/j.electacta.2008.03.062>.
- [20] I. Reche, I. Gallardo, G. Guirado, The role of cations in the reduction of 9-Fluorenone in Bis(Trifluoromethylsulfonyl)imide room temperature ionic liquids, *New J. Chem.* 38 (10) (2014) 5030–5036, <https://doi.org/10.1039/c4nj01200c>.
- [21] R. Arvai, F. Toulgoat, B.R. Langlois, J.Y. Sanchez, M. Médebielle, A simple access to metallic or onium Bistrifluoromethanesulfonimide salts, *Tetrahedron* 65 (27) (2009) 5361–5368, <https://doi.org/10.1016/j.tet.2009.04.068>.
- [22] V.D. BHATT, K. GOHIL, Ion exchange synthesis and thermal characteristics of some [N2222]⁺ based ionic liquids, *Bull. Mater. Sci.* 36 (6) (2013) 1121–1125, <https://doi.org/10.1007/s12034-013-0557-x>.
- [23] M.L. Dietz, J.A. Dzielawa, Ion-exchange as a mode of cation transfer into room-temperature ionic liquids containing crown ethers: implications for the “greenness” of ionic liquids as diluents in liquid-liquid extraction, *Chem. Commun.* (2001) 2124–2125, <https://doi.org/10.1039/b104349h>.
- [24] M.P. Jensen, J. Neufeld, J.V. Beitz, S. Skanthakumar, L. Soderholm, Mechanisms of metal ion transfer into room-temperature ionic liquids: the role of anion exchange, *J. Am. Chem. Soc.* 125 (50) (2003) 15466–15473, <https://doi.org/10.1021/ja037577b>.
- [25] P. Keil, M. Schwierz, A. König, Metathesis of ionic liquids: continuous ion exchange by Donnan dialysis, *Chem. Eng. Technol.* 37 (6) (2014) 919–926, <https://doi.org/10.1002/ceat.201200322>.
- [26] D. Zhang, T.K. Ronson, J. Mosquera, A. Martinez, J.R. Nitschke, Selective anion extraction and recovery using a Fe II/L4 cage, *Angew. Chemie – Int. Ed.* 57 (14) (2018) 3717–3721, <https://doi.org/10.1002/anie.201800459>.
- [27] M. Kuroboshi, T. Shiba, H. Tanaka, Viologen as catalytic organic reductant: electro-reductive dimerization of aryl bromides in a Pd/Viologen double mediatory system, *Tetrahedron Lett.* 54 (28) (2013) 3666–3668, <https://doi.org/10.1016/j.tetlet.2013.04.127>.
- [28] N. Nishi, K. Minami, K. Motobayashi, M. Osawa, T. Sakka, Interfacial structure at the quaternary ammonium-based ionic liquids/gold electrode Interface probed by surface-enhanced infrared absorption spectroscopy: anion dependence of the cationic behavior, *J. Phys. Chem. C* 121 (3) (2017) 1658–1666, <https://doi.org/10.1021/acs.jpcc.6b10826>.
- [29] T. Buffeteau, J. Grondin, J.-C. Lassègues, Infrared spectroscopy of ionic liquids: quantitative aspects and determination of optical constants, *Appl. Spectrosc.* 64 (1) (2010) 112–119, <https://doi.org/10.1366/000370210790572089>.
- [30] N. Mozhzhukhina, A.Y. Tesio, L.P. Mendez De Leo, E.J. Calvo, In situ infrared spectroscopy study of PYR14TFSI ionic liquid stability for Li–O₂ battery, *J. Electrochem. Soc.* 164 (2) (2017) A518–A523, <https://doi.org/10.1149/2.1391702jes>.
- [31] J.D. Tubbs, M.M. Hoffmann, Ion-pair formation of the ionic liquid 1-Ethyl-3-Methylimidazolium Bis (Triflyl) imide in low dielectric media, *J. Solut. Chem.* 33 (4) (2004) 381–394, <https://doi.org/10.1023/B:JOSL.0000036308.36052.01>.
- [32] T. De Diego, P. Lozano, S. Gmouh, M. Vaultier, J.L. Iborra, Fluorescence and CD spectroscopic analysis of the α-chymotrypsin stabilization by the ionic liquid, 1-Ethyl-3-Methylimidazolium Bis[(Trifluoromethyl)sulfonyl]amide, *Biotechnol. Bioeng.* 88 (7) (2004) 916–924, <https://doi.org/10.1002/bit.20330>.
- [33] B.-M. Su, S. Zhang, Z.C. Zhang, Structural elucidation of Thiophene interaction with ionic liquids by multinuclear NMR spectroscopy, *J. Phys. Chem. B* 108 (50) (2004) 19510–19517, <https://doi.org/10.1021/jp049027l>.
- [34] J.S. Hartman, G.J. Schrobilgen, Mixed tetrahaloborate ions. Detection and study by nuclear magnetic resonance, *Inorg. Chem.* 11 (5) (1972) 940–951, <https://doi.org/10.1021/ic50111a005>.
- [35] C.C. Cassol, G. Ebeling, B. Ferrera, J. Dupont, A simple and practical method for the preparation and purity determination of halide-free imidazolium ionic liquids, *Adv. Synth. Catal.* 348 (1–2) (2006) 243–248, <https://doi.org/10.1002/adsc.200505295>.



Article

Electrocatalytic Processes for the Valorization of CO₂: Synthesis of Cyanobenzoic Acid Using Eco-Friendly Strategies

Silvia Mena , Iluminada Gallardo and Gonzalo Guirado *

Departament de Química, Universitat Autònoma de Barcelona, Campus UAB, 08193 Bellaterra, Barcelona, Spain; silvia.mena@uab.cat (S.M.); iluminada.gallardo@uab.cat (I.G.)

* Correspondence: gonzalo.guirado@uab.cat; Tel.: +34-93-581-4882

Received: 4 March 2019; Accepted: 15 April 2019; Published: 2 May 2019



Abstract: Carbon dioxide (CO₂) is a known greenhouse gas, and is the most important contributor to global warming. Therefore, one of the main challenges is to either eliminate or reuse it through the synthesis of value-added products, such as carboxylated derivatives. One of the most promising approaches for activating, capturing, and valorizing CO₂ is the use of electrochemical techniques. In the current manuscript, we described an electrocarboxylation route for synthesizing 4-cyanobenzoic acid by valorizing CO₂ through the synergistic use of electrochemical techniques (“green technology”) and ionic liquids (ILs) (“green solvents”)—two of the major entries in the general green chemistry tool kit. Moreover, the use of silver cathodes and ILs enabled the electrochemical potential applied to be reduced by more than 0.4 V. The “green” synthesis of those derivatives would provide a suitable environmentally friendly process for the design of plasticizers based on phthalate derivatives.

Keywords: ionic liquids; carbon dioxide; electrochemistry; green chemistry; cyanobenzoic acid

1. Introduction

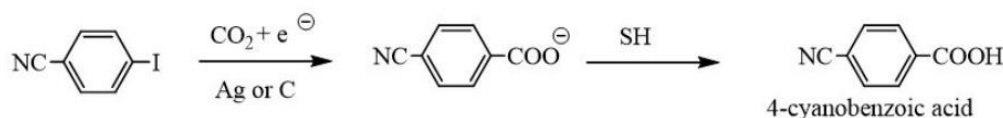
Fossil fuels in the form of coal, oil, and natural gas account for 80% of the world’s energy use and have caused increases in the Greenhouse Gas (GHG) concentrations of the atmosphere. These have led to global warming, climate change, and ozone layer depletion, with destructive impacts on human society and the economy. In the last four decades, despite global attempts to mitigate emissions, the world saw more than 100% growth in annual CO₂ emissions, which surpassed 32 billion tons in 2011. These global CO₂ emissions will continue to increase and are projected to reach 36 billion tons in 2020, and double that by 2050 if appropriate climate change mitigation measures are not put in place [1–3]. In this sense, different research strategies are currently being developed for the activating, capturing, and valorizing of CO₂. Hence, CO₂ uses are generally classified into different categories, such as direct use and/or conversion to chemicals and energy [4–11].

Carboxylic acids and esters are important classes of chemicals that are widely found in pharmaceuticals, polymers, agrochemicals, natural products, and biological systems, and they have been widely applied as versatile building blocks in organic synthesis [12–14]. For instance, the utilization of CO₂ as a C1 synthon for incorporation with lithium phenolate, or Grignard reagents for the synthesis of carboxylic acids have been well known for more than a century. On the other hand, metal-catalyzed direct insertion of CO₂ into different compounds is another valuable method for the preparation of carboxylic acids with high selectivity. This approach is widely used to obtain carboxylic analogues from carbon–halide, carbon–boron, carbon–oxygen, aromatic and alkyl reagents, etc. [15–22]. Moreover, the development of new methods that take advantage of the abundant and inexpensive CO₂ without catalysts (carbon monoxide, phenols, and others), for the transformation of aryl halides into their corresponding aryl carboxylic acid provides an attractive option for their assembly [23,24].

In this sense, the CO₂ valorization by electrochemical routes is receiving increasing attention as a way to obtain chemicals with added value, and as a promising option to chemically store renewable energy from intermittent sources like solar or wind, thus reducing our reliance on fossil fuels. Although the benefits of using electrochemical approaches to perform classic chemical reactions in the design of greener and more suitable processes are well established, the main drawbacks of performing electrochemical reactions are the use of non-volatile organic polar compounds, which are well-known hazardous substances, as well as the use of supporting electrolytes in high concentration [25–29]. In this sense, the replacement of electrolytes based on an organic solvent with ionic liquids (ILs), which are considered “green solvents” would solve this problem. Ionic liquids (ILs) are a family of solvents with unique properties that have led to their consideration as interesting alternatives and more effective solvents in many applications, including electrochemistry [30–32] and CO₂ storage and capture [33–35].

Therefore, the growing interest in the electrochemical valorization of CO₂ has resulted in different innovative attempts, including the use of ILs, in order to improve the performance of these electrochemical approaches.

In the present work, a description is presented of an electrocarboxylation route for synthesizing 4-cyanobenzoic acid by valorizing CO₂ through the synergistic use of electrochemical techniques and ILs (two of the major entries in the general green chemistry tool kit). The “green” synthesis of 4-cyanobenzoic acid is produced through the electrochemical cleavage of a carbon-iodide bond and the subsequent capture of CO₂ (Scheme 1). It was decided to perform the electrocarboxylation process from 4-iodobenzonitrile, since less energy is required to break it down than the C–F bond, the C–Cl bond, and even the C–Br bond. Moreover, electrocatalytic effects related to the nature of the cathodes and the use of ILs will also be investigated for reducing the electrochemical potential needed. The optimization of electrocarboxylation conditions would open a suitable environmentally friendly process for obtaining 4-cyanobenzoic derivatives, which can be potentially useful for the designing of “green” plasticizers based on phthalate derivatives [12].



Scheme 1. Electrocarchylation of 4-iodobenzonitrile.

2. Results and Discussion

To establish the optimal experimental conditions for the optimal electrochemical capture of CO₂, the electrochemical behavior of 4-iodobenzonitrile (**1**) was studied in different solvents and electrodes under an inert atmosphere.

2.1. Electrochemical Reduction of 4-Iodobenzonitrile under an Inert Atmosphere

Electrochemical Reduction Mechanism of 4-Iodobenzonitrile on Carbon and Silver Cathodes

Cyclic voltammograms (CVs) of a 10 mL solution of **1** in dimethylformamide (DMF) using 0.10 M of tetrabutylammonium tetrafluoroborate (TBA BF₄) were recorded at different scan rates (from 0.10 to 1.0 V s^{−1}) using glassy carbon (GC, dotted line) and Ag (solid lines) as working electrodes under a N₂ atmosphere, and are depicted in Figure 1. The same general trend was observed in both cases, a first two-electron irreversible wave followed by a second reversible one-electron wave. This second electron transfer corresponded to the electrochemical reduction of benzonitrile, which is in agreement with previous studies reported in the literature under similar experimental conditions [36]. A closer look at the CVs revealed that the reduction potential value of **1** was reduced by at least 0.46 V (from −1.83 V to −1.37 V), when Ag was used as cathode material instead of GC. The reduction of the

over-potential showed a well-defined electrochemical signal (Figure 1). Hence, the use of silver as a cathode introduced electrocatalytic properties for the current reduction processes performed in an aprotic organic electrolyte, such as DMF + 0.10 M TBA BF₄.

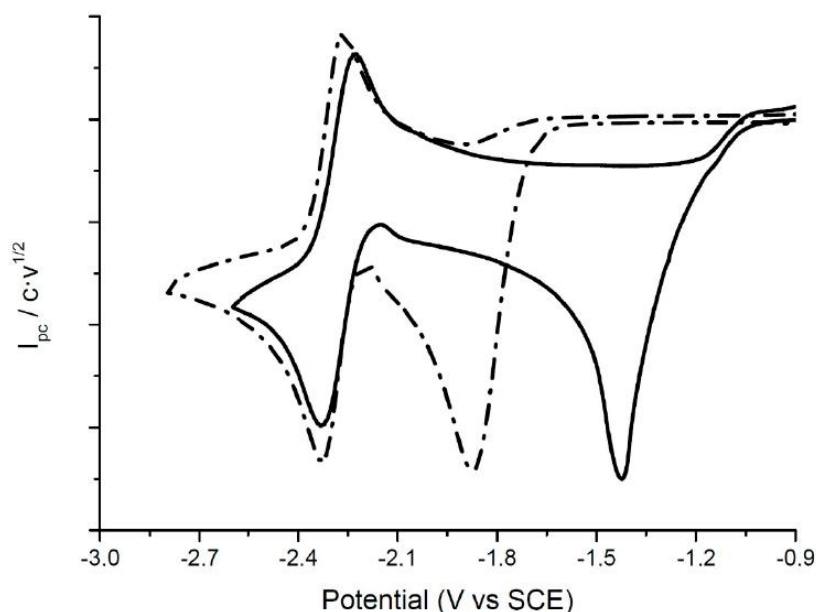


Figure 1. Cyclic voltammograms of a 5 mL DMF/0.10 M TBABF₄ solution containing 10 mM 4-iodobenzonitrile using silver, Ag, (solid line) and glassy carbon, GC, (dotted lines) under a nitrogen atmosphere. Scan rate 0.5 V s^{−1}.

The same electrocatalytic effect was observed when DMF was replaced by ionic liquids (ILs). Thus, when 1-ethyl-3-methylimidazolium bis(trifluoromethylsulfonyl)imide ([EMIM]TFSI) and 1-methyl-1-propylpiperidinium bis(trifluoromethylsulphonyl)-imide ([PP13]TFSI) were used as electrolytes, the reduction potential value of **1** was reduced by approximately (ca.) 0.5 V (Figure 2). Note that ILs can also act as a co-catalyst when silver is used as a working electrode, since the reduction potential value of **1** is ca. 0.1 V lower compared to DMF + 0.10 M TBABF₄ (Table 1). Hence, the solvation process of **1**[−] appeared to be more effective in the case of using a high concentration of cations (ILs) than tetrabutylammonium salts at low concentrations (0.1 M TBABF₄ in DMF). Besides, it seemed that the presence of pyrrolidinium cations in the IL composition led to stronger coulombic interactions, which rendered better solvation of **1**[−].

Table 1 summarizes the electrochemical data obtained for the electrochemical reduction of **1** using several solvents and cathode materials. In all the cases a fast, irreversible, two-electron reduction wave was observed, whereas the electron transfer seemed to be faster in silver than in glassy carbon, since the peak width value was reduced from ca. 100 mV (slow electron transfer) to ca. 60 mV (fast electron transfer) [37–40].

To fully establish the electrochemical reduction mechanism of **1** in ionic liquids, a controlled potential electrolysis after the first reduction wave (at a potential value of ca. 0.1 V more negative than the E_{pc}) was performed under an inert atmosphere using either carbon graphite or silver cathodes. The analysis of the sample after the electrolysis showed that, in all the cases, benzonitrile, **2**, was the only product formed after the passage of 2F (C mol^{−1}) (Figure 3). The electrochemical processes were monitored by cyclic voltammetry.

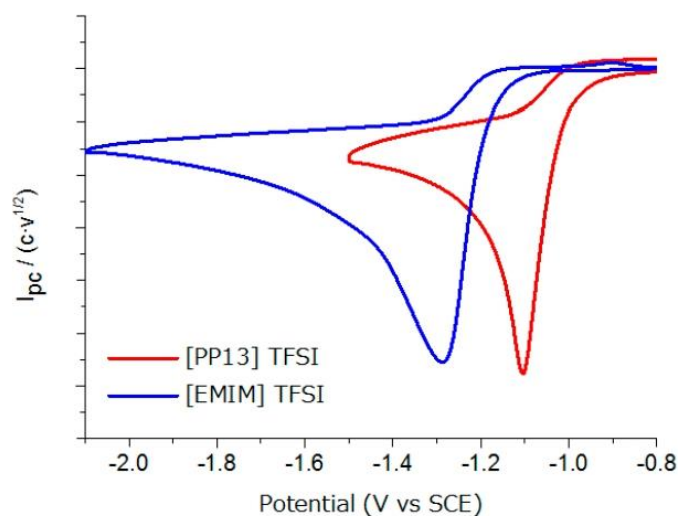


Figure 2. Cyclic voltammograms of a 5 mL solution, [PP13]TFSI (red line) and [EMIM]TFSI (blue line), containing 10 mM 4-iodobenzonitrile using Ag under a nitrogen atmosphere. Scan rate 0.5 V s^{-1} .

Table 1. Electrochemical parameters for the electrochemical reduction of **1**.

Solvent	Number of Electrons ¹	Glassy Carbon Cathode		Silver Cathode		Electrocatalytic Effect (kcal mol^{-1}) ³
		E_{pc} (V)	ΔE_{pc} (V) ²	E_{pc} (V)	ΔE_{pc} (V) ^b	
DMF ⁴	2	−1.85	0.09	−1.37	0.06	10.4
[PP13]TFSI	2	−1.83	0.12	−1.07	0.07	17.5
[EMIM]TFSI	2	−1.84	0.08	−1.29	0.06	12.7

¹ Number of electrons involved in the first electron transfer determined by comparison with a 9-Fluorenone redox probe. ² $\Delta E_{\text{p}} = E_{\text{pc}} - E_{\text{pc}/2}$. ³ Electrocatalytic effect: $E_{\text{pc}}(\text{GC}) - E_{\text{pc}}(\text{Ag})$. ⁴ DMF contains 0.10 M TBABF₄.

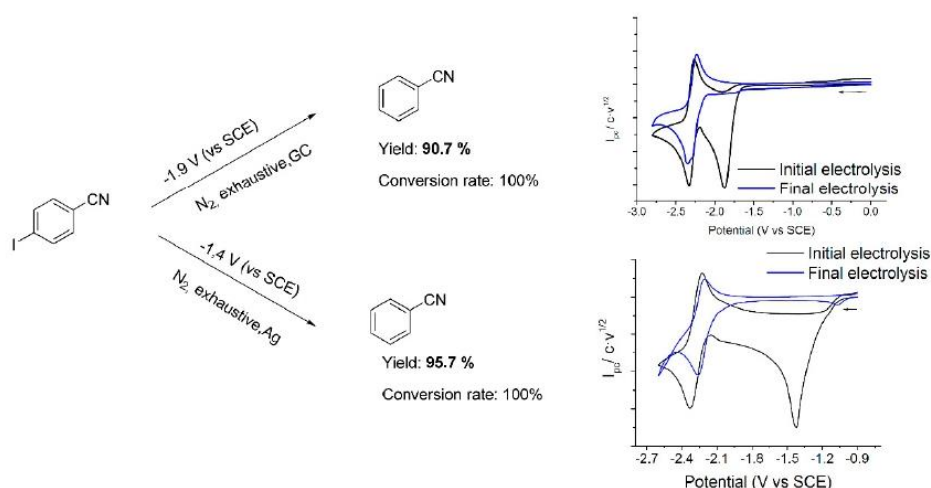
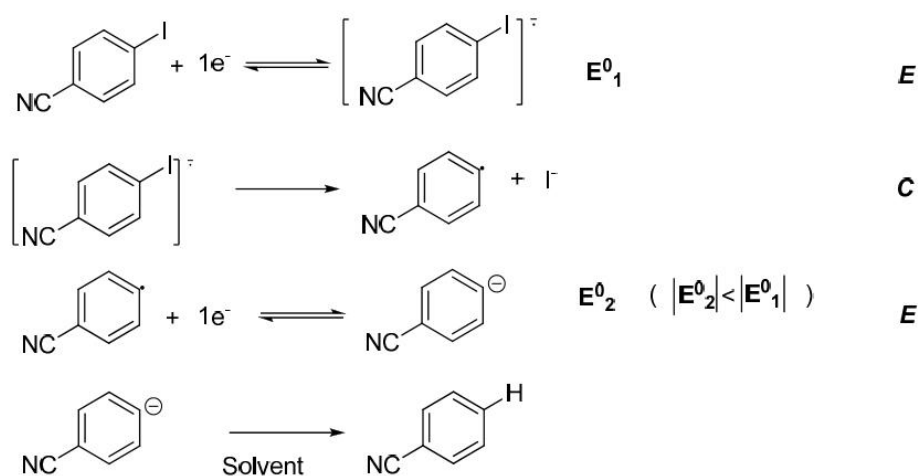


Figure 3. Experimental conditions and the cyclic voltammogram of a 5 mL solution of **1** (10 mM) before (black line) and after (blue line) controlled potential electrolysis under an inert atmosphere with a glassy carbon electrode (top) and silver electrode (bottom). Scan rate: 0.5 V s^{-1} .

Taking into account the cyclic voltammetry and controlled potential electrolysis experiments, it is possible to conclude that **1** followed the Electron transfer, Chemical reaction, Electron transfer (ECE) mechanism. Hence, in a first electrochemical step (E) the radical anion, $1^{\cdot-}$, was generated. A chemical reaction (C) coupled to this first electron transfer led to a benzonitrile radical and an iodide anion through a C–I bond cleavage reaction. Finally, the radical was reduced to an anion at the electrode surface (E), which later protonated by reacting with the solvent (Scheme 2). Note that the electrochemical generation of benzonitrile anion, which acts as a nucleophile leading to benzonitrile, opened the door to incorporate CO_2 via nucleophile-electrophile reaction through the electrochemical reduction of **1**.



Scheme 2. ECE mechanism proposal for the electrochemical reduction of **1** for both media.

2.2. Electrochemical Reduction of 4-Iodobenzonitrile under a Carbon Dioxide (CO_2) Atmosphere

Electrochemical Reduction Mechanism of 4-Iodobenzonitrile on Carbon and Silver Cathodes

4-Iodobenzonitrile (**1**) showed a different electrochemical behavior at GC and silver cathodes in DMF under a CO_2 atmosphere. When GC was used, two reduction peaks were observed at -1.83 V and -2.35 V, the first one corresponding to the electrochemical reduction of **1**, and the second one to the electrochemical reduction of benzonitrile (Figure 4a). It is worth noting that in the presence of CO_2 there was an increase in the peak current value of this second reduction peak and a loss of reversibility, which indicated that the benzonitrile was acting as an organic mediator for the reduction of CO_2 through a homogeneous indirect catalytic process [41,42]. In the corresponding anodic counter scan, a new oxidation peak was observed at 0.45 V, which corresponded to the oxidation of the oxalate anion generated in the CO_2 reduction process under a saturated CO_2 atmosphere [43] (Scheme 3). Note that the peaks at higher oxidation potential values corresponded to the oxidation of iodide and triiodide, respectively. Due to the low oxidation potential value of silver, it was not possible to record any anodic counter scan so as to detect the nature of the anionic products formed.

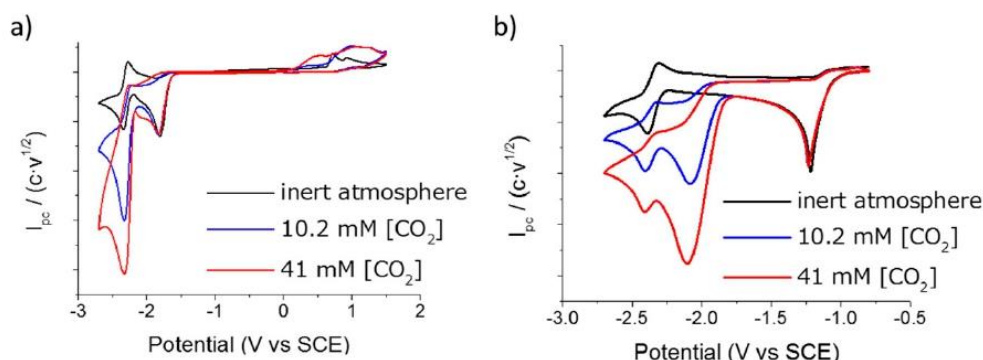
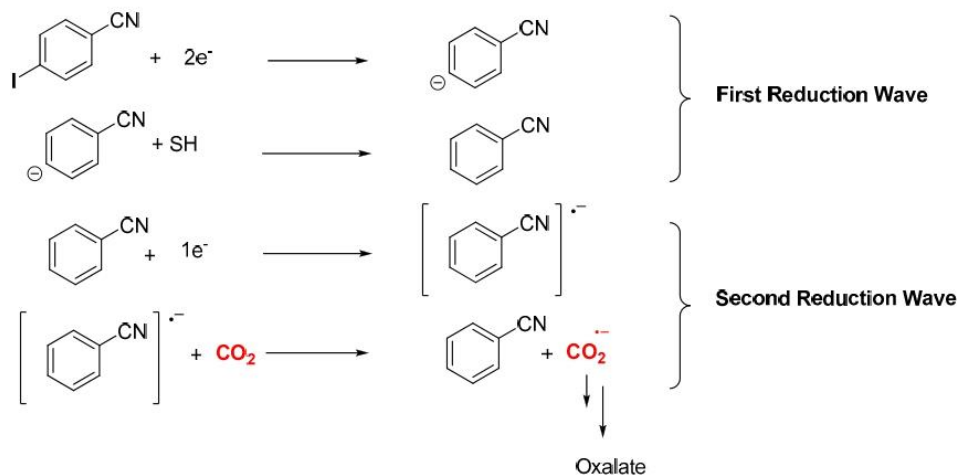


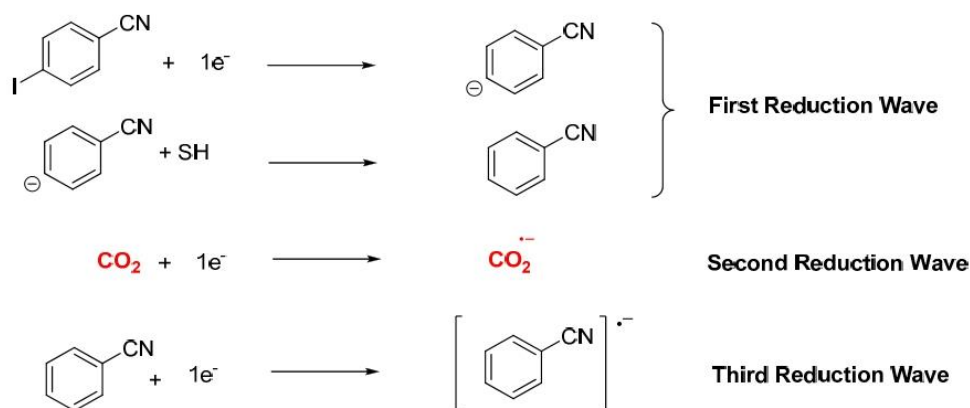
Figure 4. Cyclic voltammograms of 5 mL solution in DMF/0.10 M TBABF₄ containing 10.2 mM 4-iodobenzonitrile under a nitrogen atmosphere and CO₂ atmosphere using (a) GC and (b) Ag. Scan rate 0.5 V s⁻¹.



Scheme 3. Mechanism proposal for the electrochemical reduction of **1** using a GC electrode under a CO₂ atmosphere.

The CV of **1** at the silver cathode under a CO₂ atmosphere in DMF showed three reduction peaks at −2.23 V, −2.09, and −2.40 V vs. SCE. The first and third peaks corresponded to the electrochemical reduction of **1** and benzonitrile, respectively. The second peak corresponded to the electrochemical reduction of CO₂. This assignment of the second reduction peak to the electrochemical reduction of CO₂ can be confirmed since the peak current value was directly linked to the CO₂ concentration, as it can be seen in Figure 4b. In the case of using silver as a working electrode, the electrochemical processes and their associated reactivity were easily controlled by the applied potential. Note that in this case, since the electrochemical reduction of CO₂ occurred prior to the benzonitrile reduction, no electrocatalytic processes were observed related to the role of benzonitrile as a redox mediator (Scheme 4).

The same general electrochemical trend was observed when DMF was replaced by [PP13]TFSI under a N₂ and a CO₂ atmosphere at the GC and silver electrodes. However, when using [EMIM]TFSI, the electrochemical reduction of benzonitrile was not detected in any of the cases due to the fact that the reduction of the imidazolium cation appeared at less negative potentials either in inert or CO₂ atmospheres [44].



Scheme 4. Mechanism proposal for the electrochemical reduction of **1** using an Ag electrode under a CO₂ atmosphere.

2.3. Electrochemicarboxylation of 4-Iodobenzonitrile

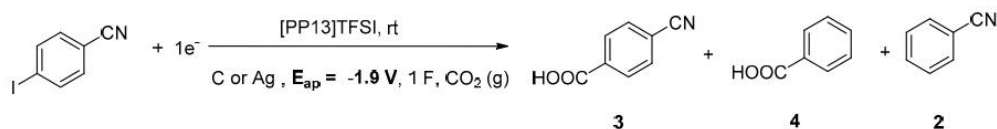
Once the electrochemical reduction mechanism was disclosed, electrocarboxylation processes were performed using a carbon graphite rod and a silver foil electrode after its first reduction wave (ca. −1.9 V) under a CO₂ atmosphere. The results are summarized in Table 2. It is important to note that, when silver was used as a cathode, the electrochemical potential required was 0.5 V lower. A closer look at the data when carbon electrode was used indicates that when the electrocarboxylation process was performed in [EMIM]TFSI, there was a loss of efficiency and no electrocarboxylation products were obtained (entry 1). Those facts can be easily explained by taking into account the IL electrochemical window and the acidity of the C₂–H of the imidazolium moiety. The replacement of the carbon cathode for silver allowed the efficiency of the electrosynthesis to increase, since the reduction potential applied was less negative, although no electrocarboxylated product was observed, again due to the acidity of the IL cation (entry 4).

Table 2. Results of the electrocarboxylation of **1**.

Entries	Solvent	Cathode	Electrochemical Conditions		Yield		
					Electrocarboxylated Products (Conversion Rate)		Ar-H
			E _{applied} (V)	F (C mol ^{−1})	3	4	
1	[EMIM]TFSI	Carbon	−1.9	3.3	–	–	45%
2	[PP13]TFSI	Carbon	−1.9	2.0	8% (19%)	2% (19%)	33%
3	[PP13]TFSI	Carbon	−1.9	3.0	–	12% (21%)	44%
4	[EMIM]TFSI	Silver	−1.4	1.5	–	–	95%
5	[PP13]TFSI	Silver	−1.4	1.0	5% (10%)	–	45%
6	[PP13]TFSI	Silver	−1.4	2.5	26% (29%)	–	66%
7	[PP13]TFSI	Silver	−1.4	3.0	30% (30%)	–	70%
8	[BMPyr]TFSI	Silver	−1.4	1.0	10% (33%)	–	20%
9	[N1114]TFSI	Silver	−1.4	2.4	29% (38%)	–	48%

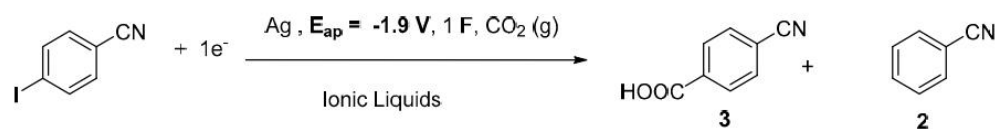
The use of an IL composed of non-acidic cations enabled electrocarboxylated products to be obtained. When [PP13]TFSI was used, around 10% of electrocarboxylated products (p-cyanobenzoic acid (**3**) and benzoic acid (**4**)) were obtained using carbon electrodes (Scheme 5, entries 2 and 3). The use of a high reduction potential value caused the appearance of an unexpected carboxylation product, **4**, which should be related to the further electrochemical reactions of compound **3** that take place under these electrochemical conditions. Note that when the charge passed to the system increased, the only

product obtained was **4** in a 12% yield (entry 3). To confirm this hypothesis, a controlled potential electrolysis of **3** was performed under the same electrochemical and chemical conditions previously described in entry 3, revealing the formation of benzoic acid in a ca. 25% yield.



Scheme 5. Electrocarboxylation of **1** acid under CO₂ atmosphere using graphite as a cathode.

The use of silver cathodes allowed working under milder conditions, and as a consequence, not only were the electrocarboxylation yields almost three times higher, but also the selectivity of the increases, and only **3** was obtained as a carboxylation product in [PP13]TFSI (entries 5–7). Only compounds **2** and **3** were obtained in 70% and 30% yields, respectively, when exhaustive controlled potential electrolysis was performed. These results can also be reproduced using two different ILs consisting of non-acidic cations, such as 1-butyl-1-methylpyrrolidinium bis(trifluoromethylsulphonyl)imide ([BMPyr]TFSI) and *N*-trimethyl-*N*-butylammonium methylimidazolium bis(trifluoromethylsulphonyl)imide ([N1114]TFSI), entries 8 and 9 respectively. In all the cases, conversion rates ca. 30% were obtained (Scheme 6).



Scheme 6. Electrocarboxylation of **1** under CO₂ atmosphere using silver as a cathode.

3. Materials and Methods

3.1. Materials

Carbon dioxide (CO₂) and nitrogen (N₂) were purchased from Carbueros Metálicos S.A. (Cornellà de Llobregat, Spain), purity of 99.9999%). All of the commercially available reagents, *p*-cyanobenzoic acid, 4-iodobenzonitrile, benzonitrile, *N,N*-dimethylformamide (DMF) and tetrabutylammonium tetrafluoroborate (TBABF₄) were acquired from Sigma-Aldrich (Madrid, Spain) with maximum purity and used as received. 1-Ethyl-3-methylimidazolium bis(trifluoromethylsulfonyl)imide ([EMIM]TFSI), 1-methyl-1-propylpiperidinium bis(trifluoromethylsulphonyl)imide ([PP13]TFSI), 1-butyl-1-methylpyrrolidinium bis(trifluoromethylsulphonyl)imide ([BMPyr]TFSI) and *N*-trimethyl-*N*-butylammonium methylimidazolium bis(trifluoromethylsulphonyl)imide ([N1114]TFSI) were acquired from Solvionic (Toulouse, France) and were dried with activated molecular sieves for 24 h in order to guarantee that the amount of water was always less than 100 ppm.

3.2. Electrochemical Experiments

An electrochemical conical cell was used for the set-up of the three-electrode system. For cyclic voltammetry (CV) experiments, the working electrode was a silver disk with a diameter of 1.6 mm and a glassy carbon disk with a diameter of 1 mm. It was polished using a 1 mm diamond paste. The counter electrode was a Pt disk <1 mm in diameter. All of the potentials were reported versus an aqueous saturated calomel electrode (SCE) isolated from the working electrode compartment by a salt bridge. The salt solution of the reference calomel electrode was separated from the electrochemical solution by a salt bridge ended with a frit, which was made of a ceramic material, allowing ionic conduction between the two solutions and avoiding appreciable contamination. Ideally, the electrolyte solution present in the bridge is the same as the one used for the electrochemical solution, in order

to minimize junction potentials. The error associated with the potential values was less than 5 mV. The ohmic drop can be one of the main sources of error when ILs are used as solvents, since they are more resistive media than polar aprotic solvents with 0.10 M concentration of supporting electrolytes.

Due to the low conductivity and larger viscosity of RTILs (Room Temperature Ionic Liquids), in order to facilitate the direct comparison between the cyclic voltammograms in the different media, the current values obtained were first normalized by the concentration and the scan rate ($I_p/cv^{1/2}$). Later, those values were also normalized and the relationship between the four solvents can be expressed by a total normalization coefficient. This coefficient can be expressed as a ratio between DMF/[EMIM]TFSI, DMF/[PP13]TFSI, DMF/[N1114]TFSI, and DMF/[BMPyr]TFSI 3.0, 1.7, 6.0, and 2.7, respectively.

For electrolysis experiments, the disc working electrodes were replaced by a graphite carbon bar and a silver foil. The counter (Pt bar) and reference (SCE) electrodes were separated from the electrochemical solution by a salt bridge filled by the electrolyte solution. The salt bridge ended with a frit, which was made of a ceramic material, avoiding appreciable contamination. Compounds were electrolyzed at a negative potential of 0.10 V more negative than the E_{pc} potential value under nitrogen- or carbon-saturated solutions. When the reaction was completed, the mixture was extracted into water/ether mixtures. The organic layer was dried with Na_2SO_4 and evaporated to yield a residue. All products obtained were characterized by Proton Nuclear Magnetic Resonance (1H -NMR) and Gas Chromatography (GC) by comparison with their respective pure commercially available analogues.

3.3. Determination of the CO_2 Concentration in ILs

A thermal mass flow meter of modular construction with a 'laboratory style' pc-board housing (EL-FLOW® Mass Flow Meter/Controller, Bronkhorst Hi-Tec, Ruurlo, Netherlands) was used to monitor the CO_2 concentrations in the solution [28]. Control valves are integrated to measure and control a gas flow from the lowest range of 0.2–10 mL/min.

4. Conclusions

This manuscript describes a new "environmentally-friendly" electrochemical approach for producing highly valuable compounds using CO_2 as a building block in ILs. The selection of the solvent and the nature of the cathode material are crucial, since it helps to overcome the main drawbacks associated with previous processes reported in the literature, in which organic solvents, redox mediators and large quantities of supporting electrolytes are employed. The use of silver instead of carbon cathodes enables p-cyanobenzoic acid to be obtained from the electrochemical reduction of 4-iodobenzonitrile under mild experimental conditions with moderate yields and conversion rates under a CO_2 atmosphere. The use of non-acidic ILs also makes the electrocarboxylation process more environmentally friendly, since it is not only able to avoid the use of organic solvents and large quantities of supporting electrolytes, but also the solvation process of 1^- appears to be more effective. Hence, the use of ILs (high concentration of cations) instead of tetrabutylammonium salts at low concentrations (0.1 M TBABF₄ in DMF) enables the electrochemical potential applied to be also reduced. This study opens the door to develop new strategies for the synthesis of similar derivatives, such as phthalates, by following this "greener" route.

Author Contributions: G.G. conceived and designed the experiments; S.M. performed the experiments and analyzed the data. G.G. and I.G. wrote the paper and approved the final version for its publication.

Funding: This research was funded by MINECO/FEDER (project CTQ2015-65439-R).

Acknowledgments: This work was supported by project CTQ2015-65439-R from the MINECO/FEDER. S.M. thanks the Universitat Autònoma de Barcelona for pre-doctoral PIF fellowships.

Conflicts of Interest: The authors declare no conflict of interests.

References

1. Veríssimo, D.; Macmillan, D.C.; Smith, R.J.; Crees, J.; Davies, Z.G. Has Climate Change Taken Prominence over Biodiversity Conservation? *Bioscience* **2014**, *64*, 625–629. [\[CrossRef\]](#)
2. Oertel, C.; Matschullat, J.; Zurba, K.; Zimmermann, F.; Erasmí, S. Greenhouse Gas Emissions from Soils—A Review. *Chemie der Erde-Geochemistry* **2016**, *76*, 327–352. [\[CrossRef\]](#)
3. Nejat, P.; Jomehzadeh, F.; Taheri, M.M.; Gohari, M.; Muhl, M.Z. A Global Review of Energy Consumption, CO₂ emissions and Policy in the Residential Sector (with an Overview of the Top Ten CO₂ Emitting Countries). *Renew. Sustain. Energy Rev.* **2015**, *43*, 843–862. [\[CrossRef\]](#)
4. Albo, J.; Alvarez-Guerra, M.; Castaño, P.; Irabien, A. Towards the Electrochemical Conversion of Carbon Dioxide into Methanol. *Green Chem.* **2015**, *17*, 2304–2324. [\[CrossRef\]](#)
5. Brunel, P.; Monot, J.; Kefalidis, C.E.; Maron, L.; Martin-Vaca, B.; Bourissou, D. Valorization of CO₂: Preparation of 2-Oxazolidinones by Metal-Ligand Cooperative Catalysis with SCS Indenediide Pd Complexes. *ACS Catal.* **2017**, *7*, 2652–2660. [\[CrossRef\]](#)
6. Bobbink, F.D.; Van Muyden, A.P.; Gopakumar, A.; Fei, Z.; Dyson, P.J. Synthesis of Cross-Linked Ionic Poly(Styrenes) and Their Application as Catalysts for the Synthesis of Carbonates from CO₂ and Epoxides. *Chempluschem* **2017**, *82*, 144–151. [\[CrossRef\]](#)
7. Cheah, W.Y.; Ling, T.C.; Juan, J.C.; Lee, D.J.; Chang, J.S.; Show, P.L. Biorefineries of Carbon Dioxide: From Carbon Capture and Storage (CCS) to Bioenergies Production. *Bioresour. Technol.* **2016**, *215*, 346–356. [\[CrossRef\]](#)
8. Huang, C.H.; Tan, C.S. A Review: CO₂ Utilization. *Aerosol Air Qual. Res.* **2014**, *14*, 480–499. [\[CrossRef\]](#)
9. Kurllov, A.; Broda, M.; Hosseini, D.; Mitchell, S.J.; Pérez-Ramírez, J.; Müller, C.R. Mechanochemically Activated, Calcium Oxide-Based, Magnesium Oxide-Stabilized Carbon Dioxide Sorbents. *ChemSusChem* **2016**, *9*, 2380–2390. [\[CrossRef\]](#)
10. Pan, S.Y.; Chiang, P.C.; Pan, W.; Kim, H. Advances in State-of-Art Valorization Technologies for Captured CO₂ toward Sustainable Carbon Cycle. *Crit. Rev. Environ. Sci. Technol.* **2018**, *48*, 471–534. [\[CrossRef\]](#)
11. Yadav, N.; Seidi, F.; Crespy, D.; D’Elia, V. Polymers Based on Cyclic Carbonates as Trait D’Union Between Polymer Chemistry and Sustainable CO₂ Utilization. *ChemSusChem* **2018**. [\[CrossRef\]](#)
12. Bocqué, M.; Voirin, C.; Lapinte, V.; Caillol, S.; Robin, J.J. Petro-Based and Bio-Based Plasticizers: Chemical Structures to Plasticizing Properties. *J. Polym. Sci. Part A Polym. Chem.* **2016**, *54*, 11–33. [\[CrossRef\]](#)
13. Cacaval, D.; Blaga, A.C.; Cmru, M.; Galaction, A.I. Comparative Study on Reactive Extraction of Nicotinic Acid with Amberlite LA-2 and D2EHPA. *Sep. Sci. Technol.* **2007**, *42*, 389–401. [\[CrossRef\]](#)
14. Diniz, L.F.; Souza, M.S.; Carvalho, P.S.; da Silva, C.C.P.; D’Vries, R.F.; Ellena, J. Novel Isoniazid Cocrystals with Aromatic Carboxylic Acids: Crystal Engineering, Spectroscopy and Thermochemical Investigations. *J. Mol. Struct.* **2018**, *1153*, 58–68. [\[CrossRef\]](#)
15. Cokoja, M.; Bruckmeier, C.; Rieger, B.; Herrmann, W.A.; Kühn, F.E. Transformation of Carbon Dioxide with Homogeneous Transition-Metal Catalysts: A Molecular Solution to a Global Challenge? *Angew. Chemie Int. Ed.* **2011**, *50*, 8510–8537. [\[CrossRef\]](#)
16. Darensbourg, D.J. Making Plastics from Carbon Dioxide: Salen Metal Complexes as Catalysts for the Production of Polycarbonates from Epoxides and CO₂. *Chem. Rev.* **2007**, *107*, 2388–2410. [\[CrossRef\]](#) [\[PubMed\]](#)
17. Gao, W.Y.; Wu, H.; Leng, K.; Sun, Y.; Ma, S. Inserting CO₂ into Aryl C–H Bonds of Metal–Organic Frameworks: CO₂ Utilization for Direct Heterogeneous C–H Activation. *Angew. Chemie. Int. Ed.* **2016**, *55*, 5472–5476. [\[CrossRef\]](#)
18. León, T.; Correa, A.; Martin, R. Ni-Catalyzed Direct Carboxylation of Benzyl Halides with CO₂. *J. Am. Chem. Soc.* **2013**, *135*, 1221–1224. [\[CrossRef\]](#)
19. Mizuno, H.; Takaya, J.; Iwasawa, N. Rhodium(I)-Catalyzed Direct Carboxylation of Arenes with CO₂ via Chelation-Assisted C–H Bond Activation. *J. Am. Chem. Soc.* **2011**, *133*, 1251–1253. [\[CrossRef\]](#)
20. Schmeier, T.J.; Dobereiner, G.E.; Crabtree, R.H.; Hazari, N. Secondary Coordination Sphere Interactions Facilitate the Insertion Step in an Iridium(III) CO₂ Reduction Catalyst. *J. Am. Chem. Soc.* **2011**, *133*, 9274–9277. [\[CrossRef\]](#)
21. Yu, D.; Teong, S.P.; Zhang, Y. Transition Metal Complex Catalyzed Carboxylation Reactions with CO₂. *Coord. Chem. Rev.* **2015**, *293–294*, 279–291. [\[CrossRef\]](#)

22. Xie, J.N.; Yu, B.; Zhou, Z.H.; Fu, H.C.; Wang, N.; He, L.N. Copper(I)-Based Ionic Liquid-Catalyzed Carboxylation of Terminal Alkynes with CO₂ at Atmospheric Pressure. *Tetrahedron Lett.* **2015**, *56*, 7059–7062. [CrossRef]
23. Isse, A.A.; Ferlin, M.G.; Gennaro, A. Electrocatalytic Reduction of Arylethyl Chlorides at Silver Cathodes in the Presence of Carbon Dioxide: Synthesis of 2-Arylpropanoic Acids. *J. Electroanal. Chem.* **2005**, *581*, 38–45. [CrossRef]
24. Senboku, H.; Nagakura, K.; Fukuhara, T.; Hara, S. Three-Component Coupling Reaction of Benzylic Halides, Carbon Dioxide, and N,N-Dimethylformamide by Using Paired Electrolysis: Sacrificial Anode-Free Efficient Electrochemical Carboxylation of Benzylic Halides. *Tetrahedron* **2015**, *71*, 3850–3856. [CrossRef]
25. Cruz, H.; Gallardo, I.; Guirado, G. Electrochemically Promoted Nucleophilic Aromatic Substitution in Room Temperature Ionic Liquids—An Environmentally Benign Way to Functionalize Nitroaromatic Compounds. *Green Chem.* **2011**, *13*, 2531–2542. [CrossRef]
26. Dokania, A.; Ramirez, A.; Bavykina, A.; Gascon, J. Heterogeneous Catalysis for the Valorization of CO₂: Role of Bifunctional Processes in the Production of Chemicals. *ACS Energy Lett.* **2018**, *4*, 167–176. [CrossRef]
27. Isse, A.A.; Durante, C.; Gennaro, A. One-Pot Synthesis of Benzoic Acid by Electrocatalytic Reduction of Bromobenzene in the Presence of CO₂. *Electrochem. Commun.* **2011**, *13*, 810–813. [CrossRef]
28. Senboku, H.; Katayama, A. Electrochemical Carboxylation with Carbon Dioxide. *Curr. Opin. Green Sustain. Chem.* **2017**, *3*, 50–54. [CrossRef]
29. Zhao, G.; Huang, X.; Wang, X.; Wang, X. Progress in Catalyst Exploration for Heterogeneous CO₂ reduction and Utilization: A Critical Review. *J. Mater. Chem. A* **2017**, *5*, 21625–21649. [CrossRef]
30. Tahara, H.; Uranaka, K.; Hirano, M.; Ikeda, T.; Sagara, T.; Murakami, H. Electrochromism of Ferrocene and Viologen-Based Redox-Active Ionic Liquids Composite. *ACS Appl. Mater. Interfaces* **2018**, *11*, 1–6. [CrossRef]
31. Mao, X.; Wu, M.; Xu, X.; Jiang, L.; Yan, J.; Du, Z.; Li, J.; Hou, S. Fabrication of an Electrochemical Sensor for NO_x Based on Ionic Liquids and MoS₂. *Int. J. Electrochem. Sci.* **2018**, *13*, 11038–11048. [CrossRef]
32. Thompson, M.W.; Matsumoto, R.; Sacci, R.L.; Sanders, N.C.; Cummings, P.T. Scalable Screening of Soft Matter: Case Study of Mixtures of Ionic Liquids and Organic Solvents. *J. Phys. Chem. B* **2019**, *123*, 1340–1347. [CrossRef] [PubMed]
33. Reche, I.; Gallardo, I.; Guirado, G. Electrochemical Studies of CO₂ in Imidazolium Ionic Liquids Using Silver as a Working Electrode: A Suitable Approach for Determining Diffusion Coefficients, Solubility Values, and Electrocatalytic Effects. *RSC Adv.* **2014**, *4*, 65176–65183. [CrossRef]
34. Alvarez-Guerra, M.; Albo, J.; Alvarez-Guerra, E.; Irabien, A. Ionic Liquids in the Electrochemical Valorisation of CO₂. *Energy Environ. Sci.* **2015**, *8*, 2574–2599. [CrossRef]
35. Chong, F.K.; Andiappan, V.; Ng, D.K.S.; Foo, D.C.Y.; Eljack, F.T.; Atilhan, M.; Chemmangattuvalappil, N.G. Design of Ionic Liquid as Carbon Capture Solvent for a Bioenergy System: Integration of Bioenergy and Carbon Capture Systems. *ACS Sustain. Chem. Eng.* **2017**, *5*, 5241–5252. [CrossRef]
36. Gallardo, I.; Soler, S. Electrochemically Promoted Arylation of Iodoaromatics. *J. Electroanal. Chem.* **2017**, *799*, 9–16. [CrossRef]
37. Isse, A.A.; Falcicola, L.; Mussini, P.R.; Gennaro, A. Relevance of Electron Transfer Mechanism in Electrocatalysis: The Reduction of Organic Halides at Silver Electrodes. *Chem. Commun.* **2006**, *1*, 344–346. [CrossRef]
38. Isse, A.A.; Gottardello, S.; Durante, C.; Gennaro, A. Dissociative Electron Transfer to Organic Chlorides: Electrocatalysis at Metal Cathodes. *Phys. Chem. Chem. Phys.* **2008**, *10*, 2409–2416. [CrossRef]
39. Isse, A.A.; Berzi, G.; Falcicola, L.; Rossi, M.; Mussini, P.R.; Gennaro, A. Electrocatalysis and Electron Transfer Mechanisms in the Reduction of Organic Halides at Ag. *J. Appl. Electrochem.* **2009**, *39*, 2217–2225. [CrossRef]
40. Arnaboldi, S.; Bonetti, A.; Giussani, E.; Mussini, P.R.; Benincori, T.; Rizzo, S.; Isse, A.A.; Gennaro, A. Electrocatalytic Reduction of Bromothiophenes on Gold and Silver Electrodes: An Example of Synergy in Electrocatalysis. *Electrochem. commun.* **2014**, *38*, 100–103. [CrossRef]
41. Costentin, C.; Robert, M.; Savéant, J.-M. Catalysis of the Electrochemical Reduction of Carbon Dioxide. *Chem. Soc. Rev.* **2013**, *42*, 2423–2436. [CrossRef] [PubMed]
42. Gennaro, A.; Isse, A.A.; Save, J.; Severin, M.; Vianello, E.; Pado, V.; Loredan, V.; Diderot, D.; Cedex, P.; February, R.V.; et al. Homogeneous Electron Transfer Catalysis of the Electrochemical Reduction of Carbon Dioxide. Do Aromatic Anion Radicals React in an Outer-Sphere Manner? *J. Am. Chem. Soc.* **1996**, *118*, 7190–7196. [CrossRef]

43. Chang, M.M.; Saji, T.; Bard, A.J. Electrogenated Chemiluminescence. 30. Electrochemical Oxidation of Oxalate Ion in the Presence of Luminescers in Acetonitrile Solutions. *J. Am. Chem. Soc.* **1977**, *99*, 5399–5403. [[CrossRef](#)]
44. Hayyan, M.; Mjalli, F.S.; Hashim, M.A.; AlNashef, I.M.; Mei, T.X. Investigating the Electrochemical Windows of Ionic Liquids. *J. Ind. Eng. Chem.* **2013**, *19*, 106–112. [[CrossRef](#)]



© 2019 by the authors. Licensee MDPI, Basel, Switzerland. This article is an open access article distributed under the terms and conditions of the Creative Commons Attribution (CC BY) license (<http://creativecommons.org/licenses/by/4.0/>).



Article

Electrochemical Tuning of CO₂ Reactivity in Ionic Liquids Using Different Cathodes: From Oxalate to Carboxylation Products

Silvia Mena and Gonzalo Guirado *

Departament de Química, Universitat Autònoma de Barcelona, Campus UAB, 08193 Bellaterra, Spain; silvia.mena@uab.cat

* Correspondence: gonzalo.guirado@uab.cat; Tel.: +34-93-581-4882

Received: 16 April 2020; Accepted: 21 May 2020; Published: 26 May 2020

Abstract: There is currently quite a lot of scientific interest in carbon dioxide (CO₂) capture and valorization with ionic liquids (ILs). In this manuscript, we analyze the influence of the potential applied, the nature of the cathode and the electrolyte using different organic mediators, such as nitro or cyano aromatic derivatives, to promote the electrochemical activation of CO₂. An electrocatalytic process using a homogeneous catalysis is seen when nitroderivatives are used, yielding to oxalate in organic electrolytes and ILs. Turnover frequency (TOF) values and Faraday efficiencies were slightly higher in *N,N'*-dimethylformamide (DMF) than in ILs probably due to the viscosity of the electrolyte. The use of cyano derivatives allows to tune the electrochemical reactivity in function of the reduction potential value applied from electrocarboxylated products (via a nucleophile-electrophile reaction) to oxalate. These electrochemical reactions were also performed using three different cathodes, organic electrolytes and ionic liquids. The use of copper, as a cathode, and ionic liquids, as electrolytes, would be a cheaper and greener alternative for activating carbon dioxide.

Keywords: CO₂; electrochemistry; ionic liquid; catalysis; carboxylation; green chemistry

1. Introduction

Nowadays methane, nitrous oxide and carbon dioxide (CO₂) emissions represents approximately 98% of the total greenhouse gas (GHG) inventory worldwide [1–3], and their share are expected to increase this twenty-first century. CO₂ represents the most important GHG, which represents approximately the 77% of the global GHG emissions (considering its global warming potential) worldwide. Moreover, the change in atmospheric CO₂ concentration has been considered the most important driver of global warming. In 2019 carbon dioxide emissions from energy stagnated at 33 Gt, which are mainly due to anthropogenic activities. Besides, it is expected to increase to 40.3 Gt by 2030 and to 50 Gt by 2050, if proper measures are not taken [4–7].

In the last decade, new concepts have been developed as a suitable approaches for facing the challenges of the current global scenario; so biomimetic [8] and circular economy models have been formulated. All the approaches involve a first capture step for an efficient removal of CO₂ from common points sources prior to the release of gases into atmosphere [9–12].

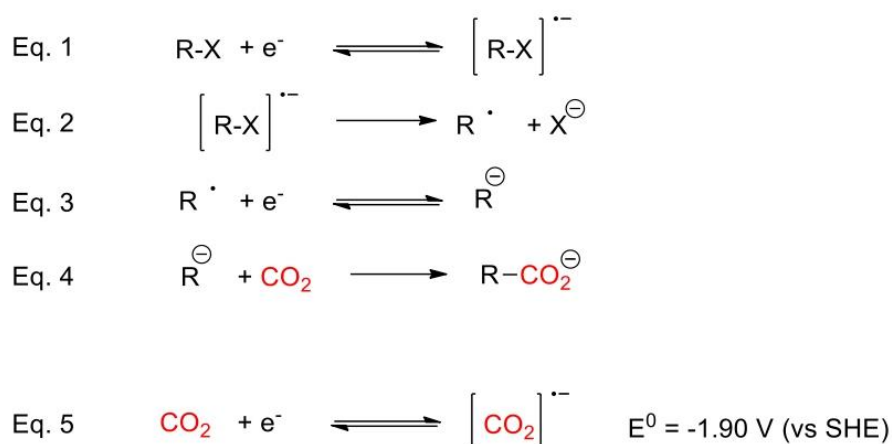
Carbon capture and storage (CCS) approaches include planning the confinement of CO₂ into depleted oil and gas wells, deep oceans, and aquifers [13]. Capture approaches based on chemical absorption and desorption using an aqueous amine solution are also one of the most promising option for separating CO₂ from fossil-fuel-derived flue gas due to its simple operation, high absorption efficiency, cost-effectiveness and maturity [14,15]. However, all these strategies only partially solve the problem, so approaches to recover valuable products from its conversion through

a circular economy vision are highly desirable [16,17]. In this sense, some conversion routes are designed for the reuse of fuels, especially when inexpensive renewable energy processes are available.

New approaches that transform CO₂ in fine chemicals or value-added products are also being deeply investigating. The remunerability of the product is much higher and can economically support the development of the technologies involved. However, the volume of the potential market of these fine chemicals can hardly match with the volume of CO₂ emissions, needing the development of a network of parallel CCU technologies. Hence, different strategies, including biological methods, have been developed either for directly producing reduced products (i.e., carbonic anhydrase, hydrogenation of CO₂ to formate, reduction of CO₂ to methane, CO₂ conversion into methanol by enzyme cascade) or to store CO₂ in biomass (e.g., algae) [18–20]. The photocatalytic reduction approaches also allow to synthesize a wide spectrum of CO₂ reduction products, such as HCOOH, HCHO, CH₃OH, or CH₄, and can be effectively used by using visible responsive materials [21–27]. Adsorption, CO₂ activation and further reduction to produce value-added products are crucial steps for photocatalytic processes. Sharma et al. reported a combined theoretical and experimental study describing the selective reduction of CO₂ into methane through a robust visible-light photocatalyst based on single-phase ternary sulfide (CTS) [28]. Zhou et al. proposed the use of aqueous suspensions of cubic ZnS nanocrystals for the photocatalytic reduction of CO₂ into formate [29]; and the development of heterostructures, such as Cu₂O/TiO₂ for artificial photosynthesis [30].

Chemical catalytic strategies for CO₂ reduction have been proposed mainly based on the Sabatier reaction [31]. Finally, it is worthy to highlight that in the last years, it has been also reported that the development of electrochemical technologies to capture and transform CO₂ into high-added value products is a suitable and green way for activating CO₂ compared to others Carbon Capture, Utilization and Storage (CCUS) strategies [32].

Direct carboxylation of carbon nucleophile using CO₂ as an electrophile is a straightforward route to prepare carboxylic acids. The main drawback associated to this process is related to the use of toxic reagents and the production of a large amounts of waste [33]. For instance, the conventional route for synthesizing 6-aminonicotinic acid from the corresponding nitriles involves low yields, hazardous chemicals (such as cyanide and ammonia gas) and high temperatures [34–36]. Nevertheless, using organic electrochemistry techniques improve environmental conditions [37–50]. One of the most widely used approaches for valorizing CO₂, is to use organic halides with electrochemical techniques, which makes it possible to activate the CO₂ (Scheme 1, Equations (1)–(4)); In a first step, a one electron transfer process generates the organic radical anion, which later converts to an anion through a second reduction electron transfer and a halide anion. The key to this approach relies on the reduction potential value of the organic halides and the stability of the organic anion formed after the reduction process [51–65].



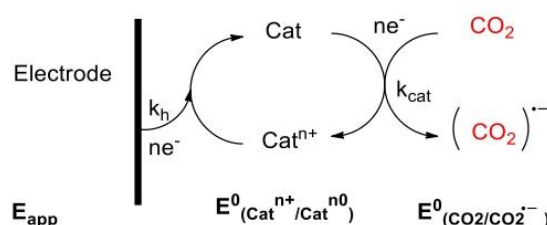
Scheme 1. Electrochemical strategies to valorize CO₂.

The development of selective electrocatalysis processes for the reduction of carbon dioxide (CO_2) to yield C_1 products (such as CO ($2e^-$), or higher C_n products) would allow the use of CO_2 as a carbon feedstock (Scheme 1). Nevertheless, it is necessary to overcome high-energy barriers for the direct reduction of CO_2 , which commonly implies reduction potential values significantly more negative than the corresponding thermodynamic reduction potential value of CO_2 . In this sense, different types of electrodes have been studied for direct reduction of CO_2 . These cathodes are classified based on the nature of the main product obtained in the electrochemical process in aqueous and non-aqueous supporting electrolytes [66]. Moreover, it has also been developed other kinds of modified or doped electrodes (with immobilized enzymes, nanoparticles or metallic oxides) to catalyze CO_2 direct reduction [67–69]. Hence, the improvement of electrocatalytic processes could lower overpotential requirements while maintaining appropriate catalytic rates and selectivity [70–91].

One of the most common techniques to analyze electrocatalysis is cyclic voltammetry, which provides direct and rapid information regarding the relationship between driving force (i.e., overpotential) and catalytic turnover (i.e., current) compared to rather complicated alternative methods monitored by spectroscopy or other means. However, understanding detailed mechanistic schemes behind voltammograms is quite challenging due to complicated and intertwining processes, such as mass transport, electron transfer, chemical reaction and interfacial chemistry between electrode and reactants. In this sense, developing the foot of the wave analysis (FOWA) of cyclic voltammetry by Savéant and Costentin has provided a feasible method to benchmark molecular electrocatalysts by turnover frequency (TOF) and turnover number (TON) [92–96].

Molecular catalysts are an attractive option owing to the high degree of tunability of electronic and geometric parameters, which allows for systematic reactivity studies that can lead to new catalyst design guidelines. The well-defined structure of the catalytic sites also allows the establishment of a precise structural model for better analysis of the multiple proton-coupled electron transfer processes involved in CO_2 reduction and better understanding of the CO_2 reduction mechanism. For example, Leung et al. proposed a mechanism for CO production using Co-based porphyrins [97,98], where the $[\text{Co}(\text{P})-(\text{CO}_2)]^{2-}$ intermediate will be protonated to form $[\text{Co}(\text{P})-(\text{COOH})]^-$. Later, it will decompose to provide CO . Koper and co-workers proposed a different mechanism [99], where the formation of the CO_2^- anion intermediate, will be protonated yielding to $[\text{Co}(\text{P})-(\text{COOH})]^0$ intermediate. Then, $[\text{Co}(\text{P})-(\text{COOH})]^0$ will decompose to CO . Finally, Yao et al. proposed a pre-activation process to form a local proton source could facilitate CO_2 reduction [100].

The electrocatalysts participates in an electron transfer reaction (on the electrode surface) and facilitates acceleration of a chemical reaction. Both electron transfer and chemical kinetics must be fast for an efficient electrocatalyst. In addition, an optimal electrocatalyst must display a good thermodynamic match between the redox potential (E^0) for the electron transfer reaction and the chemical reaction that is being catalyzed (in this work; CO_2 reduction). Chemical tuning of the electrocatalyst can optimize these factors. A general approach for an electrocatalytic system is given in Scheme 2.



Scheme 2. General approach for CO_2 electrocatalytic system.

The electrocatalytic activity can be analyzed in terms of in cyclic voltammetry (CV). In a CV under a dry inert atmosphere, an electrocatalyst should show a reversible redox couple. Upon addition of the reagent which is catalyzed (i.e., CO_2), the diffusion limited current should increase significantly, while the potential shifts anodically, and the reversibility in the return oxidation wave

is lost due to the chemical reaction between reagent and electrocatalyst. Electrocatalyst offer critical solutions to lowering the overpotentials, improving selectivity, and increasing the reaction kinetics of carbon dioxide conversion [101]. There are a lot of different catalysts reported in literature, although most of them involve the use of metal complexes, such as salen ones [102,103], offering high values of TOF with orders of h^{-1} . On the other side, ionic liquids have been developed as a new catalyst, with a high dependence between TOF and the nature of the cation and anion which form the ionic liquid [104]. The order of TOF in these cases are in order of s^{-1} , allowing avoiding but the use of metals.

Up to now, the main disadvantage of electrochemical technologies is the use of organic solvents such as *N,N*-dimethylformamide, which are well-known to be hazardous and flammable, as well as the use of large amount of supporting electrolyte [105]. For this reason, replacing organic aprotic solvents by ionic liquids (ILs), which are considered a greener option, would improve the process [106–109]. Ionic liquids are a family of solvents with unique properties that have led to their consideration as interesting alternatives, especially for electrochemical applications. Its wide electrochemical windows and good conductivities are obtained combining unsymmetrical bulky organic cations combined with hydrophobic anions [110–123]. For electrocarboxylation process, the use of ionic liquids offers the possibility of recycling the solvent as well as to improve the CO_2 capture due to their high solubility and conductivities [124–141].

Therefore, this work shows different strategies to valorize CO_2 using electrochemical technologies in ionic liquids. In one hand, with a series of nitro-compounds (Figure 1) using three different cathodes (carbon, copper and silver). On the other hand, the replacement of the nitro-group for a cyano- group, involves changes in the reaction mechanism and tune the CO_2 reduction products.

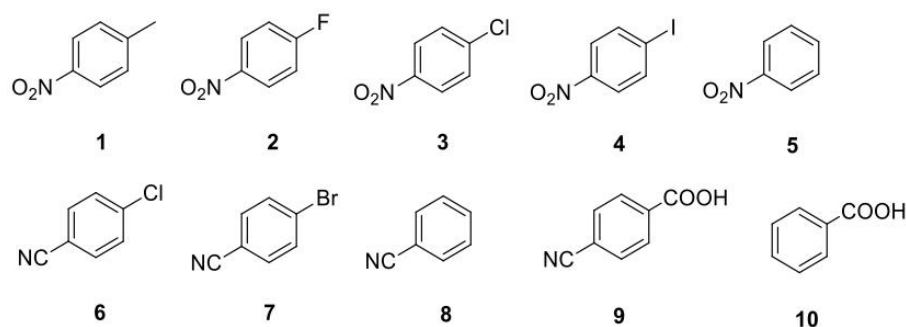


Figure 1. Structures of discussed compounds.

2. Materials and Methods

2.1. Materials

Carbueros Metálicos S.A. (Cornellà de Llobregat, Spain) provided the inert atmosphere gases (nitrogen, N_2 , or argon Ar) and carbon dioxide (CO_2) with purity of 99.9999%. All nitro- and cyano-compounds were obtained from Sigma-Aldrich (Madrid, Spain) and used without further purification. Anhydrous *N,N*-dimethylformamide (DMF) solvent (99.8%) was purchased from SDS (Madrid, Spain). The ionic liquid 1-methyl-1-ethylimidazolium bis(trifluoro-methanesulfonyl)imide (EMIM TFSI, purity 99%, $\text{H}_2\text{O} \leq 0.2\%$) was acquired from Solvionic (Toulouse, France) and was dried under vacuum using activated molecular sieves for 24 h to make sure that the amount of water was always less than $\text{H}_2\text{O} \leq 0.001\%$ [142].

2.2. Methods

2.2.1. Cyclic Voltammetry

All electrochemical experiments were performed in an electrochemical conical cell with a set-up of the three-electrode system. For CV experiments, the working electrode is a vitreous carbon disk (1 mm diameter), silver disk (3 mm diameter) and copper disk (3 mm electrode). The counter electrode is a Pt disk (<1 mm diameter). All electrodes are polished using a 1 mm diamond paste. All the electrochemical potentials were measured using a saturated calomel electrode, SCE (+0.2411 V vs. SHE) isolated from the working electrode compartment by a salt bridge (salt-solution of the reference calomel electrode is separated from the electrochemical solution by a salt-bridge ended with a ceramic material frit, allowing ionic conduction between the two solutions and avoiding appreciable contamination). Ideally, the electrolyte solution present in the bridge is the same as the one used for the electrochemical solution in order to minimize junction potentials. When such a bridge is used, the ions in the bridge are present in large excess at the junction and they carry almost the whole of the current across the boundary. In our case were used DMF/0.1M TBA BF₄ (trying to weigh the same amount of support electrolyte that in the electrolyte solution) or EMIM TFSI, in both cases without electroactive substance. The error associated with the potential values is less than 5 mV. The ohmic drop can be one of the main sources of error when ILs are used as solvents, since they are more resistive media than aprotic polar solvents with 0.1 M concentration of supporting electrolyte. Before and after performing any electrochemical experiments, the solution is purged with inert gas (nitrogen or argon) for 20 min to avoid secondary reactions associated to OER and ORR due to dissolved oxygen in the solution [143,144].

The number of electrons involved in the first reduction process of nitro-compounds were determined by comparison with very well-known one-electron reduction of 9-fluorenone (redox probe), in the same medium using the same electrochemical set-up, by terms of cyclic voltammetry.

It is used 9-fluorenone and nitrobenzene as probe because both compounds have the same magnitude value of diffusion coefficient without further limitations (DMF (10^{-9} m²·s⁻¹) nor ionic liquids (10^{-11} m²·s⁻¹) [145,146]. The number of electrons involved in this first electron transfer was also confirmed by controlled-potential electrolysis.

2.2.2. Electrocarboxylation Processes

Cyano-compounds were electrolyzed at a negative potential of ~0.1 V more negative than the E_{pc} potential value under nitrogen/argon or carbon dioxide saturated solutions. When the reaction is completed, the resulting solution in the electrolysis is extracted with ether. The organic layer is dried with Na₂SO₄ and evaporated to yield a residue that is analyzed by gas chromatography-mass spectrometry, and Proton Nuclear Magnetic Resonance (¹H-NMR). Thus, all products obtained, and the commercial analogues were characterized by ¹H-NMR. Measurements were made using a DPX360 (250 MHz) spectrometer (Bruker, Billerica, MA, USA) spectrometer. Proton chemical shifts were reported in ppm (d) (CDCl₃, δ 7.26, or CD₃CN, δ 1.94). The *J* values are reported in Hz.

Benzonitrile (8). Colorless liquid, 31–35% yield. ¹H-NMR (CDCl₃) δ (ppm): 7.70–7.55 (m, 3H), 7.47 (t, *J* = 7.4 Hz, 2H).

4-Cyanobenzoic acid (9). Yellow pale solid, 15–20% yield. ¹H-NMR (CDCl₃) δ (ppm): 8.19 (d, *J* = 8.5 Hz, 2H), 7.78 (d, *J* = 7.6 Hz, 2H).

Benzoic acid (10). Colorless solid, 7–12% yield. ¹H-NMR (CDCl₃) δ (ppm): 8.13 (d, *J* = 7.5 Hz, 2H), 7.62 (t, *J* = 6.8 Hz, 1H), 7.48 (t, *J* = 6.9 Hz, 2H).

When pure IL is used as electrolyte, the products of the electrolyzed solution are extracted with ether, allowing one to recover almost an 80% of the IL at the end of the experiment [147].

2.2.3. Determination of CO₂ Concentration

A thermal mass flowmeter of modular construction with a 'laboratory style' pc-board housing (EL-FLOW® Mass Flow Meter/Controller) from Bronkhorst Hi-Tec (Ruurlo, Netherlands), was used to monitor the CO₂ concentrations in the solution. Control valves were integrated to measure and control a gas flow from the lowest range of 0.2 up to 10 mL·min⁻¹.

3. Results and Discussion

3.1. Electrochemical Behaviour of Nitro-Compounds under Inert Atmosphere

The electrochemical behavior of a sequence of four *p*-nitro-compounds was studied in different solvents, and electrodes under inert atmosphere.

Cyclic voltammograms (CVs) of a 3–10 mL solution of **1–4** in DMF using 0.10 M of tetrabutylammonium tetrafluoroborate (TBA BF₄), and 1-methyl-1-ethylimidazolium bis(trifluoromethanesulfonyl)imide (EMIM TFSI) were recorded at different scan rates (from 0.10 to 1.0 V s⁻¹) using glassy carbon (C, blue lines), Ag (black lines) and copper, Cu (red lines) as working electrodes under a N₂ atmosphere (Figure 2). Focusing in the first wave, the same general trend was observed in all electrodes and both solvents. Compounds **1–3** shows a monoelectronic fast reversible electron transfer, whereas compound **4** has an irreversible electron transfer (Table 1).

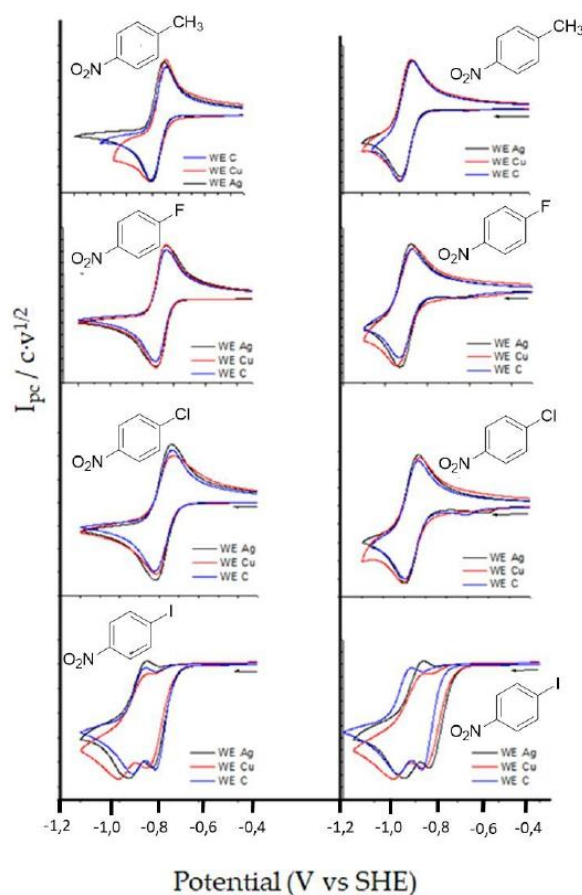
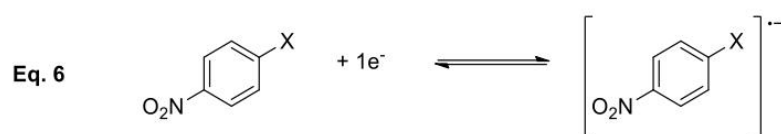


Figure 2. Cyclic voltammetry of 10 mM *p*-nitro compounds **1–4** with Ag (black line), Cu (red line) and C (blue line), under nitrogen atmosphere. Scan rate: 0.5 V·s^{−1}. Solution of DMF/0.1M TBA BF₄ (left) and solution of 3 mL EMIM TFSI (right).

Table 1. Standard potential (E°), cathodic peak potential (in V vs. SCE, E_{pc}) and peak width (ΔE_p (mV)) for **1–4** in different solvents using different working electrodes (WE) at 20 °C.

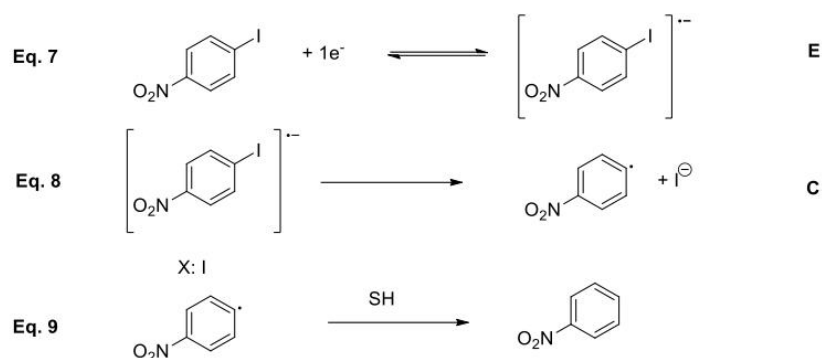
DMF/0.1M TBA BF ₄					
Entry	Nitro Derivative	WE	E _{pc} (V vs. SHE)	E ⁰ (V vs. SHE)	ΔE _p (mV)
1	1	Ag	−0.969	−0.919	72
2		Cu	−0.989	−0.889	70
3		C	−0.969	−0.899	70
4	2	Ag	−0.869	−0.839	60
5		Cu	−0.869	−0.839	72
6		C	−0.869	−0.839	60
7	3	Ag	−0.779	−0.699	67
8		Cu	−0.779	−0.689	68
9		C	−0.779	−0.689	67
10	4	Ag	−0.819	−0.719	83
11		Cu	−0.869	−0.699	90
12		C	−0.809	−0.769	70
EMIM TFSI					
Entry	Nitro Derivative	WE	E _{pc} (V vs. SHE)	E ⁰ (V vs. SHE)	ΔE _p (mV)
13	1	Ag	−0.949	−0.919	58
14		Cu	−0.949	−0.919	58
15		C	−0.959	−0.919	64
16	2	Ag	−0.889	−0.859	59
17		Cu	−0.899	−0.859	64
18		C	−0.889	−0.859	60
19	3	Ag	−0.859	−0.829	58
20		Cu	−0.859	−0.819	64
21		C	−0.859	−0.829	58
22	4	Ag	−0.889	−0.829	60
23		Cu	−0.919	−0.839	70
24		C	−0.929	−0.869	62

A closer look in CVs shows that of 4-iodonitrobenzene has irreversible wave at low scan rate, however it is possible to calculate the E° and the value of the kinetic constant associated to the chemical reaction ($k \sim 2 \cdot 10^4 \text{ s}^{-1}$) by increasing the scan rate (Scheme 3).



Scheme 3. Electron transfer followed by compounds **1–4**.

The cyclic voltammogram of **4** also shows a second monoelectronic reversible wave following the first irreversible one. To check the nature of the product obtained after this first electron transfer, a control potential electrolysis of **4** was performed, being nitrobenzene (**5**) the only product obtained. Considering cyclic voltammetry and control potential electrolysis experiments under inert atmosphere, it is possible to conclude that 4-iodonitrobenzene follows an electron transfer mechanism (E) followed by a chemical reaction (C). Hence, in a first electrochemical step (E) the radical anion, **4**^{•−}, was generated, which evolves to cleavage C-I bond, obtaining nitrobenzene radical which produces nitrobenzene and iodine with an EC mechanism (Scheme 4).



Scheme 4. Proposal mechanism for 4-nitrobenzene electrochemical reduction under inert atmosphere.

3.2. Electrochemical Behaviour of Nitro-Compounds under CO₂ Atmosphere

Compounds **1-4** shows a clearly different behaviour when the cyclic voltammograms are recorded under CO₂ atmosphere, although they show the same general trend in aprotic solvent and ionic liquid. Also they follow the same tendency in C, Ag and Cu working electrodes; there was a rising in current value of the reduction peak and its reversibility was lost (Figure 3), which indicates that p-nitrocompounds **1-4** follow a demeanor of an organic mediator for CO₂ indirect reduction through a homogeneous catalytic process (Scheme 5).

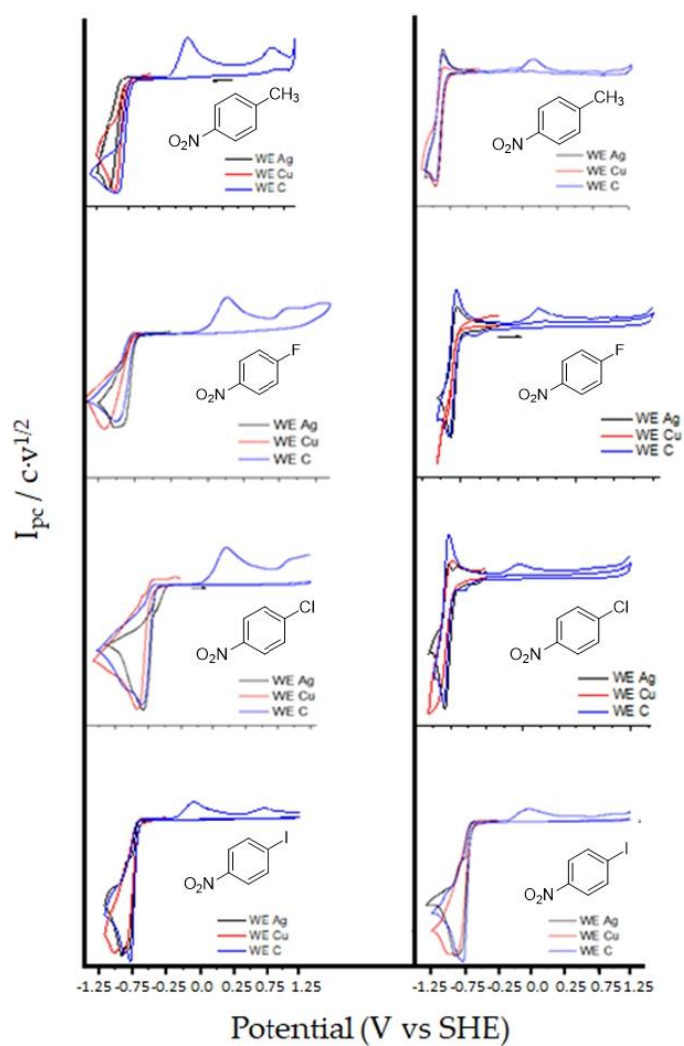
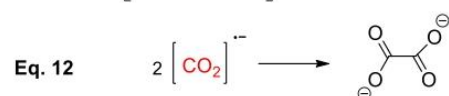
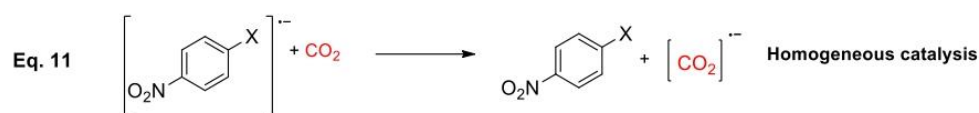
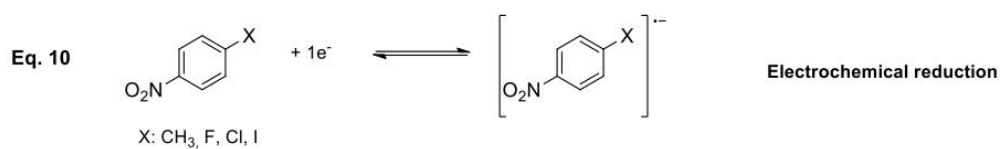


Figure 3. Cyclic voltammetry of 10 mM *p*-nitro compounds 1–4 with Ag (black line), Cu (red line) and C (blue line), under CO₂ atmosphere. Scan rate: 0.5 V·s^{−1}. Solution of DMF/0.1M TBA BF₄ (left) and solution of 3 mL EMIM TFSI (right).



Scheme 5. Proposal mechanism for general catalytic process between CO₂ and *p*-nitrobenzene halides.

In the case of carbon cathode, C, it is possible to see an oxidation peak in the corresponding anodic counter scan (copper and silver electrodes would be oxidized under this experimental conditions) between +0.19 and +0.44 V (vs. SHE). In all cases this peak corresponds to the oxidation of oxalate anion [149], which is formed after reducing the nitroaromatic compound. It is important to remark that the oxidation potential value obtained for oxalate is strongly dependent of the amount of water present in the solvent (Figure 4). The same results are obtained for a sample of pure tetrabutylammonium oxalate, since different amount of water are the oxalate oxidation peak shifts to higher oxidation potentials. Moreover, by using a carbon cathode it is possible to determine the concentration of oxalate formed upon reduction using CV, since the anodic peak current value is related with the oxalate concentration. Hence, we built a calibration curve using pure tetrabutylammonium oxalate for determining the amount of oxalate obtained upon reduction for each *p*-nitro compound. Finally, the TOF values were obtained using through FOWA's method. All the values were summarized in Table 2.

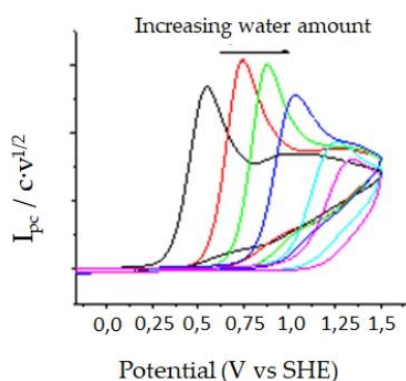


Figure 4. Cyclic voltammetry of 5 mM TBA₂C₂O₄ with glassy carbon under N₂ atmosphere. Scan rate: 0.5 V·s⁻¹.

Table 2. Catalytic parameters in homogeneous catalysis of CO₂.

Entry	Cat.	WE	E ⁰ _{catalyst} (V vs. SHE)		η (V)		TOF (s ⁻¹)		[C ₂ O ₄ ²⁻] (mM)	
			DMF/0.1 M TBA BF ₄	EMIM TFSI	DMF/0.1 M TBA BF ₄	EMIM TFSI	DMF/0.1 M TBA BF ₄	EMIM TFSI	DMF/0.1 M TBA BF ₄	EMIM TFSI
1	1	Ag	−0.919	−0.919	0.90	0.92	7	6	−	−
2		Cu	−0.889	−0.919	0.88	0.92	24	11	−	−
3		C	−0.899	−0.919	0.90	0.91	9	6	18.2	3.41
4	2	Ag	−0.839	−0.859	1.00	0.98	10	7	−	−
5		Cu	−0.80	−0.859	1.00	0.97	8	13	−	−
6		C	−0.839	−0.859	1.00	0.98	10	5	33.4	6.57
7	3	Ag	−0.699	−0.829	1.09	1.01	29	7	−	−
8		Cu	−0.689	−0.819	1.09	1.01	22	5	−	−
9		C	−0.689	−0.829	1.09	1.01	17	6	38.1	9.37
10	4	Ag	−0.719	−0.829	1.05	0.98	8	7	−	−
11		Cu	−0.699	−0.839	1.00	0.95	14	6	−	−
12		C	−0.769	−0.869	1.06	0.94	17	5	3.56	1.12

Knowing that with carbon cathode it is possible to determine oxalate's peak with CV, with a calibration curve is determined the amount of oxalate obtained with each *p*-nitro compound. Also, it is possible to obtain TOF values through Fowa's method [92–96]. All the values were summarized in Table 2. Note that changing a methyl group by halides, the standard potential is lowered between 80–200 mV depending on electrode and halide. TOF values and oxalate amount obtained in DMF

were higher than in EMIM TFSI. Faraday efficiencies were slightly higher in DMF solutions (from 30% to 88%) than in EMIM TFSI (from 10 to 51%) depending on the organic mediator used. These results can be explained due to low viscosity of the ionic liquid and coefficient diffusion value of CO₂ (Table 3).

Table 3. Viscosities and coefficient diffusion values of DMF and EMIM TFSI.

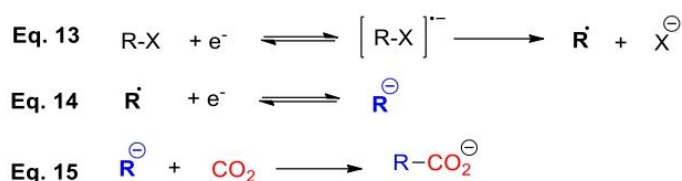
Entry	Solvent	Viscosity (mPa) ^a	Coefficient Diffusion (m ² /s) ^b
1	DMF	0.92	3.6 · 10 ⁻⁹
2	EMIM TFSI	37.3	9.7 · 10 ⁻¹¹

^a Data obtained from Sigma Aldrich/Solvionic Safety Data Sheet (MSDS). ^b Data obtained from our laboratory research group [131].

Note, that it is possible to see an improvement in overpotential values with the use of ionic liquid instead DMF when *p*-nitrocompound has a halide group in its structure. Finally, note that it is possible to use small organic compound and ionic liquids to obtaining similar TOF values (in the order of s⁻¹) to previously published one for organometallic and more sophisticated organic compounds [89,138,148–150]. On the other hand, we observed that for compound **4** the anion radical generated after electron transfer evolves to nitrobenzene radical at the same time that the CO₂ reduction is electrocatalyzed. To check if it is possible to obtain electrocarboxylation product of **5** upon reaction of its radical with CO₂, a control potential electrolysis at −0.96 V (vs. SHE) was performed. After the passage of 1F, no electrocarboxylated aromatic compounds were formed, being oxalate the only electroreduced product of CO₂ formed. These results seem to indicate that the nitrobenzene radical formed upon reduction of **4** (Scheme 4) show a low nucleophilicity, being not able to attack and capture CO₂.

3.3. Electrocatalysis of Cyano-Compounds **6** and **7** under CO₂ Atmosphere

According to previous results obtained in our research group [151], 4-iodobenzonitrile follows an ECE reduction mechanism in ionic liquids (Scheme 6). In the presence of CO₂ the electrogenerated anion intermediate leads to the corresponding carboxylation process. Hence, with the aim to obtain a stronger electrogenerated nucleophile, R[•] (Scheme 6), we decided to move from nitro to cyano aromatic compounds. Thus, two new different *p*-cyanobenzene halides (4-chlorobenzonitrile (**6**) and 4-bromobenzonitrile (**7**)) were explored in this section.



Scheme 6. General overview for an ECE electrocarboxylation mechanism.

Figure 5 shows CVs at DMF/0.1M TBA BF₄ and one example in EMIM TFSI obtained under inert atmosphere and CO₂ atmosphere. All electrochemical parameters are summarized in Table 4. The same general trend was observed in aprotic solvents and ionic liquids. Moreover, not significant differences were detected when the nature of the working electrode was changed.

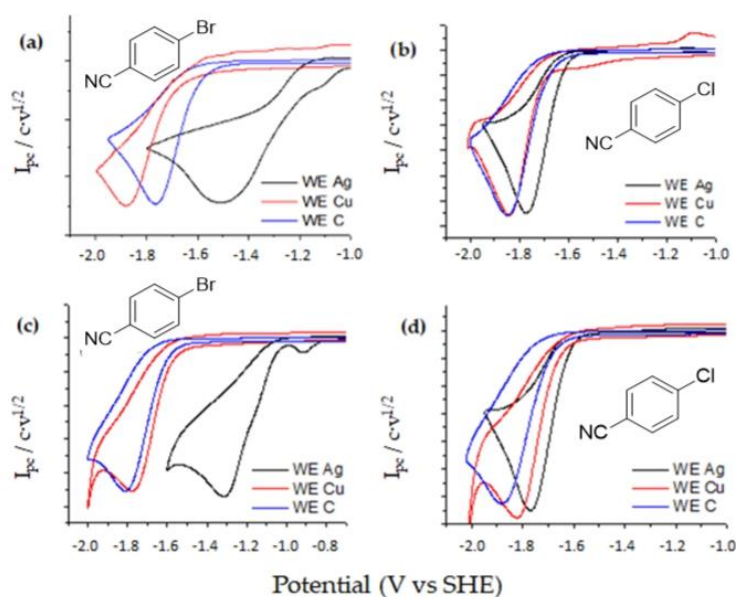


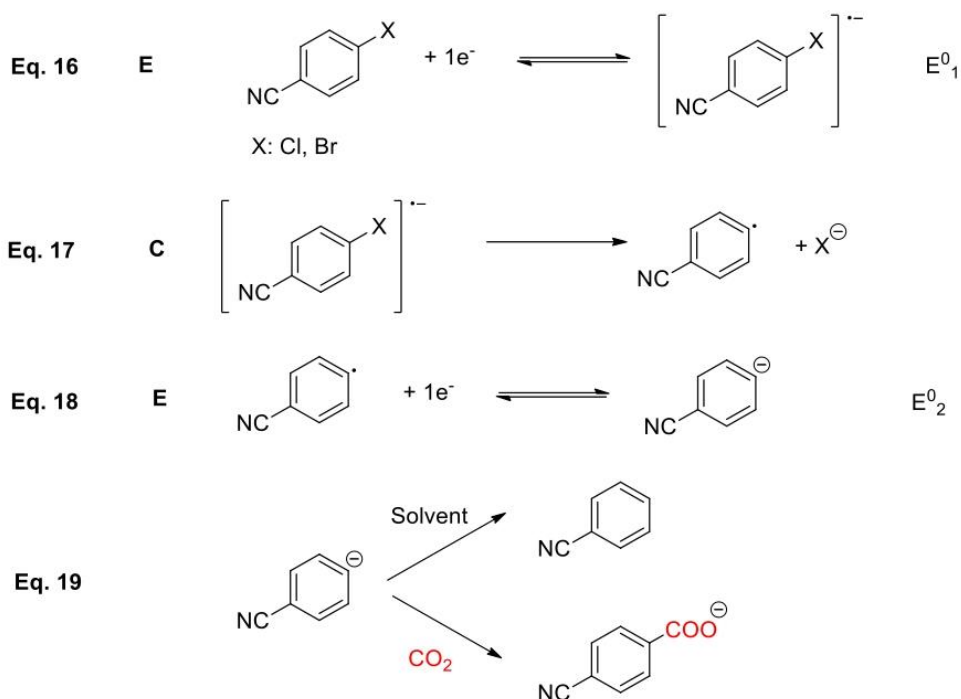
Figure 5. Cyclic voltammetry of 10 mM *p*-cyano compounds **6** and **7** in DMF/0.1M TBA BF₄ with Ag (black line), Cu (red line) and C (blue line), under inert atmosphere (left) and CO₂ atmosphere (right). Scan rate: 0.5 V·s⁻¹.

Table 4. Electrochemical parameters for electroreduction of compounds **6** and **7** in DMF/0.1M TBA BF₄ and EMIM TFSI.

DMF/0.1M TBA BF ₄				
Entries	Cyano Derivative	WE	E _{pc} (V vs. SHE)	ΔE _p (mV)
1	6	Ag	−1.73	85
2		Cu	−1.80	78
3		C	−1.81	96
4	7	Ag	−1.47	201
5		Cu	−1.87	140
6		C	−1.73	99
EMIM TFSI				
7	6	Ag	−1.80	52
8		Cu	−1.80	65
9		C	−1.78	68
10	7	Ag	−1.61	70
11		Cu	−1.85	80
12		C	−1.71	72

As it was expected compounds **6** and **7** exhibit an irreversible bielectronic wave under nitrogen atmosphere for any of the working electrodes investigated (Figures 5a,b). The same electrochemical behavior is observed when DMF is replaced by EMIM TFSI. A closer look to cyclic voltammograms reveals the electrocatalytic properties of silver as a working electrode, since the peak potential value of the reduction peak is shifted to less negative potentials. In order to determine the nature of the product formed upon reduction, a controlled potential electrolysis was performed. In all the cases benzonitrile, **8**, was the only product obtained after the passage of 2F. Taking into account CVs and the electrochemical data obtained from the electrolysis, it is possible to conclude that compound **6** and **7** follows an ECE mechanism. In a first electrochemical step, the radical anion of benzonitrile halide was generated. After that, a chemical reaction coupled to this first electron transfer led to a benzonitrile radical and the corresponding halide anion through a C-X cleavage reaction. Later, benzonitrile radical was reduced to its corresponding anion at the electrode surface (Scheme 7). It is

important to remark that when cyano derivatives are used, it is possible to electrogenerate a strong nucleophile (benzonitrile anion), which is stable enough under our experimental conditions for reacting with CO₂ leading to the corresponding electrocarboxylated product.



Scheme 7. ECE proposal mechanism for the electrochemical reduction of 6 and 7.

Figures 5c,d show that halobenzonitriles showed the same electrochemical behavior, a first two-electron reduction wave is observed for halobenzonitriles (Figures 5a,b) in nitrogen and carbon dioxide atmosphere. In none of the cases the presence of oxalate anion was detected.

Once the electrochemical reduction mechanism of halobenzonitriles under CO₂ atmosphere was disclosed, electrocarboxylation process were performed using carbon graphite rod. For all the compounds the applied potential was 0.1 V more negative than potential of the first reduction wave. The results of carboxylation reactions were summarized in Table 5. It could observe that *p*-cyanobenzoic acid (**9**) and benzoic acid (**10**) were obtained in moderated yields after the passage of 2F. Benzonitrile (**8**) is also obtained, showing that there was a competition between carboxylation and protonation process. Benzoic acid obtention would be explained because at the potential of electrolysis, *p*-cyanobenzoic acid is also reduced, since its reduction potential is c. a. −1.36 V (vs. SHE).

Table 5. Results of the electrocarboxylation of 6 and 7 at 2F.

Entries	Reagent	Cathode	Solvent	Electrochemical Conditions	% Yield (Conversion Rate)			Reagent
					Carboxylated Products		Ar-H	
				E_{ap} (V vs. SHE)	9	10	8	
1	6	C	DMF	−1.86	20 (32%)	10 (32%)	32	38
2			EMIM TFSI	−1.86	15 (26%)	7 (26%)	35	43
3	7	C	DMF	−1.81	18 (28%)	12 (28%)	34	36
4			EMIM TFSI	−1.81	16 (28%)	10 (28%)	31	43

3.3.1. Electrocatalytic Behaviour of Cyano-Compounds 6 and 7 under CO₂ Atmosphere

Figure 6 shows several cyclic voltammograms of 6 and 7 under nitrogen and CO₂ atmosphere using silver and glassy carbon (GC) as a cathode. The use of DMF as a solvent and GC as a cathode allows to see a second mono-electronic fast reversible wave after the first one (Figure 5). This second wave corresponds to the electrochemical reduction of benzonitrile, which is the only product obtained after the reduction of compounds 6 and 7. It is noticeable that benzonitrile acts as a redox mediator for CO₂ reduction when the reaction is performed under CO₂ atmosphere, since there is an increase of the peak current value and a loss of reversibility of this second reduction wave (homogeneous indirect CO₂ reduction catalytic process (Figures 6a,c)).

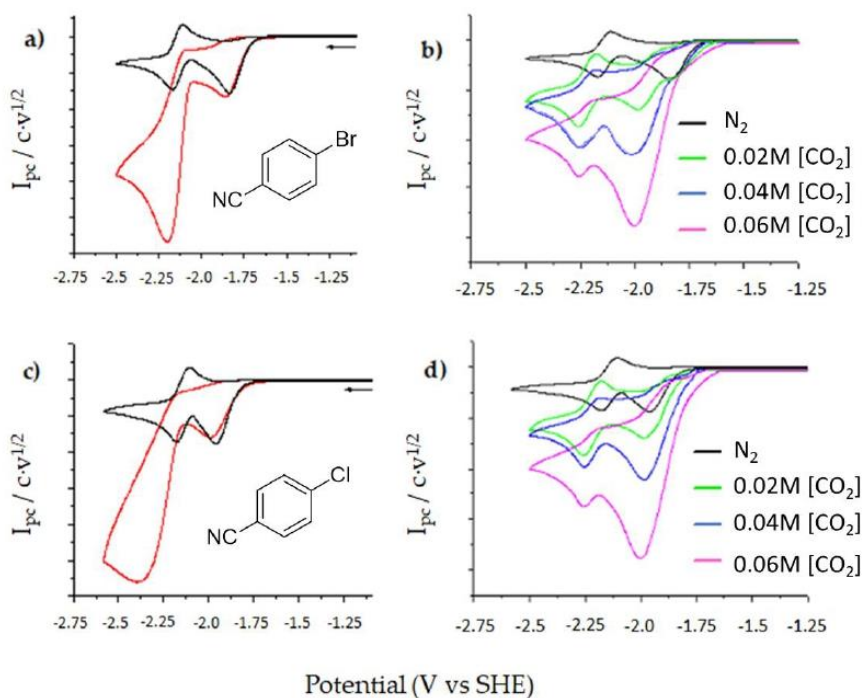


Figure 6. Cyclic voltammograms in DMF/0.1M under nitrogen atmosphere and 20–60 mM [CO₂] atmosphere using a solution of 10 mM of 6 (a) with GC (b) Ag. A solution of 10 mM of 7 with (c) GC and (d) Ag. Scan rate 0.5 V s^{−1}.

The use of silver electrode allows to tune the CO₂ reduction mechanism. In this case the current value of the first reduction is increasing as well as the peak potential value is shifting when the concentration of CO₂ is rising. These results can be explained taking into account that under these experimental conditions two electrochemical processes are happening at the electrode surface at same potential; the reduction of the cyanoaromatic halide and the direct reduction of CO₂ (Figures 6b,d). The same trend is observed with the use of copper cathode and a ionic liquid with wide

electrochemical window, such as 1-methyl-1-propylpiperidinium bis(trifluoromethylsulphonyl)-imide ([PP13] TFSI). Note that in this cases EMIM TFSI cannot be used as a IL, since the reduction of the EMIM cation takes place c.a. -2.06 V vs. SHE.[151].

4. Conclusions

In conclusion, we describe an efficient approach for producing high value products using CO₂ as building blocks. The methodology employed is based on electrochemical techniques and ILs, which provide eco-friendly chemistry solutions. These can be employed to offer a potential long-term strategy for using CO₂ feedstocks. There are two different strategies to obtain a CO₂ valorization product depending on the functional group, nitro or cyano, of the aromatic halide. An electrocatalytic process using a homogeneous catalysis, which provides an easy way of obtaining oxalate is seen when nitro derivatives are used, removing metal complexes as a catalyst. The use of cyano derivatives allows to tune the reactivity in function of the reduction potential value applied from electrocarboxylated products (via a nucleophile-electrophile reaction) to oxalate. These electrochemical reactions were performed with three different electrodes and in aprotic solvents and ionic liquids, which all showed the same trend. This opens the possibility of using a cooper electrode and ionic liquids to valorize CO₂, which would be a cheaper and greener alternative.

Author Contributions: G.G. conceptualized the research topic, conceived and designed the experiments; S.M. perform the experiments, G.G. and S.M. analyzed and interpreted the results. S.M. and G.G. prepared the manuscript. All authors corrected the draft. G.G. obtained the funds for the research.

Funding: This research was funded by MINECO/FEDER (project CTQ2015-65439-R)

Acknowledgments: This work was supported by project CTQ2015-65439-R from the MINECO/FEDER. S.M. thanks the Universitat Autònoma de Barcelona for a predoctoral PIF fellowship.

Conflicts of Interest: The authors declare no conflict of interest.

References

- Holtsmark, B. Quantifying the global warming potential of CO₂ emissions from wood fuels. *GCB Bioenergy* **2015**, *7*, 195–206.
- Hu, L.; Song, Y.; Jiao, S.; Liu, Y.; Ge, J.; Jiao, H.; Zhu, J.; Wang, J.; Zhu, H.; Fray, D.J. Direct Conversion of Greenhouse Gas CO₂ into Graphene via Molten Salts Electrolysis. *ChemSusChem* **2016**, *9*, 588–594.
- Kramm, G.; Dlugi, R. Scrutinizing the atmospheric greenhouse effect and its climatic impact. *Nat. Sci.* **2011**, *3*, 971–998.
- Mohan, S.V.; Modestra, J.A.; Amulya, K.; Butti, S.K.; Velvizhi, G. A circular bioeconomy with biobased products from CO₂ sequestration. *Trends Biotechnol.* **2016**, *34*, 506–519.
- Schleussner, C.F.; Lissner, T.K.; Fischer, E.M.; Wohland, J.; Perrette, M.; Golly, A.; Rogelj, J.; Childers, K.; Schewe, J.; Frieler, K.; et al. Differential climate impacts for policy-relevant limits to global warming: The case of 1.5 °C and 2 °C. *Earth Syst. Dyn.* **2016**, *7*, 327–351.
- Szulejko, J.E.; Kumar, P.; Deep, A.; Kim, K.H. Global warming projections to 2100 using simple CO₂ greenhouse gas modeling and comments on CO₂ climate sensitivity factor. *Atmos. Pollut. Res.* **2017**, *8*, 136–140.
- Song, C. Global challenges and strategies for control, conversion and utilization of CO₂ for sustainable development involving energy, catalysis, adsorption and chemical processing. *Catal. Today* **2006**, *115*, 2–32.
- Cuce, E.; Nachan, Z.; Cuce, P.M.; Sher, F.; Neighbour, G.B. Strategies for ideal indoor environments towards low/zero carbon buildings through a biomimetic approach. *Int. J. Ambient Energy* **2019**, *40*, 86–95.
- De Guido, G.; Compagnoni, M.; Pellegrini, L.A.; Rossetti, I. Mature versus emerging technologies for CO₂ capture in power plants: Key open issues in post-combustion amine scrubbing and in chemical looping combustion. *Front. Chem. Sci. Eng.* **2018**, *12*, 315–325.
- Borhani, T.N.; Wang, M. Role of solvents in CO₂ capture processes: The review of selection and design methods. *Renew. Sustain. Energy Rev.* **2019**, *114*, 109299.
- Asif, M.; Suleman, M.; Haq, I.; Jamal, S.A. Post-combustion CO₂ capture with chemical absorption and hybrid system: Current status and challenges. *Greenh. Gases Sci. Technol.* **2018**, *8*, 998–1031.
- Zhu, X.; Li, S.; Shi, Y.; Cai, N. Recent advances in elevated-temperature pressure swing adsorption for

- carbon capture and hydrogen production. *Prog. Energy Combust. Sci.* **2019**, *75*, 100784, doi:10.1016/j.pecs.2019.100784.
13. Sambo, C.; Ifeobi, C.C.; Babasafari, A.A.; Rezaei, S.; Akanni, O.A. The role of 4d time lapse seismic technology as reservoir monitoring and surveillance tool: A comprehensive review. *J. Nat. Gas Sci. Eng.* **2020**, 103312, doi:10.1016/j.jngse.2020.103312.
 14. Thompson, J.G.; Combs, M.; Abad, K.; Bhatnagar, S.; Pelgen, J.; Beaudry, M.; Rochelle, G.; Hume, S.; Link, D.; Figueroa, J.; et al. Pilot testing of a heat integrated 0.7 MWe CO₂ capture system with two-stage air-stripping: Emission. *Int. J. Greenh. Gas Control* **2017**, *64*, 267–275.
 15. Thompson, J.G.; Bhatnagar, S.; Combs, M.; Abad, K.; Onneweer, F.; Pelgen, J.; Link, D.; Figueroa, J.; Nikolic, H.; Liu, K. Pilot testing of a heat integrated 0.7 MWe CO₂ capture system with two-stage air-stripping: Amine degradation and metal accumulation. *Int. J. Greenh. Gas Control* **2017**, *64*, 23–33.
 16. Rafiee, A.; Khalilpour, K.R.; Milani, D.; Panahi, M. Trends in CO₂ conversion and utilization: A review from process systems perspective. *J. Environ. Chem. Eng.* **2018**, *6*, 5771–5794.
 17. Hassan, M.H.A.; Sher, F.; Zarren, G.; Suleiman, N.; Tahir, A.A.; Snape, C.E. Kinetic and thermodynamic evaluation of effective combined promoters for CO₂ hydrate formation. *J. Nat. Gas Sci. Eng.* **2020**, *78*, 103313.
 18. Bhatia, S.K.; Bhatia, R.K.; Jeon, J.-M.; Kumar, G.; Yang, Y.-H. Carbon dioxide capture and bioenergy production using biological system—A review. *Renew. Sustain. Energy Rev.* **2019**, *110*, 143–158.
 19. Cheng, J.; Zhu, Y.; Zhang, Z.; Yang, W. Modification and improvement of microalgae strains for strengthening CO₂ fixation from coal-fired flue gas in power plants. *Bioresour. Technol.* **2019**, *291*, 121850.
 20. Cheng, F.; Porter, M.D.; Colosi, L.M. Is hydrothermal treatment coupled with carbon capture and storage an energy-producing negative emissions technology? *Energy Convers. Manag.* **2020**, *203*, 112252.
 21. Kim, J.; Kwon, E.E. Photoconversion of carbon dioxide into fuels using semiconductors. *J. CO₂ Util.* **2019**, *33*, 72–82.
 22. Galli, F.; Compagnoni, M.; Vitali, D.; Pirola, C.; Bianchi, C.L.; Villa, A.; Prati, L.; Rossetti, I. CO₂ photoreduction at high pressure to both gas and liquid products over titanium dioxide. *Appl. Catal. B Environ.* **2017**, *200*, 386–391.
 23. Bahadori, E.; Tripodi, A.; Villa, A.; Pirola, C.; Prati, L.; Ramis, G.; Rossetti, I. High pressure photoreduction of CO₂: Effect of catalyst formulation, hole scavenger addition and operating conditions. *Catalysts* **2018**, *8*, 430.
 24. Compagnoni, M.; Ramis, G.; Freyria, F.S.; Armandi, M.; Bonelli, B.; Rossetti, I. Innovative photoreactors for unconventional photocatalytic processes: The photoreduction of CO₂ and the photo-oxidation of ammonia. *Rend. Lincei* **2017**, *28*, 151–158.
 25. Rossetti, I.; Bahadori, E.; Tripodi, A.; Villa, A.; Prati, L.; Ramis, G. Conceptual design and feasibility assessment of photoreactors for solar energy storage. *Sol. Energy* **2018**, *172*, 225–231.
 26. Bahadori, E.; Tripodi, A.; Villa, A.; Pirola, C.; Prati, L.; Ramis, G.; Dimitratos, N.; Wang, D.; Rossetti, I. High pressure CO₂ photoreduction using Au/TiO₂: Unravelling the effect of co-catalysts and of titania polymorphs. *Catal. Sci. Technol.* **2019**, *9*, 2253–2265.
 27. Rossetti, I.; Villa, A.; Pirola, C.; Prati, L.; Ramis, G. A novel high-pressure photoreactor for CO₂ photoconversion to fuels. *RSC Adv.* **2014**, *4*, 28883–28885.
 28. Sharma, N.; Das, T.; Kumar, S.; Bhosale, R.; Kabir, M.; Ogale, S. Photocatalytic Activation and Reduction of CO₂ to CH₄ over Single Phase Nano Cu₃SnS₄: A Combined Experimental and Theoretical Study. *ACS Appl. Energy Mater.* **2019**, *2*, 5677–5685.
 29. Zhou, R.; Guzman, M.I. CO₂ reduction under periodic illumination of ZnS. *J. Phys. Chem. C* **2014**, *118*, 11649–11656.
 30. Aguirre, M.E.; Zhou, R.; Eugene, A.J.; Guzman, M.I.; Grela, M.A. Cu₂O/TiO₂ heterostructures for CO₂ reduction through a direct Z-scheme: Protecting Cu₂O from photocorrosion. *Appl. Catal. B Environ.* **2017**, *217*, 485–493.
 31. Navarro, J.C.; Centeno, M.A.; Laguna, O.H.; Odriozola, J.A. Policies and motivations for the CO₂ valorization through the sabatier reaction using structured catalysts. A review of the most recent advances. *Catalysts* **2018**, *8*, 578, doi:10.3390/catal8120578.
 32. Al-Shara, N.K.; Sher, F.; Yaqoob, A.; Chen, G.Z. Electrochemical investigation of novel reference electrode Ni/Ni(OH)₂ in comparison with silver and platinum inert quasi-reference electrodes for electrolysis in eutectic molten hydroxide. *Int. J. Hydrogen Energy* **2019**, *44*, 27224–27236.
 33. Hudlicky, T. Benefits of Unconventional Methods in the Total Synthesis of Natural Products. *ACS Omega* **2018**, *3*, 17326–17340.

34. Dummel, R.J.; Mosher, H.S. Some Nitropyridine Derivatives. *J. Org. Chem.* **1959**, *24*, 1007–1009.
35. Gennaro, A.; Sánchez-Sánchez, C.M.; Isse, A.A.; Montiel, V. Electrocatalytic synthesis of 6-aminonicotinic acid at silver cathodes under mild conditions. *Electrochem. commun.* **2004**, *6*, 627–631.
36. Ramesh Raju, R.; Krishna Mohan, S.; Jayarama Reddy, S. Electroorganic synthesis of 6-aminonicotinic acid from 2-amino-5-chloropyridine. *Tetrahedron Lett.* **2003**, *44*, 4133–4135.
37. Amatore, C.; Savéant, J.M. Mechanism and Kinetic Characteristics of the Electrochemical Reduction of Carbon Dioxide in Media of Low Proton Availability. *J. Am. Chem. Soc.* **1981**, *103*, 5021–5023.
38. Frontana-Urbe, B.A.; Little, R.D.; Ibanez, J.G.; Palma, A.; Vasquez-Medrano, R. Organic electrosynthesis: A promising green methodology in organic chemistry. *Green Chem.* **2010**, *12*, 2099.
39. Gennaro, A.; Isse, A.A.; Severin, M.-G.; Vianello, E.; Bhugun, I.; Savéant, J.-M. Mechanism of the electrochemical reduction of carbon dioxide at inert electrodes in media of low proton availability. *J. Chem. Soc. Faraday Trans.* **1996**, *92*, 3963–3968.
40. Isse, A.A.; Galia, A.; Belfiore, C.; Silvestri, G.; Gennaro, A. Electrochemical reduction and carboxylation of halobenzophenones. *J. Electroanal. Chem.* **2002**, *526*, 41–52.
41. Machado, A.S.R.; Nunes, A.V.M.; da Ponte, M.N. Carbon dioxide utilization-Electrochemical reduction to fuels and synthesis of polycarbonates. *J. Supercrit. Fluids* **2018**, *134*, 150–156.
42. Mateos, R.; Escapa, A.; Vanbroekhoven, K.; Patil, S.A.; Moran, A.; Pant, D. Microbial Electrochemical Technologies for CO₂ and Its Derived Products Valorization. In *Microbial Electrochemical Technology*; Mohan, S.V., Varjani, S., Pandey, A., Eds.; Elsevier: Amsterdam, The Netherlands, 2018; pp. 777–796, ISBN 9780444640529.
43. Matthessen, R.; Franssaer, J.; Binnemans, K.; De Vos, D.E. Electrocarboxylation: Towards sustainable and efficient synthesis of valuable carboxylic acids. *Beilstein J. Org. Chem.* **2014**, *10*, 2484–2500.
44. Senboku, H.; Katayama, A. Electrochemical carboxylation with carbon dioxide. *Curr. Opin. Green Sustain. Chem.* **2017**, *3*, 50–54.
45. Tokuda, M. Efficient fixation of carbon dioxide by electrolysis—Facile synthesis of useful carboxylic acids—*J. Nat. Gas. Chem.* **2006**, *15*, 275–281.
46. Whipple, D.T.; Kenis, P.J.A. Prospects of CO₂ utilization via direct heterogeneous electrochemical reduction. *J. Phys. Chem. Lett.* **2010**, *1*, 3451–3458.
47. Windle, C.D.; Perutz, R.N. Advances in molecular photocatalytic and electrocatalytic CO₂ reduction. *Coord. Chem. Rev.* **2012**, *256*, 2562–2570.
48. Yuan, X.; Lu, B.; Liu, J.; You, X.; Zhao, J.; Cai, Q. Electrochemical conversion of methanol and carbon dioxide to dimethyl carbonate at graphite-Pt electrode system. **2012**, *159*, 183–186.
49. Zhang, W.; Lü, X. Synthesis of carboxylic acids and derivatives using CO₂ as carboxylative reagent. *Chin. J. Catal.* **2012**, *33*, 745–756.
50. Damodar, J.; Krishna Mohan, S.; Khaja Lateef, S.K.; Jayarama Reddy, S. Electrosynthesis of 2-arylpropionic acids from α -methylbenzyl chlorides and carbon dioxide by [Co(Salen)]. *Synth. Commun.* **2005**, *35*, 1143–1150.
51. Correa, A.; Martin, R. ChemInform abstract: Palladium-catalyzed direct carboxylation of aryl bromides with carbon dioxide. *ChemInform* **2010**, *41*, 15974–15975.
52. Damodar, J.; Krishna Mohan, S.R.; Jayarama Reddy, S.R. Synthesis of 2-arylpropionic acids by electrocarboxylation of benzylchlorides catalysed by PdCl₂(PPh₃)₂. *Electrochem. Commun.* **2001**, *3*, 762–766.
53. Durante, C.; Isse, A.A.; Todesco, F.; Gennaro, A. Electrocatalytic activation of aromatic carbon-bromine bonds toward carboxylation at silver and copper cathodes. *J. Electrochem. Soc.* **2013**, *160*, G3073–G3079.
54. Durante, C.; Isse, A.A.; Sandonà, G.; Gennaro, A. Electrochemical hydrodehalogenation of polychloromethanes at silver and carbon electrodes. *Appl. Catal. B Environ.* **2009**, *88*, 479–489.
55. Isse, A.A.; De Giusti, A.; Gennaro, A.; Falcicola, L.; Mussini, P.R. Electrochemical reduction of benzyl halides at a silver electrode. *Electrochim. Acta* **2006**, *51*, 4956–4964.
56. Isse, A.A.; Durante, C.; Gennaro, A. One-pot synthesis of benzoic acid by electrocatalytic reduction of bromobenzene in the presence of CO₂. *Electrochem. Commun.* **2011**, *13*, 810–813.
57. Isse, A.A.; Falcicola, L.; Mussini, P.R.; Gennaro, A. Relevance of electron transfer mechanism in electrocatalysis: The reduction of organic halides at silver electrodes. *Chem. Commun.* **2006**, *1*, 344–346.
58. Isse, A.A.; Gennaro, A. Electrochemical synthesis of cyanoacetic acid from chloroacetonitrile and carbon dioxide. *J. Electrochem. Soc.* **2002**, *149*, D113.
59. Isse, A.A.; Gottardello, S.; Durante, C.; Gennaro, A. Dissociative electron transfer to organic chlorides: Electrocatalysis at metal cathodes. *Phys. Chem. Chem. Phys.* **2008**, *10*, 2409–2416.

60. Isse, A.A.; Ferlin, M.G.; Gennaro, A. Electrocatalytic reduction of arylethyl chlorides at silver cathodes in the presence of carbon dioxide: Synthesis of 2-arylpropanoic acids. *J. Electroanal. Chem.* **2005**, *581*, 38–45.
61. Korsager, S.; Taaning, R.H.; Skrydstrup, T. Effective palladium-catalyzed hydroxycarbonylation of aryl halides with substoichiometric carbon monoxide. *J. Am. Chem. Soc.* **2013**, *135*, 2891–2894.
62. Lugaresi, O.; Minguzzi, A.; Locatelli, C.; Vertova, A.; Rondinini, S.; Amatore, C. Benzyl chloride electroreduction on Ag cathodes in CH₃CN in the presence of small amounts of water: Evidences of quantitative effects on reaction rates and mechanism. *Electrocatalysis* **2013**, *4*, 353–357.
63. Scialdone, O.; Galia, A.; Filardo, G.; Isse, A.A.; Gennaro, A. Electrocatalytic carboxylation of chloroacetonitrile at a silver cathode for the synthesis of cyanoacetic acid. *Electrochim. Acta* **2008**, *54*, 634–642.
64. Yoo, W.J.; Kondo, J.; Rodríguez-Santamaría, J.A.; Nguyen, T.V.Q.; Kobayashi, S. Efficient synthesis of α -trifluoromethyl carboxylic acids and esters through fluorocarboxylation of gem-difluoroalkenes. *Angew. Chem. Int. Ed.* **2019**, *58*, 6772–6775.
65. Yamauchi, Y.; Hara, S.; Senboku, H. Synthesis of 2-aryl-3,3,3-trifluoropropanoic acids using electrochemical carboxylation of (1-bromo-2,2,2-trifluoroethyl)arenes and its application to the synthesis of β,β,β -trifluorinated non-steroidal anti-inflammatory drugs. *Tetrahedron* **2010**, *66*, 473–479.
66. Scibioh, M.A.; Viswanathan, B. Electrochemical reduction of carbon dioxide: A status report. *Proc. Indian Natl. Sci. Acad.* **2004**, *70*, 407–462.
67. Schlager, S.; Dumitru, L.M.; Haberbauer, M.; Fuchsbauer, A.; Neugebauer, H.; Hiemetsberger, D.; Wagner, A.; Portenkirchner, E.; Sariciftci, N.S. Electrochemical reduction of carbon dioxide to methanol by direct injection of electrons into immobilized enzymes on a modified electrode. *ChemSusChem* **2016**, *9*, 631–635.
68. Ensafi, A.A.; Alinajafi, H.A.; Rezaei, B. Pt-modified nitrogen doped reduced graphene oxide: A powerful electrocatalyst for direct CO₂ reduction to methanol. *J. Electroanal. Chem.* **2016**, *783*, 82–89.
69. Liu, S.; Liu, Q.; Luo, J.-L. In-situ exsolved alloy nanoparticles on perovskite for direct CO₂ reduction. *ECS Trans.* **2017**, *75*, 1–6.
70. Savéant, J.M. Molecular catalysis of electrochemical reactions. Mechanistic aspects. *Chem. Rev.* **2008**, *108*, 2348–2378.
71. Feng, D.M.; Zhu, Y.P.; Chen, P.; Ma, T.Y. Recent advances in transition-metal-mediated electrocatalytic CO₂ reduction: From homogeneous to heterogeneous systems. *Catalysts* **2017**, *7*, doi:10.3390/catal7120373.
72. Kang, P.; Chen, Z.; Brookhart, M.; Meyer, T.J. Electrocatalytic Reduction of Carbon Dioxide: Let the molecules do the work. *Top. Catal.* **2015**, *58*, 30–45.
73. Hammouche, M.; Lexa, D.; Savéant, J.M.; Momenteau, M. Chemical catalysis of electrochemical reactions. Homogeneous catalysis of the electrochemical reduction of carbon dioxide by iron (“0”) porphyrins. Role of the addition of magnesium cations. *J. Am. Chem. Soc.* **1991**, *113*, 8455–8466.
74. Laitar, D.S.; Müller, P.; Sadighi, J.P. Efficient homogeneous catalysis in the reduction of CO₂ to CO. *J. Am. Chem. Soc.* **2005**, *127*, 17196–17197.
75. Zhang, S.; Fan, Q.; Xia, R.; Meyer, T.J. CO₂ reduction: From homogeneous to heterogeneous electrocatalysis. *Acc. Chem. Res.* **2020**, *53*, 255–264.
76. Wang, W.; Zhang, J.; Wang, H.; Chen, L.; Bian, Z. Photocatalytic and electrocatalytic reduction of CO₂ to methanol by the homogeneous pyridine-based systems. *Appl. Catal. A Gen.* **2016**, *520*, 1–6, doi:10.1016/j.apcata.2016.04.003.
77. Theaker, N.; Strain, J.M.; Kumar, B.; Brian, J.P.; Kumari, S.; Spurgeon, J.M. Heterogeneously catalyzed two-step cascade electrochemical reduction of CO₂ to ethanol. *Electrochim. Acta* **2018**, *274*, 1–8.
78. Geri, J.B.; Ciatti, J.L.; Szymczak, N.K. Charge effects regulate reversible CO₂ reduction catalysis. *Chem. Commun.* **2018**, *54*, 7790–7793.
79. Benson, E.E.; Kubiak, C.P.; Sathrum, A.J.; Smieja, J.M. Electrocatalytic and homogeneous approaches to conversion of CO₂ to liquid fuels. *Chem. Soc. Rev.* **2009**, *38*, 89–99.
80. Grills, D.C.; Ertem, M.Z.; McKinnon, M.; Ngo, K.T.; Rochford, J. Mechanistic aspects of CO₂ reduction catalysis with manganese-based molecular catalysts. *Coord. Chem. Rev.* **2018**, *374*, 173–217.
81. Luan, Y.X.; Ye, M. Transition metal-mediated or catalyzed hydrocarboxylation of olefins with CO₂. *Tetrahedron Lett.* **2018**, *59*, 853–861.
82. Xie, J.N.; Yu, B.; Zhou, Z.H.; Fu, H.C.; Wang, N.; He, L.N. Copper(I)-based ionic liquid-catalyzed carboxylation of terminal alkynes with CO₂ at atmospheric pressure. *Tetrahedron Lett.* **2015**, *56*, 7059–7062.
83. Mizuno, H.; Takaya, J.; Iwasawa, N. Rhodium(I)-catalyzed direct carboxylation of arenes with CO₂ via chelation-assisted C-H bond activation. *J. Am. Chem. Soc.* **2011**, *133*, 1251–1253.

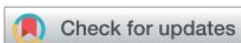
84. Honda, M.; Tamura, M.; Nakagawa, Y.; Tomishige, K. Catalytic CO₂ conversion to organic carbonates with alcohols in combination with dehydration system. *Catal. Sci. Technol.* **2014**, *4*, 2830–2845.
85. Tappe, N.A.; Reich, R.M.; D'Elia, V.; Kühn, F.E. Current advances in the catalytic conversion of carbon dioxide by molecular catalysts: An update. *Dalt. Trans.* **2018**, *47*, 13281–13313.
86. Kleij, A.W.; North, M.; Urakawa, A. CO₂ Catalysis. *ChemSusChem* **2017**, *10*, 1036–1038.
87. Dey, G.R.; Belapurkar, A.D.; Kishore, K. Photo-catalytic reduction of carbon dioxide to methane using TiO₂ as suspension in water. *J. Photochem. Photobiol. A Chem.* **2004**, *163*, 503–508.
88. Veselovskaya, J.V.; Parunin, P.D.; Netskina, O.V.; Kibis, L.S.; Lysikov, A.I.; Okunev, A.G. Catalytic methanation of carbon dioxide captured from ambient air. *Energy* **2018**, *159*, 766–773.
89. Zhao, G.; Huang, X.; Wang, X.; Wang, X. Progress in catalyst exploration for heterogeneous CO₂ reduction and utilization: A critical review. *J. Mater. Chem. A* **2017**, *5*, 21625–21649.
90. Dokania, A.; Ramirez, A.; Bavykina, A.; Gascon, J. Heterogeneous Catalysis for the Valorization of CO₂: Role of Bifunctional Processes in the Production of Chemicals. *ACS Energy Lett.* **2018**, *4*, 167–176.
91. Gennaro, A.; Isse, A.A.; Savéant, J.M.; Severin, M.G.; Vianello, E. Homogeneous electron transfer catalysis of the electrochemical reduction of carbon dioxide. Do aromatic anion radicals react in an outer-sphere manner? *J. Am. Chem. Soc.* **1996**, *118*, 7190–7196.
92. Costentin, C.; Savéant, J.-M. Multielectron, multistep molecular catalysis of electrochemical reactions: Benchmarking of homogeneous catalysts. *ChemElectroChem* **2014**, *1*, 1226–1236.
93. Costentin, C.; Savéant, J.M. Homogeneous catalysis of electrochemical reactions: The steady-state and nonsteady-state statuses of intermediates. *ACS Catal.* **2018**, *8*, 5286–5297.
94. Costentin, C.; Robert, M.; Savéant, J.M. Catalysis of the electrochemical reduction of carbon dioxide. *Chem. Soc. Rev.* **2013**, *42*, 2423–2436.
95. Costentin, C.; Savéant, J.M. Homogeneous molecular catalysis of electrochemical reactions: Catalyst benchmarking and optimization strategies. *J. Am. Chem. Soc.* **2017**, *139*, 8245–8250.
96. Zhang, B.A.; Ozel, T.; Elias, J.S.; Costentin, C.; Nocera, D.G. Interplay of homogeneous reactions, mass transport, and kinetics in determining selectivity of the reduction of CO₂ on gold electrodes. *ACS Cent. Sci.* **2019**, *5*, 1097–1105.
97. Nielsen, I.M.B.; Leung, K. Cobalt-porphyrin catalyzed electrochemical reduction of carbon dioxide in water. 1. A density functional study of intermediates. *J. Phys. Chem. A* **2010**, *114*, 10166–10173.
98. Leung, K.; Nielsen, I.M.B.; Sai, N.; Medforth, C.; Shelnutt, J.A. Cobalt-porphyrin catalyzed electrochemical reduction of carbon dioxide in water. 2. Mechanism from first principles. *J. Phys. Chem. A* **2010**, *114*, 10174–10184.
99. Shen, J.; Kolb, M.J.; Göttle, A.J.; Koper, M.T.M. DFT Study on the mechanism of the electrochemical reduction of CO₂ catalyzed by cobalt porphyrins. *J. Phys. Chem. C* **2016**, *120*, 15714–15721.
100. Yao, C.L.; Li, J.C.; Gao, W.; Jiang, Q. Cobalt-porphine catalyzed CO₂ electro-reduction: A novel protonation mechanism. *Phys. Chem. Chem. Phys.* **2017**, *19*, 15067–15072.
101. Bard, J.A.; Faulkner, L.R. *Fundamentals and Applications*, 2nd ed.; Harris, D., Swain, E., Robey, C., Aiello, E., Eds.; Wiley: Austin, TX, USA, 1990; ISBN 0471043729.
102. Darensbourg, D.J. Making Plastics from Carbon Dioxide: Salen Metal Complexes as Catalysts for the Production of Polycarbonates from Epoxides and CO₂. *Chem. Rev.* **2007**, *107*, 2388–2410.
103. Sakakura, T.; Choi, J.C.; Yasuda, H. Transformation of carbon dioxide. *Chem. Rev.* **2007**, *107*, 2365–2387.
104. Feng, J.; Zeng, S.; Feng, J.; Dong, H.; Zhang, X. CO₂ electroreduction in ionic liquids: A review. *Chin. J. Chem.* **2018**, *36*, 961–970.
105. Gallardo, I.; Soler, S. Electrochemically promoted arylation of iodoaromatics. *J. Electroanal. Chem.* **2017**, *799*, 9–16.
106. Das, R.N.; Roy, K. Development of classification and regression models for *Vibrio fischeri* toxicity of ionic liquids: Green solvents for the future. *Toxicol. Res.* **2012**, *1*, 186–195.
107. Armand, M.; Endres, F.; Mac Farlane, D.R.; Ohno, H.; Scrosati, B. Ionic-liquid materials for the electrochemical challenges of the future. *Nature Mater.* **2009**, *8*, 621–629.
108. Allen, G.D.; Buzzee, M.C.; Davies, I.G.; Villagrán, C.; Hardacre, C.; Compton, R.G. A comparative study on the reactivity of electrogenerated bromine with cyclohexene in acetonitrile and the room temperature ionic liquid, 1-Butyl-3-methylimidazolium bis[(trifluoromethyl)sulfonyl]imide. *J. Phys. Chem. B* **2004**, *108*, 16322–16327.
109. Maca, J.; Sedlarikova, M.; Libich, J.; Kazda, T.; Vondrak, J. Ionic Liquids as Electrolytes and Aging Process. *ECS Trans.* **2016**, *74*, 179–184.

110. Barrosse-Antle, L.E.; Bond, A.M.; Compton, R.G.; O'Mahony, A.M.; Rogers, E.I.; Silvester, D.S. Voltammetry in room temperature ionic liquids: Comparisons and contrasts with conventional electrochemical solvents. *Chem. Asian J.* **2010**, *5*, 202–230.
111. Bhatt, V.D.; Gohil, K. Ion exchange synthesis and thermal characteristics of some [N2222]⁺ based ionic liquids. *Bull. Mater. Sci.* **2013**, *36*, 1121–1125.
112. Cruz, H.; Gallardo, I.; Guirado, G. Understanding specific effects on the standard potential shifts of electrogenerated species in 1-butyl-3-methylimidazolium ionic liquids. *Electrochim. Acta* **2008**, *53*, 5968–5976.
113. Deetlefs, M.; Seddon, K.R.; Shara, M. Predicting physical properties of ionic liquids. *Phys. Chem. Chem. Phys.* **2006**, *8*, 642–649.
114. Doherty, A.P.; Brooks, C.A. *Organic Electrochemistry in Ionic Liquids*. Rogers, R., Seddon, K.R. Eds.; American Chemical Society: Washington DC, **2003**; pp. 410–420 ISBN 978084123856.
115. Earle, M.J.; Esperança, J.M.S.S.; Gilea, M.A.; Lopes, J.N.C.; Rebelo, L.P.N.; Magee, J.W.; Seddon, K.R.; Widegren, J.A. The distillation and volatility of ionic liquids. *Nature* **2006**, *439*, 831–834.
116. Gutowski, K.E. Industrial uses and applications of ionic liquids 1. *Phys. Sci. Rev.* **2018**, *3*, doi:10.1515/psr-2017-0191.
117. Hayyan, M.; Mjalli, F.S.; Hashim, M.A.; AlNashef, I.M.; Mei, T.X. Investigating the electrochemical windows of ionic liquids. *J. Ind. Eng. Chem.* **2013**, *19*, 106–112.
118. Jensen, M.P.; Neufeind, J.; Beitz, J.V.; Skanthakumar, S.; Soderholm, L. Mechanisms of metal ion transfer into room-temperature ionic liquids: The role of anion exchange. *J. Am. Chem. Soc.* **2003**, *125*, 15466–15473.
119. Picquet, M.; Tkatchenko, I.; Tommasi, I.; Wasserscheid, P.; Zimmermann, J. Ionic Liquids, 3. Synthesis and utilisation of protic imidazolium salts in homogeneous catalysis. *Adv. Synth. Catal.* **2003**, *345*, 959–962.
120. Reche, I.; Gallardo, I.; Guirado, G. The role of cations in the reduction of 9-fluorenone in bis (trifluoromethylsulfonyl) imide room temperature ionic liquids. *New J. Chem.* **2014**, *38*, 5030–5036.
121. Seddon, K.R. Ionic Liquids for Clean Technolog. *J. Chem. Technol. Biotechnol. Int. Res. Process Environ. Clean Technol.* **1997**, *64*, 351–356.
122. Wasserscheid, P.; Welton, T. Ionic Liquids Ionic Liquids. *Top. Curr. Chem.* **1999**, *1*, 223–226.
123. Welton, T. Ionic liquids : A brief history. *Biophys. Rev.* **2018**, *10*, 691–706.
124. Zhou, F.; Liu, S.; Yang, B.; Wang, P.; Alshammari, A.S.; Deng, Y. Electrochemistry communications highly selective and stable electro-catalytic system with ionic liquids for the reduction of carbon dioxide to carbon monoxide. *Electrochem. Commun.* **2015**, *55*, 43–46.
125. Tateno, H.; Nakabayashi, K.; Kashiwagi, T.; Senboku, H.; Atobe, M. Electrochemical fixation of CO₂ to organohalides in room-temperature ionic liquids under supercritical CO₂. *Electrochim. Acta* **2015**, *161*, 212–218.
126. Tanner, E.E.L.; Batchelor-McAuley, C.; Compton, R.G. Carbon dioxide reduction in room-temperature ionic liquids: The effect of the choice of electrode material, cation, and anion. *J. Phys. Chem. C* **2016**, *120*, 26442–26447.
127. Sung, S.; Kumar, D.; Gil-Sepulcre, M.; Nippe, M. Electrocatalytic CO₂ reduction by imidazolium-functionalized molecular catalysts. *J. Am. Chem. Soc.* **2017**, *139*, 13993–13996.
128. Sun, L.; Ramesha, G.K.; Kamat, P.V.; Brennecke, J.F. Switching the reaction course of electrochemical CO₂ reduction with ionic liquids. *Langmuir* **2014**, *30*, 6302–6308.
129. Rosen, B.A.; Salehi-Khojin, A.; Thorson, M.R.; Zhu, W.; Whipple, D.T.; Kenis, P.J.A.; Masel, R.I. Ionic liquid-mediated selective conversion of CO₂ to CO at low overpotentials. *Science* **2011**, *334*, 643–644.
130. Reche, I.; Gallardo, I.; Guirado, G. Cyclic voltammetry using silver as cathode material: A simple method for determining electro and chemical features and solubility values of CO₂ in ionic liquids. *Phys. Chem. Chem. Phys.* **2015**, *17*, 2339–2343.
131. Reche, I.; Gallardo, I.; Guirado, G. Electrochemical studies of CO₂ in imidazolium ionic liquids using silver as a working electrode: A suitable approach for determining diffusion coefficients, solubility values, and electrocatalytic effects. *RSC Adv.* **2014**, *4*, 65176–65183.
132. Niu, D.; Zhang, J.; Zhang, K.; Xue, T.; Lu, J. Electrocatalytic carboxylation of benzyl chloride at silver cathode in ionic liquid BMIMBF₄. *Chin. J. Chem.* **2009**, *27*, 1041–1044.
133. Mena, S.; Sanchez, J.; Guirado, G. Electrocatalytic carboxylation of 1-chloro-(4-isobutylphenyl)ethane with a silver cathode in ionic liquids : An environmentally benign and efficient way to synthesize Ibuprofen. *RSC Adv.* **2019**, *9*, 15115–15123.
134. Mei, K.; He, X.; Chen, K.; Zhou, X.; Li, H.; Wang, C. Highly efficient CO₂ capture by imidazolium ionic liquids through a reduction in the formation of the carbene-CO₂ complex. *Ind. Eng. Chem. Res.* **2017**, *56*,

- 8066–8072.
135. Marrucho, I.M.; Branco, L.C.; Rebelo, L.P.N. Ionic liquids in pharmaceutical applications. *Annu. Rev. Chem. Biomol. Eng.* **2014**, *5*, 527–546.
 136. Liu, R.; Zhang, P.; Zhang, S.; Yan, T.; Xin, J.; Zhang, X. Ionic liquids and supercritical carbon dioxide: Green and alternative reaction media for chemical processes. *Rev. Chem. Eng.* **2016**, *32*, 587–609.
 137. Lim, H.K.; Kim, H. The mechanism of room-Temperature ionic-liquid-based electrochemical CO₂ reduction: A review. *Molecules* **2017**, *22*, 536, doi:10.3390/molecules22040536.
 138. Li, J.; Jia, D.; Guo, Z.; Liu, Y.; Lyu, Y.; Zhou, Y.; Wang, J. Imidazolium based porous hypercrosslinked ionic polymers for efficient CO₂ capture and fixation with epoxides. *Green Chem.* **2017**, *19*, 2675–2686.
 139. Lau, G.P.S.; Schreier, M.; Vasilyev, D.; Scopelliti, R.; Gra, M.; Dyson, P.J. New Insights Into the Role of Imidazolium-Based Promoters for the Electroreduction of CO₂ on a Silver Electrode. *J. Am. Chem. Soc.* **2016**, *138*, 7820–7823.
 140. Faggion, D., Jr.; Gonçalves, W.D.G.; Dupont, J. CO₂ Electroreduction in Ionic Liquids. *Front. Chem.* **2019**, *7*, 1–8.
 141. Aghaie, M.; Rezaei, N.; Zendejboudi, S. A systematic review on CO₂ capture with ionic liquids: Current status and future prospects. *Renew. Sustain. Energy Rev.* **2018**, *96*, 502–525.
 142. Williams, D.B.G.; Lawton, M. Drying of organic solvents: Quantitative evaluation of the efficiency of several desiccants. *J. Org. Chem.* **2010**, *75*, 8351–8354.
 143. Strmcnik, D. When small is big: The role of impurities in electrocatalysis. *Top. Catal.* **2015**, *58*, 1174–1180.
 144. Taylor, R.J. Electrochemical studies on glassy carbon electrodes. III. Oxygen reduction in solutions of low pH (pH < 10). *J. Electroanal. Chem.* **1975**, *64*, 85.
 145. Saveant, J.M.; Tessier, D. Potential dependence of the electrochemical transfer coefficient. Reduction of some nitro compounds in aprotic media. *J. Phys. Chem.* **1977**, *81*, 2192–2197.
 146. Brooks, C.A. *Electrochemistry in Ionic Liquids*; Torriero, A. A. J., Eds.; Springer: London, 2002; Volume 2002–19; ISBN 9783319151311.
 147. Mena, S.; Santiago, S.; Gallardo, I.; Guirado, G. Sustainable and efficient electrosynthesis of naproxen using carbon dioxide and ionic liquids. *Chemosphere* **2020**, *245*, 125557.
 148. Kumar, B.; Llorente, M.; Froehlich, J.; Dang, T.; Sathrum, A.; Kubiak, C.P. Photochemical and photoelectrochemical reduction of CO₂. *Annu. Rev. Phys. Chem.* **2012**, *63*, 541–569.
 149. Al-Omari, A.A.; Yamani, Z.H.; Nguyen, H.L. Electrocatalytic CO₂ reduction: From homogeneous catalysts to heterogeneous-based reticular chemistry. *Molecules* **2018**, *23*, 2835.
 150. Yang, N.; Waldvogel, S.R.; Jiang, X. Electrochemistry of carbon dioxide on carbon electrodes. *ACS Appl. Mater. Interfaces* **2016**, *8*, 28357–28371.
 151. Mena, S.; Gallardo, I.; Guirado, G. Electrocatalytic Processes for the Valorization of CO₂: Synthesis of cyanobenzoic acid using eco-friendly strategies. *Catalysts* **2019**, *9*, 413.



© 2020 by the authors. Licensee MDPI, Basel, Switzerland. This article is an open access article distributed under the terms and conditions of the Creative Commons Attribution (CC BY) license (<http://creativecommons.org/licenses/by/4.0/>).

Cite this: *RSC Adv.*, 2019, 9, 15115

Electrocarboxylation of 1-chloro-(4-isobutylphenyl)ethane with a silver cathode in ionic liquids: an environmentally benign and efficient way to synthesize Ibuprofen†

Silvia Mena, , Jessica Sanchez and Gonzalo Guirado *

Electrocarboxylation of organic halides is one of the most widely used approaches for valorising CO₂. In this manuscript, we report a new greener synthetic route for synthesising 2-(4-isobutylphenyl)propanoic acid, Ibuprofen, one of the most popular non-steroidal anti-inflammatory drugs (NSAIDs). The joint use of electrochemical techniques and ionic liquids (ILs) allows CO₂ to be used as a C₁-organic building block for synthesising Ibuprofen in high yields, with conversion ratios close to 100%, and under mild conditions. Furthermore, the determination of the reduction peak potential values of 1-chloro-(4-isobutylphenyl)ethane in several electrolytes (DMF, and ionic liquids) and with different cathodes (carbon and silver) makes it possible to evaluate the most "energetically" favourable conditions for performing the electrocarboxylation reaction. Hence, the use of ILs not only makes the electrolytic media greener, but they also act as catalysts enabling the electrochemical reduction of 1-chloro-(4-isobutylphenyl)ethane to be decreased by up to 1.0 V.

Received 8th March 2019

Accepted 9th May 2019

DOI: 10.1039/c9ra01781j

rsc.li/rsc-advances

1. Introduction

Carbon dioxide (CO₂) is known as a greenhouse gas and is the most important contributor to global warming. The chemical properties of CO₂ make it an interesting candidate for developing new green sustainable chemistry, since it is abundant, non-toxic, non-flammable, and a low cost material. Moreover, its C₁ carbon skeleton is interesting for making longer molecules. Therefore, one of the main challenges for the scientific community is to eliminate or re-use CO₂ in order to obtain other types of compounds with high added value, such as carboxylic derivatives. In this sense, different methodologies are currently being developed to minimise its production, such as the carbon capture and storage (CCS) and carbon capture and utilisation (CCU) technologies.^{1–6}

According to the literature,^{7–9} different organic synthetic routes have been developed using CO₂ as a reactant. Direct carboxylation of carbon nucleophile using CO₂ as an electrophile is a straightforward route to prepare carboxylic acids. On the other hand, CO₂ is highly reactive with carbon nucleophiles, such as Grignard and organolithium reagents. The main disadvantage of those processes is the use of toxic reagents that generate a large amount of waste. An attractive alternative is the

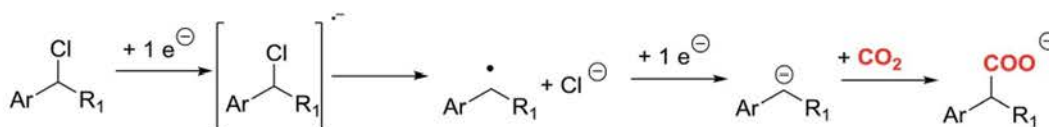
use of organic electrochemical techniques for obtaining high valuable carboxylation products, since they can improve environmental conditions. In this sense, electrochemical techniques may offer the possibility to activate the CO₂ through a electrocarboxylation process.^{10–19} Electrocarboxylation of organic halides is one of the most widely used approaches for valorising CO₂. In a first step, a one electron transfer process generates the organic radical, which later converts to an anion through a second reduction electron transfer, and a halide anion (Scheme 1).²⁰ The key step of this approach relies on the reduction potential value of the organic halides and on the stability of the organic anion formed after the reduction process. Furthermore, in the recent years, many studies have appeared in which a silver electrode is a good option to reduce the reduction potential in the carbon–halide cleavage reaction.^{21–29}

The electrochemical approach for synthesis of non-steroidal anti-inflammatory drugs (NSAIDs) (*e.g.* Naproxen³⁰ and Ibuprofen^{30–32}) has been previously performed, obtaining from moderate to good yields. However, the main drawbacks associated with those electrocarboxylation processes were the use of organic solvents, which are well-known to be hazardous and flammable,¹⁴ the use of large quantities of supporting electrolyte,¹⁶ and either the use of toxic redox mediators, or high reduction potential values. In this sense, in the current manuscript we propose an attractive alternative to these electrocarboxylation processes by: (1) the replacement of conventional electrochemical solvents with Ionic Liquids (ILs). ILs have been

Departament de Química, Universitat Autònoma de Barcelona, 08193-Bellaterra, Barcelona, Spain. E-mail: gonzalo.guirado@uab.cat

† Electronic supplementary information (ESI) available. See DOI: 10.1039/c9ra01781j





Scheme 1 Electrochemical carboxylation mechanism of benzyl halides.

widely used as environmentally friendly solvents, electrolytes, as well as catalysts,^{33–41} and (2) the use of a silver cathode for decreasing the reduction potential values required for the cleavage of the halide–carbon bond, avoiding the use of either toxic mediators. Hence, this manuscript reports a new, more environmentally friendly, approach for synthesising 2-(4-(2-methylpropyl)phenyl)propanoic acid (Ibuprofen) by using green technologies (electrochemistry), green solvents (RTILs), and CO₂ feedstock.

2. Experimental section

2.1. Materials

Carbon dioxide, CO₂, and nitrogen, N₂, were obtained from Carburos Metálicos S.A. (a purity of 99.9999%). 1-Chloro-(4-isobutylphenyl)ethane (**1**) was synthesised following that in the literature.⁴² *N*-Methyl-*N*-propylpiperidinium bis(trifluoromethanesulfonyl)imide (PP13 TFSI, purity 99.5%, H₂O ≤ 0.05%), 1-methyl-1-ethylimidazolium bis(trifluoromethanesulfonyl)imide (EMIM TFSI, purity 99%, H₂O ≤ 0.2%) were acquired from Solvionic, and were dried under vacuum using activated molecular sieves for 24 h to make sure that the amount of water was always less than H₂O ≤ 0.001% (Scheme 2).

2.2. Cyclic voltammetry experiments

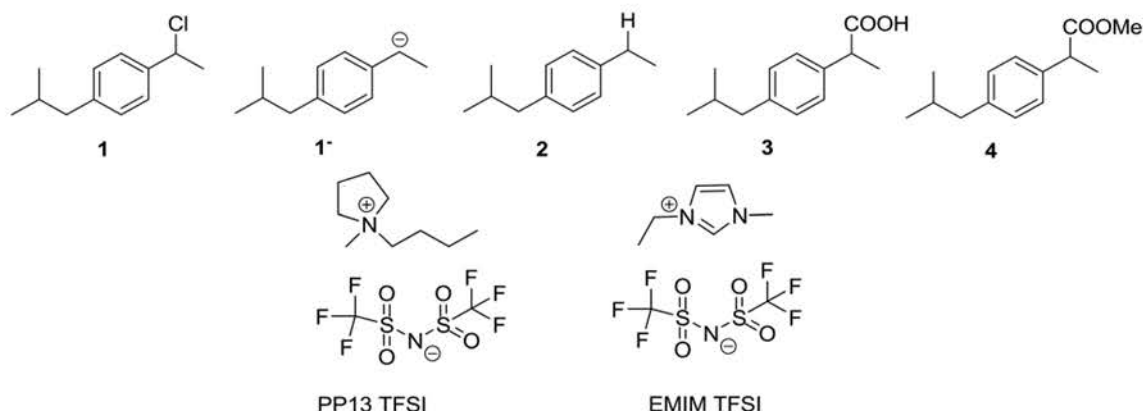
An electrochemical conical cell is used for the set-up of the three-electrode system. For CV experiments, the working electrode is a vitreous carbon disk of 1 mm diameter. It is polished using a 1 mm diamond paste. The counter electrode is a Pt disk of <1 mm diameter. All the potentials are reported *versus* an

aqueous saturated calomel electrode (SCE) isolated from the working electrode compartment by a salt bridge. The salt solution of the reference calomel electrode is separated from the electrochemical solution by a salt-bridge ended with a frit, which is made of a ceramic material, allowing ionic conduction between the two solutions and avoiding appreciable contamination. Ideally, the electrolyte solution present in the bridge is the same as the one used for the electrochemical solution, in order to minimise junction potentials. The error associated with the potential values is less than 5 mV. The ohmic drop can be one of the main sources of error when ILs are used as solvents, since they are more resistive media than aprotic polar solvents with 0.1 M concentration of supporting electrolyte.

The number of electrons involved in the first reduction process of **1** was determined by comparison with very well-known one-electron reduction of fluorenone and nitrobenzene (redox probes), in the same medium using the same electrochemical set-up, by terms of cyclic voltammetry. The number of electrons involved in this first electron transfer was also confirmed by controlled-potential electrolysis.^{43–46}

2.3. General procedure for the electrocarboxylation processes

Compound **1** was electrolysed at a negative potential of 0.1 V more negative than the *E*_{pc} potential value under nitrogen or carbon dioxide saturated solutions. When the reaction is completed, the resulting solution in the electrolysis is extracted into water/ether mixtures. The organic layer is dried with Na₂SO₄ and evaporated to yield a residue that is analysed by gas chromatography-mass spectrometry, and Proton Nuclear Magnetic Resonance (¹H-RMN). When pure ILs are used as



Scheme 2 Diagram of the structures.



Paper

electrolyte, the products of the electrolysed solution are extracted with ether, allowing to recover almost an 80% of the IL at the end of the experiment. This organic layer was lately washed with water and dried with Na_2SO_4 (Scheme 3). Besides, the IL recovered was dried and reused in a new electrochemical process without loss of Ibuprofen yield.

All products obtained, and the commercial analogues (1-chloro-(4-isobutylphenyl)ethane, 1-ethyl-4-isobutylbenzene, 2-(4-(2-methylpropyl)phenyl)propanoic acid) were characterised by $^1\text{H-NMR}$. Measurements were made using a Bruker DPX360 (360 MHz) (Billerica, MA, USA) spectrometer. Proton chemical shifts were reported in ppm (δ) (CDCl_3 , $\delta = 7.26$, or CD_3CN , $\delta = 1.94$). The J values are reported in Hz.

2.4. Determination of the CO_2 concentration in ILs

A thermal mass flowmeter of modular construction with a 'laboratory style' pc-board housing (EL-FLOW® Mass Flow Meter/Controller) from Bronkhorst Hi-Tec, was used to monitor the CO_2 concentrations in the solution.⁴⁷ Control valves were integrated to measure and control a gas flow from the lowest range of 0.2 up to 10 ml min^{-1} .

3. Results and discussion

3.1. Electrochemical reduction of 1-chloro-(4-isobutylphenyl)ethane (1) under inert atmosphere

Cyclic voltammetry of compound 1 was recorded in different solvents (DMF + 0.1 M TBABF₄, EMIM TFSI, PP13 TFSI, and a DMF-PP13 TFSI (50 : 50)), and scan rates using glassy carbon electrode as a cathode under a N_2 atmosphere. In all cases, compound 1 shows a two-electron irreversible reduction peak (Fig. 1), as was expected for these types of compounds. The number of electrons involve in the first reduction process is determined by comparison with the fluorenone, our standard, in the same medium and with the same electrochemical set-up. Hence, in a first cathodic scan, a two electron irreversible reduction wave appears between -1.9 and -2.4 V vs. SCE, depending on the solvent. The peak width value (ΔE_p) is always more than 150 mV (at 0.3 V s^{-1} , Table 1), which means that compound 1 shows a slow electron transfer (charge transfer coefficient (α) ca. 0.3).⁴⁸ The analysis of the peak current values (and their dependence with the concentration and the scan rate), the peak potential values (and their dependence with the concentration) indicates that the chemical reaction coupled to the electron transfer is a first order reaction. In the corresponding anodic counter scan an oxidation peak at ca. 1.1 V is

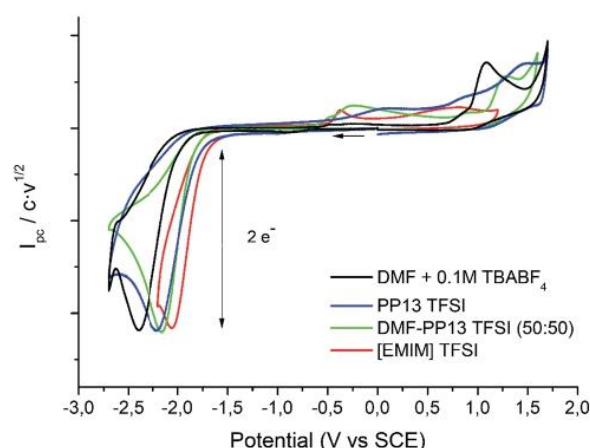
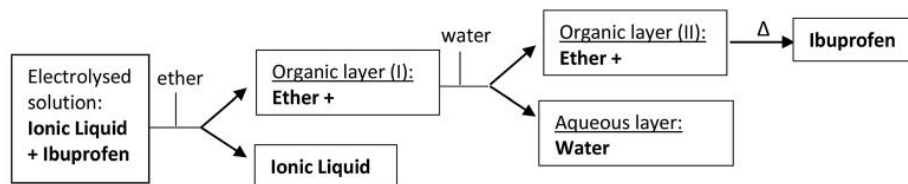


Fig. 1 Cyclic voltammograms (scan rate 0.5 V s^{-1}) at 25 $^{\circ}\text{C}$ on GC electrode of a solution of 10 mM of 1 in DMF + 0.1 M TBABF₄ (black line), PP13TFSI (blue line), DMF-PP13 TFSI (50 : 50) and EMIM TFSI (red line).

detected, which is attributed to the oxidation of chloride anion.⁴⁹ A closer look at the CVs also reveals that when EMIM TFSI is used as a solvent, a new peak appears -0.3 V vs. SCE. This new peak is oxidation related to imidazolium moieties formed after the electrochemical reduction of EMIM. This IM radical is immediately reduced at the electrode surface to its anion, and on the CV return its oxidation is observed at ca. 0.1 V vs. SCE.^{50–54} The cyclic voltammograms performed in PP13 TFSI and DMF-PP13 TFSI also show an irreversible oxidation peak at -0.28 V in the corresponding anodic counter scan. The appearance of this peak indicates that a new electroactive species is present in the solution. Hence, the oxidation peak should be associated with the oxidation of the benzylic anion intermediate $1^{\cdot-}$ (Schemes 4 and 5, Fig. 2). The irreversible wave at $E_{pa} = -0.28$ V vs. SCE disappears upon the addition of water and acid, which agrees with the presence of the anionic intermediate.

Taking the value E_{pc} value obtained for the electrochemical reduction of 1 in DMF + 0.1 M TBABF₄ as a reference value (Table 1), the E_{pc} values obtained in all the ILs are positively shifted, which means that the cation of the IL acts as a catalyst (as was previously pointed out by us and some other authors).³⁵ The reduction potential can be lowered to more than 0.30 V (7 kcal mol^{-1}) with respect to DMF + 0.1 M TBABF₄ (Table 1, entries 1–4). This fact can be explained by taking in to account that the IL is a pure ion solvent, whereas the concentration of



Scheme 3 Schematic process for Ibuprofen purification and IL recovery after the electrocarboxylation reaction.



Table 1 Cathodic peak potential (E_{pc} in V), $\Delta E_p = |E_{pc} - E_{pc/2}|$ (in mV), scan rate: 0.3 V s^{-1} , concentration ca. 5 mM, Charge transfer coefficient (α) for **1** in several solvents using glassy carbon as a working electrode at 25°C under nitrogen atmosphere

Entry	Solvent	E_{pc} (V)	ΔE_p^b (mV)	α	Number of electrons
1	DMF ^a	-2.42	180	0.26 ₁	1.9 ₅
2	EMIM TFSI	-2.03	156	0.31 ₃	2.1 ₂
3	DMF ^a -PP13 TFSI (50-50%)	-2.18	180	0.26 ₅	2.0 ₃
4	PP13 TFSI	-2.15	212	0.22 ₂	1.8 ₅

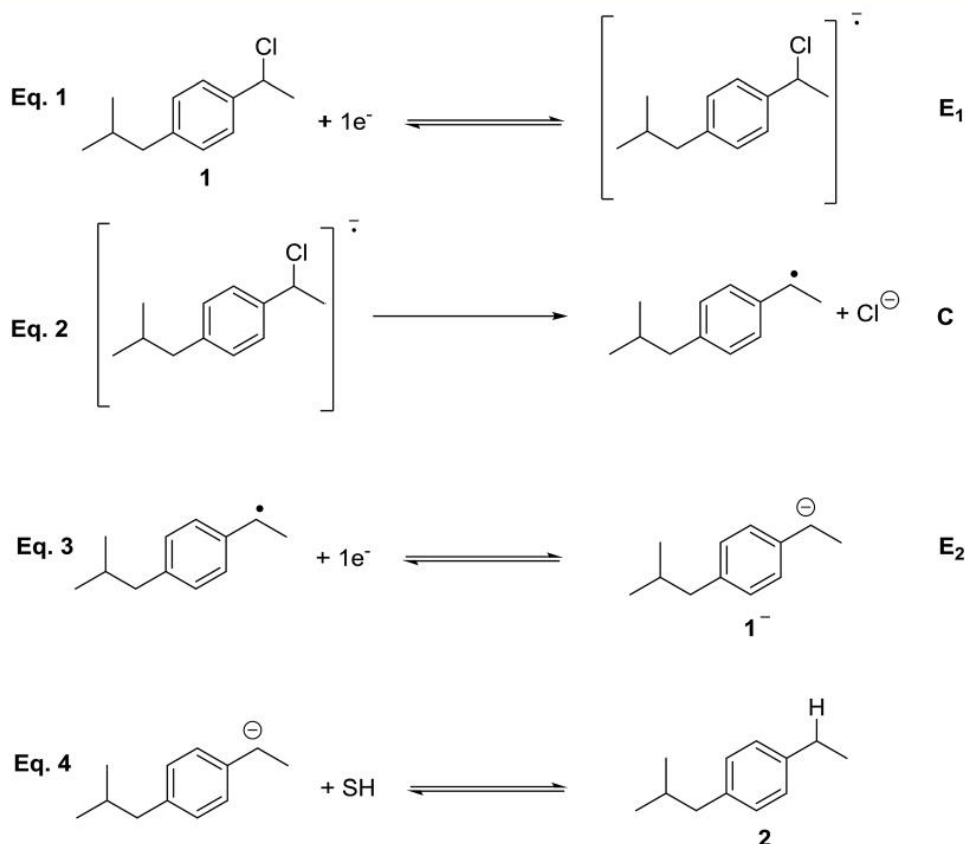
^a The DMF solution contains 0.1 M of *N*-tetrabutylammonium tetrafluoroborate (TBABF₄). ^b ΔE_p (mV) is the peak width value $E_{pc} - E_{pc/2}$ at 0.3 V s^{-1} .

the counter-cation is considerably lower the DMF solution, where “only” a 0.1 M concentration of tetrabutylammonium cation is present.

In order to determine the nature of the product formed after the first electron transfer of **1**, a control potential electrolysis at -2.2 V vs. SCE under inert atmosphere was performed in the above-mentioned electrolytic media (a control potential electrolysis at -2.5 V vs. SCE was performed in DMF). 1-Ethyl-4-isobutylbenzene, **2**, was obtained as a unique quantitative product (100%) in DMF, DMF/PP13, and PP13 after the passage of 2F. Overall, the electrochemical reduction mechanism of **1** is a two electron ECE mechanism (Scheme 4). In a first reduction step, a radical anion is formed

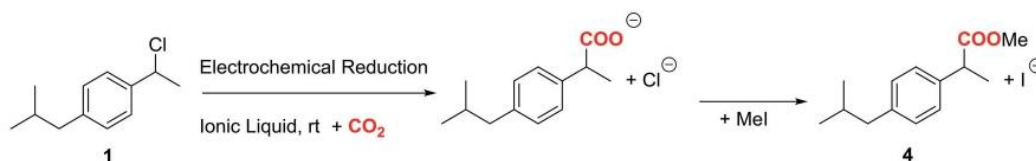
(electrochemical reaction, E), which undergoes C–Cl cleavage, leading to the corresponding organic radical and halide anion (elementary reaction step, C). The radical is reduced at this potential value, leading to the corresponding anion (electrochemical reaction, E). In a last protonation step the organic anion evolves to **2**.

When EMIM TFSI is used as solvent the reactant was recovered at the end of the process, and only decomposition products related to the reduction of EMIM cation were observed. These results can be easily rationalised taking into account that EMIM cation is reduced at -2.3 V , so the solvent is partially reduced at this potential. Thus, EMIM TFSI was discarded for the upcoming electrocarboxylation processes.



Scheme 4 Electrochemical reduction mechanism of **1**





Scheme 5 Electrocarboxylation of **1** under CO₂ atmosphere adding Mel as methylated agent at the end of the controlled-potential electrolysis.

3.2. Electrochemical reduction of 1-chloro-(4-isobutylphenyl)ethane (**1**) under CO₂ atmosphere with carbon vitreous working electrode

Fig. 2 shows the cyclic voltammograms of **1** in one of the electrolytic media employed under CO₂ atmosphere. In all the cases, a two electron reduction wave was observed at *ca.* −2.20 V *vs.* SCE in the initial cathodic scan, whereas an oxidation peak at *ca.* 1.1 V *vs.* SCE, which corresponds to the oxidation of chloride ion, is also detected in the ensuing anodic scan.

Taking advantage of the long lifetime of **1**[−] in ionic liquid based electrolytes, several electrocarboxylation processes were attempted. The selected electrolyte was previously pre-saturated with CO₂ to minimise undesired protonation side reactions. Hence controlled-potential electrolysis of **1** was performed using a graphite bar electrode under a saturated CO₂ atmosphere in DMF and ILs. The reduction processes were easily monitored by means of cyclic voltammetry (Fig. 3). In all the cases Ibuprofen was obtained in moderate to good yields (Table 2). The use of PP13 TFSI IL as a co-solvent, not only makes the reaction greener, but also increases the yield up to 75%. This result can be explained due to a higher hydrophobicity of the media, since these electrocarboxylation reactions are very sensitive to the presence of water. Finally, when pure IL electrolyte is used, the product yield increases up to *ca.* 90% over consumed reactant, with the *E*-factor being close to 1 (Table 2, entries 5 and 10). Hence, no other products apart from the Ibuprofen and the starting material were recovered. Moreover,

a methylated agent, such as iodomethane, was added it is possible to obtain methylated Ibuprofen, **4** (Scheme 5). Finally, note, that for obtaining yields close to 100%, the IL should be previously dried, the use of commercial IL (≤0.05% water content) also leads also to 20% of protonated compound **2**.

3.3. Electrochemical reduction of 1-chloro-(4-isobutylphenyl)ethane (**1**) under CO₂ atmosphere with silver working electrode

It is well-known that the use of silver cathodes reduces the reduction potential value where the carbon–halide cleavage reaction takes place.^{21–29} Due to the electrocatalytic effect of silver, it was decided to use a silver electrode as a cathode for the electrocarboxylation process in ILs.

Cyclic voltammetry of compound **1** was recorded, using a silver electrode as a cathode under N₂ atmosphere, in EMIM TFSI (to try to improve the results obtained with the carbon electrode) and PP13 TFSI (Fig. 4). In all cases, compound **1** shows the same general behaviour as in the case of using a glassy carbon electrode. Hence, in a first cathodic scan, a two electron irreversible reduction wave appears between −1.7 and −2.0 V *vs.* SCE depending on the ionic liquid. Taking the *E*_{pc} value obtained for the electrochemical reduction of **1** in the ionic liquids with glassy carbon electrode as a reference value (Table 1), the *E*_{pc} values obtained using silver electrode are considerably positively shifted. The reduction potential can be lowered to more than 0.07 V (1.61 kcal mol^{−1}) and 0.49 V

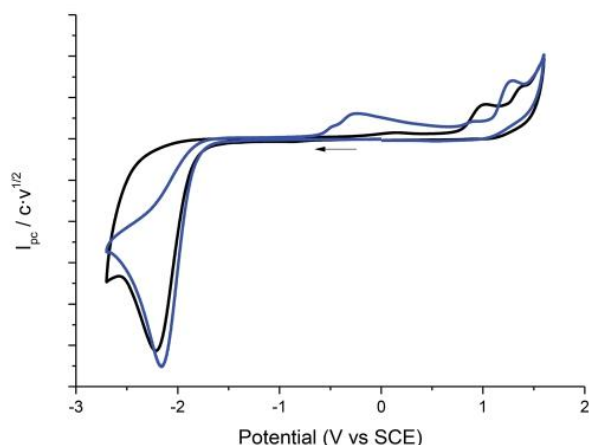


Fig. 2 Cyclic voltammograms (scan rate 0.5 V s^{−1}) at 25 °C on a GC electrode of 10 mM of **1** at CO₂ atmosphere (blue line), inert atmosphere (black line) in PP13 TFSI–DMF (1 : 1).

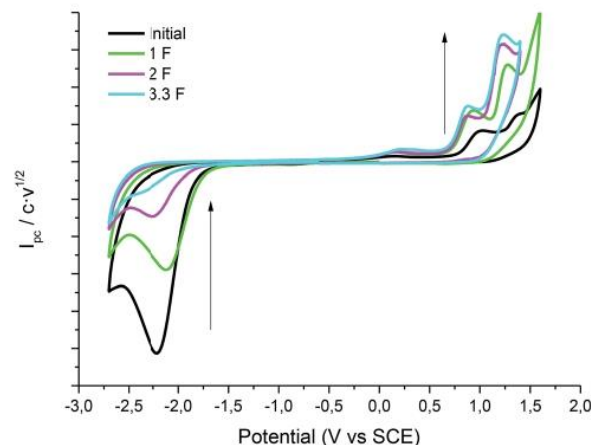


Fig. 3 Cyclic voltammograms (scan rate 0.5 V s^{−1}) at 25 °C on a GC electrode showing controls of the control potential electrolysis of **1** at CO₂ atmosphere in DMF–PP13 TFSI (1 : 1).



Table 2 Results of electrocarboxylation of **1** to obtain R-COOH/Me

Entry	Solvent	E_{applied}	$C \text{ mol}^{-1}$	R-COOH (Ibuprofen isolated yield)		Reagent recovery (%)	R-H (%)
				Yield ^a (%)	Conversion rate ^b (%)		
1	DMF ^c	−2.6	3.0	61	82	26	13
2	EMIM TFSI	−2.2	3.0	—	—	—	—
3	DMF-IL ^d (50–50%)	−2.4	3.3	75	83	10	15
4	PP13 TFSI ^e	−2.4	1.7	25	57	56	19
5	PP13 TFSI ^f	−2.4	1.7	47	94	50	3

	Solvent	E_{applied}	$C \text{ mol}^{-1}$	R-COOMe (methylated Ibuprofen isolated yield)		Reagent recovery (%)	R-H (%)
				Yield (%)	Conversion rate		
6	DMF ^c	−2.6	3.0	61	87	30	9
7	EMIM TFSI	−2.2	3.0	—	—	—	—
8	DMF-IL ^d (50–50%)	−2.4	3.0	86	86	—	14
9	PP13 TFSI ^e	−2.4	1.7	26	67	61	13
10	PP13 TFSI ^f	−2.4	1.7	48	96	50	2

^a Percent yield over isolated product. ^b Percent of Ibuprofen over consumed reactant. ^c The DMF solution contains 0.1 M of *N*-tetrabutylammonium tetrafluoroborate (TBABF₄) dried under vacuum and molecular sieves (less than 0.01% of water). ^d Mixture 1 : 1 of DMF + 0.1 M TBABF₄ and PP13 TFSI dried under vacuum and molecular sieves (less than 0.01% of water). ^e PP13 TFSI commercially available 0.05% of water. ^f PP13 TFSI dried under vacuum and molecular sieves (less than 0.01% of water).

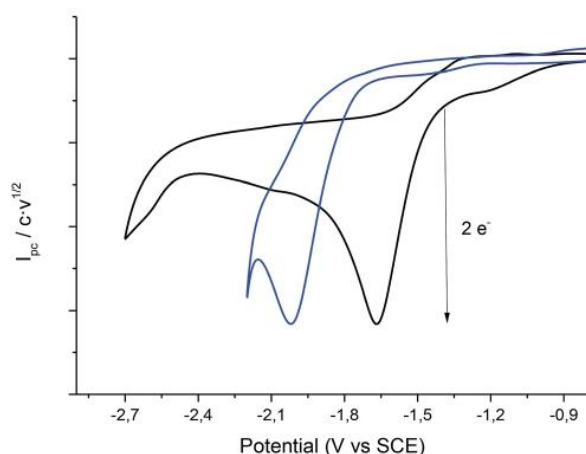


Fig. 4 Cyclic voltammograms (scan rate 0.5 V s^{-1}) at 25°C on a silver electrode of a solution of 20 mM of **1** in PP13 TFSI (black line), EMIM TFSI (blue line) under nitrogen atmosphere.

(11 kcal mol^{−1}) with respect to the glassy carbon electrode in EMIM TFSI and PP13 TFSI, respectively (Table 3, entries 1 and 2).

Table 3 Cathodic peak potential (E_{pc} in V), $\Delta E_{\text{p}} = |E_{\text{pc}} - E_{\text{pc}/2}|$ (in mV), scan rate: 0.5 V s^{-1} , concentration ca. 50 mM, charge transfer coefficient (α) for **1** in several solvents using silver as a working electrode at 25°C under nitrogen atmosphere

Entry	Solvent	E_{pc} (V)	ΔE_{p} (mV)	α	Number of electrons
1	EMIM TFSI	−1.96	95	0.46	2.3
2	PP13 TFSI	−1.66	130	0.37	1.9

Fig. 5 shows the cyclic voltammogram of **1** in PP13 TFSI under CO₂ atmosphere. A two electron reduction wave was observed at ca. -1.7 V vs. SCE , which corresponds to the reduction of **1**. Moreover, in the cathodic scan a new reduction peak at -2.00 V vs. SCE is also detected, which is ascribed to the electrochemical reduction of CO₂ in the IL. The peak current value of this second reduction peak grows when the concentration of CO₂ in the ionic liquid increases.

In order to obtain the products **3** and **4**, control potential electrolyses at -1.75 V vs. SCE under saturated CO₂ atmosphere were performed in the above-mentioned electrolytic media with silver foil (a control potential electrolysis at -2.1 V vs. SCE was

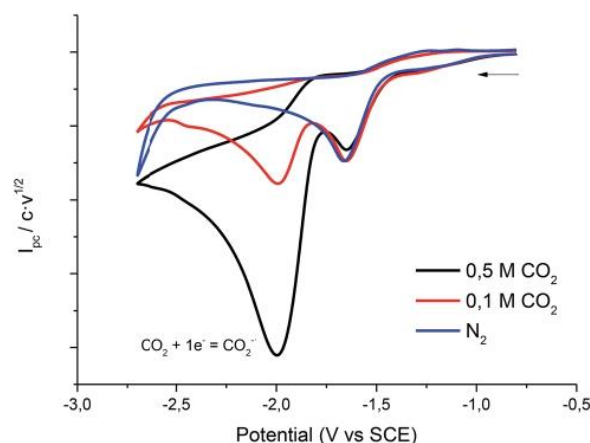


Fig. 5 Cyclic voltammograms (scan rate 0.5 V s^{-1}) at 25°C on a silver electrode of 10 mM of **1** at different concentrations of CO₂ in PP13 TFSI.



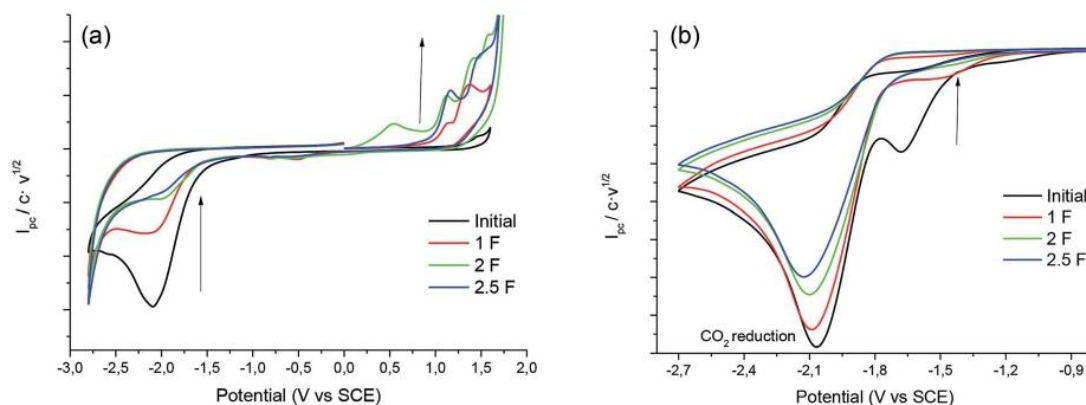


Fig. 6 Cyclic voltammograms (scan rate 0.5 V s^{-1}) at 25°C showing controls of the control potential electrolysis of **1** at CO_2 atmosphere in PP13 TFSI on Ag electrode (a) GC electrode (b) Ag electrode.

Table 4 Results of electrocarboxylation of **1** to obtain R-COOH/Me

Entry	Solvent	E_{applied}	$C \text{ mol}^{-1}$	R-COOH (Ibuprofen isolated yield)			R-H (%)
				Yield ^a (%)	Conversion rate ^b (%)	Reagent recovery (%)	
1	EMIM TFSI	-2.10	2.3	17	34	50	33
2	PP13 TFSI ^c	-1.75	2.0	9	38	76	15
3	PP13 TFSI ^d	-1.75	2.5	82	85	3	15

Entry	Solvent	E_{applied}	$C \text{ mol}^{-1}$	R-COOMe (methylated Ibuprofen isolated yield)			R-H (%)
				Yield (%)	Conversion rate	Reagent recovery (%)	
4	EMIM TFSI	-2.10	2.3	18	35	49	33
5	PP13 TFSI ^c	-1.75	2.0	8	35	77	15
6	PP13 TFSI ^d	-1.75	2.5	83	83	0	17

^a Percent yield over isolated product. ^b Percent of Ibuprofen over consumed reactant. ^c PP13 TFSI commercially available (0.05% of water). ^d PP13 TFSI dried under vacuum and molecular sieves (less than 0.01% of water).

performed in EMIM TFSI). The reduction processes were easily monitored by means of cyclic voltammetry with a silver electrode and a glassy carbon electrode (Fig. 6), showing the disappearance of **1**. In all the cases Ibuprofen and its methylated analogue (when iodomethane was added as electrophile) were obtained with moderate to good yields (Table 4). As previously mentioned, it should be noted that, for obtaining yields close to 100% the IL should be previously dried. The use of commercial IL ($\leq 0.05\%$ water content) also yields a 20% of protonated compound **2**.

Finally, the use of silver as a working electrode also allows the electrocarboxylation synthesis of Ibuprofen to be performed in EMIM TFSI. Furthermore, the electrochemical potential required is lower than in carbon electrodes and within the electrochemical window of the IL. However, when electrochemical synthesis is performed in EMIM TFSI, only 30% of **2** is obtained due to the acidity of the C2-H of the imidazolium moiety.

4. Conclusions

In conclusion, a description is presented of an efficient approach for producing high value compounds using CO_2 as building block. The methodology employed is based on electrochemical techniques and ILs, which allow eco-friendly chemistry solutions to be used and maintain the aim of offering a potential long-term strategy for using CO_2 feedstocks. The use of dried PP13 TFSI as electrolyte helps to overcome the main drawbacks associated with previous processes reported in the literature, where organic solvents, redox mediators, and large quantities of supporting electrolytes are employed. It is important to highlight the economic feasibility and viability of replacing organic aprotic solvents that contain 0.1 M TBABF₄ of supporting electrolyte by ILs. Although the price of a single experiment in IL is double that of DMF + 0.1 M of TBABF₄, the fact that the IL can be recovered and reused in almost 80% at the end of the experiment makes this methodology highly viable and attractive. Moreover, changing the nature of the working



electrode, the synthesis, in terms of potential applied, is improved and allows the use of ionic liquids with a narrow electrochemical window, such as imidazolium ionic liquids. Controlled potential electrolysis of 1-chloro-(4-isobutylphenyl) ethane under CO₂ atmosphere allows Ibuprofen to be obtained in good yields and excellent conversion rates. This methodology offers a new “green” route for the synthesis of different carboxylic acids that can be potential non-steroidal anti-inflammatory drugs (NSAIDs) in a more environmentally friendly way.

Conflicts of interest

There are no conflicts to declare.

Acknowledgements

This work was supported by project CTQ2015-65439-R from the MINECO/FEDER. S. M. acknowledges the Autonomous University of Barcelona for her predoctoral research grant (PIF fellowship).

References

- G. Yadav and R. Sen, *J. CO₂ Util.*, 2017, **17**, 188–206.
- P. Brunel, J. Monot, C. E. Kefalidis, L. Maron, B. Martin-Vaca and D. Bourissou, *ACS Catal.*, 2017, **7**, 2652–2660.
- P. Nejat, F. Jomehzadeh, M. M. Taheri, M. Gohari and M. Z. Muhd, *Renewable Sustainable Energy Rev.*, 2015, **43**, 843–862.
- R. M. Cuéllar-Franca and A. Azapagic, *J. CO₂ Util.*, 2015, **9**, 82–102.
- C. Song, *Catal. Today*, 2006, **115**, 2–32.
- Y. Xu, L. Isom and M. A. Hanna, *Bioresour. Technol.*, 2010, **101**, 3311–3319.
- Q. Liu, L. Wu, R. Jackstell and M. Beller, *Nat. Commun.*, 2015, **6**, 1–15.
- C. H. Huang and C. S. Tan, *Aerosol Air Qual. Res.*, 2014, **14**, 480–499.
- T. Sakakura, J. C. Choi and H. Yasuda, *Chem. Rev.*, 2007, **107**, 2365–2387.
- N. Yang, S. R. Waldvogel and X. Jiang, *ACS Appl. Mater. Interfaces*, 2016, **8**, 28357–28371.
- A. Gennaro, C. M. Sánchez-Sánchez, A. A. Isse and V. Montiel, *Electrochem. Commun.*, 2004, **6**, 627–631.
- H. Tateno, K. Nakabayashi, T. Kashiwagi, H. Senboku and M. Atobe, *Electrochim. Acta*, 2015, **161**, 212–218.
- J. Albo, M. Alvarez-Guerra, P. Castaño and A. Irabien, *Green Chem.*, 2015, **17**, 2304–2324.
- B. A. Frontana-Urbe, R. D. Little, J. G. Ibanez, A. Palma and R. Vasquez-Medrano, *Green Chem.*, 2010, **12**, 2099.
- A. Gennaro, A. A. Isse, M.-G. Severin, E. Vianello, I. Bhugun and J.-M. Savéant, *J. Chem. Soc., Faraday Trans.*, 1996, **92**, 3963–3968.
- A. A. Isse, M. G. Ferlin and A. Gennaro, *J. Electroanal. Chem.*, 2005, **581**, 38–45.
- A. S. R. Machado, A. V. M. Nunes and M. N. da Ponte, *J. Supercrit. Fluids*, 2018, **134**, 150–156.
- M. A. Scibioh and B. Viswanathan, *Proc. Indian Natl. Sci. Acad.*, 2004, **70**, 407–462.
- I. Reche, I. Gallardo and G. Guirado, *RSC Adv.*, 2014, **4**, 65176–65183.
- R. Matthesen, J. Fransaer, K. Binnemans and D. E. De Vos, *Beilstein J. Org. Chem.*, 2014, **10**, 2484–2500.
- A. A. Isse, S. Gottardello, C. Durante and A. Gennaro, *Phys. Chem. Chem. Phys.*, 2008, **10**, 2409–2416.
- E. E. L. Tanner, C. Batchelor-McAuley and R. G. Compton, *J. Phys. Chem. C*, 2016, **120**, 26442–26447.
- A. A. Isse, A. Galia, C. Belfiore, G. Silvestri and A. Gennaro, *J. Electroanal. Chem.*, 2002, **526**, 41–52.
- A. A. Isse, A. De Giusti, A. Gennaro, L. Falciola and P. R. Mussini, *Electrochim. Acta*, 2006, **51**, 4956–4964.
- O. Scialdone, A. Galia, G. Filardo, A. A. Isse and A. Gennaro, *Electrochim. Acta*, 2008, **54**, 634–642.
- O. Lugaresi, A. Minguzzi, C. Locatelli, A. Vertova, S. Rondinini and C. Amatore, *Electrocatalysis*, 2013, **4**, 353–357.
- P. Khalili, K. Y. Tshai and I. Kong, *Composites, Part A*, 2017, **100**, 194–205.
- D. Niu, J. Zhang, K. Zhang, T. Xue and J. Lu, *Chin. J. Chem.*, 2009, **27**, 1041–1044.
- A. A. Isse and A. Gennaro, *Chem. Commun.*, 2002, 2798–2799.
- J. Damodar, S. Krishna Mohan, S. K. Khaja Lateef and S. Jayarama Reddy, *Synth. Commun.*, 2005, **35**, 1143–1150.
- J. F. Fauvarque, A. Jutand and M. Francois, *J. Appl. Electrochem.*, 1988, **18**, 109–115.
- J. F. Fauvarque, A. Jutand, M. Francois and M. A. Petit, *J. Appl. Electrochem.*, 1988, **18**, 116–119.
- R. Liu, P. Zhang, S. Zhang, T. Yan, J. Xin and X. Zhang, *Rev. Chem. Eng.*, 2016, **32**, 587–609.
- I. Reche, I. Gallardo and G. Guirado, *Phys. Chem. Chem. Phys.*, 2015, **17**, 2339–2343.
- H. K. Lim and H. Kim, *Molecules*, 2017, **22**, 536.
- D. T. Whipple and P. J. A. Kenis, *J. Phys. Chem. Lett.*, 2010, **1**, 3451–3458.
- J. Li, D. Jia, Z. Guo, Y. Liu, Y. Lyu, Y. Zhou and J. Wang, *Green Chem.*, 2017, **19**, 2675–2686.
- M. Alvarez-Guerra, J. Albo, E. Alvarez-Guerra and A. Irabien, *Energy Environ. Sci.*, 2015, **8**, 2574–2599.
- S. Mena, I. Gallardo and G. Guirado, *Catalysts*, 2019, **9**, 413.
- L. Sun, G. K. Ramesha, P. V. Kamat and J. F. Brennecke, *Langmuir*, 2014, **30**, 6302–6308.
- B. A. Rosen, A. Salehi-Khojin, M. R. Thorson, W. Zhu, D. T. Whipple, P. J. A. Kenis and R. I. Masel, *Science*, 2011, **334**, 643–644.
- R. A. KJonaas, P. E. Williams, D. A. Counce and L. R. Crawley, *J. Chem. Educ.*, 2011, **88**, 825–828.
- H. Cruz, I. Gallardo and G. Guirado, *Electrochim. Acta*, 2008, **53**, 5968–5976.
- H. Cruz, I. Gallardo and G. Guirado, *Green Chem.*, 2011, **13**, 2531–2542.
- I. Reche, I. Gallardo and G. Guirado, *New J. Chem.*, 2014, **38**, 5030–5036.



Paper

- 46 I. Reche, I. Gallardo and G. Guirado, *ChemElectroChem*, 2014, **1**, 2104–2109.
- 47 D. Kodama, K. Sato, M. Watanabe, T. Sugawara, T. Makino and M. Kanakubo, *J. Chem. Eng. Data*, 2018, **63**, 1036–1043.
- 48 L. R. Faulkner and A. J. Bard, *Electrochemical Methods: Fundamentals and Applications*, University of Texas at Austin, 2nd edn, 2000, vol. 30.
- 49 I. Gallardo, G. Guirado and J. Marquet, *J. Electroanal. Chem.*, 2000, **488**, 64–72.
- 50 E. W. Oliver, D. H. Evans and J. V. Caspar, *J. Electroanal. Chem.*, 1996, **403**, 153–158.
- 51 E. W. Oliver and D. H. Evans, *J. Electroanal. Chem.*, 1997, **432**, 145–151.
- 52 L. Xiao and K. E. Johnson, *J. Electrochem. Soc.*, 2003, **150**, 307–311.
- 53 B. Gorodetsky, T. Ramnial, N. R. Branda and J. A. C. Clyburne, *Chem. Commun.*, 2004, 1972–1973.
- 54 G. H. Lane, *Electrochim. Acta*, 2012, **83**, 513–528.





Sustainable and efficient electrosynthesis of naproxen using carbon dioxide and ionic liquids

Silvia Mena, Sara Santiago, Iluminada Gallardo, Gonzalo Guirado*

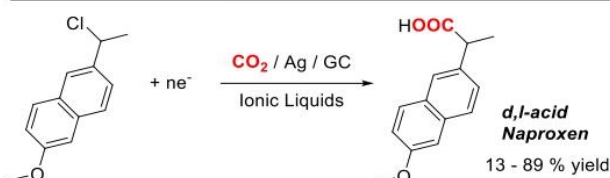
Departament de Química, Universitat Autònoma de Barcelona, 08193-Bellaterra, Barcelona, Spain



HIGHLIGHTS

- Electrocarboxylation of 2-(1-chloroethyl)-6-methoxynaphthalene using CO₂ and Ionic Liquids for synthesizing Naproxen.
- Electrochemical reactivity of CO₂ in function of the nature of the cathode and the electrolyte.
- Electrochemical Synthesis of Naproxen with high yields (89 %) and conversion rates (90 %).
- New "greener" route for the synthesis of Nonsteroidal anti-inflammatory drugs (NSAIDs).

GRAPHICAL ABSTRACT



ARTICLE INFO

Article history:

Received 11 August 2019
Received in revised form
28 November 2019
Accepted 5 December 2019
Available online 11 December 2019

Handling editor: Ignasi Sires

Keywords:

Ionic liquids
Electrochemistry
Carbon dioxide
Naproxen

ABSTRACT

The use of CO₂ as a C1 carbon source for synthesis is raising increasing attention both as a strategy to bring value to carbon dioxide capture technologies and a sustainable approach towards chemicals and energy. The presented results focus on the application of electrochemical methods to incorporate CO₂ into organic compounds using ionic liquids as electrolytes, which provides a green alternative to the formation of C–C bonds. In this sense, the current manuscript shows that Naproxen (6-Methoxy- α -methyl-2-naphthaleneacetic acid) can be synthesized in high yield (89%) and conversion rates (90%) through an electrocarboxylation process using CO₂ and ionic liquids. The role of the cathode and solvent, which can potentially enhance the synthesis, is also discussed. The "green" route described in the current work would open a new sustainable strategy for the electrochemical production of pharmaceutical compounds.

© 2019 Elsevier Ltd. All rights reserved.

1. Introduction

Nonsteroidal anti-inflammatory drugs (NSAID) (Ruelius et al., 1987), such as Ibuprofen or Naproxen that are the 2-arylpropionic acid (profen) derivatives, are commonly used to treat pain,

menstrual cramps, inflammatory diseases such as rheumatoid arthritis, and fever (Adelman et al., 2007; Janssens et al., 2008; Uziel et al., 2000). Naproxen was firstly commercialized by Syntex in 1976 (Harrington and Lodewijk, 1997), its manufacture started from β -naphthol and produced 500 kg in 1970 (Harrison et al., 1970). However, this process involved several undesirable associated reagents: nitroaromatic compounds (used in acylation), ammonium sulfide (for performing the Willgerodt reaction), sodium hydride, as well as methyl iodide ((Fig. S1. Route A).

These disadvantages were overcome with a new procedure to

* Corresponding author.

E-mail addresses: gonzalo.guirado@uab.es, gonzalo.guirado@uab.cat (G. Guirado).

obtain naproxen that was also created at Syntex in 1972–1975 (Fig. S1, Route B1). In this manufacturing process, there were also significant associated problems associated to this second synthetic strategy; First, a stoichiometric amount of zinc chloride was used for the naphthylzinc coupling reaction, hence large amounts of zinc hydroxide by-product were also produced. Second, this coupling reaction not only showed poor yields but also led to undesirable side products such as 2-methoxynaphthalene, which is volatile, and large amounts of binaphthyl, a highly insoluble “dimer” by product.

Focusing on the major problems resulting from the naphthylzinc coupling reaction, an alternative coupling was introduced to this second manufacturing process (Fig. S1, Route B2). Besides, from 1984 to 1993 the yield increased, from less than 50% to a 90%, after a series of process improvements introduced to the above-mentioned synthetic approach. At this point it is important to highlight that overall atom economy for the previously described modern Syntex process described (Fig. S1, Route B2) was a **24%**. Considering that 98% of N-alkylglucamine was recoverable by cycle, the atom economy raised to **34%**. However, it is important not to forget that the bromination and the coupling reactions still produce high amounts of waste.

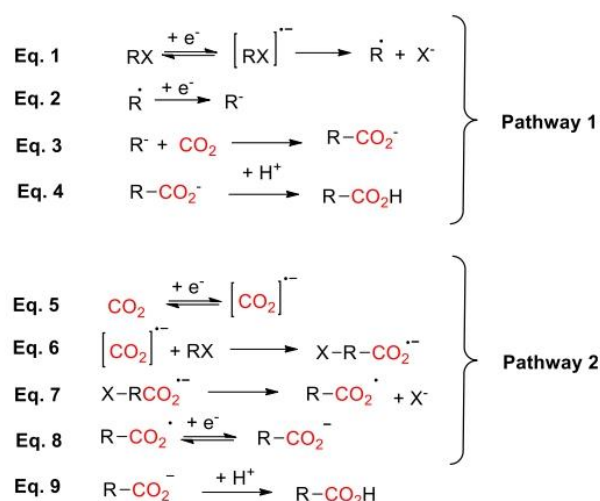
In order to ameliorate the manufacture processes of Naproxen new approaches have been explored and discussed in the last years. Nate Shaw and Steve Schlitzer (Shaw and Schlitzer, 2015) introducing the use of safer solvents and auxiliaries (Scheme 1); sulfolane, as well as gaseous reagents (H_2 and CO in steps 2 and 3). Moreover, catalysts (SiO_2 , Raney Nickel, Palladium catalyst, tosylic acid, LiCl, virtually all recoverable) were employed. So, its atom economy is higher (**39.4%**, which rises to **77.7%** when considering recoverability of resolving agent) than in the case of Syntex and reduces the use of halogens and alkali metals as much as possible. On the other hand, this adapted synthesis required the use of a sophisticated catalyst and CO, which are well-known pollutants.

Carbon dioxide (CO_2) can be described as a carbon source for chemical synthesis. In this sense, the use of electrochemical methods for triggering the formation of C–C bonds by coupling CO_2 to organic compounds is a very attractive “green” alternative (Matthessen et al., 2014; Senboku and Katayama, 2017; Tokuda, 2006). Hence, the use of CO_2 as a feedstock is perceived as a promising attractive strategy for obtaining carboxylic acids via electrochemical fixation of CO_2 (Frontana-Urbe et al., 2010). One of the most important examples of its application can be found in NSAIDs such as Ibuprofen or Naproxen (Fauvarque et al., 1988a,

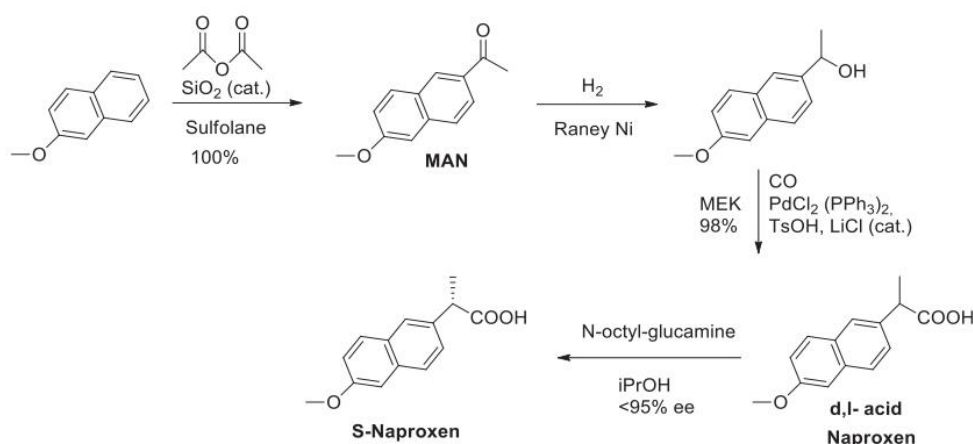
1988b; Mena et al., 2019b). The CO_2 incorporation to organic skeleton can be easily reached at low CO_2 pressure and under mild conditions with the use of a suitable of electrodes, electrolytes and catalysts in the electrolysis. In terms of green and sustainable chemistry, this approach is essentially environmentally benign and carbon dioxide is an eco-friendly C1 source (Yamauchi et al., 2010, 2008; Yoo et al., 2019).

Electrocarboxylation reactions of organic compounds using CO_2 is achieved via two different reaction pathways. The first one is depicted in Scheme 2, Eq. 1–4, and this involves the generation of organic anionic intermediates. The carbanions electrochemically formed upon the passage of two electron undergo a nucleophilic attack on carbon dioxide to yield the corresponding carboxylic acids. This mechanism takes place when the reduction potentials of the organic substrates are less negative than that of carbon dioxide (Amatore and Savéant, 1981; Costentin et al., 2013; Gennaro et al., 1996b).

In turn, reaction pathway 2 occurs when the reduction potentials of the organic substrates are more negative than those of carbon dioxide (Scheme 2, Eq. 5–9). Via this mechanism, the electrogenerated anion radical of carbon dioxide reacts with



Scheme 2. Electrochemical carboxylation of organic compounds with CO_2 .



Scheme 1. Schlitzer/Shaw adapted synthesis.

organic substrates leading to the corresponding carboxylic acids (Damodar et al., 2001; Isse et al., 2005; Liu et al., 2015).

Both strategies are associated to several advantages compared with the classical carboxylation process. However, electrochemical carboxylation processes usually uses organic aprotic solvents that are toxic and flammable (Alvarez-Guerra et al., 2015). Hence, our strategy for electrochemically synthesizing CO₂ will be based on the replacement of those organic solvents with ionic liquids (ILs).

In the last decade the use of ILs has been considered a sustainable solvent choice for several organic transformations, including the preparation of pharmaceutical drugs (Marrucho et al., 2014). Chemical and electrochemical reactions in ILs usually do not require special apparatus or methodologies. Focusing on electrochemical synthesis in ILs, a large array of different cations and anions available today in the IL toolbox. Wide electrochemical windows and good conductivities are obtained by combining unsymmetrical bulky organic cations combined and hydrophobic anions such as [BF₄]⁻ or [NTf₂]⁻. For electrocarboxylation process, the use of ILs offers the possibility to recycle the solvent at the end of the reaction (Chen et al., 2016; Lim and Kim, 2017; Pappenfus et al., 2009; Sun et al., 2014; Tateno et al., 2015; Zhou et al., 2015).

Our strategy for electrochemically synthesizing NSAIDs involve the use of CO₂ as reagent, which is valorised through an electrocarboxylation process that would allow the synthesis of Naproxen. We also introduce electrochemistry as a technology to enhance the synthesis with the use of milder conditions, easy control and monitoring of the process, selectivity and the use of electrodes as cheap, green catalysts. Hence, this manuscript reports a sustainable, green and new approach to synthesise 2-(6-methoxy-2-naphthyl)propanoic acid (Naproxen) using electrochemical methods, ILs, and CO₂ feedstock.

2. Experimental section

2.1. Chemicals

Reagents: Carbon dioxide, CO₂, and nitrogen, N₂, were obtained from Carburos Metálicos S.A. (purity of 99.9999%). 2-(1-chloroethyl)-6-methoxynaphthalene (**1**) was obtained from SigmaAldrich and employed without further purification.

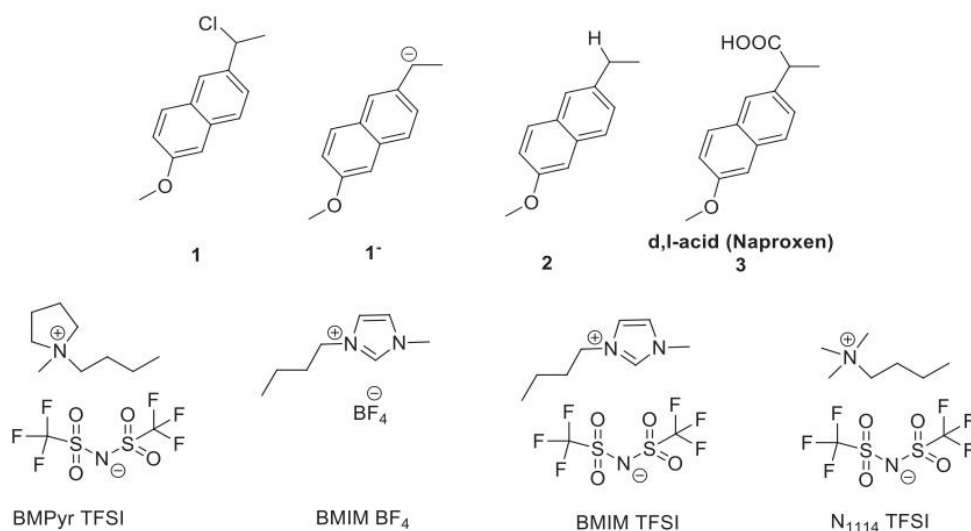
Solvents and Electrolytes: *N,N*-dimethylformamide anhydrous

(DMF), 99.8%, was obtained from Sigma Aldrich. Ionic Liquids were purchased from Solvionic (N-Butyl-N-methylpyrrolidonium bis(trifluoromethanesulfonyl)imide (BMPyr TFSI, purity 99.5%, H₂O ≤ 0.02%), 1-Butyl-3-methylimidazolium bis(trifluoromethanesulfonyl)imide (BMIM TFSI, purity 99%, H₂O ≤ 0.5%), 1-Butyl-3-methylimidazolium tetrafluoroborate (BMIM BF₄, purity 99%, H₂O ≤ 0.5%), N-trimethyl-N-butylammonium bis(trifluoromethanesulfonyl)imide (N₁₁₁₄ TFSI, purity 99.5%, H₂O ≤ 0.02%) (Scheme 3). Tetrabutylammonium tetrafluoroborate (TBABF₄), 99%, was obtained from SigmaAldrich and employed without further purification. After received all the solvents and electrolytes prepared, they were dried under vacuum using activated molecular sieves for 48 h in order to make sure that the amount of water was always less than H₂O ≤ 0.001% (Williams and Lawton, 2010). The physical chemical parameters of the electrolytes used in the current work in terms of viscosity, density and water content are conveniently summarised in Table 1.

2.2. Experimental procedures and instrumentation

Electrochemical measurements were performed in a one-compartment cell using the three-electrode configuration. All experiments have been carried out at room temperature. Cyclic voltammetry experiments were recorded using a potentiostat equipped with positive feedback compensation and current measurer previously described (Cruz et al., 2011, 2008; Gallardo and Soler, 2017; Mena et al., 2019a, 2019b, 2018; Reche et al., 2015, 2014a, 2014b). The working electrode was a 1 mm diameter glassy carbon or 3 mm diameter silver electrode disk carefully polished with 1 μm diamond paste (DP-Paste, P) and rinsed with ethanol. The counter electrode was a 2 mm platinum electrode disk and the reference electrode a Saturated Calomel Electrode (SCE) separated from the solution by a sintered-glass disk. All potentials were reported versus this reference.

It is worthy to remark the current values obtained for the cyclic voltammograms in the different electrolytes were first normalized by the concentration and the scan rate ($I_p/cv^{1/2}$) due to the moderate conductivity and larger viscosity of the ionic liquids. Under these experimental conditions the diffusion coefficient of the electroactive compounds was determined and normalized taking into account their relationship. Hence, the normalization



Scheme 3. Diagram of the structures.

Table 1
Physical-Chemical properties and recyclability of selected Ionic Liquids.

Ionic Liquid	Viscosity ^a (mPa·s)	Conductivity ^a (mS·cm ⁻¹)	Density ^a (g·cm ⁻³)	H ₂ O content before drying (%)	H ₂ O content after drying (%)	Recyclability (%)
BMIM TFSI	68.8	3.23	1.44	≤ 0.5	≤ 0.001	93
BMIM BF₄	103	3.15	1.20	≤ 0.5	≤ 0.001	76
N₁₁₁₄ TFSI	138	1.60	1.40	≤ 0.02	≤ 0.001	57
BMPyr TFSI	998	2.21	1.39	≤ 0.02	≤ 0.001	61

^a Data obtained from Solvionic Safety data sheet (MSDS) for each the selected ionic liquids.**Table 2**Cathodic Peak Potential (E_{pc} in V), $\Delta E_p = |E_{pc} - E_{pc2}|$ (in mV), Charge transfer coefficient (α), scan rate: 0.5 V s⁻¹ for solutions of **1** ca. 5–10 mM **1** in different electrolytes at 25 °C under N₂ atmosphere.

Entry	Electrode	Solvent	E_{pc} (V)	ΔE_p (mV)	α	Number of electrons
1	Carbon	DMF + Et ^[a]	-2.14	160	0.33	2.1 ₅
2	Carbon	BMIM TFSI	-1.97	200	0.24	2.1 ₈
3	Carbon	BMPyr TFSI	-1.95	210	0.22	2.2 ₀
4	Carbon	N ₁₁₁₄ TFSI	-1.90	190	0.25	2.2 ₀
5	Silver	DMF + Et ^[a]	-2.09	130	0.37	2.0 ₁
6	Silver	BMIM BF ₄	-1.76	110	0.43	2.1 ₅
7	Silver	BMPyr TFSI	-1.94	100	0.45	1.9 ₉
8	Silver	N ₁₁₁₄ TFSI	-1.83	110	0.40	2.0 ₆

[a] DMF + 0.1 M of *N*-tetrabutylammonium tetrafluoroborate (TBABF₄)

Note that the E_{pc} values obtained in all the ILs for both electrodes are positively shifted (Fig. S2a), which means that the cation of the IL may have a role as a co-catalyst (as was previously pointed out by ourselves and some other authors). The reduction potential can be lowered to more than 0.24 V (5.5 kcal mol⁻¹) and 0.33 V (7.6 kcal mol⁻¹) with respect to DMF + 0.1 M TBABF₄ in carbon electrode and silver electrode (Table 2, entries 1–4 and Table 2, entries 5–8), respectively. This can be explained because the concentration of the counter-cation is considerably lower in DMF than in IL solutions. Moreover, a slightly electrocatalytic effect, 0.07 V (4.8 kcal mol⁻¹), can also be observed when silver is used a cathode (Fig. S2b). This effect has been previously shown for electrochemical cleavage of carbon-halide reactions (Amaboldi et al., 2014; Durante et al., 2013, 2009; Gennaro et al., 2004; Isse et al., 2009, 2008; 2006b, 2006a; Isse and Gennaro, 2002; Lugaresi et al., 2013; Mena et al., 2019a; Niu et al., 2009).

coefficients expressed as a ratio were the following: 4.1, 8.1, 6.0, and 2.7 for DMF + 0.1 M TBABF₄/[BMIM]TFSI, DMF + 0.1 M TBABF₄/[BMIM]BF₄, DMF + 0.1 M TBABF₄/[N₁₁₁₄] TFSI, and DMF + 0.1 M TBABF₄/[BMPyr]TFSI, respectively.

Controlled potential electrolysis were carried out using a potentiostat EG&G PRINCETON APPLIED RESEARCH model 273 A following a previous described methodology (Cruz et al., 2011, 2008; Gallardo and Soler, 2017; Mena et al., 2019a, 2019b). The working electrode was a graphite bar or a silver foil; the counter electrode, a platinum bar separated from the solution by a sintered-glass disk; and the reference, the SCE electrode. Electrocarboxylation reactions were performed under CO₂ atmosphere using a Mass Flow Meter to control the CO₂ concentrations and flows. These experiments were also monitored using Cyclic Voltammetry. When the electrolysis was completed, Naproxen was extracted from the IL using diethylether (Scheme 4). Later, the organic phase was washed with water and dried with anhydrous sulphate sodium. The organic solvent was removed under high vacuum. After that the residue was dissolved in dichloromethane and characterised by gas chromatography, gas chromatography–mass spectrometry, and Proton Nuclear

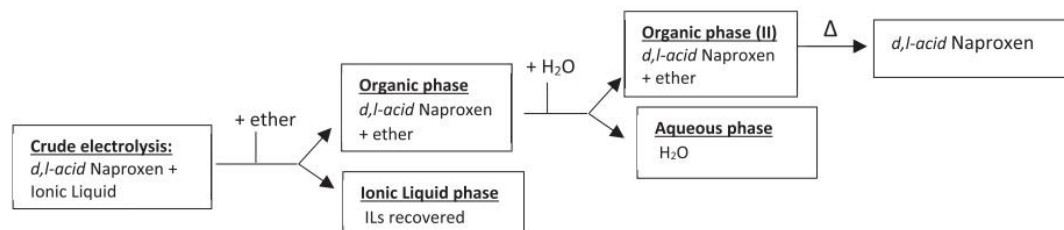
Magnetic Resonance (¹H-RMN). Finally, it is important to highlight that, in all the cases, more than a half of the IL used as electrolyte can be recovered, recycle and reused after a purification process for a new set of electrochemical experiments (Table 1).

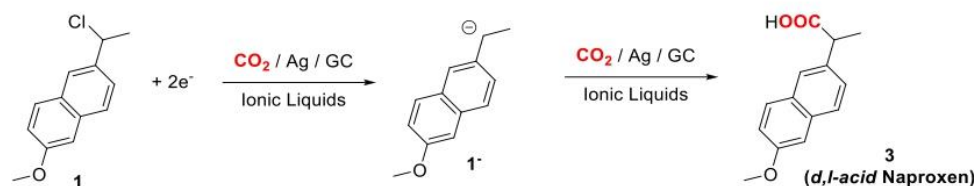
The ¹H NMR spectra were recorded on a Bruker DPX250 operating at 250.13 MHz. Gas chromatography (GC) were performed with a Clarus 500 from PerkinElmer (vector gas: Helium, column: Elite 5, l = 30 m, d = 0.25 mm). Apparatus for gas phase chromatography coupled with mass spectrometry was a Hewlett Packard 6890 and the detector were Hewlett Packard 5973.

3. Results and discussion

2-(6-methoxy-2-naphthyl)propanoic acid (**3**, Naproxen) was obtained by taking a new environmentally friendly approach that combines electrochemical techniques and ionic liquids as green solvents to valorise CO₂ with an electrocarboxylation process (Scheme 5).

For this reason, compound **1** must be electrochemically characterised in an inert and CO₂ saturated atmosphere to find out whether its relative anion, **1**⁻, is stable enough to catch CO₂.

**Scheme 4.** Schematic process for Naproxen purification and Ionic Liquid recovery after electrocarboxylation reaction.

Scheme 5. Electrocarboxylation of **1** under CO₂ atmosphere.

3.1. Electrochemical reduction of 2-(1-chloroethyl)-6-methoxynaphthalene (**1**) in inert atmosphere

Compound **1** was characterised with cyclic voltammetry (CV) at several scan rates (and in different solvents (DMF + 0.1 M TBA BF₄, BMIM TFSI, BMIM BF₄, N₁₁₁₄ TFSI, and a BMPyr TFSI) using either glassy carbon (GC) or silver (Ag) cathodes in N₂ atmosphere (Figs. 1a and S2). In all the cases, compound **1** shows a two-electron irreversible reduction peak followed by a one-electron reversible one. The analysis of the peak current and potential values as well as their dependence on the concentration and the scan rate reveals that the chemical reaction coupled to the electron transfer is a first order reaction. The shape of CVs, peak width value (ΔE_p), is always more than 100 mV (at 0.5 V s⁻¹, Table 1), which means that compound **1** involves slow electron transfer with charge transfer coefficient (α) between 0.2 and 0.4.

Finally, the second reversible one-electron transfer can be assigned to the reduction of **2**. Fig. 1b shows a cyclic voltammogram of pure samples of **1** and **2**, the second electrochemical reduction wave of **1** and the first reduction wave of **2**, which have the same shape and cathodic peak potential value for both electrodes.

In order to confirm this hypothesis, control potential electrolysis at -2.0 V vs SCE in ILs and at -2.2 V vs SCE in DMF under N₂ atmosphere was carried out. After the passage of 2F, for all the electrolytes investigated, compound **2** was obtained as a unique quantitative product (100%) (Fig. S3). The use altogether of electrochemical techniques (such as CV and Controlled potential electrolysis) allows to establish an ECE mechanism for the electrochemical reduction of **1** (Scheme 6). A radical anion is firstly formed (Eq. 1, electrochemical reaction, E). After that, a chemical reaction coupled to this electron transfer leads to the corresponding organic radical, **1**•, and halide anion (Eq. 2, chemical reaction step, C). Finally, the organic radical formed is reduced at the electrode surface yielding the corresponding anion (Eq. 3, electrochemical reaction, E), which evolves to compound **2** after a protonation reaction (Eq. 4).

3.2. Electrochemical reduction of 2-(1-chloroethyl)-6-methoxynaphthalene (**1**) in CO₂ atmosphere

3.2.1. Carbon vitreous working electrode

The voltammetric response of **1** in CO₂ was the same for all the electrolytes tested (Fig. S4). Hence, in the initial cathodic scan a two-electron reduction wave was detected c. a. -2.0 V vs. SCE. The oxidation of chloride ion is detected in the ensuing anodic scan, since an oxidation peak at c. a. 1.1 V vs. SCE is observed (Fig. S5a).

Note that the second reduction wave at -2.60 V vs. SCE becomes irreversible and increases its intensity in CO₂ atmosphere. This behaviour typically describes a catalytic process, where product **2** would act as a catalyst to reduce CO₂ through a homogeneous catalytic process (Gennaro et al., 1996a), producing CO₂^{•-} (Scheme 7).

At this point several electrocarboxylation processes were attempted under CO₂ atmosphere, after pre-saturated with CO₂ the selected electrolyte. Controlled-potential electrolysis of **1**, after its first reduction wave, was performed in DMF and ILs using a carbon graphite bar as a cathode. Cyclic voltammograms were recorded after the passage of different charge amounts in order to monitor the process (Fig. S5b). In all cases, naproxen was obtained in reasonable yields (Table 2), the behaviour and results being the same for classic organic aprotic solvents and ionic liquids. A closer look reveals that the best yields were obtained for imidazolium ionic liquids, since the conductivity and the viscosity of the solution is higher and lower, respectively (Tables 1 and 3, entries 4 and 5). Only when using BMPyr TFSI is the yield as well as the conversion rate of naproxen reduced probably due to its high viscosity (Tables 1 and 3, entry 3).

3.2.2. Silver working electrode

Considering the enhanced results obtained with a silver electrode in comparison to a carbon working electrode, thanks to the electrocatalytic effect of the silver electrode in carbon-halogen cleavage reactions, we expected the moderate yields obtained in

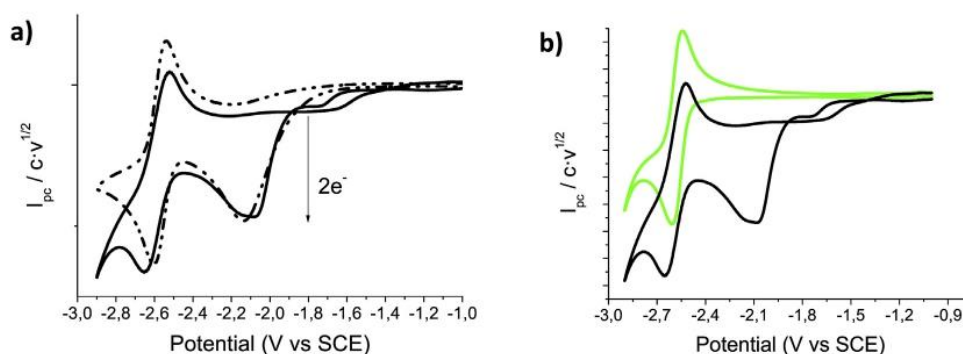
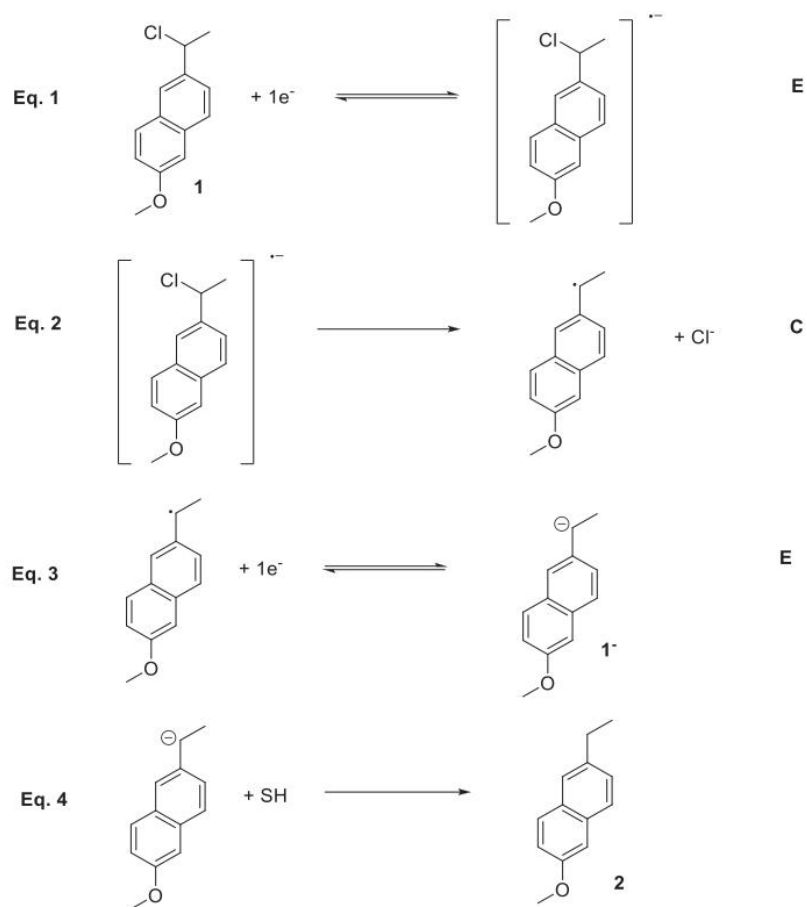
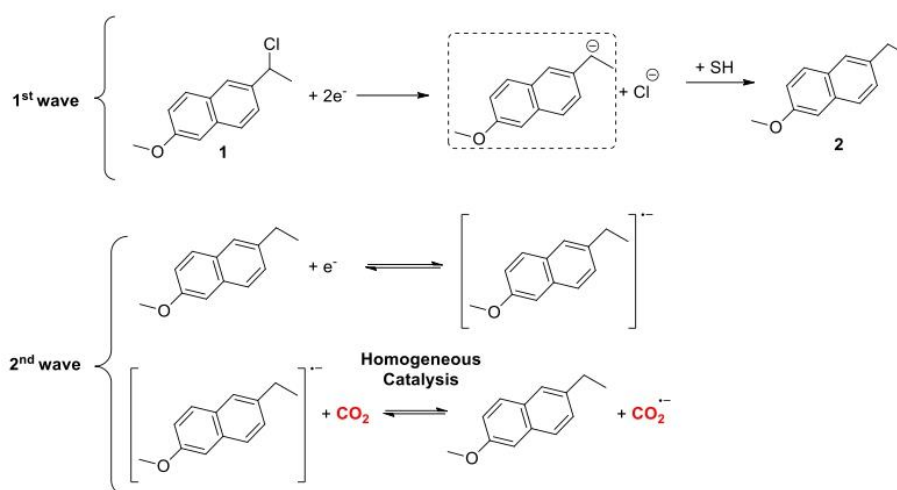


Fig. 1. Cyclic voltammograms in DMF + TBABF₄ (scan rate 0.5 V s⁻¹) at 25 °C a) of **1** on a GC (dotted line) and Silver (solid line) electrodes b) **1** (black line) and **2** (green line) on a GC in inert atmosphere. (For interpretation of the references to colour in this figure legend, the reader is referred to the Web version of this article.)

Scheme 6. Electrochemical reduction mechanism of **1**.Scheme 7. Electrochemical reduction mechanism that describes cyclic voltammogram in CO₂ atmosphere.

electrocarboxylation reactions with a carbon cathode to improve with the use of the silver electrode.

Fig. 2 shows the CV of **1** in the different solvents in CO₂

atmosphere with a silver electrode. A reduction peak of between c. a. -1.8 or -2.40 V vs. SCE is detected, when ILs or DMF is used as an electrolyte. This reduction peak is assigned to the reduction of **1** and

Table 3
Results of Exhaustive Electrolysis of **1** under CO₂ atmosphere to obtain Naproxen (**3**).

Entry	Solvent	E _{applied} (V)	R-COOH (Naproxen isolated, 3) Yield (% conversion rate)	Reactant (1)(%)	R-H (2)(%)
1	DMF + Et ^[a]	-2.25	29 (36%)	20	51
2	N ₁₁₁₄ TFSI	-2.1	26 (31%)	15	59
3	BMPyr TFSI	-2.1	13 (14%)	6	81
4	BMIM TFSI	-2.1	32 (34%)	6	62
5	BMIM BF ₄	-2.1	40 (42%)	5	55

[a] DMF + 0.1 M of TBABF₄

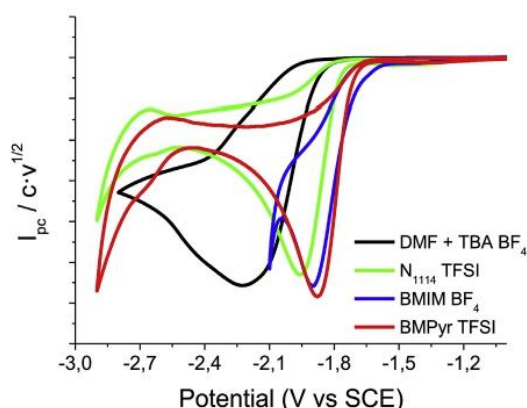
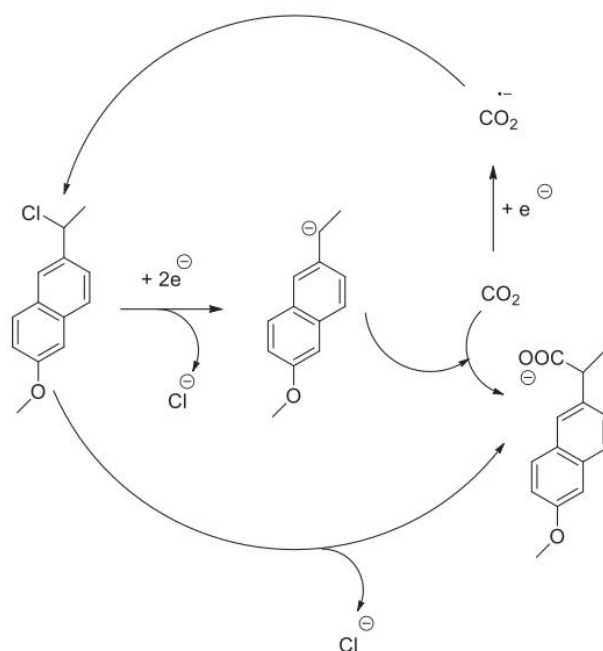


Fig. 2. Cyclic voltammograms (scan rate 0.5 V s⁻¹) at 25 °C on Ag electrode of 5 mM of **1** and 40 mM of CO₂ in the different electrolytes.

CO₂ at the same time. It has already been reported by some of us that the electrochemical reduction potential of CO₂ reduction with a silver electrode surface is lower in ILs than in the case of organic aprotic solvents (Reche et al., 2015, 2014a). Hence, the cyclic voltammogram (Fig. 2) shows a reduction, which not only involves the electrochemical reduction peak of **1** but also the direct reduction of CO₂ at silver surface.

Controlled-potential electrolysis of **1** was performed using a silver sheet cathode under CO₂ atmosphere in DMF and ILs applying a potential 0.1 V after the first electron transfer, which was obtained in an inert atmosphere. The electrochemical processes were easily monitored by means of cyclic voltammetry using glassy carbon as a working electrode instead of silver because, CO₂ reduction does not occur with carbon. The behaviour and results being the same for classic organic aprotic solvents and ionic liquids. However, there was an improvement in Naproxen yields from moderate to good compared when silver (Table 4) was used instead of carbon as a working electrode (Table 3). For all the electrolytes the same general trends, in terms of yield and conversion rates of Naproxen, were seen for both cathodes. The use of ILs with high conductivity



Scheme 8. Nucleophilic substitution mechanism operates concurrently.

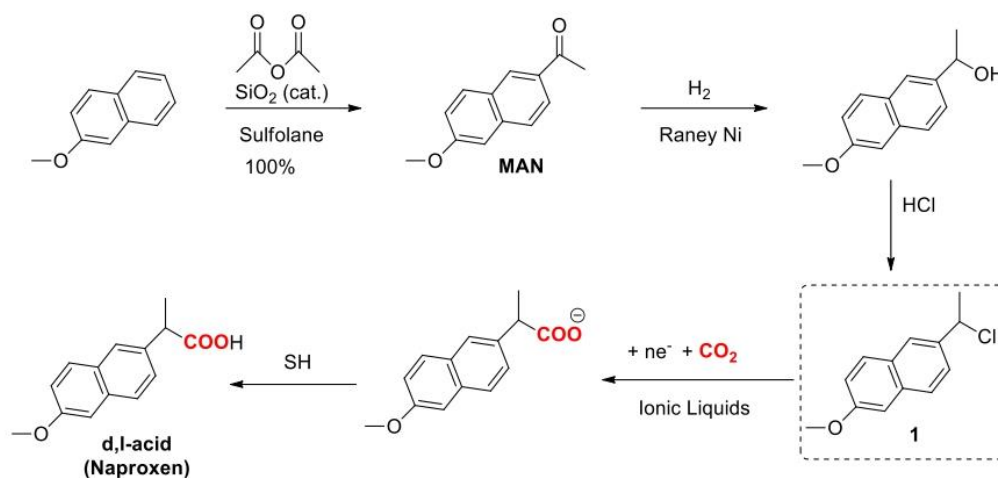
and low viscosity enhances the yields and the conversion rates, allowing to reach values close to the 90% when BMIM BF₄ and silver are used as electrolyte and cathode, respectively. (Table 3, entry 4). Finally, it is important to highlight that in all the cases the use of silver as a cathode allowed to obtain Naproxen as a main product with conversion rates higher than 50%.

Focusing on our electrochemical procedure, two kinds of mechanism operate concurrently in this reaction depending on the working electrode, and which are summarised in Scheme 8. On the one hand, with the use of the glassy carbon working electrode the mechanism goes through **1**^{•-} anion, which improves its nucleophilic

Table 4
Results of Exhaustive Electrolysis of **1** under CO₂ atmosphere to obtain Naproxen (**3**).

Entry	Solvent	E _{applied} (V)	R-COOH (Naproxen isolated, 3) Yield (% conversion rate)	Reactant (1) (%)	R-H (2) (%)
1	DMF + Et ^[a]	-2.15	55 (58.5%)	6	39
2	N ₁₁₁₄ TFSI	-2.0	65 (66%)	2	33
3	BMPyr TFSI	-2.0	52 (55%)	6	42
4	BMIM BF ₄	-1.8	88.5 (90%)	1.5	10
5	BMIM TFSI	-2.0	70 (63%)	5	35

[a] The DMF + 0.1 M of TBABF₄



Scheme 9. Naproxen proposed synthesis.

behaviour and attaches CO_2 , which acts as an electrophile, to its structure (Table 3, entries 1–5). In turn, there is a radical mechanism with the use of a silver electrode, where CO_2 is reduced to obtain CO_2^- on the electrode's surface, and in this case, CO_2 acts as a nucleophile and reacts with **1** (Table 4, entries 1–5). The electrochemically triggered dual reactivity enhances the yield of Naproxen through a carboxylation process (see Scheme 9).

3.3. Sustainability of “our” electrocarboxylation approach

Our proposed synthesis of Naproxen (Scheme 9) presents an alternative to the other two strategies described in the introduction. In our case, two first steps were obtained as in the case of the Shaw/Schlitzer synthesis. However, we propose to replace the OH substituent of the starting material for a chloride group, since it is a better leaving group (Ayers et al., 2005). Then, with the use of an electrochemical carboxylation process, CO_2 is incorporated into the reactant. In the atom economy analysis (Table 5) of our proposal, we obtain **36%** (65% considering recoverability of the resolving agent). These results are very similar to those achieved by Shaw and Schlitzer. Moreover, in our case, despite the use of halogens, one of the catalysts we used were electrons, which are heterogeneous and much cheaper and more widely available than the others, and the use of CO_2 instead of CO enhances the process.

Note that a similar approach was used in the past for the electrochemical synthesis of Naproxen (Fauvarque et al., 1988a), as it has been previously pointed in the introduction section. This work

identified tetramethylurea (TMU) as the most suitable solvent for performing the electrochemical synthesis in terms of moderate toxicity, high reaction yields and conversion rates. However, the use of TMU as a solvent for electrochemistry involves large quantities of supporting electrolyte (usually tetralkylammonium salts) due to its moderate conductivity as well as large-energy-consuming processes for solvent recovery. In this sense, our electrocarboxylation approach, based on the recyclability of green electrolytes (ILs), would allow to overcome those environmental limitations. This “greener” approach can be potentially applied to more sophisticated NSAIDs as well as other carboxylation products.

In this sense, cost-effectiveness analysis to determine whether an electrocarboxylation approach is a low-cost alternative would strongly depend on the electricity prices and the energy conversion efficiencies. It is reported that for electrosynthesis to become economical viable with traditional fossil fuel-derived processes the electricity generation should come from renewable sources, being the electrochemical conversion efficiencies at least 60% and the electricity price below 4 cents per kWh (De Luna et al., 2019). In 2019, non-household electricity prices in the European Union are between 0.17 and 0.07 cents per kWh depending on the country and 0.13 cents per kWh in United States. Hence, apart from the technical challenges of using electrochemistry for manufacturing marketable products; the main challenge would be to reduce the electricity price between 2 and 4 times. Focusing on electrochemical approach for synthesizing Naproxen, note that when silver is used as cathode not only yields and the conversion

Table 5
Atom economy analysis –Our proposed synthesis.

Reagent		Used in Naproxen		Unused in Naproxen	
Formula	MW	Formula	MW	Formula	MW
$\text{C}_{10}\text{H}_7\text{OCH}_3$	158.3	$\text{C}_{10}\text{H}_6\text{OCH}_3$	157.3	H	1.0
$\text{C}_4\text{H}_6\text{O}_3$	102.1	C_2H_3	27.0	$\text{C}_2\text{H}_3\text{O}_3$	75.1
H_2	2.0	H	1.0	H	1.0
HCl	36.5	—	—	HCl	36.5
e^-	—	e^-	—	—	—
CO_2	44.0	CO_2	44.0	—	—
H	1.0	H	1.0	—	—
$\text{C}_{14}\text{H}_{31}\text{NO}_5$	293.4	—	—	$\text{C}_{14}\text{H}_{31}\text{NO}_5$	293.4
Total		Naproxen		Waste	
$\text{C}_{43}\text{H}_{63}\text{NO}_{11}\text{Cl}_2$	637.3	$\text{C}_{14}\text{H}_{14}\text{O}_3$	230.3	$\text{C}_{16}\text{H}_{36}\text{NO}_5\text{Cl}_2$	407

efficiencies are around 90% but also ca. 75% the electrolyte can be recycled and reused at the end of the process.

4. Conclusions

A description of a sustainable and highly efficient chemical route for synthesizing useful compounds using CO₂ as a C1 synptom through electrocarboxylation reactions is presented. This strategy deals with the used of electrochemical techniques and ILs, which allow introduce some of the Green Chemistry principles for the synthesis of NSAIDs. Controlled potential electrolysis 2-(1-chloroethyl)-6-methoxynaphthalene in CO₂ atmosphere obtains Naproxen in good yields and excellent atom economy compared with the initial ones. This methodology offers a “green” way for the synthesis of different carboxylic acids that could potentially displace the petrochemical process in a future.

Declaration of competing interest

The authors declare no conflicts of interest.

Acknowledgments

The authors thank financial support though the project CTQ 2015-65439-R from the MINECO/FEDER. S.M. acknowledges the Autonomous University of Barcelona for her predoctoral PIF grant. This work was also supported by the Spanish network of Excellence E3TECH (“Environmental and Energy Applications of the Electrochemical Technology”, CTQ 2017-90659-REDT).

Appendix A. Supplementary data

Supplementary data to this article can be found online at <https://doi.org/10.1016/j.chemosphere.2019.125557>.

Author contributions

G and GG conceptualized the research topic, conceived and designed the experiments; S.M. did the main part of the experiments, and was assisted by S.S.; S.M., S.S. and G.G. analyzed the data; S.M., I.G. and G.G. interpreted the results. S.M. and G.G. prepared the draft. All authors corrected the draft. I.G. and G.G. obtained the funds for the research.

References

- Adelman, J.U., Alexander, W.J., Barrett, P.S., Brandes, J.L., Kudrow, D., Lener, S.E., O'Carroll, C.P., O'Donnell, F.J., Spruill, S.E.S.S., 2007. Sumatriptan-naproxen for acute treatment of migraine. *Jama* 297, 1443–1454.
- Alvarez-Guerra, M., Albo, J., Alvarez-Guerra, E., Irabien, A., 2015. Ionic liquids in the electrochemical valorisation of CO₂. *Energy Environ. Sci.* 8, 2574–2599. <https://doi.org/10.1039/C5EE01486G>.
- Amatore, C., Savéant, J.M., 1981. Mechanism and kinetic characteristics of the electrochemical reduction of carbon dioxide in media of low proton availability. *J. Am. Chem. Soc.* 103, 5021–5023. <https://doi.org/10.1021/ja00407a008>.
- Amaboldi, S., Bonetti, A., Giussani, E., Mussini, P.R., Benincori, T., Rizzo, S., Isse, A.A., Gennaro, A., 2014. Electrocatalytic reduction of bromothiophenes on gold and silver electrodes: an example of synergy in electrocatalysis. *Electrochem. Commun.* 38, 100–103. <https://doi.org/10.1016/j.elecom.2013.10.025>.
- Janssens, H.J., Janssen, M., Van de Lisdonk, E.H., van Riel, P.L., Van Weel, C., 2008. Use of oral prednisolone or naproxen for the treatment of gout arthritis: a double-blind, randomised equivalence trial. *Lancet* 371, 1854–1860.
- Ayers, P.W., Anderson, J.S.M., Rodriguez, J.J., Jawed, Z., 2005. Indices for predicting the quality of leaving groups. *Phys. Chem. Chem. Phys.* 7, 1918–1925. <https://doi.org/10.1039/b500996k>.
- Chen, L., Guo, S.-X., Li, F., Bentley, C., Horne, M., Bond, A.M., Zhang, J., 2016. Electrochemical reduction of CO₂ at metal electrodes in a distillable ionic liquid. *ChemSusChem* 9, 1271–1278. <https://doi.org/10.1002/cssc.201600359>.
- Costentin, C., Robert, M., Savéant, J.M., 2013. Catalysis of the electrochemical reduction of carbon dioxide. *Chem. Soc. Rev.* 42, 2423–2436. <https://doi.org/10.1039/c2cs35360a>.
- Cruz, H., Gallardo, I., Guirado, G., 2008. Understanding specific effects on the standard potential shifts of electrogenerated species in 1-butyl-3-methylimidazolium ionic liquids. *Electrochim. Acta* 53, 5968–5976. <https://doi.org/10.1016/j.electacta.2008.03.062>.
- Cruz, H., Gallardo, I., Guirado, G., 2011. Electrochemically promoted nucleophilic aromatic substitution in room temperature ionic liquids - an environmentally benign way to functionalize nitroaromatic compounds. *Green Chem.* 13, 2531–2542. <https://doi.org/10.1039/c1gc15303j>.
- Damodar, J., Krishna Mohan, S.R., Jayarama Reddy, S.R., 2001. Synthesis of 2-arylpropionic acids by electrocarboxylation of benzylchlorides catalysed by PdCl₂(PPh₃)₂. *Electrochem. Commun.* 3, 762–766. [https://doi.org/10.1016/S1388-2481\(01\)00263-6](https://doi.org/10.1016/S1388-2481(01)00263-6).
- De Luna, P., Hahn, C., Higgins, D., Jaffer, S.A., Jaramillo, T.F., Sargent, E.H., 2019. What would it take for renewably powered electrosynthesis to displace petrochemical processes? *Science* 80, 364. <https://doi.org/10.1126/science.aav3506>.
- Durante, C., Isse, A.A., Sandona, G., Gennaro, A., 2009. Electrochemical hydrodehalogenation of polychloromethanes at silver and carbon electrodes. *Appl. Catal. B Environ.* 88, 479–489. <https://doi.org/10.1016/j.apcatb.2008.10.010>.
- Durante, C., Isse, A.A., Todesco, F., Gennaro, A., 2013. Electrocatalytic activation of aromatic carbon-bromine bonds toward carboxylation at silver and copper cathodes. *J. Electrochem. Soc.* 160, G3073–G3079. <https://doi.org/10.1149/2.008307jes>.
- Fauvarque, J.F., Jutand, A., Francois, M., 1988a. Nickel catalysed electrosynthesis of anti-inflammatory agents. Part I - synthesis of aryl-2 propionic acids, under galvanostatic conditions. *J. Appl. Electrochem.* 18, 109–115. <https://doi.org/10.1007/BF01016213>.
- Fauvarque, J.F., Jutand, A., Francois, M., Petit, M.A., 1988b. Nickel catalysed electrosynthesis of anti-inflammatory agents. Part II - monitoring of the electrolyses by HPLC analysis. Role of the catalyst. *J. Appl. Electrochem.* 18, 116–119. <https://doi.org/10.1007/BF01016214>.
- Frontana-Urbe, B.A., Little, R.D., Ibanez, J.G., Palma, A., Vasquez-Medrano, R., 2010. Organic electrosynthesis: a promising green methodology in organic chemistry. *Green Chem.* 12, 2099. <https://doi.org/10.1039/c0gc00382d>.
- Gallardo, I., Soler, S., 2017. Electrochemically promoted arylation of iodoaromatics. *J. Electroanal. Chem.* 799, 9–16. <https://doi.org/10.1016/j.jelechem.2017.05.034>.
- Gennaro, A., Isse, A.A., Savéant, J.M., Severin, M.G., Vianello, E., 1996a. Homogeneous electron transfer catalysis of the electrochemical reduction of carbon dioxide. Do aromatic anion radicals react in an outer-sphere manner? *J. Am. Chem. Soc.* 118, 7190–7196. <https://doi.org/10.1021/ja960605o>.
- Gennaro, A., Isse, A.A., Severin, M.-G., Vianello, E., Bhugun, I., Savéant, J.-M., 1996b. Mechanism of the electrochemical reduction of carbon dioxide at inert electrodes in media of low proton availability. *J. Chem. Soc., Faraday Trans. 92*, 3963–3968. <https://doi.org/10.1039/FT9969203963>.
- Gennaro, A., Sánchez-Sánchez, C.M., Isse, A.A., Montiel, V., 2004. Electrocatalytic synthesis of 6-aminonicotinic acid at silver cathodes under mild conditions. *Electrochem. Commun.* 6, 627–631. <https://doi.org/10.1016/j.elecom.2004.04.019>.
- Harrington, P.J., Lodewijk, E., 1997. Twenty years of naproxen technology. *Org. Process Res. Dev.* 1, 72–76. <https://doi.org/10.1021/op960009e>.
- Harrison, I.T., Lewis, B., Nelson, P., Rooks, W., Roszkowski, A., Tomolonis, A., Fried, J.H., 1970. Nonsteroidal antiinflammatory agents. I. 6-Substituted 2-naphthylacetic acids. *J. Med. Chem.* 13, 203–205. <https://doi.org/10.1021/jm00296a008>.
- Isse, A.A., Gennaro, A., 2002. Electrocatalytic carboxylation of benzyl chlorides at silver cathodes in acetonitrile the reductive carboxylation of benzyl chlorides (RCI): in trials that are about 0.6 V more positive than those of the acids in good to excellent yields. *Chem. Commun.* 2798–2799.
- Isse, A.A., Ferlin, M.G., Gennaro, A., 2005. Electrocatalytic reduction of arylethyl chlorides at silver cathodes in the presence of carbon dioxide: synthesis of 2-arylpropanoic acids. *J. Electroanal. Chem.* 581, 38–45. <https://doi.org/10.1016/j.jelechem.2005.04.007>.
- Isse, A.A., De Giusti, A., Gennaro, A., Falciola, L., Mussini, P.R., 2006a. Electrochemical reduction of benzyl halides at a silver electrode. *Electrochim. Acta* 51, 4956–4964. <https://doi.org/10.1016/j.electacta.2006.01.039>.
- Isse, A.A., Falciola, L., Mussini, P.R., Gennaro, A., 2006b. Relevance of electron transfer mechanism in electrocatalysis: the reduction of organic halides at silver electrodes. *Chem. Commun.* 1, 344–346. <https://doi.org/10.1039/B513801A>.
- Isse, A.A., Gottardello, S., Durante, C., Gennaro, A., 2008. Dissociative electron transfer to organic chlorides: electrocatalysis at metal cathodes. *Phys. Chem. Chem. Phys.* 10, 2409–2416. <https://doi.org/10.1039/b719936h>.
- Isse, A.A., Berzi, G., Falciola, L., Rossi, M., Mussini, P.R., Gennaro, A., 2009. Electrocatalysis and electron transfer mechanisms in the reduction of organic halides at Ag. *J. Appl. Electrochem.* 39, 2217–2225. <https://doi.org/10.1007/s10800-008-9768-z>.
- Lim, H.K., Kim, H., 2017. The mechanism of room-Temperature ionic-liquid-based electrochemical CO₂ reduction: a Review. *Molecules* 22. <https://doi.org/10.3390/molecules22040536>.
- Liu, Q., Wu, L., Jackstell, R., Beller, M., 2015. Using carbon dioxide as a building block in organic synthesis. *Nat. Commun.* 6, 1–15. <https://doi.org/10.1038/ncomms6933>.
- Lugaresi, O., Minguzzi, A., Locatelli, C., Vertova, A., Rondinini, S., Amatore, C., 2013. Benzyl chloride electroreduction on Ag cathodes in CH₃CN in the presence of small amounts of water: evidences of quantitative effects on reaction rates and mechanism. *Electrocatalysis* 4, 353–357. <https://doi.org/10.1007/s12678-013-0080-0>.

- 0161–2.
- Marrucho, I.M., Branco, L.C., Rebelo, L.P.N., 2014. Ionic liquids in pharmaceutical applications. *Annu. Rev. Chem. Biomol. Eng.* 5, 527–546. <https://doi.org/10.1146/annurev-chembioeng-060713-040024>.
- Matthessen, R., Fransaer, J., Binnemans, K., De Vos, D.E., 2014. Electrocarboxylation: towards sustainable and efficient synthesis of valuable carboxylic acids. *Beilstein J. Org. Chem.* 10, 2484–2500. <https://doi.org/10.3762/bjoc.10.260>.
- Mena, S., Mirats, A., Caballero, A.B., Guirado, G., Barrios, L.A., Teat, S.J., Rodríguez-Santiago, L., Sodupe, M., Gamez, P., 2018. Drastic effect of the peptide sequence on the copper-binding properties of tripeptides and the electrochemical behaviour of their copper(II) complexes. *Chem. Eur. J.* 24, 5153–5162. <https://doi.org/10.1002/chem.201704623>.
- Mena, S., Gallardo, I., Guirado, G., 2019a. Electrocatalytic processes for the valorization of CO₂: synthesis of cyanobenzoic acid using eco-friendly strategies. *Catalysts* 9, 413. <https://doi.org/10.3390/catal9050413>.
- Mena, S., Sanchez, J., Guirado, G., 2019b. Electrocarboxylation of 1-chloro-(4-isobutylphenyl)ethane with a silver cathode in ionic liquids: an environmentally benign and efficient way to synthesize Ibuprofen. *RSC Adv.* 9, 15115–15123. <https://doi.org/10.1039/C9RA01781J>.
- Niu, D., Zhang, J., Zhang, K., Xue, T., Lu, J., 2009. Electrocatalytic carboxylation of benzyl chloride at silver cathode in ionic liquid BMIMBF₄. *Chin. J. Chem.* 27, 1041–1044. <https://doi.org/10.1002/cjoc.200990174>.
- Pappenfus, T.M., Lee, K., Thoma, L.M., Dukart, C.R., 2009. Wind to ammonia: electrochemical processes in room temperature ionic liquids. *ECS Trans* 16, 89–93. <https://doi.org/10.1149/1.3159311>.
- Reche, I., Gallardo, I., Guirado, G., 2014a. Electrochemical studies of CO₂ in imidazolium ionic liquids using silver as a working electrode: a suitable approach for determining diffusion coefficients, solubility values, and electrocatalytic effects. *RSC Adv.* 4, 65176–65183. <https://doi.org/10.1039/c4ra11297k>.
- Reche, I., Gallardo, I., Guirado, G., 2014b. The role of cations in the reduction of 9-fluorenone in bis(trifluoromethylsulfonylethyl)imide room temperature ionic liquids. *New J. Chem.* 38, 5030–5036. <https://doi.org/10.1039/c4nj01200c>.
- Reche, I., Gallardo, I., Guirado, G., 2015. Cyclic voltammetry using silver as cathode material: a simple method for determining electro and chemical features and solubility values of CO₂ in ionic liquids. *Phys. Chem. Chem. Phys.* 17, 2339–2343. <https://doi.org/10.1039/c4cp05409a>.
- Ruelius, W., Johns, C., Mouelhi, M.E.L., Fenselau, H., Dulik, M.M., 1987. SPECIES-DEPENDENT enantioselective glucuronidation OF three 2-ARYLPROPIONIC acids: naproxen, ibuprofen, and benoxaprofen. *Drug Metab. Dispos.* 15, 767–772.
- Senboku, H., Katayama, A., 2017. Electrochemical carboxylation with carbon dioxide. *Curr. Opin. Green Sustain. Chem.* 3, 50–54. <https://doi.org/10.1016/j.cogsc.2016.10.003>.
- Shaw, N., Schlitzer, S., 2015. Green Synthesis: Naproxen [WWW Document]. <https://es.slideshare.net/NathanShaw3/green-chemistry-synthesis-of-naproxen-54358185>.
- Sun, L., Ramesha, G.K., Kamat, P.V., Brennecke, J.F., 2014. Switching the reaction course of electrochemical CO₂ reduction with ionic liquids. *Langmuir* 30, 6302–6308. <https://doi.org/10.1021/la5009076>.
- Tateno, H., Nakabayashi, K., Kashiwagi, T., Senboku, H., Atobe, M., 2015. Electrochemical fixation of CO₂ to organohalides in room-temperature ionic liquids under supercritical CO₂. *Electrochim. Acta* 161, 212–218. <https://doi.org/10.1016/j.electacta.2015.01.072>.
- Tokuda, M., 2006. Efficient fixation of carbon dioxide by electrolysis - facile synthesis of useful carboxylic acids -. *J. Nat. Gas Chem.* 15, 275–281. [https://doi.org/10.1016/S1003-9953\(07\)60006-1](https://doi.org/10.1016/S1003-9953(07)60006-1).
- Uziel, Y., Hashkes, P.J., Kassem, E., Padeh, S., Goldman, R., Vollach, B., 2000. The use of naproxen in the treatment of children with rheumatic fever. *J. Pediatr.* 137, 269–271. <https://doi.org/10.1067/mpd.2000.107158>.
- Williams, D.B.G., Lawton, M., 2010. Drying of organic solvents: quantitative evaluation of the efficiency of several desiccants. *J. Org. Chem.* 75, 8351–8354. <https://doi.org/10.1021/jo101589h>.
- Yamauchi, Y., Fukuhara, T., Hara, S., Senboku, H., 2008. Electrochemical carboxylation of α,α -difluorotoluene derivatives and its application to the synthesis of α -fluorinated nonsteroidal anti-inflammatory drugs. *Synlett* 428–442. <https://doi.org/10.1055/s-2008-1032069>.
- Yamauchi, Y., Hara, S., Senboku, H., 2010. Synthesis of 2-aryl-3,3,3-trifluoropropanoic acids using electrochemical carboxylation of (1-bromo-2,2,2-trifluoroethyl)arenes and its application to the synthesis of β,β -trifluorinated non-steroidal anti-inflammatory drugs. *Tetrahedron* 66, 473–479. <https://doi.org/10.1016/j.tet.2009.11.053>.
- Yoo, W.J., Kondo, J., Rodríguez-Santamaría, J.A., Nguyen, T.V.Q., Kobayashi, S., 2019. Efficient synthesis of α -trifluoromethyl carboxylic acids and esters through fluorocarboxylation of gem-difluoroalkenes. *Angew. Chem. Int. Ed.* 58, 6772–6775. <https://doi.org/10.1002/anie.201902779>.
- Zhou, F., Liu, S., Yang, B., Wang, P., Alshammari, A.S., Deng, Y., 2015. Electrochemistry Communications Highly selective and stable electro-catalytic system with ionic liquids for the reduction of carbon dioxide to carbon monoxide. *Electrochem. Commun.* 55, 43–46.

Appendix:

Theoretical fundamentals
of Electrochemistry

Appendix. Theoretical fundamentals of Electrochemistry

Considering the reaction at the electrode $O + ne^- \rightleftharpoons R$, the current or electrode reaction rate is governed by the following processes (Figure 42).

1. Mass transfer.
2. Electronic transfer on the electrode surface.
3. Chemical reactions before or after the electron transfer, which could be homogeneous (bulk solution) or heterogeneous (electrode).
4. Other surface reactions: adsorption, desorption or crystallization.

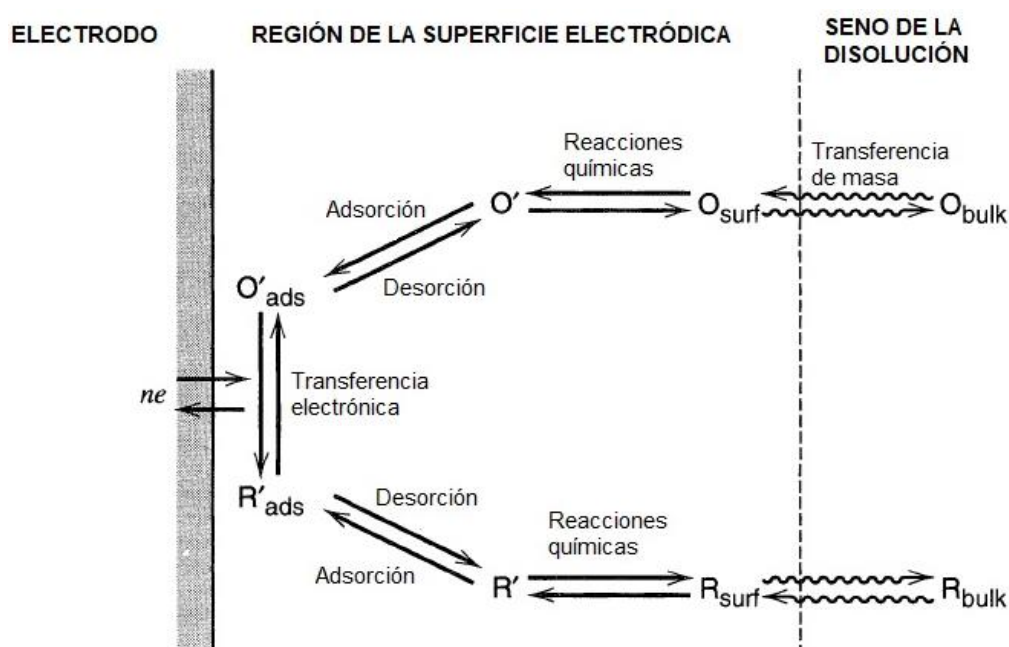


Figure 42. Electrochemical processes.

The I-E-t, curves provide information about the kinetics of the electrochemical reaction. The scan rate of an electrochemical reaction is defined as:

$$v = k_f \cdot C_{Ox} - k_b \cdot C_{Red} = \frac{I}{zFS} \quad (8)$$

$$I = FS \cdot [k_f \cdot C_{Ox} - k_b \cdot C_{Red}] \quad (9)$$

Under conditions where there are not mass transport, chemical reactions or processes of adsorption and desorption on the electrode surface, it is possible to apply the Butler-Volmer equation:

$$I = \pm F A k_s^{ap} \exp \left[\pm \frac{\alpha F}{RT} (E - E^0) \right] \cdot \left\{ (C_{Ox})_0 - (C_{Red})_0 \cdot \exp \left[\pm \frac{F}{RT} (E - E^0) \right] \right\} \quad (10)$$

Where C_{ox} and C_{red} are the oxidizing and reducing species concentrations, respectively, on the electrode surface. S is the electrode surface area. E is the potential applied to the electrode, E^0 is the standard potential, α is the electronic transfer coefficient ($0 < \alpha < 1$), k_s^{ap} is the apparent electronic transfer rate constant, and Φ is the external plane of Helmontz.

$$k_s^{ap} = k_s \exp \left(\frac{-\alpha F \phi}{RT} \right) \quad (11)$$

$$k_s = k_f(E = E^0) = k_b(E = E^0) \quad (12)$$

Due to during the electron transfer the amount of oxidizing (Ox) and reducing (Red) species change on the electrode surface, the mas transfer is a determining factor. In this situation, the Butler-Volmer equation shown as equation (10) is no longer valid.

To introduce the mass transport, is important to define the kind of transport that take place (diffusion, migration or convection), and therefore, which electrochemical method must be used.

The mass transport (J) follows the next equation:

$$\vec{J} = \frac{c_j D_j}{RT} \cdot \frac{\delta \mu_j}{\delta x} + c_j v_x \quad (13)$$

Where c_j is the concentration of j specie in the solution, v_x is the solution speed, D_j is the diffusion coefficient of specie j , and μ_i is the electrochemical potential.

The equation (2) includes different mass transports which can be take place; the first term includes diffusive and migration transport, and it is added with the term related to the convection of the electroactive substance (EAS).

Depending on how the mass is transported to the electrode surface, electrochemical methods can be divided into two groups:

○ Stationary electrochemical methods.

The transport of the mass related to EAS from bulk solution to the electrode surface takes place by diffusion and forced convection (agitation).

○ Non-stationary or transient electrochemical methods.

The transport of the mass related to EAS to the electrode surface takes place only by diffusion. These methods are subdivided as:

- a. Potentiostatic methods, which a controlled potential is applied, and the intensity is obtained as a function of time.
- b. Galvanostatic methods, which a current is applied as a function of time and the potential as a function of time is obtained as a response.

Under normal working conditions for transient electrochemical methods, the electroactive substance (EAS) is transferred from the bosom of the solution to the electrode surface by diffusion only. Thus, the differential equations with respect to time in the homogeneous kinetics are replaced by partial differential equations with respect to time and space that separate the electroactive species from the electrode surface (Fick's Laws).

Linear Voltammetry and Cyclic Voltammetry

The linear voltammetry (LV) is a transient electrochemical method. The applied signal in this technique is a potential ramp which varies linearly with time, and with respect to a reference electrode. The signal is applied to the system by means of a signal generator where the potential is applied to the working electrode.

Cyclic voltammetry (CV), is based on the application of a triangular sweep of potential; a potential ramp in the direct sense and another in the opposite direction (Figure 43a). The sweep starts at an initial value of potential (E_i) to a cutoff value (E_c), and then reverses the sweep to reach the initial potential again. In this disturbance, the slope of the potential variation is known as “potential sweep rate” (v).

$$E = E_i \pm vt \quad (14)$$

The characteristic time of the technique, θ (s) is inversely proportional related to the potential sweep rate, $\theta = RT/Fv$.

As a response, a Current-Potential (I-E) curves is registered. For a reversible system, the I-E response is obtained as shown in Figure 43b.

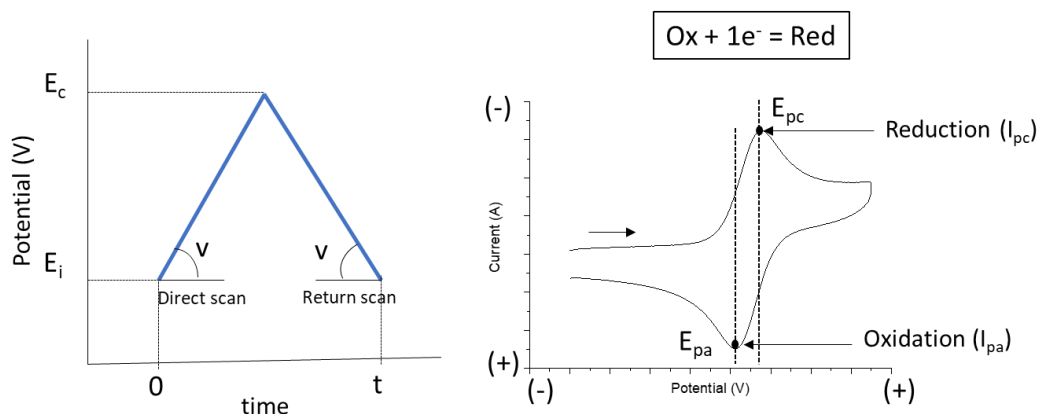


Figure 43. Signal $E=f(t)$ applied in CV (left). Response I-E for a reversible electrochemical reaction (right).

From the I-E curves, the characteristic parameters of electronic transfer can be determined: the peak potential at which a substance is oxidized or reduced (E_p), as well as the peak intensity (I_p) and the average wavelength (ΔE_p). The scan rate (v) is a determining parameter of this technique and can vary from 0.05 to 1000 V/s, in case of using microelectrodes (mm), but the use of ultra-microelectrodes (μm) and high-speed potentiostats, allows the application of much higher scanning rates, in the order of 10^6 V/s.

Current-Potential curves (I-E)

The I-E-t curves also gives electron transfer kinetic information.

Electron transfer (E)

The kinetic equations which take into account diffusion and electronic transfer are the following:

$$\left(\frac{\delta c_{Ox}}{\delta t}\right) = D_{Ox} \left(\frac{\delta^2 c_{Ox}}{\delta x^2}\right) \quad (15)$$

$$\left(\frac{\delta c_{Red}}{\delta t}\right) = D_{Red} \left(\frac{\delta^2 c_{Red}}{\delta x^2}\right) \quad (16)$$

Assuming the use of a flat electrode, to solve the system of differential equations are needed boundary conditions:

1. The diffusion takes place in a single direction, linear diffusion, since the working electrode is flat.
2. $D_{Ox} = D_{Red}$.
3. At time $t = 0 \rightarrow x \geq 0$
In a time: $t \geq 0$ y $x = \infty \rightarrow c_{Ox} = c_{Ox}^0$ y $c_{Red} = 0$
4. When $x = 0$ and $t > 0$ (parameters indicating the surface of the electrode), the Nerst/Volmer equation is fulfilled and there is no accumulation of matter.

$$\left(\frac{\delta c_{Ox}}{\delta x}\right) + \left(\frac{\delta c_{Red}}{\delta x}\right) = 0 \quad \text{(Nerst/Volmer)}$$

$$c_{Ox} = c_{Red} \cdot e^{\left(\frac{(E-E^0)F}{RT}\right)} \quad (17)$$

Where E is the applied potential, $E = E_i + vt$ and the current is defined by:

$$I = FSD \cdot \left(\frac{\delta c_{Ox}}{\delta x}\right) \quad (18)$$

For a rapid electronic transfer step (E), solving the system of differential equations associated with the theoretical study of the variation of the concentrations of the Ox and Red species, and with the Nerst equation, the following theoretical expressions are obtained for the values of the characteristic voltamperometric parameters.

$$I_p = 0.446 \cdot F \cdot A \cdot c^0 \cdot D^{1/2} \cdot \left(\frac{Fv}{RT}\right)^{1/2} \quad (19)$$

$$E_p = E^0 - 1.11 \cdot \left(\frac{RT}{F}\right) \quad (20)$$

$$\Delta E_p = E_p - E_{p1} = 2.20 \cdot \left(\frac{RT}{F}\right) \quad (21)$$

$$E_{p1} = E_{(I=\frac{I_1}{2})} \quad (22)$$

From the expressions obtained for a fast electronic transfer process, it can be concluded that the values of $I_p/c \cdot v^{-1/2}$, E_p and ΔE_p do not depend on the potential sweep rate ($\delta E_p / \delta \log v$) = 0, and the quotient of intensities $I_{pa}/I_{pc} = 1$.

In the case where only the electron transfer process (E) is observed, the value of E^0 (standard potential) is determined from the half-sum of the anodic and cathode peak potentials.

$$E^0 = \frac{1}{2}(E_{p,c} + E_{p,a}) \quad (23)$$

It is possible to distinguish two different of electron transfer processes:

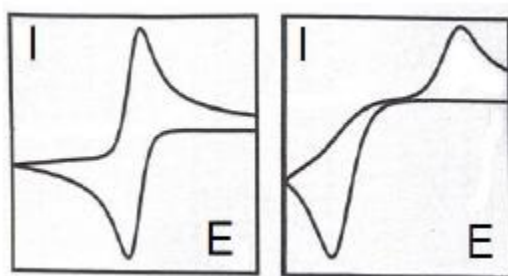


Figure 44. Electron transfer processes. Faster electron transfer (left) and slow electron transfer (right).

Obtaining a fully reversible voltamperometric wave (Figure 44, left) indicates that there are no chemical reactions associated with the electron transfer step and that a stable species has been generated on the electrode surface.

A slow electronic transfer process (Figure 44, right) is characterized by presenting apart from the thermodynamic parameter E^0 and two kinetic parameters, k_s^{ap} (apparent electronic transfer rate constant) and α (electronic transfer coefficient). With identical kinetic equations to those used for fast electron transfer, but considering Volmer, the quantitative analysis of the characteristic parameters give rise to the following expressions:

$$I_p = 0.496 \cdot F \cdot A \cdot c^0 \cdot D^{1/2} \cdot \alpha^{1/2} \cdot v^{1/2} \left(\frac{F \cdot v}{RT} \right)^{1/2} \quad (24)$$

$$E_p = E^0 - 0.78 \cdot \left(\frac{RT}{\alpha F} \right) - \left(\frac{RT}{2F} \right) \cdot \ln \left(\frac{\alpha D F}{RT} \right) + \left(\frac{RT}{\alpha F} \right) \cdot \ln k_s^{ap} - \left(\frac{RT}{2\alpha F} \right) \cdot \ln v \quad (25)$$

$$\Delta E_p = E_p - E_{p\frac{1}{2}} = 1.875 \cdot \left(\frac{RT}{F\alpha} \right) \quad (26)$$

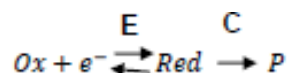
Unlike the case of fast electron transfer, in the case of a slow electron transfer, there is a dependence of E_p on the speed of potential variation, $(\delta E_p / \delta \log v) = -\frac{29}{\alpha}$ at 298 K.

Chemical reaction associated to Electron transfer (EC_x)

The two cases described above referred to processes where stable intermediates are formed (reversible I-E curves). In cases where the intermediates evolve in the electrolytic reaction medium (chemical reactions associated with the electronic transfer stage), irreversible cyclic voltammograms are obtained. Depending on the applied potential sweep rate and the characteristic time of the technique.

EC₁ Mechanism

It consists of a first step of fast electron transfer (E) followed by a first order associated chemical reaction step (C₁).



The concentrations of the species involved in the charge transfer chemical reaction are:

$$\left(\frac{\delta c_{Ox}}{\delta t}\right) = D_{Ox} \left(\frac{\delta^2 c_{Ox}}{\delta x^2}\right) \quad (27)$$

$$\left(\frac{\delta c_{Red}}{\delta t}\right) = D_{Red} \left(\frac{\delta^2 c_{Red}}{\delta x^2}\right) - k \cdot c_{Red} \quad (28)$$

The initial and boundary conditions are the same as those described for a fast electron transfer (Nerst equation). But, in the case of an EC₁ mechanism, a new term appears called λ , which contains the kinetic information of the chemical reaction associated to the electron transfer, it is a measure of the competition between the chemical reaction and the diffusion.

$$\lambda = \left(\frac{RT}{F}\right) \left(\frac{k}{v}\right) \quad (29)$$

- If $\lambda \rightarrow 0$ ($k \rightarrow 0$ or $v \rightarrow \infty$), there is control by diffusion only. In this case the cyclic voltammogram does not describe the effect of the chemical reaction since it is slower than diffusion. In this particular case, the resolution of the

system gives rise to the following equations for the parameters that describe the wave obtained, which coincide with those obtained for a fast electron transfer.

$$I_p = 0.446 \cdot F \cdot A \cdot c^0 \cdot D^{1/2} \cdot \left(\frac{Fv}{RT}\right)^{1/2} \quad (30)$$

$$E_p = E^0 - 1.11 \cdot \left(\frac{RT}{F}\right) \quad (31)$$

$$\Delta E_p = E_p - E_{p1/2} = 2.20 \cdot \left(\frac{RT}{F}\right) \quad (32)$$

$$\left(\frac{\delta E_p}{\delta \log v}\right) = 0 \quad (33)$$

- If $\lambda \rightarrow \infty$ ($k \rightarrow \infty$ or $v \rightarrow 0$), there is control by chemical reaction. In this case, the expressions for the parameters which describe the wave obtained are:

$$I_p = 0.496 \cdot F \cdot S \cdot c^0 \cdot D^{1/2} \cdot \alpha^{1/2} \cdot v^{1/2} \left(\frac{F}{RT}\right)^{1/2} \quad (34)$$

$$E_p = E^0 - 0.78 \cdot \left(\frac{RT}{F}\right) - \left(\frac{RT}{2F}\right) \cdot \ln\left(\frac{kc}{v} \cdot \frac{RT}{F}\right) \quad (35)$$

$$\Delta E_p = E_p - E_{p1/2} = 1.875 \cdot \left(\frac{RT}{F\alpha}\right) \quad (36)$$

$$\left(\frac{\delta E_p}{\delta \log v}\right) = -29.6 \text{ (mV)} \quad (37)$$

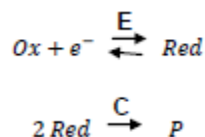
The main parameters that allow to distinguish between an EC₁ mechanism and a slow electronic transfer stage (irreversible wave) are the width of the wave obtained, ΔE_p , and the variation of the peak potential with the scanning rate ($\delta E_p / \delta \log v$). In all cases there is a dependence of E_p with $\log v$, but in the case of a slow ET stage, ΔE_p is approximately 94 mV while in an EC₁ mechanism, the value of ΔE_p is lower, 47 mV.

Therefore, by increasing the speed of potential variation it will be possible to go from an irreversible wave (at low sweep rates) to a reversible one (sufficiently

high sweep rates) and at that point, the value of the rate constant of the chemical reaction associated with the electronic transfer stage can be determined.

EC₂ Mechanism

It consists of a first step of fast electron transfer (E) followed by a second order associated chemical reaction step (C₂).



The concentrations of the species involved in the charge transfer chemical reaction are:

$$\left(\frac{\delta c_{\text{Ox}}}{\delta t} \right) = D_{\text{Ox}} \left(\frac{\delta^2 c_{\text{Ox}}}{\delta x^2} \right) \quad (38)$$

$$\left(\frac{\delta c_{\text{Red}}}{\delta t} \right) = D_{\text{Red}} \left(\frac{\delta^2 c_{\text{Red}}}{\delta x^2} \right) - 2k \cdot c_{\text{Red}} \quad (39)$$

The term λ contains the kinetic information of the chemical reaction associated to the electron transfer, it is a measure of the competition between the chemical reaction and the diffusion.

$$\lambda = \left(\frac{RT}{F} \right) \left(\frac{k}{v} \right) \quad (40)$$

- If $\lambda \rightarrow 0$ ($k \rightarrow 0$ or $v \rightarrow \infty$), there is control by diffusion only. In this case the cyclic voltammogram does not describe the effect of the chemical reaction since it is slower than diffusion. In this particular case, the resolution of the system gives rise to the following equations for the parameters that describe the wave obtained, which coincide with those obtained for a fast electron transfer.
- If $\lambda \rightarrow \infty$ ($k \rightarrow \infty$ or $v \rightarrow 0$), there is control by chemical reaction. The expressions for the parameters which describe the wave obtained are:

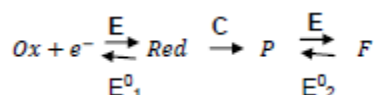
$$I_p = 0.496 \cdot F \cdot S \cdot c^0 \cdot D^{1/2} \cdot \alpha^{1/2} \cdot v^{1/2} \left(\frac{F}{RT} \right)^{1/2} \quad (41)$$

$$E_p = E^0 - 0.78 \cdot \left(\frac{RT}{F} \right) - \left(\frac{RT}{2F} \right) \cdot \ln \left(\frac{kc}{v} \cdot \frac{RT}{F} \right) \quad (42)$$

$$\Delta E_p = E_p - E_{p1} = 1.875 \cdot \left(\frac{RT}{F\alpha} \right) \quad (43)$$

ECE Mechanism

It can be said that in an ECE mechanism a first electrochemical step of electron transfer (E) is produced, followed by a chemical reaction (C), and subsequently, an electrochemical reaction occurs because the product formed is electroactive.



In the specific case that the product obtained is more easily reducible than the initial reagent ($|E^0_2| < |E^0_1|$). At low sweep rate an irreversible two-electron wave will be obtained, which as the speed increases should become a reversible mono- electron wave. Since the electron transfer rate becomes superior to the speed of the associated chemical reaction.

To sum up, once the variations of I_p , E_p , ΔE_p are known experimentally, with the concentration of the species under study and the potential sweep rate (v), it is possible to determine the mechanism of electrochemical reaction.

In the following table there are summarized $(\delta E_p / \delta \log v)$ and $(\delta E_p / \delta \log c)$ for the exposed mechanism:

Table 8. Potential variation versus sweep rate and concentration for different mechanisms.		
Mechanism	$\delta E_p / \delta \log v$	$\delta E_p / \delta \log c$
Fast E	0	0
Slow E	$\pm 29.6 / \alpha$	0
EC ₁	± 29.6	0
EC ₂	± 19.6	± 19.6
ECE	± 29.6	0

Bibliography

- (1) J. Bard, A.; A. Faulkner, L. *Electrochemical Methods: Fundamentals and Applications*, Ed. 2.; Wiley, Ed.; Texas, 2001.